SUPPORTING INFORMATION

Self-assembly of achiral building blocks into chiral cyclophanes using non-directional interactions

Yuan Zhang,[a] Benjamin Ourri,[b] Pierre-Thomas Skowron,[a] Emeric Jeamet,[b] Titouan Chetot,[b] Christian Duchamp,[b] Ana M. Belenguer,[c] Nicolas Vanthuyne,[c] Olivier Cala,[d] Elise Dumont,[e] Pradeep K. Mandal,[f] Ivan Huc,[f] Florent Perret,[b] Laurent Vial,[*b] and Julien Leclaire[*b]

[a] *Institut des Sciences Moléculaires de Marseille, UMR 7313 CNRS – Université d'Aix-Marseille – École Centrale Marseille, Avenue Escadrille Normandie-Niemen, 13397 Marseille Cedex 20, France*
[b] *Univ Lyon, Univ Lyon 1, CNRS, INSA, CPE, ICBMS, F-69622 Lyon, France*
[c] *Yusuf Hamied Department of Chemistry, University of Cambridge Lensfield Road, CambridgeCB2 1EW, UK*
[d] *Institut des Sciences Analytiques, UMR 5280 CNRS, Université Claude Bernard Lyon, France*
[e] *ENS Lyon, Univ Lyon 1, CNRS, Laboratoire de Chimie, F-69364, France*
[f] *Department of Pharmacy and Center for Integrated Protein Science, Ludwig-Maximilians-Universität Butenandtstr., 5–13, 81377 München, Germany*
[*] laurent.vial@univ-lyon1.fr; julien.leclaire@univ-lyon1.fr

I. GENERAL METHODS

1. Synthesis

Following commercial reagents were used as received and were purchased from Sigma Aldrich: Dimethyl acetylenedicarboxylate (reference D138401, 99 %, CAS 762-42-5), spermine (reference 85590, ≥99.0%, CAS 71-44-3), p-benzoquinone (reference B10358, reagent grade, ≥98%, 106-51-4), dicyclopentadiene (reference 454338, contains BHT as stabilizer, CAS 77-73-6), dimethylthiocarbamoyl chloride (reference 135895, 97 %, CAS 16420-13-6). NaH (reference 452912, 60 % dispersion in mineral oil, CAS 7646-69-7) and carbonyldihydridotris(triphenylphosphine)ruthenium(II) $RuH_2(CO)(PPh_3)_3$, reference 335002, quality level 100, CAS 25360-32-1). Sodium hydride was washed with pentane prior to use to remove mineral oil. Cyclopentadiene was obtained by heating and distillation of dicyclopentadiene and was used directly. Triethylamine was freshly dried by stirring with KOH followed by distillation and then was stored on 4 Å molecular sieves[1]. Dichloromethane, tetrahydrofuran and chloroform were purchased at

reagent grade and then freshly dried by distillation on CaH_2 and then were stored on 4 Å molecular sieves[1]. Similarly, methanol and ethanol were freshly dried by distillation on KOH and then were stored on 3 Å molecular sieves[1]. Dry N,N-dimethylacetamide (reference 271012, anhydrous, 99.8%, CAS 127-19-5) and dry N,N-dimethylformamide (reference 227056, both anhydrous, 99.8 %, CAS 68-12-2) were purchased from Sigma Aldrich. Diphenyl ether was purchased from Sigma Aldrich (ReagentPlus®, ≥99%). All reactions were carried out under nitrogen or argon. Column chromatography was performed using silica gel (Sigma Aldrich, technical grade, pore size 60 Å, 230-400 mesh particle size, 40-63 µm particle size). Reactions were monitored via TLC on a silica gel plate and visualised under UV light. ^{1}H NMR and ^{13}C NMR spectra were recorded for intermediate compounds on a Bruker DRX at 400 MHz or on a Bruker ALS at 300 MHz. J values are given in Hz. Likewise, for intermediate compounds, mass spectra were acquired on an LCQ Advantage ion trap instrument, detecting positive or negative ions in the ESI mode. Melting points were determined by a Buchï Melting point B-540.

2. Semi-preparative chiral HPLC

The diastereoisomeric mixture **BC-4** was separated into pure diastereoisomers **B-4** and **C-4** by HPLC on a chiral stationary phase: Lux-Amylose-2 (amylose tris(5-chloro-2-methylphenylcarbamate, 3 µm) coated on silica). On the analytical column, Lux-Amylose-2 (250 x 4.6 mm, 3 microns), with heptane / ethanol (8/2) mixture as mobile phase, flow-rate = 1 mL/min and UV detection at 254 nm, the two diastereomers were separated with a selectivity of 1.29 and a resolution of 4.4, Rt (**B-4**) = 6.79 mn, k(**B-4**) = 1.30, Rt (**C-4**) = 7.90 mn, k(**C-4**) = 1.68.

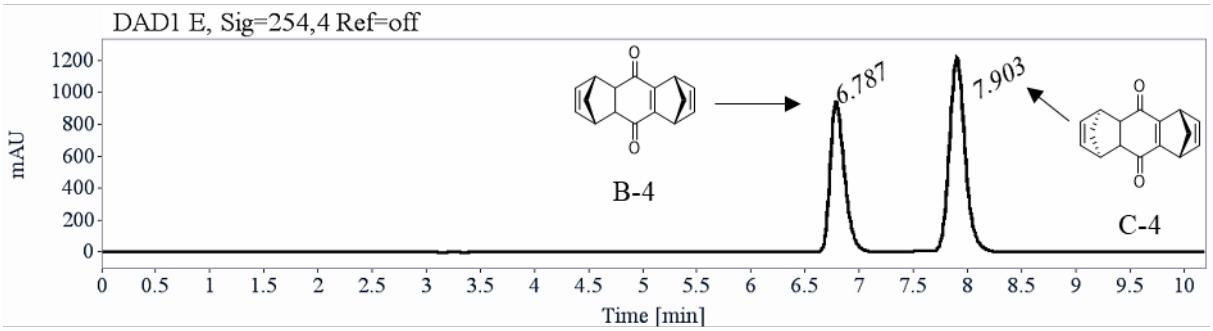

Figure S1 : *UV chromatogram (254 nm) of the analytical separation of **B-4** and **C-4** on Lux-Amylose-2*

On the preparative column, Lux-Amylose-2 (250 x 10 mm, 5 microns), with hexane / ethanol (8/2) mixture as mobile phase, flow-rate = 5 mL/min and UV detection at 290 nm, 21 mg of the mixture could be loaded. From 11 grams of the mixture, 4.5 grams of **B-4** and 4.7 grams of **C-4** were obtained, after 525 stacked injections (cycle time = 4 minutes).

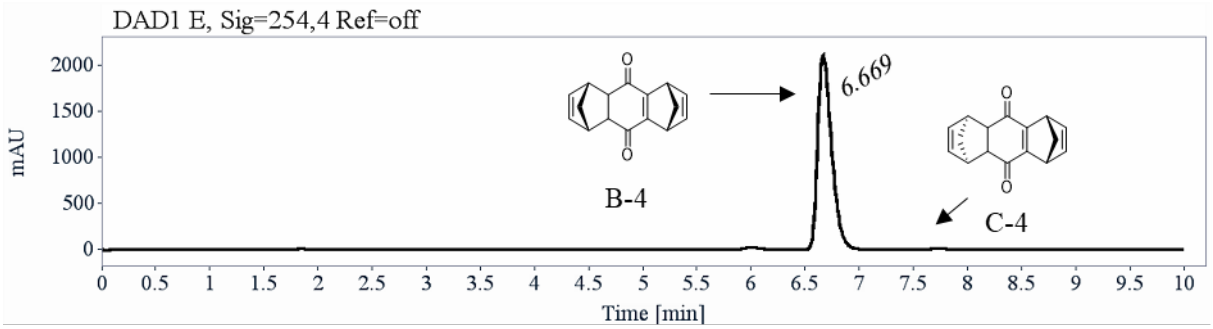

*Figure S2: UV chromatogram (254 nm) of **B-4** diastereomer on the analytical Lux-Amylose-2*

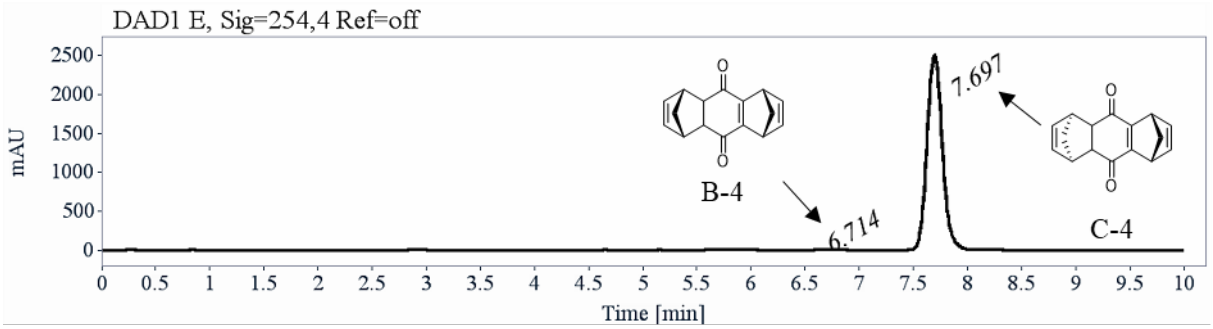

*Figure S3: UV chromatogram (254 nm) of **C-4** diastereomer on the analytical Lux-Amylose-2*

3. Potentiometric titrations

Experiments were performed on a Metrohm 848 Titrino plus at 25°C. The machine was calibrated prior use with adequate buffer solution (7.00; 10.01). NaOH solution was calibrated prior use with analytical grade potassium hydrogen phthalate. 11.0 mg of $\mathbf{B_4}$ were dissolved in 1 mL HCl (0,0958 mM) + 9 mL milliQ water. The solution was then titrated with a solution of NaOH solution (49.0 mM). The same experiment was performed without the macrocycle.

4. Liquid state NMR analyses

Liquid state NMR spectra of synthetic intermediates were recorded in $CDCl_3$, DMSO-d_6, methanol-d_4, heavy water buffered with $CD_3CO_2ND_4$ on spectrometers operating at 300, 400 (BBFO probe with z gradients) and 500 MHz (BBFO and BBI probes with z gradients) respectively for ^1H and ^{13}C. Solvent residual signals were used as internal standard (when necessary, water suppression by presaturation was used). Chemical shifts (δ) and coupling constants (J) are given in ppm and Hz respectively. The peaks patterns are indicated as the following format multiplicity (s: singlet; d: doublet; t: triplet; q: quartet; sept: septuplet; m: multiplet; dd: doublet of doublet; dt: doublet of triplet; etc.). The prefix br. indicates a broadened signal. Temperature was set to 22 degrees unless otherwise specified.

Liquid-state 1D (^1H) using excitation sculpting for water suppression and 2D (COSY, TOCSY, HSQC and HMBC) NMR spectra of $\mathbf{B_4}$-$\mathbf{B_8}$ were recorded in $CD_3CO_2ND_4$ at 283 K on an Avance Neo 1000MHz NMR spectrometer (Bruker Biospin) equipped with a 5 mm CP-TCI-H-C/N-D cryoprobe with standard Z gradient.

DOSY experiments on **B** and **B_4-B_8** where driven on a 500 MHz NMR Bruker Avance III spectrometer with BBFO or BBI probes with standard 50G/cm Z gradient. To avoid convection due to inhomogeneous temperature in the sample, the height of liquid was limited to approximatively 37 mm. Pulses were calibrated prior acquisition. The standard ledbpgp1s where generally used, except when convection was suspected we used the standard dstegp3s sequence. The gradient pulses δ and the delay Δ were adjusted to reach an attenuation of approximatively 95-98 % at maximum gradient. Processing used the Topspin package and Dynamics centre. The data were acquired and processed using TOPSPIN 3.5pl7 software.

Stoichiometric amounts of 1,4-dioxane were introduced for each dyn[n]arene. Stokes-Einstein equation (S1) was used to evaluate hydrodynamic radii in the solvent of analysis from diffusion coefficients.

For each analysis, either the reported values of the viscosity η of the medium in the same experimental conditions (temperature, concentration), following reported DOSY analyses or reported hydrodynamic radii values of the reference in the same experimental conditions (solvent, concentration and temperature) was used through equation (2) derived from (1):

$$R_H = \frac{k_B T}{6\pi n D} \quad (1)$$

$$R_H = \frac{R_H(ref) D(ref)}{D} \quad (2)$$

All solid-state NMR experiments were recorded on a Bruker Avance Neo spectrometer operating at ^{1}H and ^{13}C Larmor frequencies of 800 MHz and 201 MHz, respectively. Cross-polarization (CP) MAS spectra were recorded with a 3.2 mm triple resonance probe at 22 kHz MAS. ^{13}C chemical shifts were referenced to the CH_2 resonance observed for adamantane at 38.48 ppm with respect to the signal for neat TMS. The data were acquired and processed using TOPSPIN 4.0.6 software.

5. UPLC and UPLC-MS analyses

The LCMS method was developed in the Department of Chemistry, University of Cambridge using a modular Agilent 1200 Series HPLC system. This is composed of a HPLC high pressure binary pump, autosampler with injector programming capabilities, Peltier type column oven with 6 µl heat exchanger and a Diode Array Detector (DAD). The large column static mixer was replaced by a much lower volume semiprep frit inside its housing acting as a low volume solvent mixer to significantly reduce the delay of the gradient start. The DAD was fitted with a semi-micro flow cell (1.6 µl, 6 mm pathlength) to reduce peak dispersion when using narrow HPLC columns as in this case. The flow-path was connected using 0.12 mm ID flexible stainless-steel tubing to minimize peak dispersion. The flow from the outlet of the DAD flowcell was connected using a 0.12 mm ID flexible stainless-steel tubing to the "waste/source" divert valve build-in into the IonTrap XCT model from Agilent. This allows the solvent front containing very ionic compounds to be directed away from the Electrospray (ESI) ion source

avoiding contamination, flowing directly to waste. From the switching valve, the flow is directed to a zero dead volume, stainless-steel T-piece, designed as a splitter to avoid more than 100 µL/min to be sprayed directly into the ESI source, this strategy improving the signal to noise. A 5 cm, Peeksil capillary tubing was connected between the outlet of the stainless-steel T-piece and the inlet of the ESI nebuliser capillary needle, this avoiding the capillary to be in direct contact with metal. Peeksil is a silica capillary coated with PEEK for protection. The HPLC/UV data was acquired using Agilent on-line ChemStation software while the MS data was acquired using Bruker Daltronics data acquisition software.

We used Phenomenex Kinetex C18, 100 A 2.6 µm 100 x 2.1 mm as this HPLC column chemistry presented the best separation for the different oligomers. The use of 0.1% TFA in the mobile phase with a very low pH around 1.8, was necessary to obtain the separation of these multi-carboxylate analytes. TFA is transparent to UV above 190 nm, but supresses ionisation to ESI.

The final LCMS method is as follows.

- HPLC column: Kinetex C18 2.6um 100x2.1 mm
- Solvent A: H_2O (0.1%TFA)
- Solvent B: MeCN (0.1%TFA)
- Gradient : 0-8 min 15-42%B; postrun 4min; 12 min run time
- Flowrate ; 0.4 mL/min; 3uL injection ; column oven : 45°C ;
- Detection : λ = 261&310 nm (16 nm bandwidth), reference λ_{ref} = 550 nm (100 nm)

The iontrap was set up in (-)-ESP and the MS was scanned in the Standard enhanced mode (50-2200 m/z at 8,100 m/z/sec)

Nebuliser pressure : 20 psi

Dry gas flow (nitrogen) : 8 L/min

Dry temperature : 350 °C

UPLC analysis were performed using a DIONEX ultimate 3000 Thermo Scientific system. The column used was a phenomenex Kinetex C_{18} 100 A 2.6 µm 100 x 2.1 mm V_{inj} = 4 µL, flowrate 0.4 mL/mn), at 45 °C. Gradient water + 0.1 % TFA / MeCN + 0.1 % TFA in 8 min method (t_0 15/85, t_8 42/58)

Time (mn)	MeCN + 0.1 % TFA (%)	H_2O + 0.1 % TFA (%)
0	15	85
8	42	58

Table S1 : Method of UPLC analysis

6. ESI-MS analyses

High Resolution Mass Spectra of synthetic intermediates and building blocks were recorded with an Atmospheric Pressure Ionization (API) source (positive or negative mode) or a Time Of Flight (TOF) analyzer.

Preliminary ESI-MS monitoring of B and C oligomerization. Experiments were performed on a Q-TOF mass spectrometer (AB Sciex QStar), equipped with a pneumatic assisted electrospray ionization source (nebulization gas: air at 20 psi) operated in the negative ion mode (electrospray voltage: -4200 V; declustering potential: -75 V). Sample solutions (in methanol containing 3 mM ammonium acetate) were introduced in the electrospray source at a 10 µL/min flow rate using a syringe pump.

B_4/B_8 semi-quantitative calibration studies: correlation of relative ESI-MS intensity and integration vs q^{1}H NMR with varying injection volume

This procedure was performed on a hybrid high resolution QTOF spectrometer (Impact II, Bruker) with the following parameters:

- *E*lectrospray ionization in negative mode (ESI -)
- *Capillary voltage* : 4500 V
- *nebulizer gas pressure* : 0.3 bar
- *dry gas* : 4.0 L/min
- *dry gas temperature* : 200 °C
- *Scan range* : 50 – 2000 m/z

The methodology followed was inspired from a recent proof of feasibility published by Lehn and coll. on hydrazine based DCLs[2]. A **B_4/B_8** sample obtained from a 4 mM **B** library stirred at 500 rpm for 48 h and precipitated by TFA was used. The final mother solution was prepared by dissolving this solid in $CD_3CO_2ND_4$ 50 mM D_2O at a 4 mM concentration. q^{1}H NMR analysis of the same sample in deuterated media in the presence of 1 mM dioxane as an internal standard indicated a 80 % content in **B_4** ie a **B_8/B_4** molar ratio of 0.2 (see Figure S121)

Dilution was conducted by mixing 10 µL of mother liquor (10-100 µL micropipette, Thermo Scientific) with 1 mL ESI-CCSM solvent (micropipette 100-1000 µL Thermo Scientific)
The ESI-CCSM Solvent was made of:
- Methanol OPTIMA®LC/MS GRADE, Fisher Chemical A456-212 …….…..... 46.1 %
- Dichloromethane HPLC GRADE Fisher Chemical D/1856/17.…….... 38.4 %
- miliQ water....…… 15.4 %
- Formic acid OPTIMA®LC/MS GRADE, Fisher Chemical A117-50. ….....0.1 %

These diluted samples were introduced into the MS source by a Hamilton syringe of 500 µL loaded into a KD Scientific Pousse-syringe model 601553 set on a flowrate of 10 µL/min

Matrix-assisted laser desorption ionization time-of-flight mass spectrometry (MALDI-TOF MS): mass spectra were acquired in negative reflectron mode (mass accuracy = 0.008%) with a Voyager-DE PRO (Sciex, Framingham, MA) equipped with a nitrogen laser emitting at 337 nm. Ions were accelerated to a final potential of 20 kV. Mass spectra were the sum of 300 shots and an external mass calibration was used (a mixture of peptides from Sequazyme™ standards kit, Sciex). Samples were prepared without any solvent by mixing in a mortar both powder of polymer and matrix (Dithranol, Sigma-Aldrich) in 1/1 (w/w) ratio. Some of the mixture was then crushed on the sample target and submitted to the laser beam.

7. X-ray diffraction

On A_4-a

General procedure for crystallization of ***A_4-a***

Stock solution of $(pR\text{-}P)_4/(pS\text{-}M)_4$-**$A_4$** noted **$A_4$-a** was prepared by dissolving 10mg of the lyophilized powder using 970µL of pure water and 26µL of 2M ammonium bicarbonate solution, to reach a concentration of ~10mM. Stock solutions of 10mM of each polyamine was prepared in pure water. For crystallization trials, 100µL of working solutions were prepared by 1:1 mixture of **A_4-a** and the corresponding polyamine.

Crystallization trials were performed using standard aqueous sitting-drop vapor diffusion method in CrystalQuick Plus 96-well polystyrene microplates, at 293 K. Screening of crystallization conditions was carried out using commercial sparse-matrix screens JBScreen Basic from Jena Bioscience. The initial sitting drops composed of 0.75µL of free-host or host-guest solution and an equal volume of the crystallization reagent. The drops were equilibrated against 50µL of the respective crystallization reagent in reservoir. X-ray quality crystallogenesis were optimized by using the hanging drop vapor diffusion method in EasyXtal 15-well plates at 293 K. The drop size was in the range of 1.0 to 1.5µL of free-host or host-guest solution and an equal volume of the crystallization reagent. The drops were equilibrated against 500 µl of the respective crystallization reagent in reservoir. Crystals appeared in a span of 1 to 5 days. The crystallization conditions are summarized in Table S2.

X-ray data collection and structure determination

Single crystals were fished using MiTeGen micro-loops and quickly soaked in cryo-protectant solution for low temperature x-ray diffraction measurements in :

1) an in-house, micro-focus, rotating anode Rigaku FRX diffractometer, with Cu Kα radiation and a hybrid pixel detector (PILATUS 200K) at the IECB X-ray facility (UMS 3033)
2) the EMBL P13 beamline[3]with a Dectris Pilatus 6M detector in Petra III DESY, Hamburg.
3) the ID30b beamline[4] with a Dectris Pilatus 6M detector in ESRF, Grenoble.

The diffraction data were processed using the program *CrysAlis*^{Pro}[5] and *XDS*[6,7]. The structures were solved with the program *SHELXT* and refined by full-matrix least-squares method on F^2 with *SHELXL-2014*[8] within *Olex2*[9]. After each refinement step, visual inspection of the model and the electron-density maps were carried out using *Olex2* and *Coot*[10]. The initial structure revealed most atoms of the macrocycle and additives from crystallization reagents. Anisotropic refinement was carried out for all non-H atoms except for those with severe disorder. SQUEEZE procedure was then used to flatten the electron density map[11]. H-atoms were placed at idealized positions using HFIX. Crystallographic data and refinement statistics are reported in Table S3.

On (*MInPIn*)$_4$-B$_8$

General procedure for crystallization of ***B$_8$***

An aqueous solution of ca. 8mM was prepared by dissolving 4.2mg of the lyophilized compound in 260µL of pure water and 4.35µL of concentrated NaOH solution. Crystallization trials were performed using standard aqueous sitting-drop vapor diffusion method in CrystalQuick Plus 96-well polystyrene microplates, at 293 K. Screening of crystallization conditions was carried out using commercial sparse-matrix screens JBScreen Basic 1 - 4 from Jena Bioscience[3,4]. Initial sitting drops composed of 0.75µL of **B$_4$-B$_8$** mixture and an equal volume of the crystallization reagent. The drops were equilibrated against 50µL of respective crystallization reagent in reservoir. Majority of the drops observed had light/heavy amorphous precipitate or liquid-liquid phase separation within 24 hours. Observation after 3 days of incubation revealed hexagonal prisms in three conditions (listed below) where precipitate occurred first.

1) JBScreen Basic 4- G1: 0.8 M KH_2PO_4, 0.8 M NaH_2PO_4, 0.1 M HEPES (pH 7.5)
2) JBScreen Basic 4- G3: 1.0 M $NH_4H_2PO_4$, 0.1 M tri-Sodium citrate (pH 5.6)
3) JBScreen Basic 4- G4: 2.0 M $NH_4H_2PO_4$, 0.1 M TRIS (pH 8.5)

Numerous X-ray diffraction analyses were performed for which the crystals were flash cooled in the presence or absence of different cryo-protectant solutions. Undesirably, none of the crystals yielded atomic resolution data sets (at best 1.5 Å) and could not be solved by *ab initio* methods.

The JBScreen XP from Jena Bioscience was then used for crystallization screening as it provides 96 of the most prominent crystallization conditions upgraded with the Anderson−Evans polyoxotungstate $[TeW_6O_{24}]^{6-}$ (TEW) additive that improves crystallization and crystal diffraction quality of challenging targets.[2] X-ray quality crystals was obtained by the addition of 1µL of **Y** and 1µL of the reservoir solution consisting of JBScreen XP-A2 i.e. 1.5 M ammonium sulfate, 12% glycerol, 0.1 M TRIS buffer (pH 8.5) and 1mM TEW. Crystals (Figure S129) appeared after 7 days after initial precipitation of the drop. A single crystal was fished with a MiTeGen microloop and plunged directly into liquid nitrogen such that the mother liquor served as cryo-protectant.

X-ray data collection and structure determination

X-ray diffraction data were collected at the P13 beamline operated by EMBL, Hamburg at the Petra III storage ring (DESY, Hamburg, Germany) with a Dectris Pilatus 6M detector[3]. Diffraction data were measured at T = 100 K and λ = 0.97625 Å (Energy 12.7 keV). The crystal was exposed for 0.04 s and 0.1° oscillation per frame. Diffraction data was processed with *CrysAlis*^{Pro} suite version 39.46[5]. Empirical absorption correction using spherical harmonics, implemented in SCALE3 ABSPACK scaling algorithm was used. The crystal belonged to the space group *P*622 with unit cell parameters: *a* = *b* = 49.495 (7) Å and *c* = 35.697 (5) Å; V = 75733 (2) Å^3 and two ¼ molecules per asymmetric unit (Z = 6). The structure was solved by intrinsic phasing with *Shelxl* and and refined by full-matrix least-squares method on F^2 with *Shelxl-2014*[8] within *Olex2*[9]. Due to the weak diffraction intensity and low resolution, all non-H atoms of the octamer were refined with anisotropic or isotropic displacement parameters (Figure S130). H atoms (except carboxylic side chains) were placed geometrically and constrained depending on their environment. Those H-atoms were refined in the riding-model approximation, with Uiso(H)=1.2Ueq(CH, CH2). DFIX, AFIX, SADI, FLAT, SIMU and EADP instructions were employed to model geometry of the molecules and temperature parameters. After several attempts to model the disordered carboxylate side chains, the *PLATON*/*SQUEEZE* procedure was used to flatten the electron density map[11]. Calculated total potential solvent accessible void volume and electron count per cell are 54147 Å^3 and 9812 respectively.

8. Molecular modelling

DFT calculations

All the molecular structures have been fully optimized using the density functional theory, with the B3LYP[12] functional (together with the Grimme's D3BJ dispersion correction), and with the Minnesota's M06-2X functional that includes an implicit dispersion correction. A Pople's triple-zeta basis set 6-311G(d,p) was employed for C, H and N atoms, whereas diffusive orbitales were included 6-311+G(d,p) to describe sulfur and oxygens atoms. All DFT calculations were performed with Gaussian 09 Rev B.02[13] series of programs. Vibrational frequencies have been computed to characterize transition states and stationary points. IRC were employed to characterize transition states with a single imaginary frequency.

Molecular dynamic simulations

All molecular dynamic simulations and post-processing were performed with the Amber 16 Molecular Dynamics software package[14]. The force-field parameters were taken from parm99[15], while the parameters for the cage were generated using the generalized AMBER force field GAFF[16]. Each compound was previously build using the Gaussview5 software and their geometries were optimized

with the Gaussian09 suite of programs[13] software using density functional theory at the B3LYP level of theory with the 6-31G(d,p) basis set. The different parameters were generated with antechamber and parmcheck subprograms, and atom point charges were computed using the RESP protocol. The guest was inserted inside the host using the xleap module. Potassium cations (K^+) and chlorine anions (Cl-) were added in order to assign a salt concentration of 0.150 M. The systems were immersed in a truncated octahedral water TIP3P[17] water box containing around 2500 water molecules. Each system was first minimized in a 5000 steps simulation, including 2500 steps of steepest descent. Then, a thermalization step was performed to heat each system from 0 to 300 K in 30 ps. The temperature was kept constant during the following steps using Langevin thermostat with a collision frequency γln of 1 ps^{-1}. A 1000 ps equilibration run was performed in NPT conditions. Finally, a 100 ns production was executed with constant pressure. After all dynamic molecular simulations, analysis of the trajectories were performed using the cpptraj module[18] of AMBER, and thermodynamic parameters were extracted using the MM/GBSA method[19] with the internal and external dielectric constants set to 4 and 80, respectively. Trajectories were visualized with the chimera software[20]. The four SS dihedral angles were monitored to ensure that a rapid conformational exchange takes place along our dynamics.

II. EXPERIMENTAL DATA

1. Compound **A_4-a**

a. Synthesis

The synthesis of **A** and **A_4-a** were conducted following our previously published procedure using spermine as a template[21].

b. ^{1}H NMR Spectra

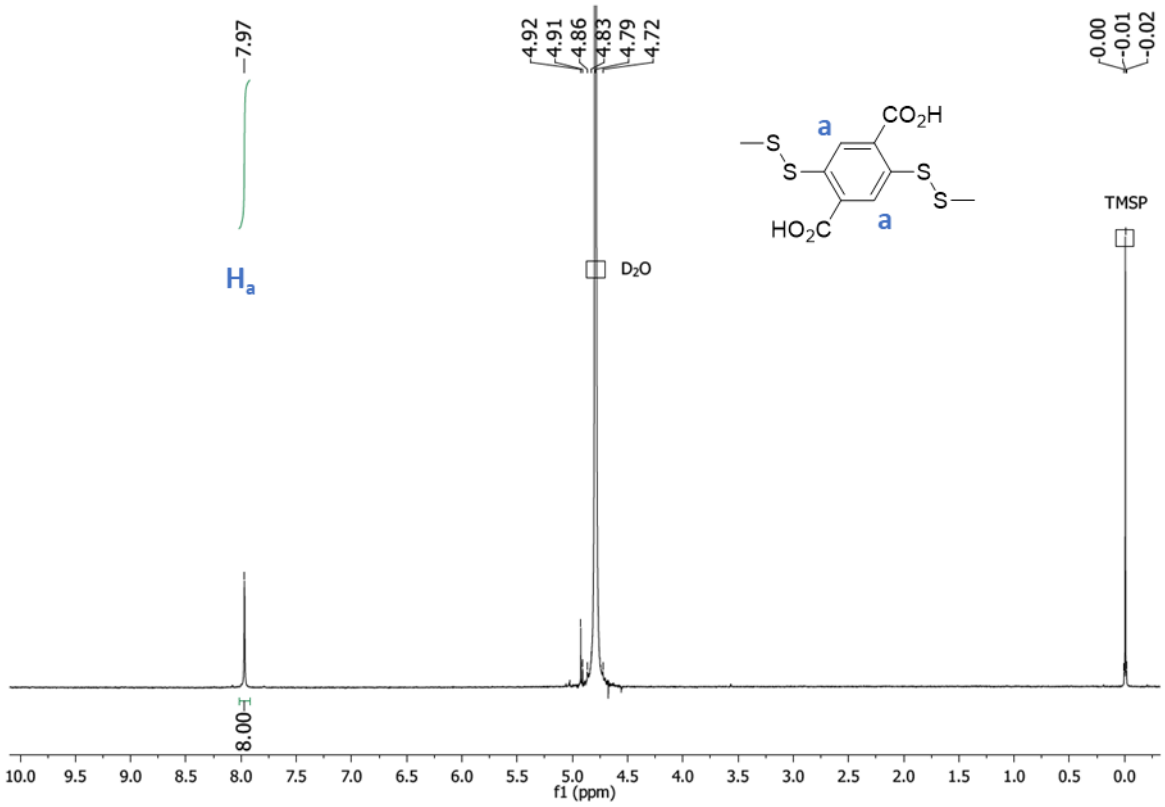

*Figure S4 : ^{1}H NMR spectra of compound **A_4-a** at 1 mM in D_2O with TMSP (1 mM) as internal standard. pH adjusted to 7.42 by addition of a solution of NaOD.*

c. Mass spectra

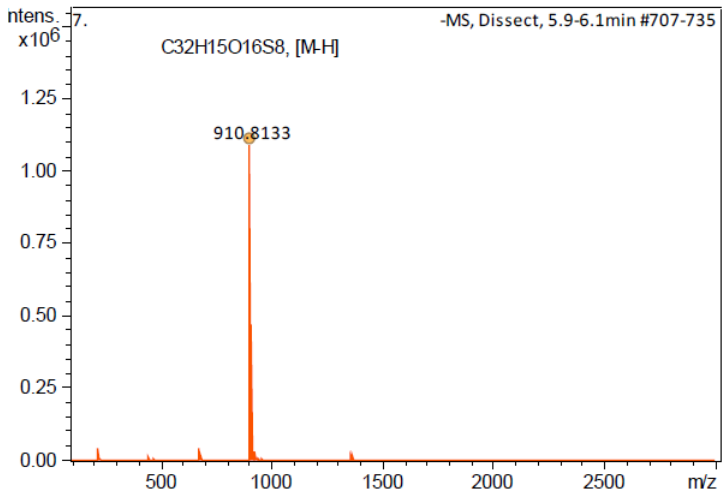

Meas. m/z	Ion Formula	m/z	err [ppm]	mSigma	Score	Adduct	z
910.8133	C32H15O16S8	910.8131	-0.1	18.9	100	M-H	1-

*Figure S5: HRMS data of **A_4-a***

d. Crystallographic data

Solution	Crystallization reagent and crystal size	Cryo protectant solution
A_4-a	2.0 M Ammonium sulfate 0.15 x 0.05 x 0.05 mm	Crystallization reagent + Paratone-N oil (2:1)
A_4-a + Putrescine	1.8 M Ammonium sulfate, 0.1M MES buffer (pH 6.5), 0.01 M $CoCl_2$ 0.15 x 0.05 x 0.03 mm	Crystallization reagent + 100% glycerol (2:1)
A_4-a + Cadaverine	2.0 M $NH_4H_2PO_4$, 0.1 M TRIS buffer (pH 8.5) 0.07 x 0.07 x 0.07 mm	Crystallization reagent + Paratone-N oil (2:1)

*Table S2: Summary of crystallization conditions and cryo-protectant solutions, *spermine from crystallization reagent was later found to form complex with **A_4-a**.*

		A_4-a	**A_4-a** + putrescine	**A_4-a** + cadaverine
CCDC number		1554744	2003290	2001333
Empirical formula		$C_{32}H_{18}O_{30}S_8$	$C_{37.5}H_{22}Co\ N_{9.75}O_{23.5}S_8$	$C_{37}H_{22}N_2O_{17.75}S_8$
Formula weight		1138.94	1300.56	1035.04
Temperature		100 K	100 K	150 K
Diffraction source		Rigaku FRX	Petra III, DESY	Rigaku FRX
Wavelength		1.5417 Å	0.8265 Å	1.5417 Å
Space group		$P2_1$	P-1	Pc
Unit cell parameter	a	10.248 (3)	10.644 (2) Å	10.749 (18) Å
	b	23.721 (5)	11.901 (2) Å	11.906 (17) Å
	c	11.087 (3)	22.630 (5) Å	19.424 (3) Å
	α	90	101.40 (3)°	90°
	β	115.08 (3)	90.57 (3)°	18.589 (14)°
	γ	90	99.40 (3)°	90°
Volume		2441.2 (12) $Å^3$	2769.7 (10) $Å^3$	2458.2 (6)
Z		2	2	2
Density		1.577 g/cm^{-3}	1.494 g/cm^{-3}	1.623 g/cm^{-3}
Absorption coefficient		4.241 mm^{-1}	1.063 mm^{-1}	3.904 mm^{-1}
F(000)		1196.0	1262.0	1077.0
Theta range for data		4.74 to 73.38°	1.99 to 53.62°	2.30 to 51.24°
Index range		*h = -10 → 12*	*h = -10 → 10*	*h = -10 → 10*
		k = -29 → 28	*k = -11 → 11*	*k = -12 → 12*
		l = -13 → 13	*l = -22 → 22*	*l = -19 → 19*
Total reflections		17097	17503	12839

Unique reflections	8784	5051	5063
R_{int}	0.0329	0.0299	0.0775
Completeness	0.8894	0.8951	0.9546
Data/restraints/parameters	8784/43/712	5045/380/645	5063/486/551
R1, wR2 (I > 2σ (I))	0.0578, 0.1660	0.1353, 0.4438	0.0917, 0.2248
R1, wR2 (all data)	0.0591, 0.1695	0.1389, 0.4583	0.1547, 0.2683
Goodness-of-fit	1.143	2.503	1.109
Largest diff. Peak/hole e/ Å^3	0.61/-0.65	1.64/-1.25	0.43/-0.37
Total potential solvent accessible void volume from SQUEEZE	-	-	365.0 Å^3
Electron count/cell	-	-	121.4

Table S3 : Crystallographic data and refinement statistics

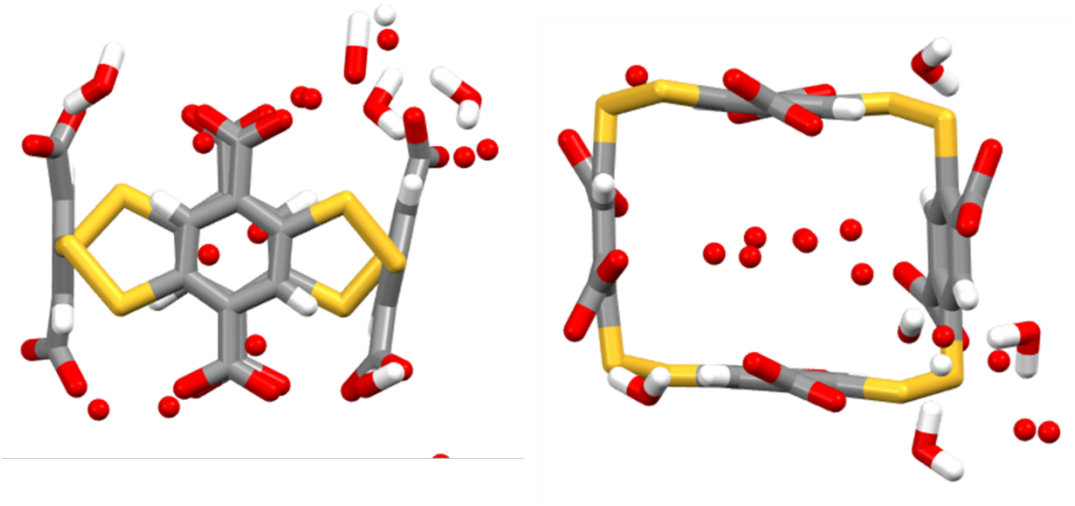

Figure S6: X-ray crystallographic structure of (MpR)$_4$-**A$_4$-a**. *Values of the torsion angles of the disulfide bridges (in degrees): 94.32, 83.11, 88.05, 80.15.*

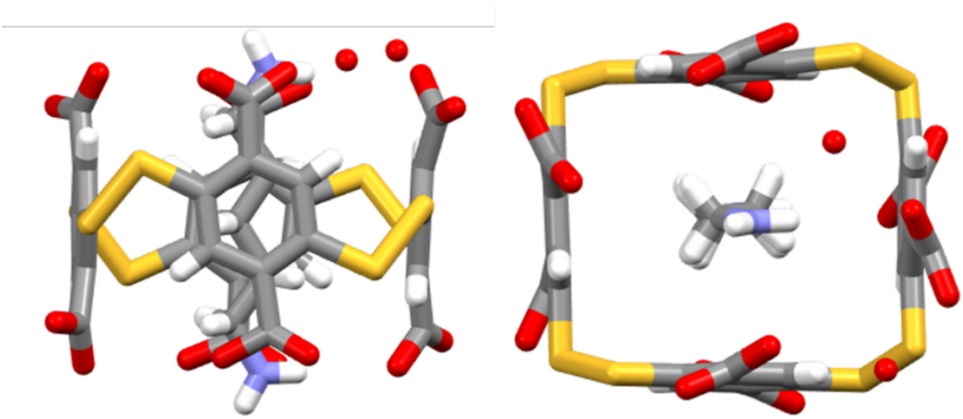

Figure S7: X-ray crystallographic structure of (PpS)$_4$-**A$_4$-a-Cadav** (Cadav = cadaverine). *Values of the torsion angles of the disulfide bridges (in degrees): - 88.34, -89.89, - 88.43, -85.01.*

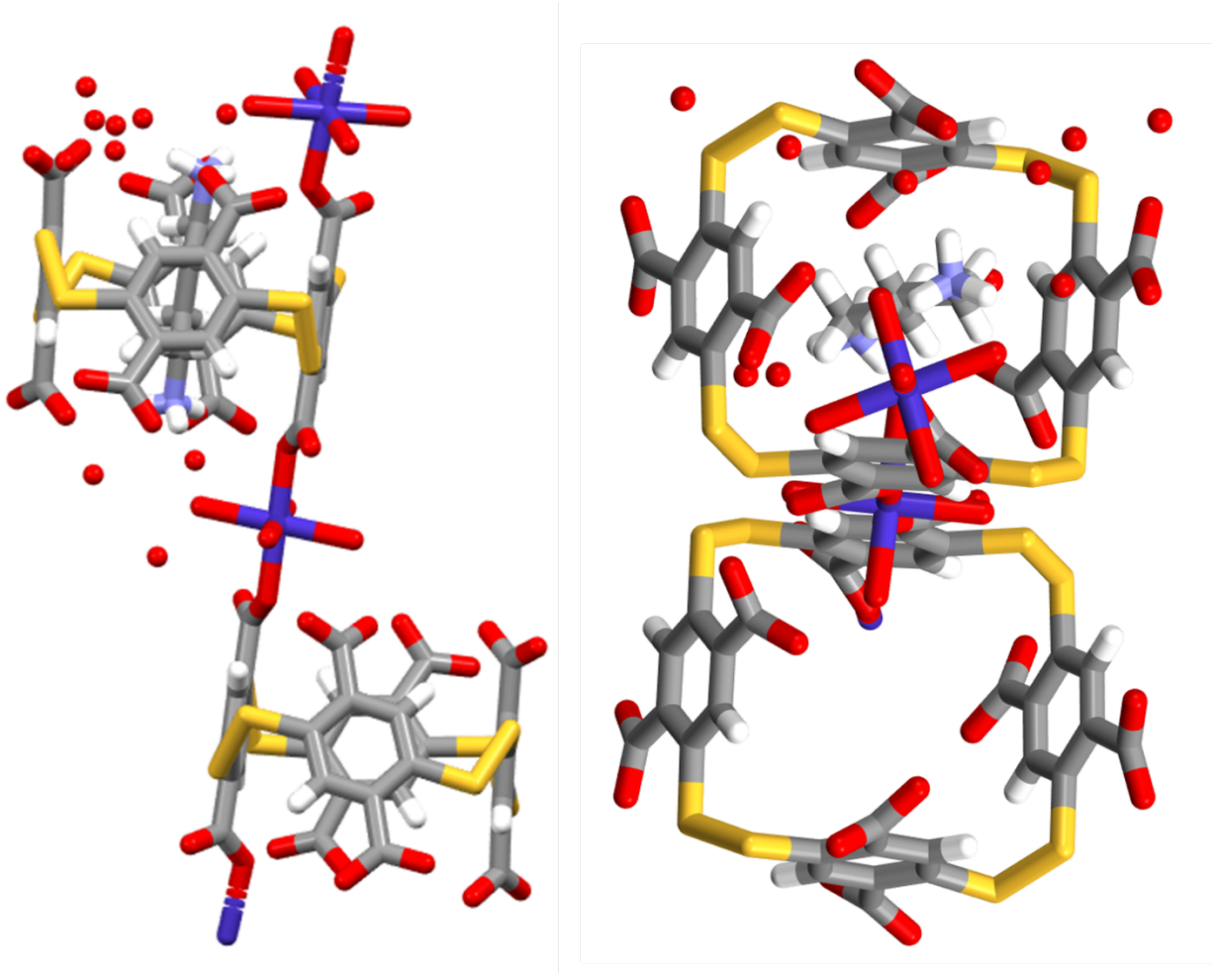

Figure S8: X-ray crystallographic structure of (MpR)$_4$-**A$_4$-a-Put** (Put = putrescine). *Values of the torsion angles of the disulfide bridges (in degrees): 83.73, 89.42, 82.62, 88.70.*

e. Modelling data

Compound (*pS*)$_4$-A$_4$-a

Entry	confo.	%	E(kcal.mol^{-1})	Esp(kcal.mol^{-1})
0	**M$_4$**	38.51	-3523116.48	-3523010.39
1	**M$_4$**	35.69	-3523113.14	-3522917.70
2	**M$_4$**	11.94	-3523116.62	-3522949.86
3	**M$_4$**	11.64	-3523114.56	-3522911.56
4	**M$_4$**	0.83	-3522546.22	-3522846.45
5	**M$_4$**	0.48	-3523007.89	-3523005.46
6	**M$_4$**	0.32	-3523104.32	-3522756.32
7	**M$_4$**	0.30	-3523100.70	-3522965.12
8	**M$_4$**	0.27	-3523004.45	-3522802.34
9	**M$_4$**	0.02	-3522890.11	-3522917.21

*Table S4: Population and energy of the 10 conformers identified upon cluster analysis and after structure optimization and single point energy minimization of $(pS)_4$-**A_4**, starting from a mismatched P_4 conformation*

Conformers	SS1	SS2	SS3	SS4
0	132,47	40,90	123,47	63,90
1	53,25	127,04	50,24	139,04
2	47,69	106,13	47,44	106,65
3	106,63	51,76	108,23	77,04
4	70,29	80,22	78,92	103,19
5	117,77	76,68	104,38	81,02
6	98,10	66,31	104,41	96,18
7	66,06	103,20	71,07	136,20
8	89,17	95,70	91,34	73,97
9	68,24	93,70	61,23	112,95

*Table S5: Dihedral angle values, in degrees, calculated for 10 conformers of $(pS\text{-}M)_4$-**A_4** identified based on cluster analysis.*

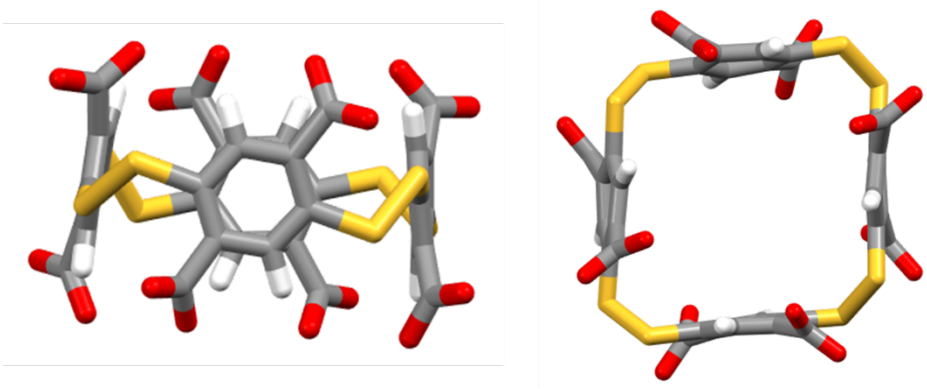

*Figure S9: DFT-modelled structure of $(PpS)_4$-**A_4-a***

Compound *pR_3pS/pS_3pR*-A_4-b

Entry	confo.	%	E(kcal.mol^{-1})	Esp(kcal.mol^{-1})
0	**M_2PC**	60.92	-3523111.98	-3522944.48
1	**M_2PC**	36.46	-3523111.90	-3522941.46
2	**M_3P**	2.17	-3523091.81	-3522911.73
3	**M_3P**	0.35	-3523074.03	-3522923.17
4	**M_3P**	0.04	-3523103.27	-3522890.45
5	**M_3P**	0.04	-3523081.45	-3522843.56
6	**MCTC**	0.01	-3523109.07	-3522902.06
7	**M_3P**	0.01	-3523090.72	-3522909.13
8	**TCTC**	0.01	-3523071.98	-3522878.67
9	**M_3P**	0.01	-3523099.52	-3522901.22

*Table S6: Population and energy of the 10 conformers identified upon cluster analysis and after structure optimization and single point energy minimization of pR_3pS/pS_3pR-**A_4-b**, starting from a mismatched P_4 conformation (**C** = cis and **T** = trans correspond to 0 +/- 20° and 180°+/- 20°)*

entry	SS1	SS2	S3	SS4
0	54,02	109,71	6,03	-117,28
1	127,34	44,39	-111,88	-1,69
2	24,63	115,46	-28,74	118,72
3	52,82	116,69	-62,77	105,70
4	124,87	60,06	109,26	-60,61
5	96,65	80,74	-104,93	25,22
6	107,04	70,23	52,57	-89,26
7	44,25	117,21	46,82	-120,90
8	162,65	29,16	-144,94	-36,04
9	26,20	100,63	-2,94	95,40

*Table S7 : Dihedral angle values, in degrees, calculated for 10 conformers of pR_3pS/pS_3pR-**A_4-b** identified based on cluster analysis.*

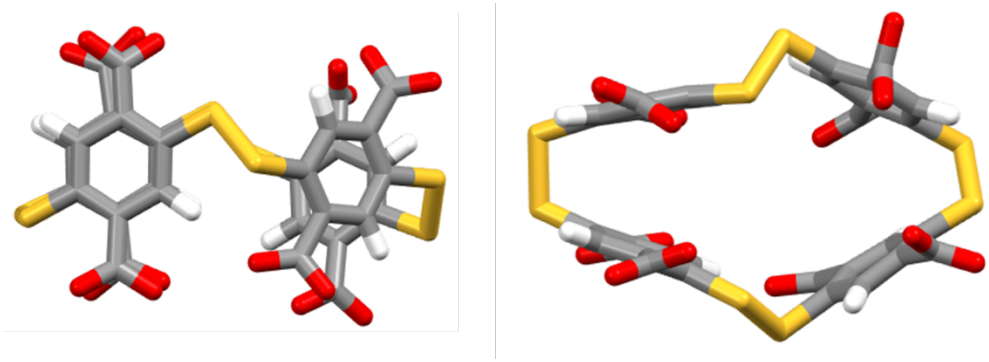

*Figure S10: DFT-modelled structure of $pS(pR)_3$-**A_4-b***

Compound *pR_2pS_2* -A_4-c

Entry	confo.	%	E(kcal.mol^{-1})	Esp(kcal.mol^{-1})
0	**CPCM**	89.58	-3523129.84	-3522985.17
1	**MCPM**	9.64	-3523112.01	-3522932.95
2	**MPM_2**	0.25	-3523120.47	-3522952.12
3	**M_2PM**	0.21	-3523109.34	-3522916.81
4	**M_2PM**	0.13	-3523097.13	-3522971.17
5	**CPM_2**	0.07	-3523107.27	-3522967.80
6	**P_3M**	0.06	-3523123.22	-3522970.54
7	**P_3M**	0.03	-3523110.12	-3522947.16
8	**MPCM**	0.02	-3523107.31	-3522987.26
9	**M_2PM**	0.01	-3523007.31	-3522952.33

*Table S8: Population and energy of the 10 conformers identified upon cluster analysis and after structure optimization and single point energy minimization of pR_2pS_2/pS_2pR_2-**A_4-c**, starting from a mismatched P_4 conformation (**C** = cis and **T** = trans correspond to 0 +/- 20° and 180°+/- 20°)*

entry	SS1	SS2	SS3	SS4
0	-11,41	122,30	-20,42	-123,52
1	-121,14	1,70	110,10	-41,62
2	-116,66	60,66	-110,62	-58,67
3	-32,27	-107,98	47,59	-122,10
4	-68,92	-69,09	80,40	-86,31
5	-19,56	107,34	-40,56	-110,31
6	51,78	74,27	74,11	-96,10
7	122,33	31,88	135,82	-47,37
8	-52,64	103,61	-5,76	-120,12
9	-105,61	-42,81	122,16	-35,78
Mean				

*Table S9: Dihedral angle values of pR_2pS_2-**A_4-c** for10 conformers identified based on cluster analysis.*

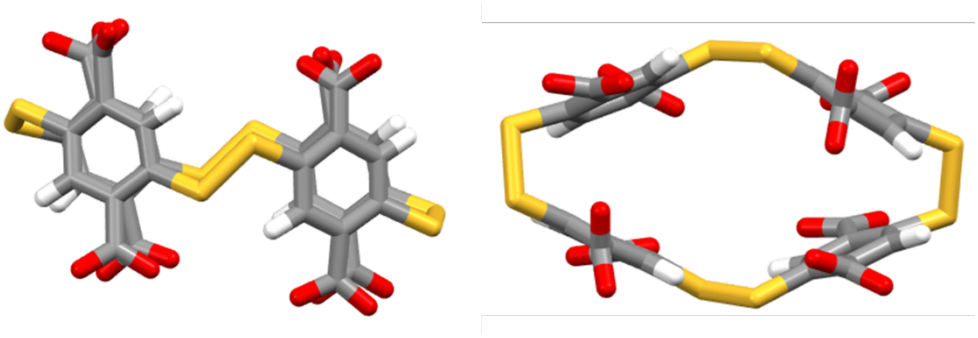

*Figure S11: DFT-modelled structure of $(pS)_2(pR)_2$-**A_4-c***

2. Compounds $(In\text{-}M\text{-}In\text{-}P)_2$-**B**$_4$ and $(P\text{-}In\text{-}M\text{-}In)_4$-**B**$_8$

a. Syntheses of building blocks **B** and **C**

Experimental procedures

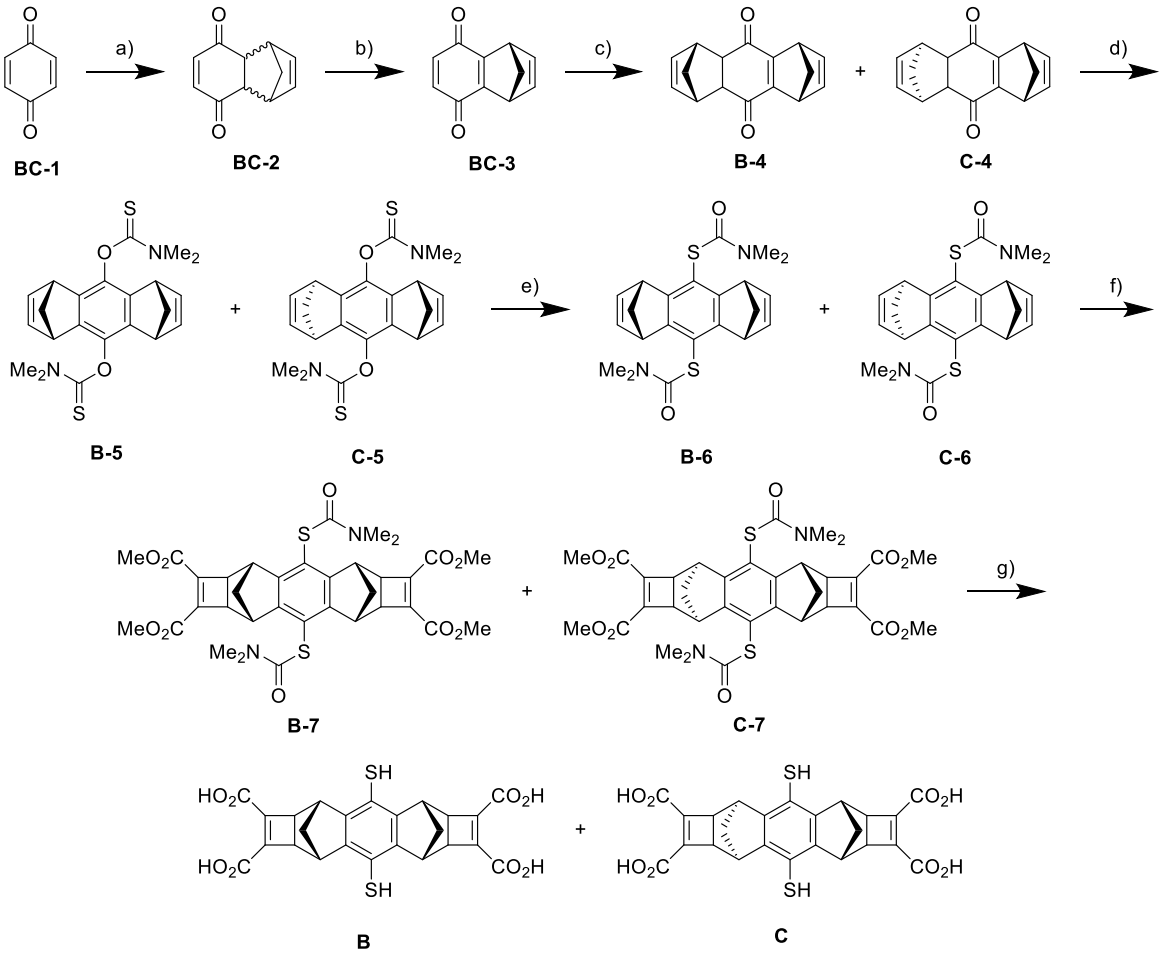

Scheme S1 : Synthesis of diastereoisomeric building blocks **B** and **C**. Their separation by chiral chromatography was conducted after step c), ie on a B-4/C-4 mixture. The subsequent steps were hence conducted on diastereoisomerically pure material, a) cyclopentadiene, MeOH, -78°C to r.t., 16 h., 98 %; b) 1. Et_3N, MeOH, r.t., 16 h., 2. benzoquinone **BC-I**, $CHCl_3$, 50°C, 5 h., 87 %; c) cyclopentadiene, MeOH, -78°C to r.t., 16 h., 44 % (**B-4**) 22 % (**C-4**) 22 %; d) dimethyl thiocarbamoyl chloride, NaH, DMF, r.t., 16 h., 99 % (**B-5**), 98 % (**C-5**); g) diphenyl-ether, 230 °C, 3 h., (**B-6**) 49 % (**C-6**) 11 %; f) $RuH_2CO(PH_3)_3$, DMAD, THF, reflux, 10 d. (**B-7**) 29 %, (**C-7**) 41 %; g) NaOH, H_2O/EtOH, reflux, 16 h., (**B**) 35 %, (**C**) 37 %.

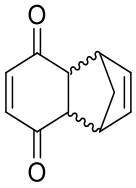

BC-2 1,4,4a,8a-tetrahydro-1,4-methanonaphthalene-5,8-dione

p-benzoquinone **BC-1** (36 g, 0.33 mol) was dissolved in 500 mL of methanol. The mixture was cooled down to -78 °C and freshly distilled cyclopentadiene (28 mL, 0.33 mol) was added. The reaction mixture was stirred at room temperature for 2 h. The solvent was removed under vacuum and the resulting solid was recrystallised in hexane if necessary, to give a brown powder (57,8 g, 99 %).

Brown powder, mp: 63,4 – 65,8 °C; HRMS (ESI) $[M + Na]^+$ found 197.0572, calculated 197.0573 for $[C_{11}H_{11}NaO_2]^+$; ^{1}H NMR (400 MHz, $CDCl_3$) δ ppm = 6.46 (s, 2 H, =C**H**$_a$-CO), 5.97 - 5.92 (m, 2 H, C**H**$_b$=C**H**$_b$), 3.44 - 3.40 (m, 2 H, C**H**$_c$-CO), 3.14 - 3.11 (m, 2 H, C**H**$_d$-CH=CH), 1.45 - 1.39 (m, 1 H, C**H**$_{2e}$), 1.36 - 1.31 (m, 1 H, C**H**$_{2e}$); ^{13}C NMR (400 MHz, $CDCl_3$) δ ppm = 199.1 (**C**$_f$O), 141.7 (=**C**$_a$H-CO), 135.0 (CH-**C**$_b$H=**C**H), 48.4 (**C**$_c$H-CO), 48.4 (**C**$_e$H$_2$), 48.0 (**C**$_d$H-CH=CH)

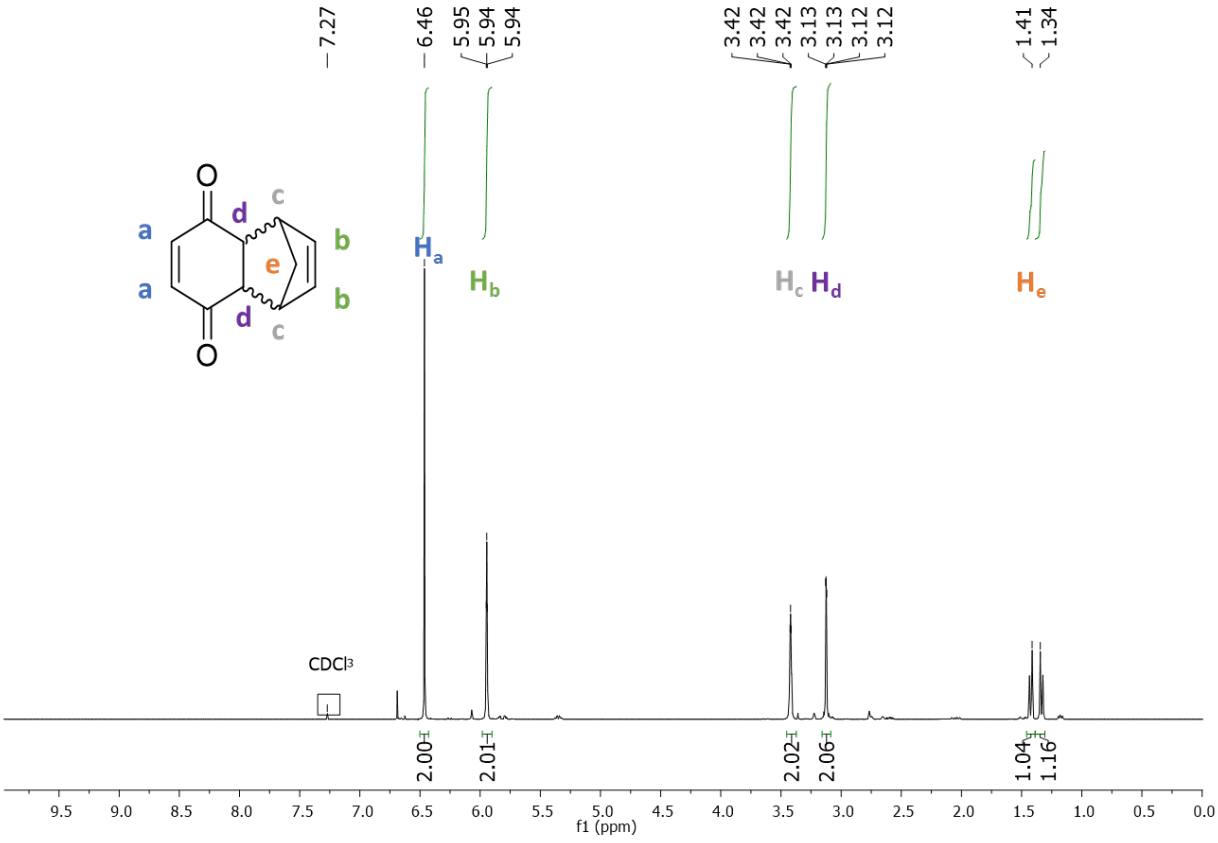

*Figure S12: ^{1}H NMR spectrum of compound **BC-2***

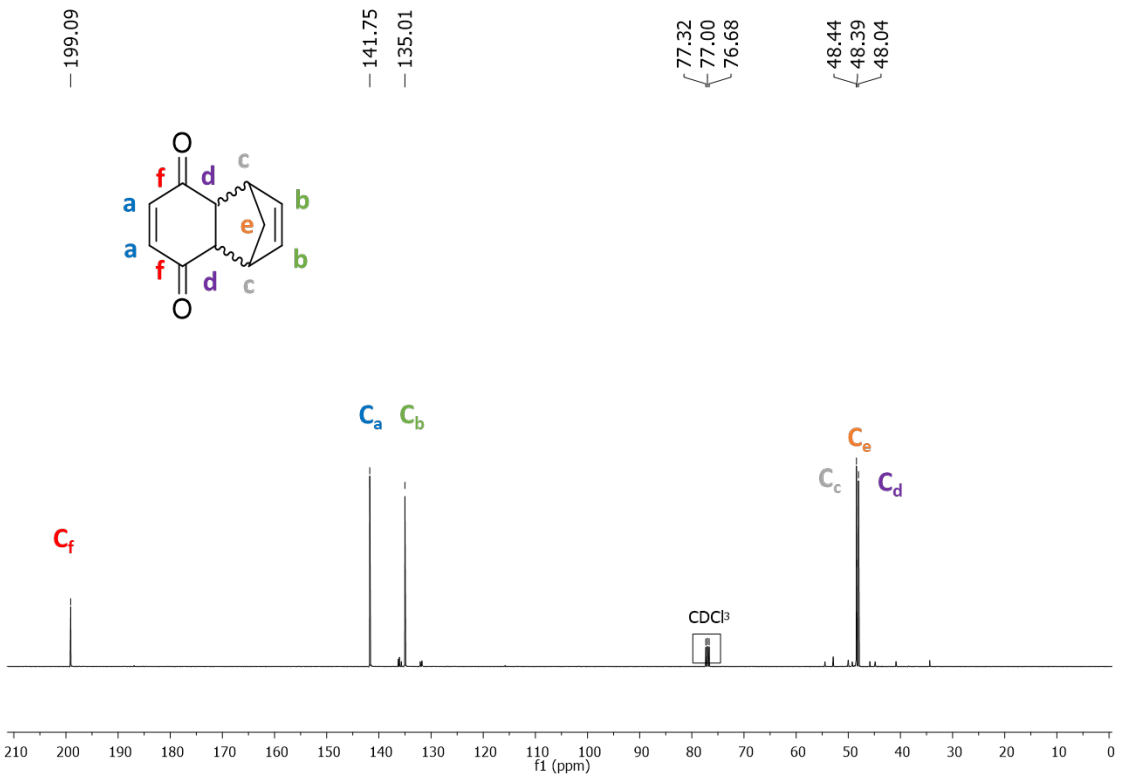

*Figure S13: ^{13}C NMR spectrum of compound **BC-2***

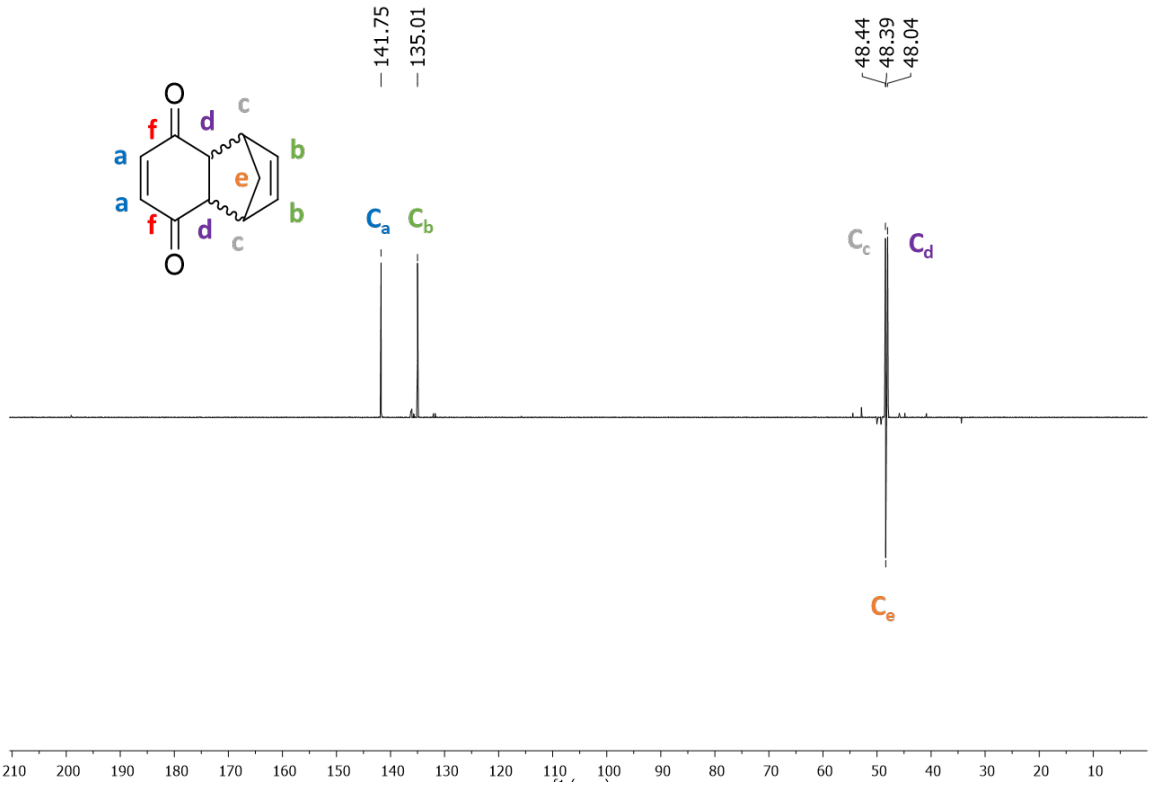

*Figure S14: DEPT ^{13}C NMR spectrum of compound **BC-2***

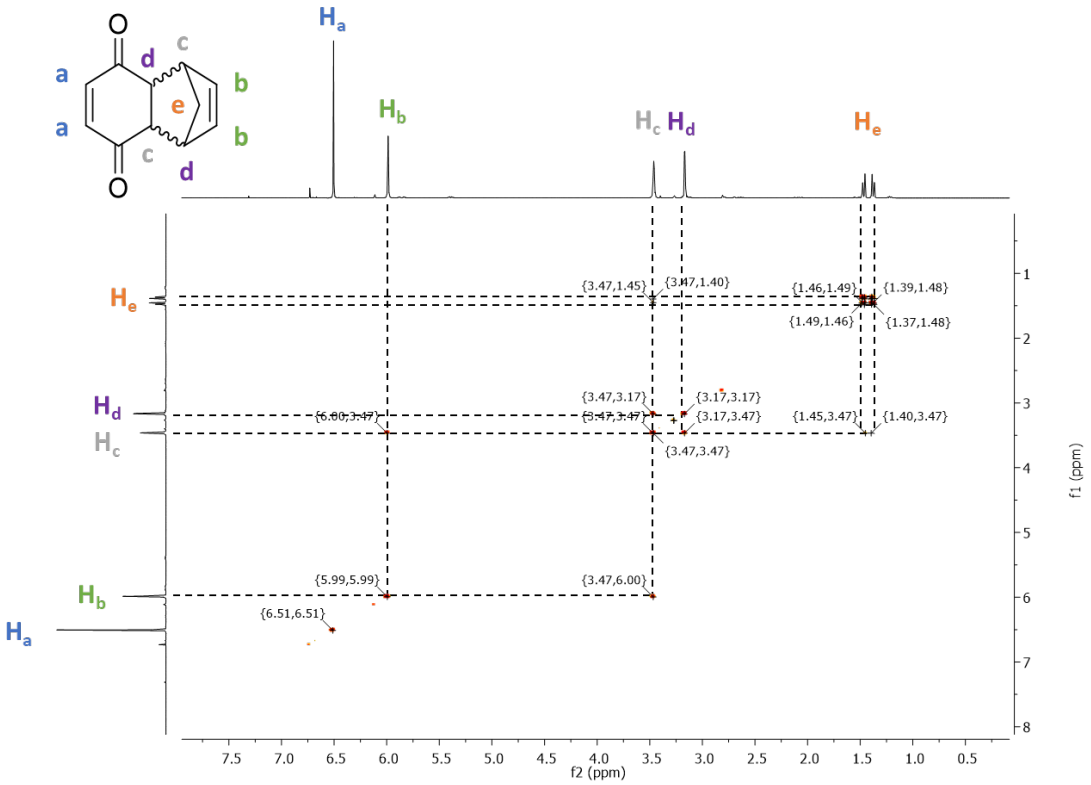

Figure S15: COSY NMR spectrum of compound ***BC-2***

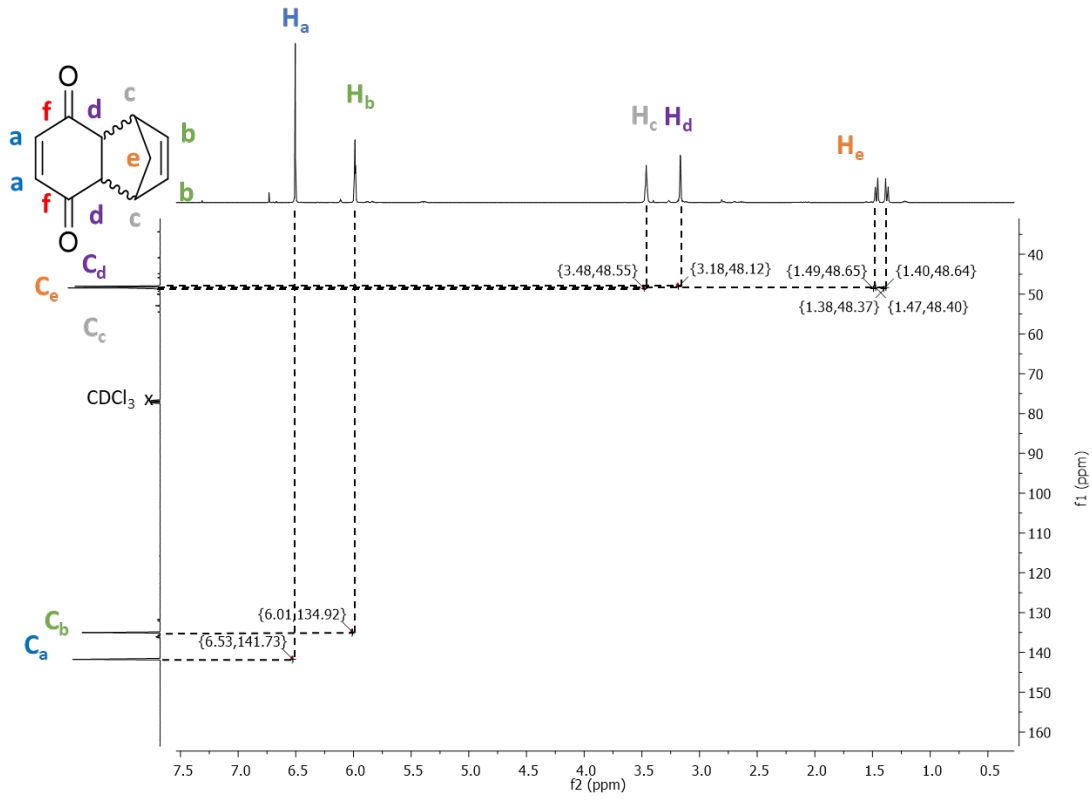

Figure S16: HSQC NMR spectrum of compound ***BC-2***

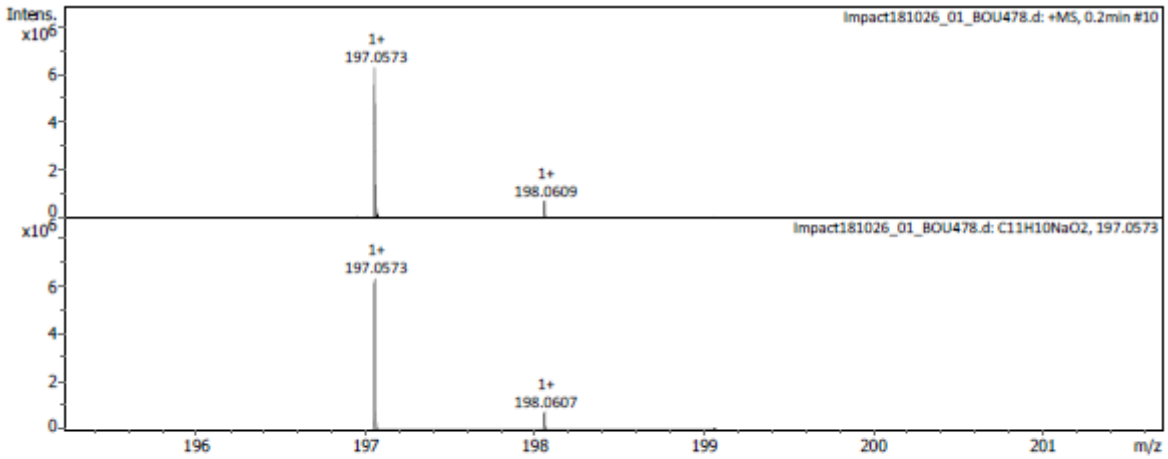

Meas. m/z	Ion Formula	m/z	Sum Formula	err [ppm]	mSigma	Adduct	z
175.0753	C11H11O2	175.0754	C11H10O2	0.2	2.4	M+H	1+
197.0573	C11H10NaO2	197.0573		0.2	3.0	M+Na	1+

Figure S17: HRMS spectrum of compound ***BC-2***

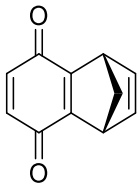

BC-3 (1R,4S)-1,4-dihydro-1,4-methanonaphthalene-5,8-dione

To 240 mL of methanol was added **BC-2** 1,4,4a,8a-tetrahydro-1,4-methanonaphthalene-5,8-dione (38 g, 216 mmol, 1 eq). The resulting solution was cooled down to 10 °C and triethylamine (0.38 mL, 2.72 mmol, 0.013 eq) was added. The reaction mixture was stirred for 5 h at 10 °C then was allowed to warm up to room temperature and was stirred for further 15 h. The solvent was removed under vacuum to give the corresponding hydroquinone form, which was suspended in p-benzoquinone (25.9 g, 238 mmol, 1.1 eq) in 590 mL of chloroform. The stirred suspension was heated firstly at 50 °C for 4 h, then at 40 °C for one more hour. The reaction mixture was cooled down to room temperature. The hydroquinone precipitate was filtered off and washed with 30 mL of chloroform. The combined chloroform layers were washed with a 1 % aqueous solution of NaOH, and then dried over $MgSO_4$. The solvent was removed under vacuum to give a yellow oil (36 g, 87 %).

Yellow powder, mp : 62.6 – 64.1; HRMS (ESI) $[M + H]^+$ found 173.0599, calculated 173.0597 for $[C_{11}H_9O_2]^+$; ^{1}H NMR (400 MHz, $CDCl_3$) δ ppm = 6.80 (t, J = 1.8 Hz, 2 H, =C$\mathbf{H_a}$-CH), 6.52 (s, 2 H, =C$\mathbf{H_b}$-CO), 4.04 (t, J = 1.3 Hz, 2 H, C$\mathbf{H_c}$), 2.30 - 2.24 (m, J = 1.5, 1.5, 7.2 Hz, 1 H, C$\mathbf{H_{2d}}$), 2.23 - 2.19 (m, J = 1.5, 1.5, 7.2 Hz, 1 H, CH_2); ^{13}C NMR (101 MHz, $CDCl_3$) δ ppm = 183.7 (**C**$_f$O), 160.4 (**C**$_{IVe}$=**C**$_{IVe}$), 142.3 (CH-**C**$_{IIIa}$=**C**$_{IIIa}$-CH), 135.5 (CO-**C**$_{IIIb}$=**C**$_{IIIb}$-CO), 73.6 (**C**$_d$H$_2$), 48.1 (**C**$_c$H)

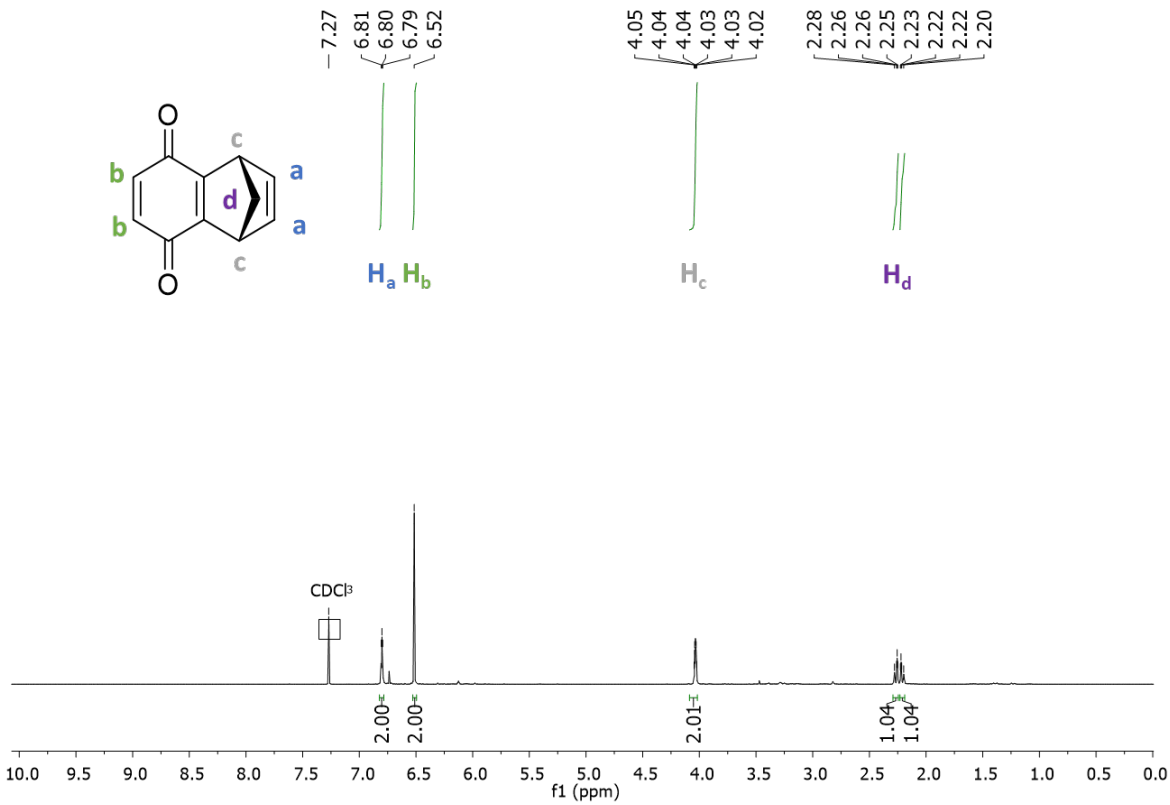

*Figure S18: [1]H NMR spectrum of compound **BC-3***

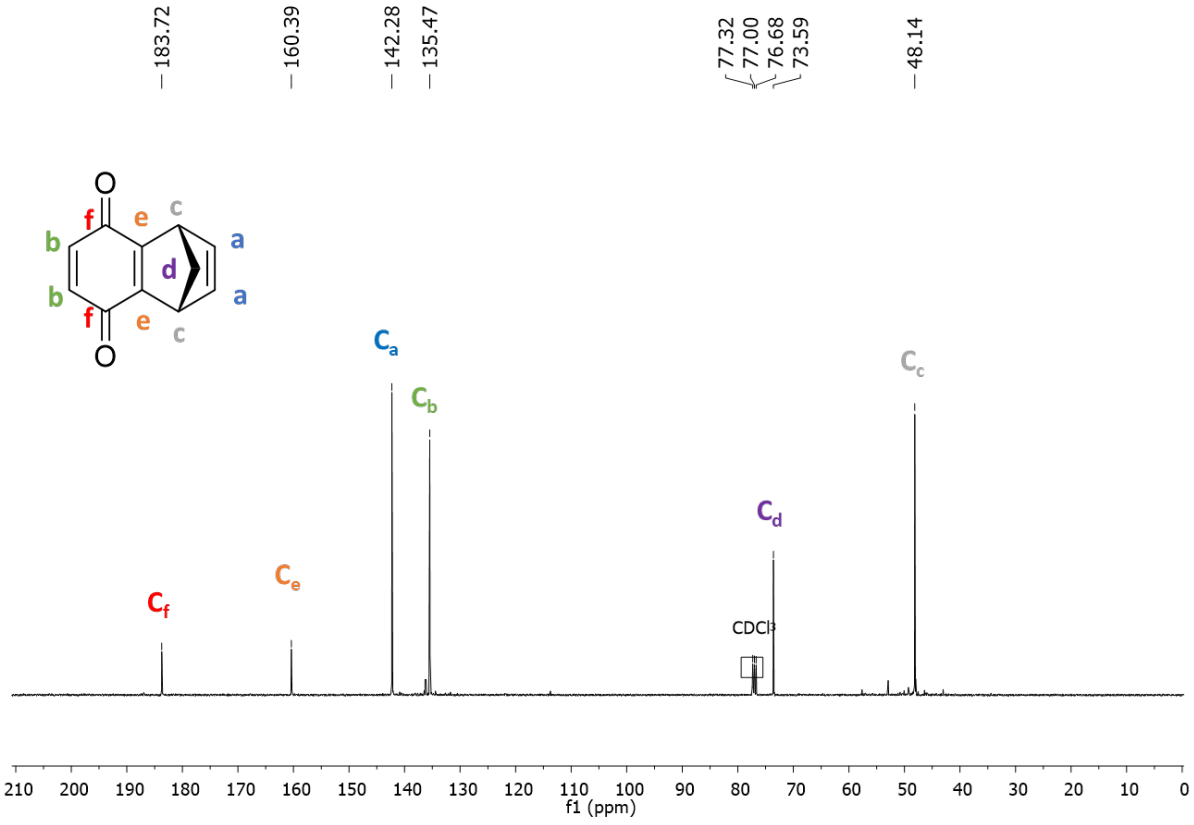

*Figure S19: [13]C NMR spectrum of compound **BC-3***

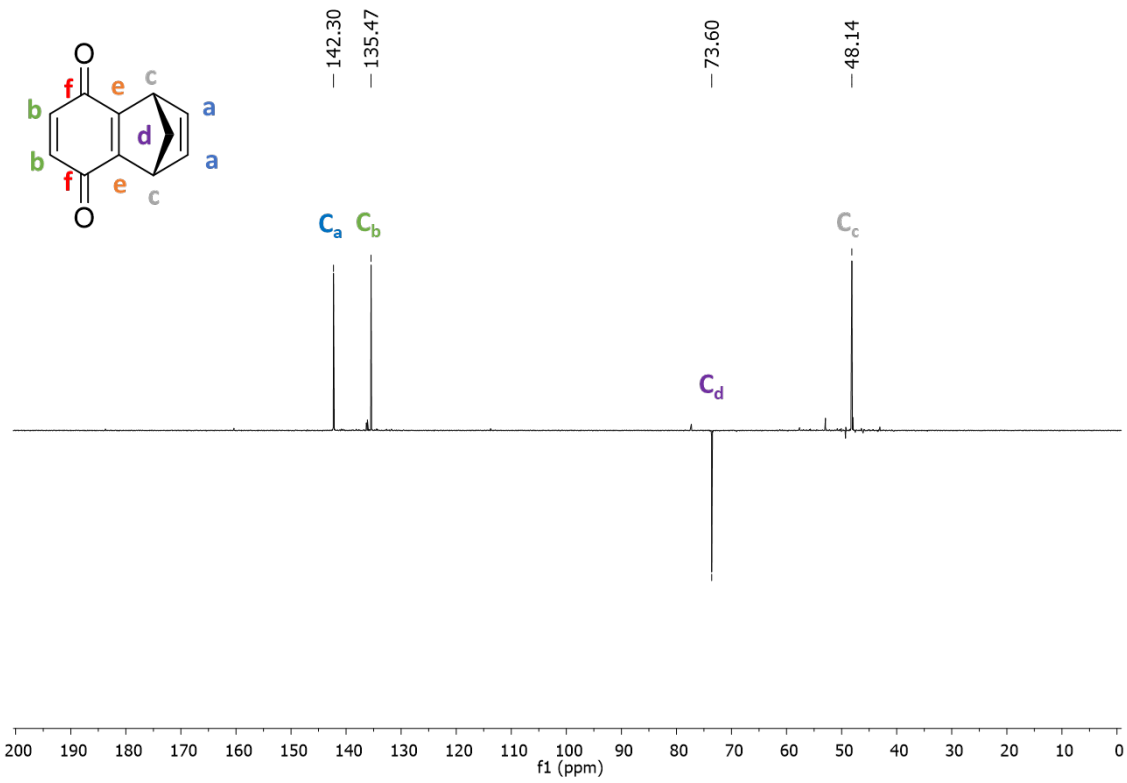

*Figure S20: DEPT ^{13}C NMR spectrum of compound **BC-3***

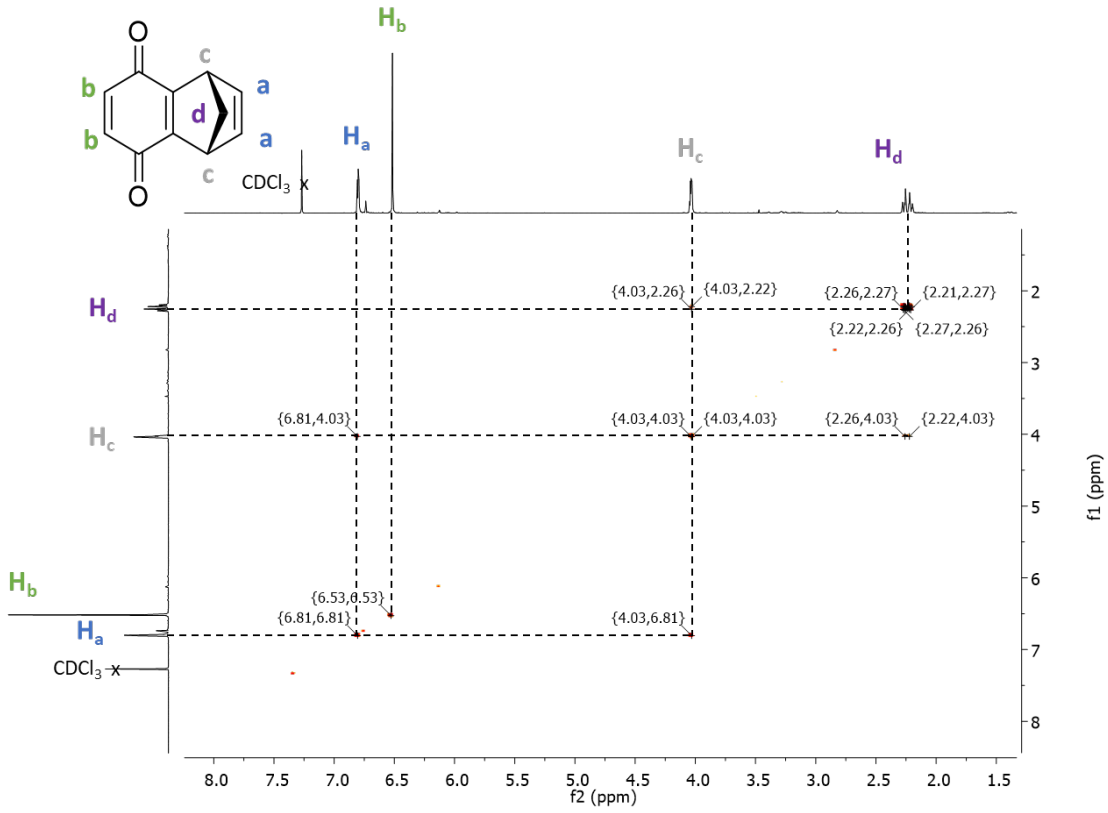

*Figure S21: COSY NMR spectrum of compound **BC-3***

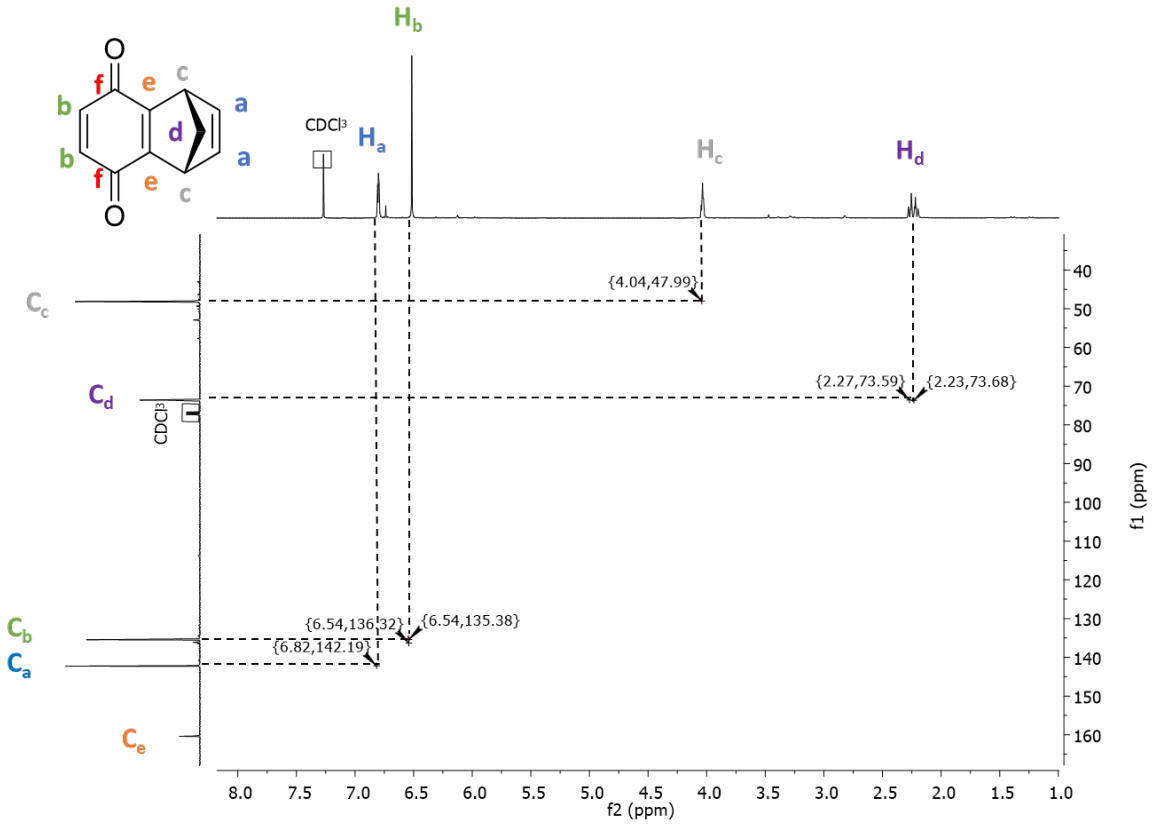

Figure S22: HSQC NMR spectrum of compound ***BC-3***

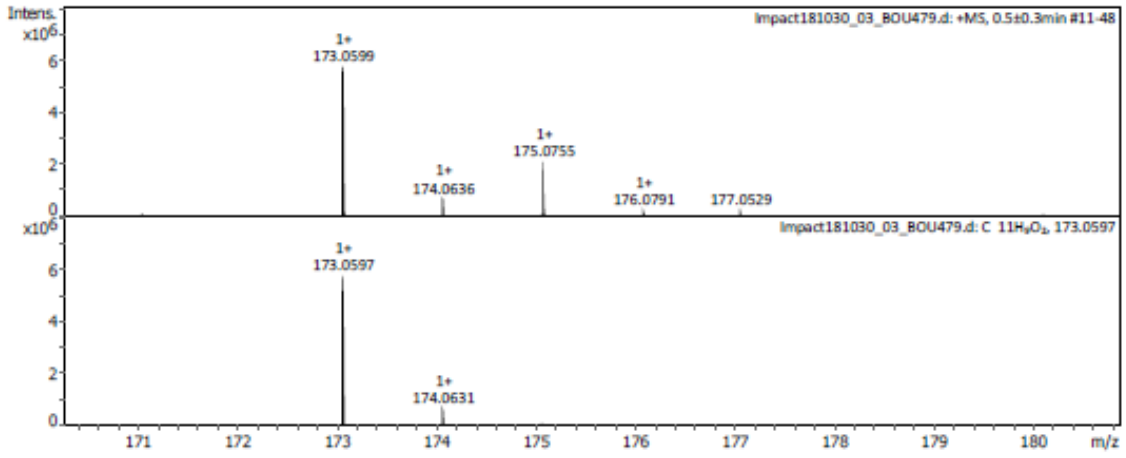

Meas. m/z	Ion Formula	m/z	Sum Formula	err [ppm]	mSigma	Adduct	z
173.0599	C11H9O2	173.0597	C11H8O2	-0.9	204.0	M+H	1+
195.0420	C11H8NaO2	195.0417		-1.9	603.5	M+Na	1+
345.1126	C22H17O4	345.1121		-1.3	17.5	2M+H	1+
367.0946	C22H16NaO4	367.0941		-1.5	39.1	2M+Na	1+

Figure S23: HRMS spectrum of compound ***BC-3***

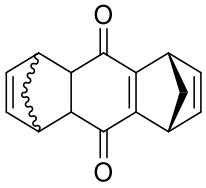

BC-4 (1R,4S,5R,8S)-1,4,4a,5,8,9a-hexahydro-1,4:5,8-dimethanoanthracene-9,10-dione

A solution of **BC-3** (1R,4S)-1,4-dihydro-1,4-methanonaphthalene-5,8-dione (37 g, 0, 189 mmol, 1 eq) in MeOH (280 mL) was maintained at -78°C and freshly distilled cyclopentadiene (16 mL, 189 mmol, 1 eq) was added at once. The stirred orange solution was allowed to warm up overnight. The solvent was removed under vacuum and the resulting yellow solid was recrystallised in ethanol, and then purified by column chromatography (SiO_2, pentane : ethyl acetate = 8:2) to give a yellow powder (21,109 g, 44 %). The diastereoisomeric mixture **BC-4** was separated into pure diastereoisomers **B-4** and **C-4** through semi-preparative chiral HPLC (Lux-Amylose-2 (250 x 10 mm), hexane : EtOH 80 : 20)

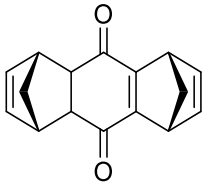

B-4 (1R,4S,5R,8S)-1,4,4a,5,8,9a-hexahydro-1,4:5,8-dimethanoanthracene-9,10-dione

Yellow powder (3.4 g, 22 %), mp : 152.8 – 155.3; HRMS (ESI) $[M + H]^+$ found 261.0890, calculated 261.0886 for $[C_{16}H_{14}NaO_2]^+$; ^1H NMR (400 MHz, $CDCl_3$) δ ppm = 6.77 (t, J = 2.0 Hz, 2 H, $\mathbf{H_a}C=C\mathbf{H_a}$, side of the central double bond), 6.04 - 5.98 (m, 2 H, $\mathbf{H_b}C=C\mathbf{H_b}$, opposite side of the central double bond), 3.92 (t, J = 2.0 Hz, 2 H, =CH-C$\mathbf{H_c}$, side of the central double bond), 3.51 - 3.31 (m, 2 H, =CH-C$\mathbf{H_d}$, opposite side of the central double bond), 3.15 (t, J = 2.2 Hz, 2 H, C$\mathbf{H_e}$-C$\mathbf{H_e}$), 2.18 (td, J = 1.5, 7.1 Hz, 1 H, C$\mathbf{H_{2f}}$, side of the central double bond), 2.03 (td, J = 1.5, 7.1 Hz, 1 H, C$\mathbf{H_{2f}}$, side of the central double bond), 1.53 (td, J = 1.7, 8.6 Hz, 1 H, C$\mathbf{H_{2g}}$, opposite side to the central double bond), 1.41 (td, J = 1.7, 8.6 Hz, 1 H, C$\mathbf{H_{2g}}$, opposite side of the central double bond); ^{13}C NMR (101 MHz, $CDCl_3$) δ ppm = 195.2 (CO), 166.7 (C_{IV}=C_{IV}), 142.2 (CH-$\mathbf{C}_{III}$=$\mathbf{C}_{III}$-CH), 134.6 (CO-$\mathbf{C}_{III}$=$\mathbf{C}_{III}$-CO), 73.5 (CH_2), 51.0 (**C**H-CO), 49.3 (**C**H-CO), 48.6 (CH), 48.2 (CH)

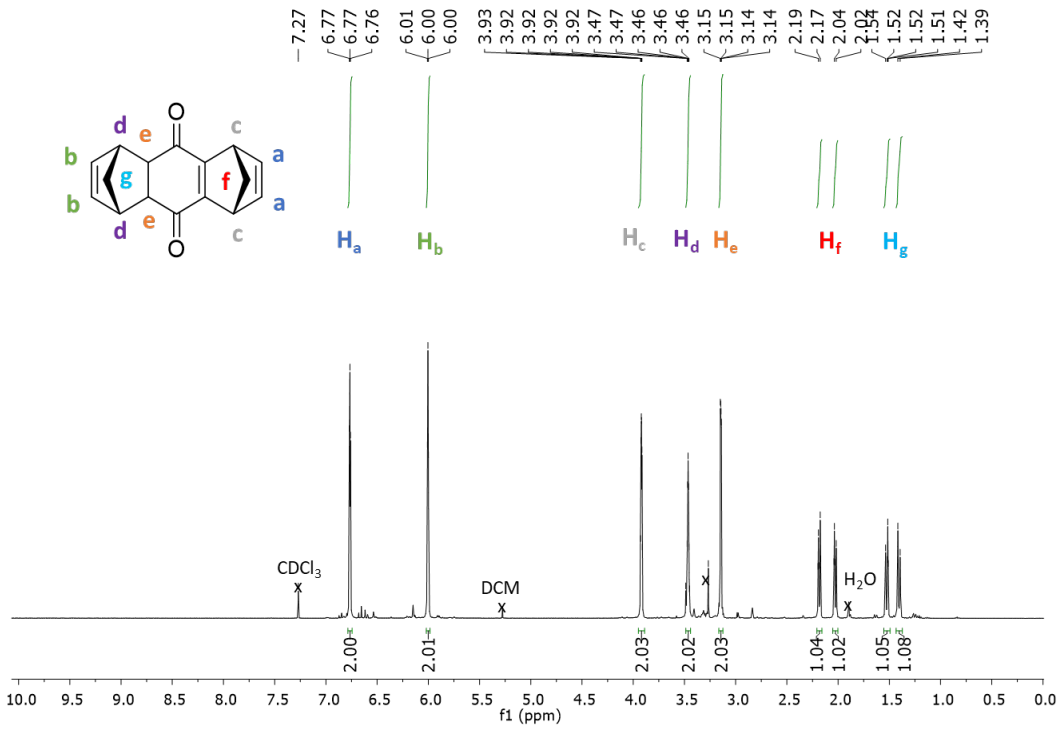

*Figure S24: ^{1}H NMR spectrum of compound **B-4***

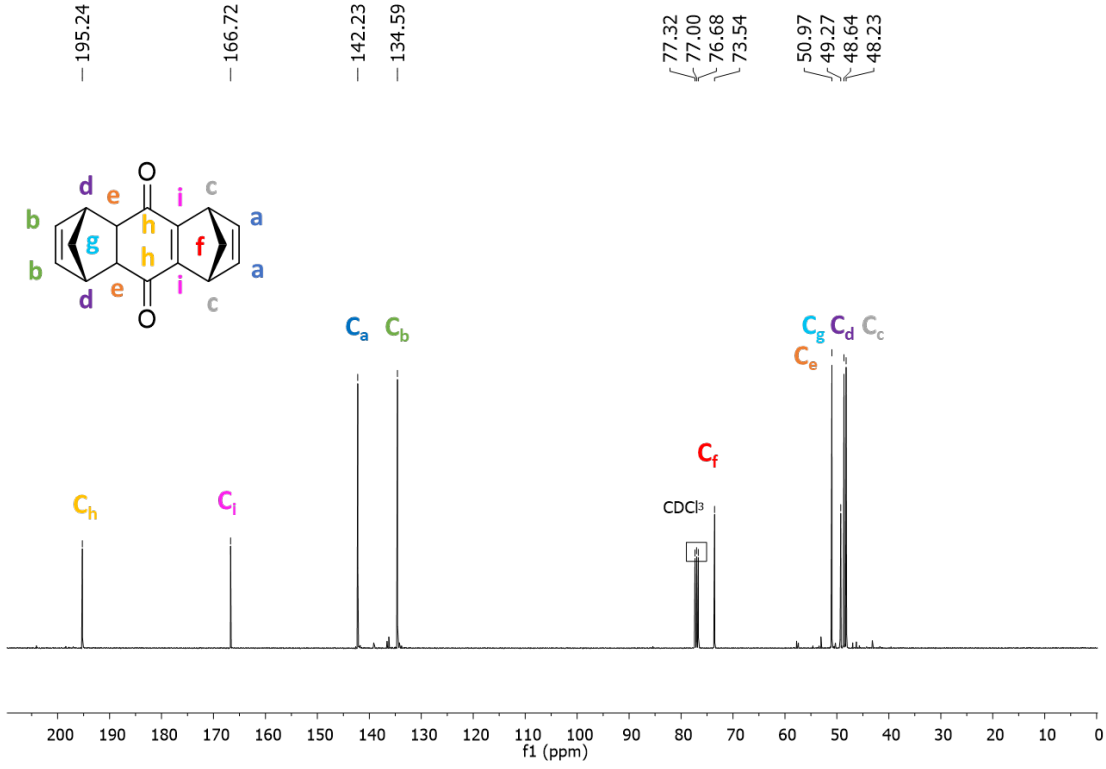

*Figure S25: ^{13}C NMR spectrum of compound **B-4***

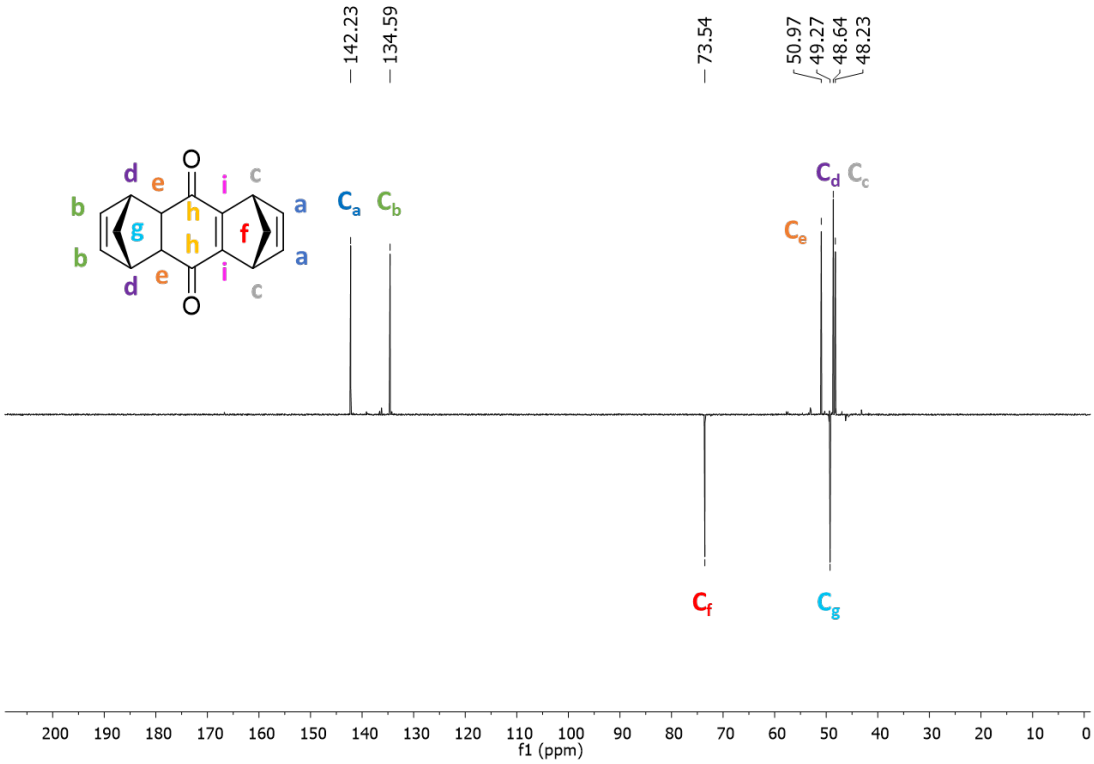

Figure S26: DEPT ^{13}C NMR spectrum of compound ***B-4***

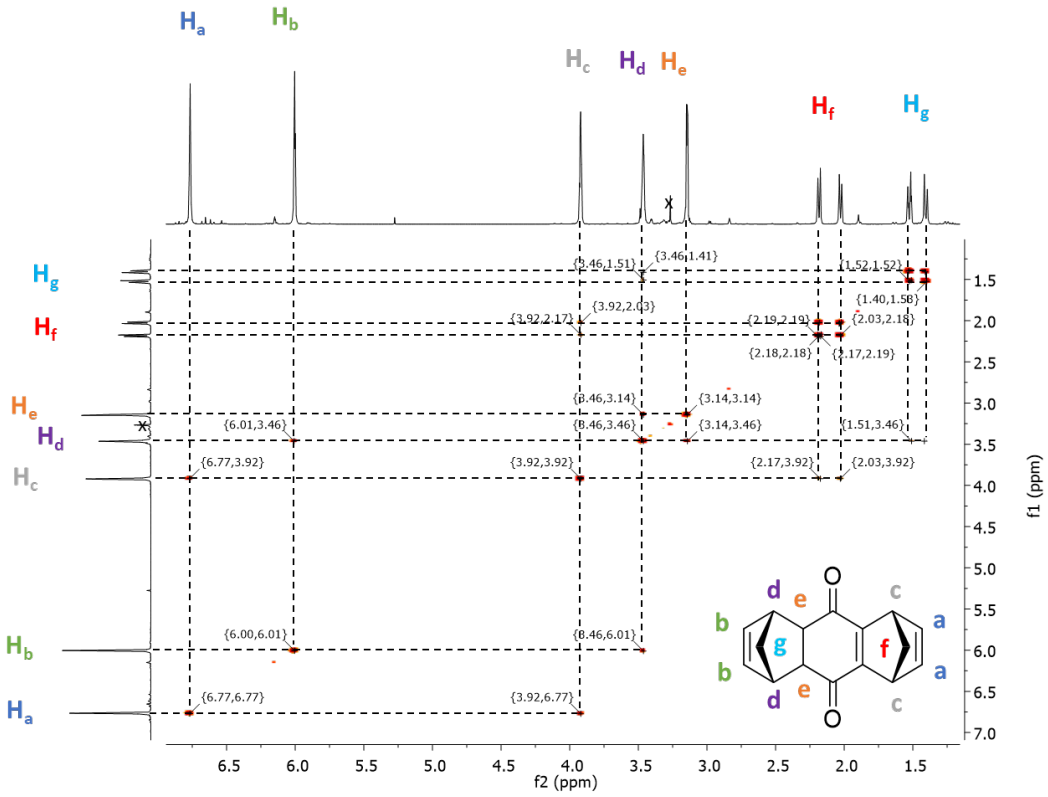

Figure S27: COSY ^{1}H NMR spectrum of compound ***B-4***

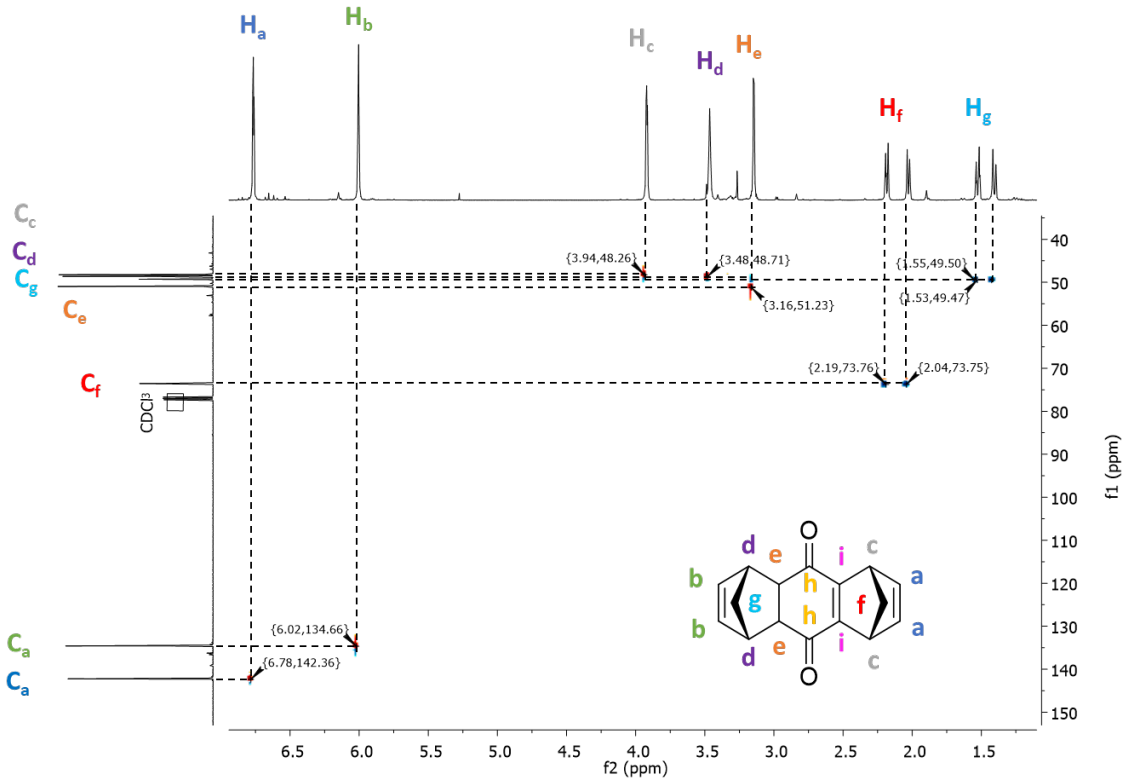

Figure S28: HSQC NMR spectrum of compound ***B-4***

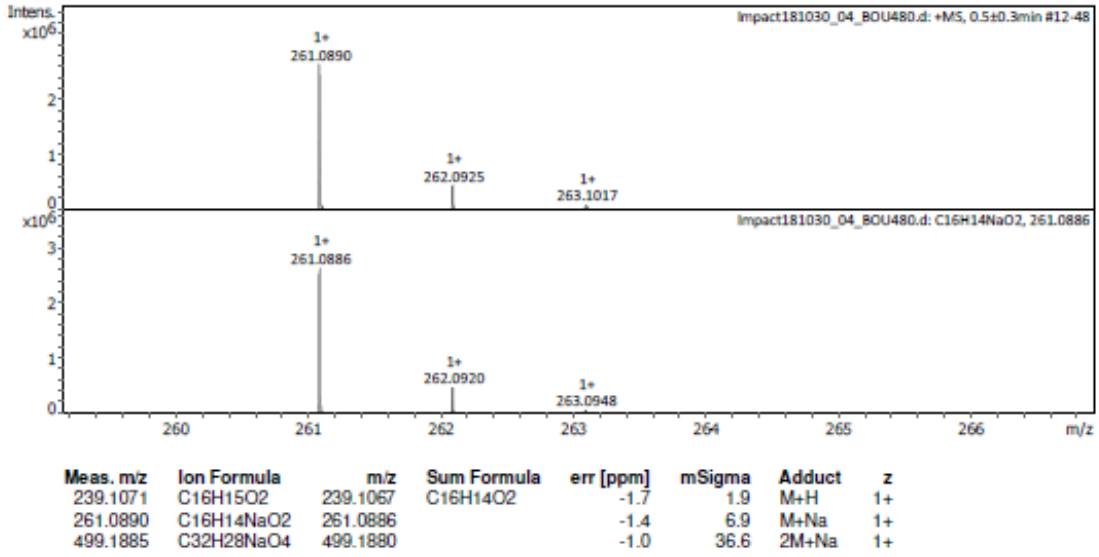

Meas. m/z	Ion Formula	m/z	Sum Formula	err [ppm]	mSigma	Adduct	z
239.1071	C16H15O2	239.1067	C16H14O2	-1.7	1.9	M+H	1+
261.0890	C16H14NaO2	261.0886		-1.4	6.9	M+Na	1+
499.1885	C32H28NaO4	499.1880		-1.0	36.6	2M+Na	1+

Figure S29: HRMS spectrum of compound ***B-4***

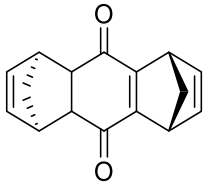

C-4 (1R,4S,5S,8R)-1,4,4a,5,8,9a-hexahydro-1,4:5,8-dimethanoanthracene-9,10-dione

Yellow powder, mp (22 %): 148.3 – 150.1; HRMS (ESI) $[M + H]^+$ found 261.0890, calculated 261.0886 for $[C_{16}H_{14}NaO_2]^+$; ^{1}H NMR (400 MHz, $CDCl_3$) δ ppm = 6.76 (t, J = 1.7 Hz, 2 H, $\mathbf{H_a}C{=}C\mathbf{H_a}$, side of the central double bond), 5.77 (t, J = 1.8 Hz, 2 H, $\mathbf{H_b}C{=}C\mathbf{H_b}$, opposite side of the central double bond), 3.96 (t, J = 1.5 Hz, 2 H, =CH-C$\mathbf{H_c}$, side of the central double bond), 3.51 - 3.38 (m, 2 H, =CH-C$\mathbf{H_d}$, opposite side of the central double bond), 3.29 - 3.16 (m, 2 H, C$\mathbf{H_e}$-C$\mathbf{H_e}$), 2.20 (m, 1 H, C$\mathbf{H_{2f}}$, side of the central double bond), 2.12 (m, 1 H, C$\mathbf{H_{2f}}$, side of the central double bond), 1.47 (m, 1 H, C$\mathbf{H_{2g}}$, opposite side to the central double bond), 1.39 (m, 1 H, C$\mathbf{H_{2g}}$, opposite side of the central double bond); ^{13}C NMR (101 MHz, $CDCl_3$) δ ppm = 195.6 (**C**$_h$O), 166.9 (**C**$_{IVi}$=**C**$_{IVi}$), 142.7 (CH-**C**$_{IIIa}$=**C**$_{IIIa}$-CH), 134.5 (CH-**C**$_{IIIb}$=**C**$_{IIIb}$-CH), 72.4 (**C**$_f$H$_2$), 50.6 (**C**H-CO), 48.8 (**C**$_g$H$_2$), 48.4 (**C**$_d$H-CH), 48.3 (**C**$_e$H-CH)

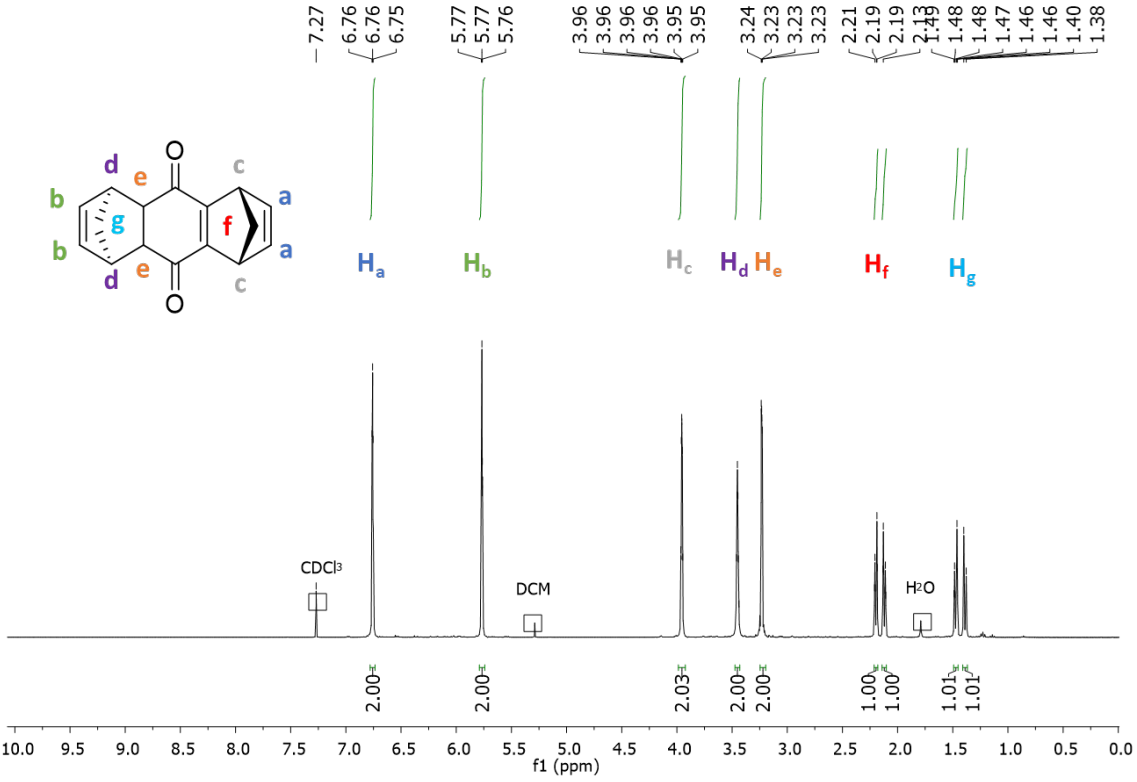

Figure S30: ^{1}H NMR spectrum of compound C-4

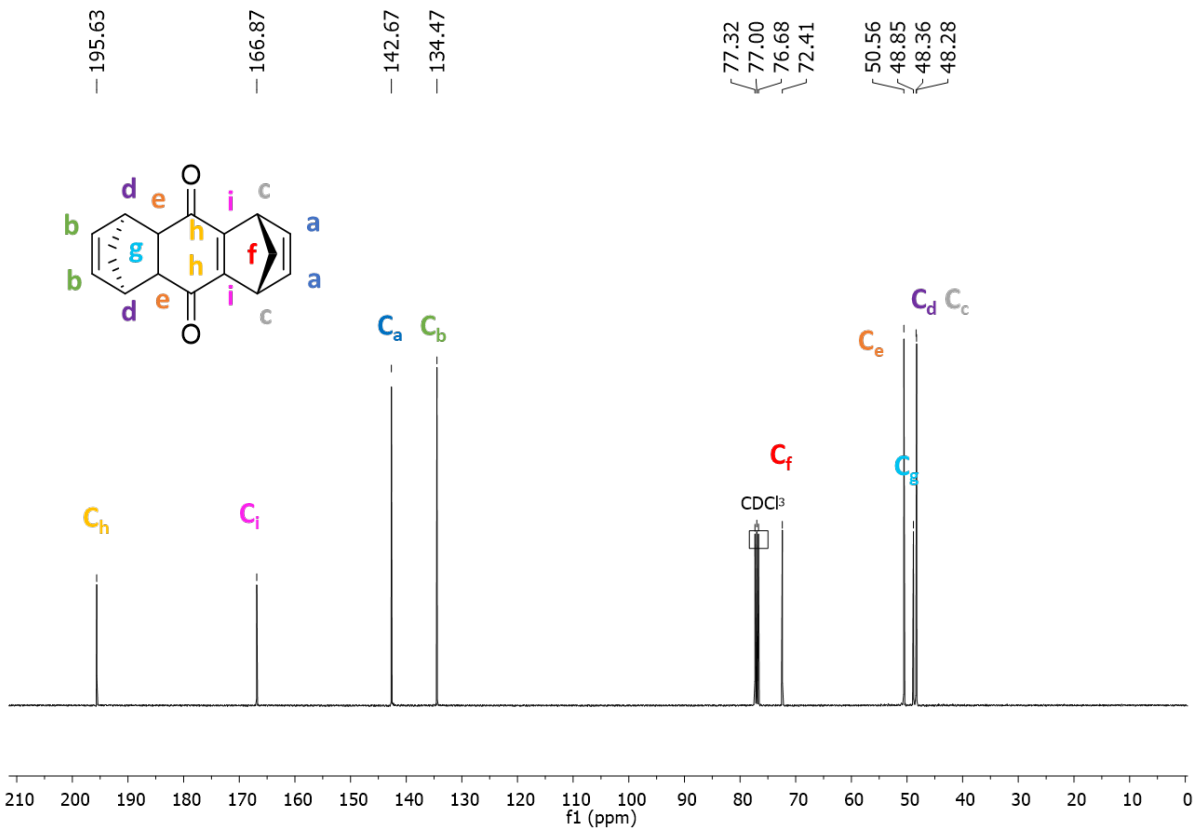

*Figure S31: ^{13}C NMR spectrum of compound **C-4***

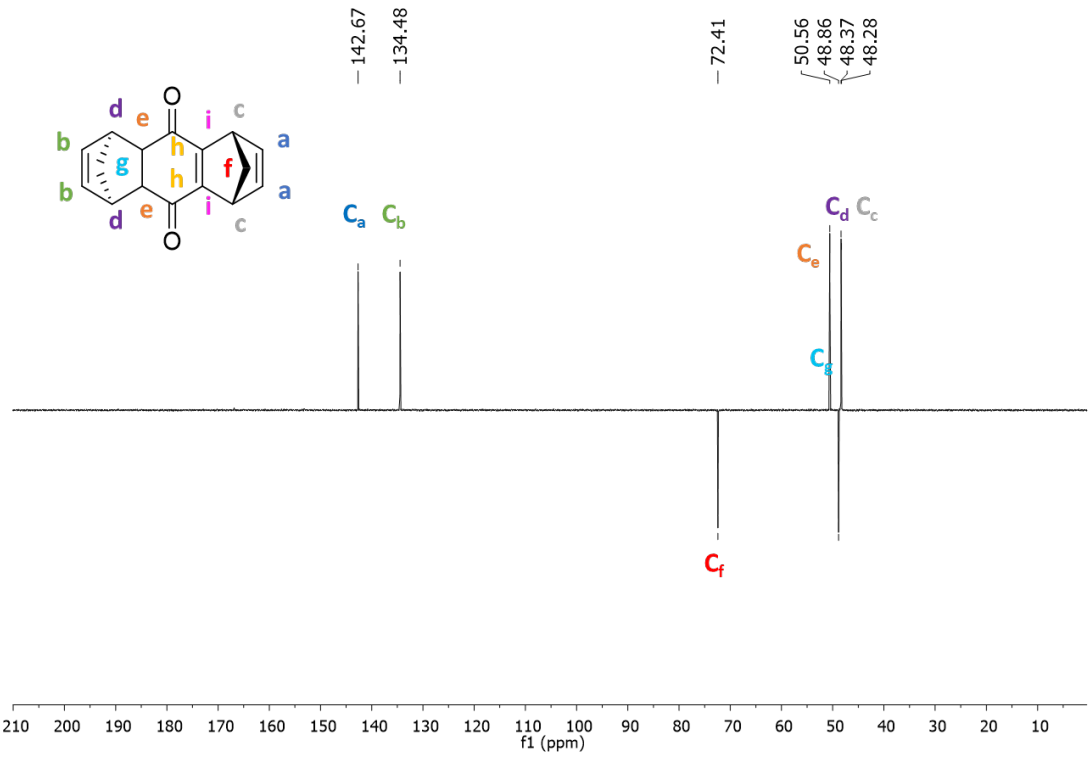

*Figure S32: DEPT ^{13}C NMR spectrum of compound **C-4***

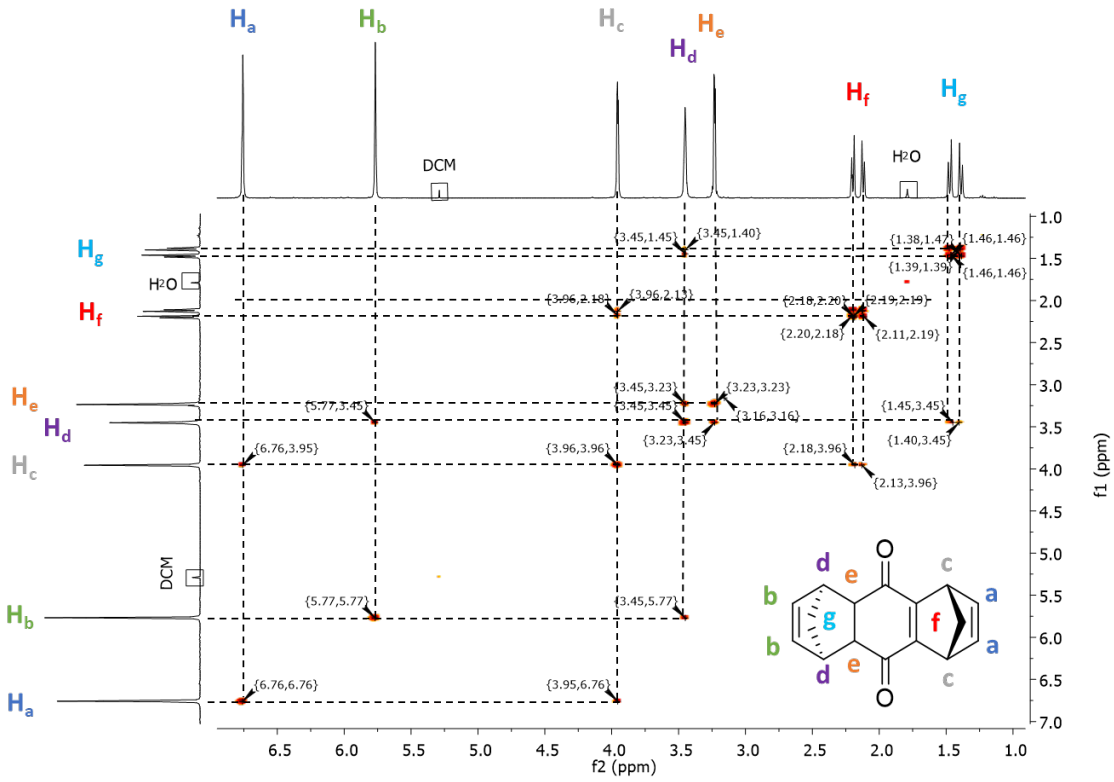

Figure S33: COSY NMR spectrum of compound ***C-4***

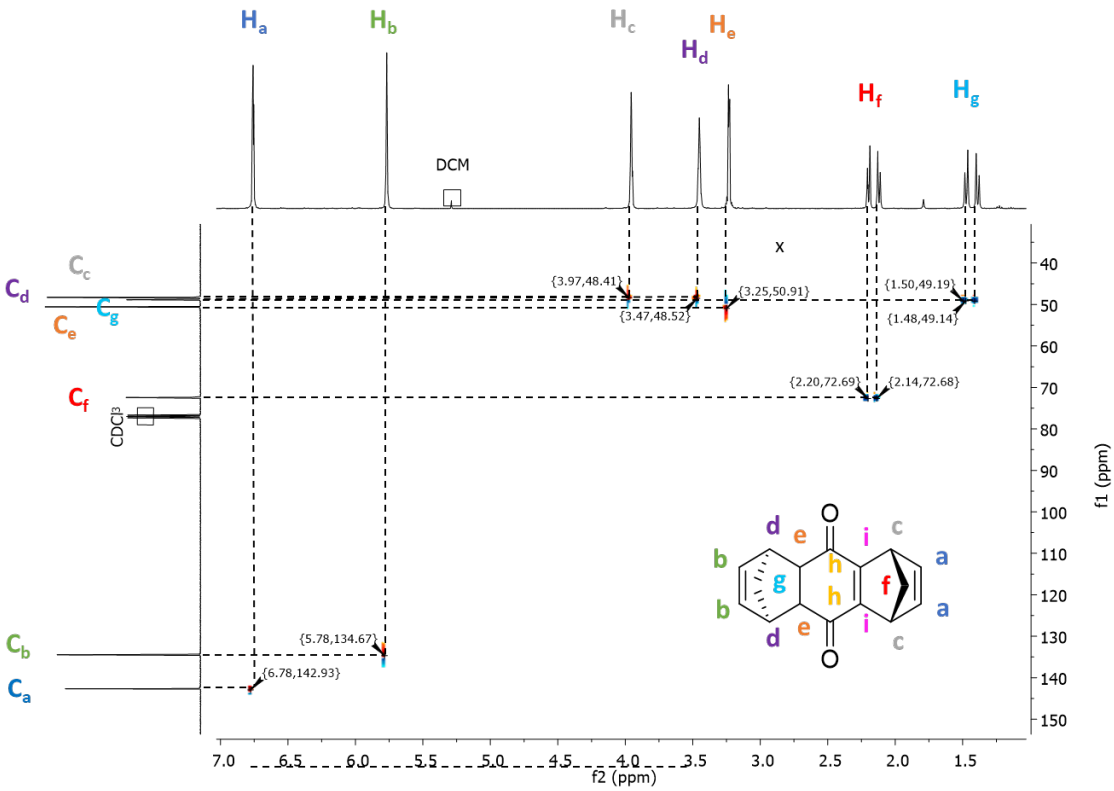

Figure S34: HSQC NMR spectrum of compound ***C-4***

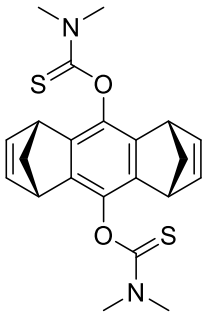

B-5 O,O'-((1R,4S,5R,8S)-1,4,5,8-tetrahydro-1,4:5,8-dimethanoanthracene-9,10-diyl) bis(dimethylcarbamothioate)

To a solution of **B-4** (1R,4S,5R,8S)-1,4,4a,5,8,9a-hexahydro-1,4:5,8-dimethanoanthracene-9,10-dione (3,400 g, 14.3 mmol, 1 eq) and NaH (1,06 g, 42.1 mmol, 4 eq) in dimethylformamide (30 mL) was added at 0°C dimethylthiocarbamoyl chloride (7.023 g, 42.1 mmol, 4 eq) in 13 mL of dry N, N-dimethylacetamide. The mixture was stirred at room temperature for 24 h. The precipitate was then filtrated and washed extensively with water. Drying of the resulting solid gave a brown powder (5.843 g, 99 %).

Brown powder, mp: degradation, 260.1 °C; HRMS (ESI) $[M + H]^+$ found 413.1351, calculated 413.1352 for $[C_{22}H_{25}N_2O_2S_2]^+$; ^{1}H NMR (400 MHz, $CDCl_3$) δ ppm = 6.78 (t, J = 1.5 Hz, 4 H, $\mathbf{H_a}C{=}C\mathbf{H_a}$), 3.82 (t, J = 1.7 Hz, 4 H, $C\mathbf{H_b}$), 3.49 (s, 6 H, $C\mathbf{H_{3c}}$), 3.38 (s, 6 H, $C\mathbf{H_{3d}}$), 2.33 (td, J = 1.6, 6.8 Hz, 2 H, $C\mathbf{H_{2e}}$), 2.21 (td, J = 1.5, 7.1 Hz, 2 H, $C\mathbf{H_{2e}}$); ^{13}C NMR (101 MHz, $CDCl_3$) δ ppm = 187.6 ($\mathbf{C_f}S$), 142.7 ($H\mathbf{C_a}{=}\mathbf{C_a}H$), 140.6 ($\mathbf{C_{ArIVg}}$-O), 69.5 ($\mathbf{C_e}H_2$), 47.5 ($\mathbf{C_c}H$), 43.2 ($\mathbf{C_b}H_3$), 38.5 ($\mathbf{C_d}H_3$)

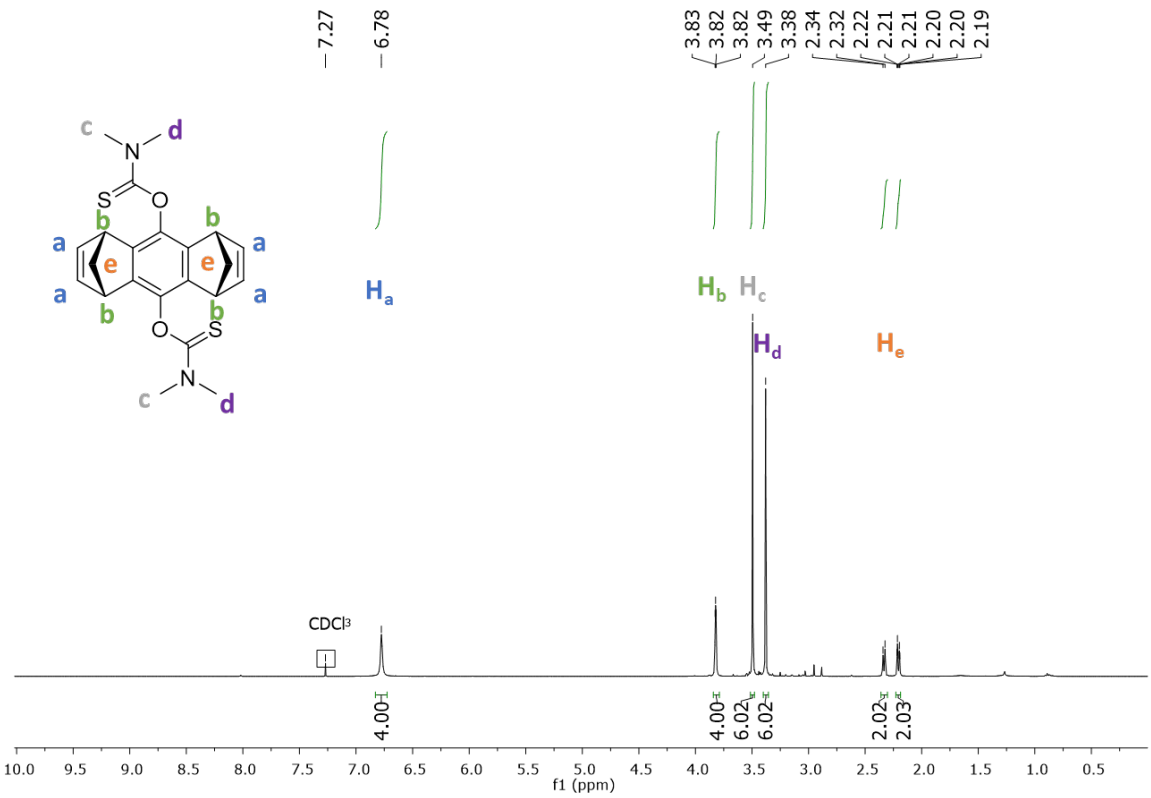

*Figure S35: ^{1}H NMR spectrum of compound **B-5***

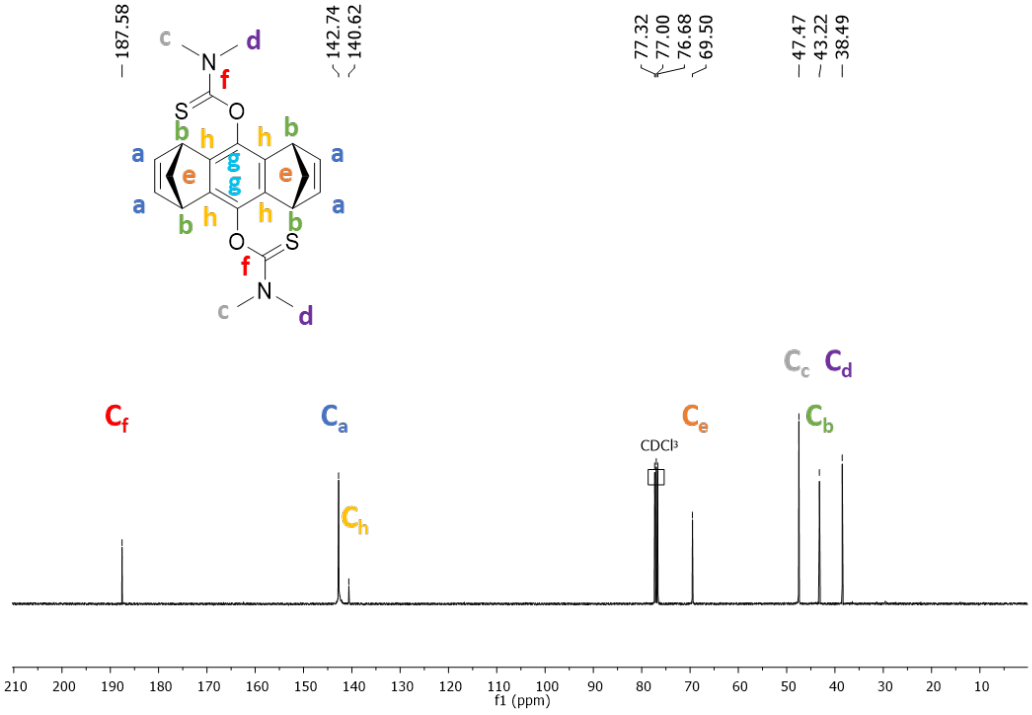

*Figure S36: ^{13}C NMR spectrum of compound **B-5***

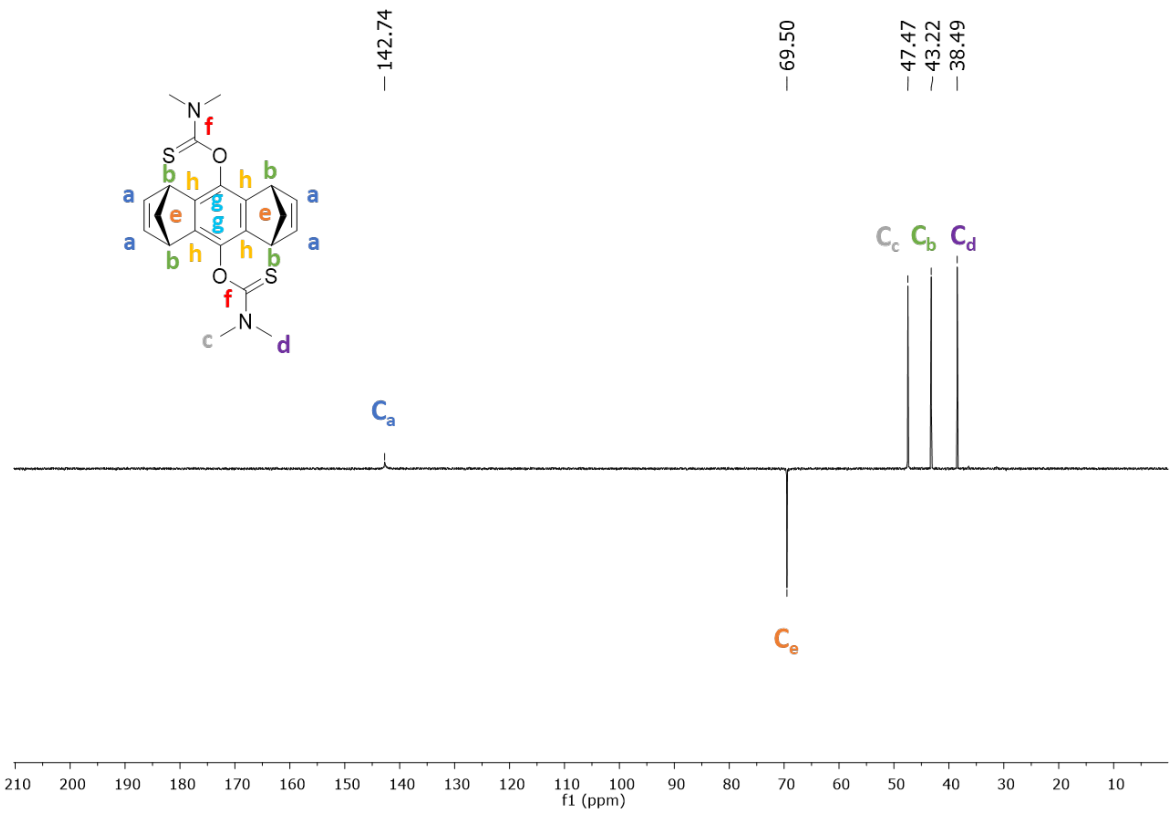

Figure S37: DEPT ^{13}C NMR spectrum of compound ***B-5***

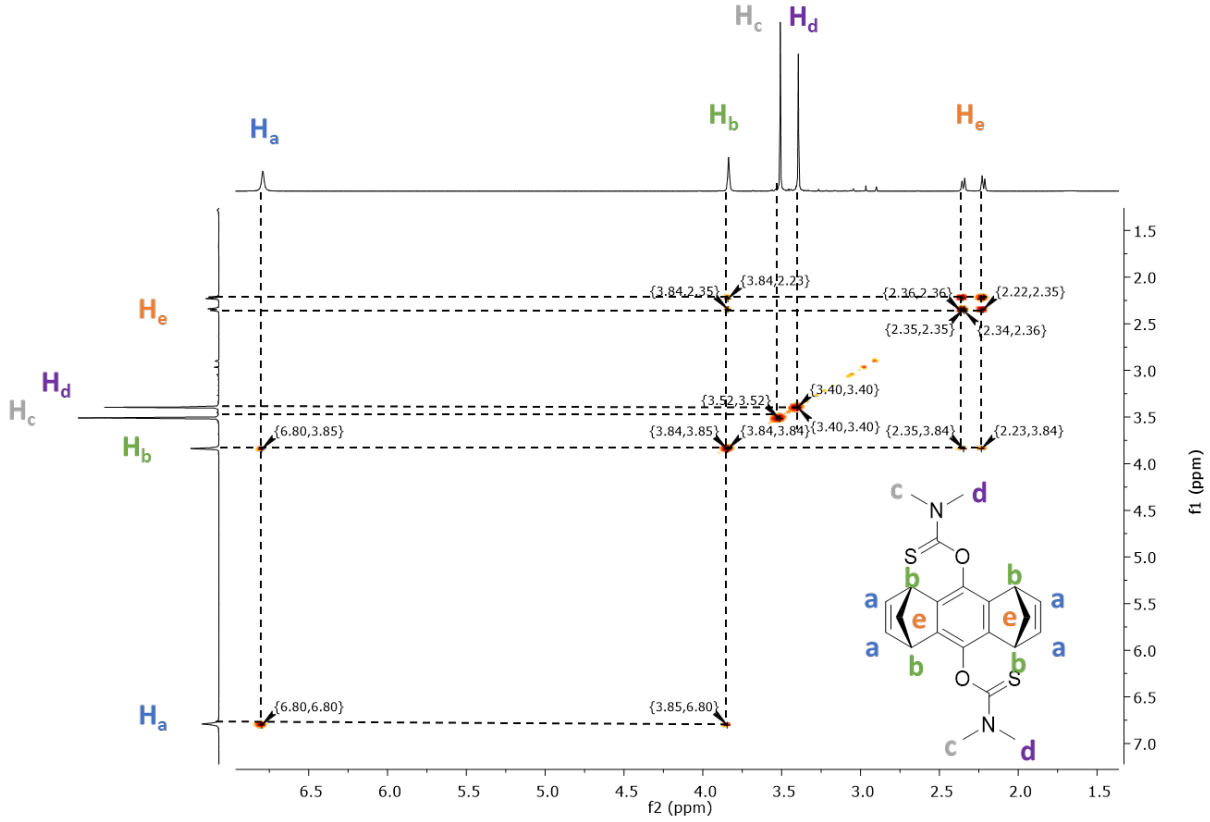

Figure S38: COSY NMR spectrum of compound ***B-5***

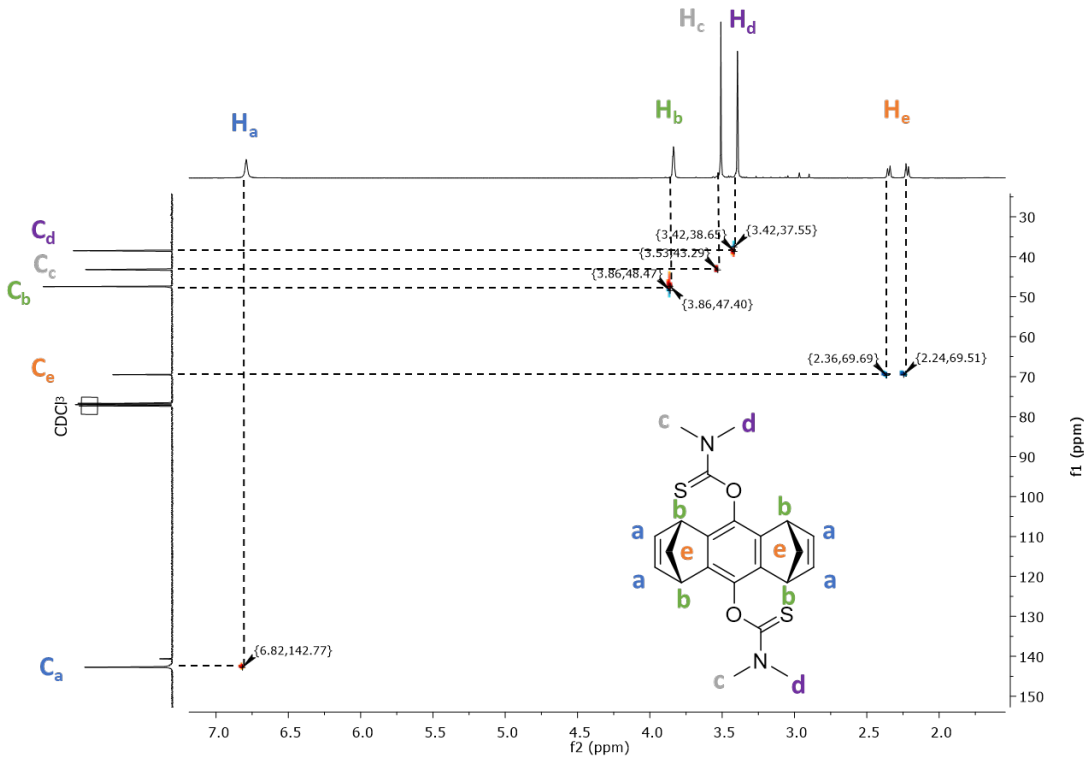

Figure S39: HSQC NMR spectrum of compound ***B-5***

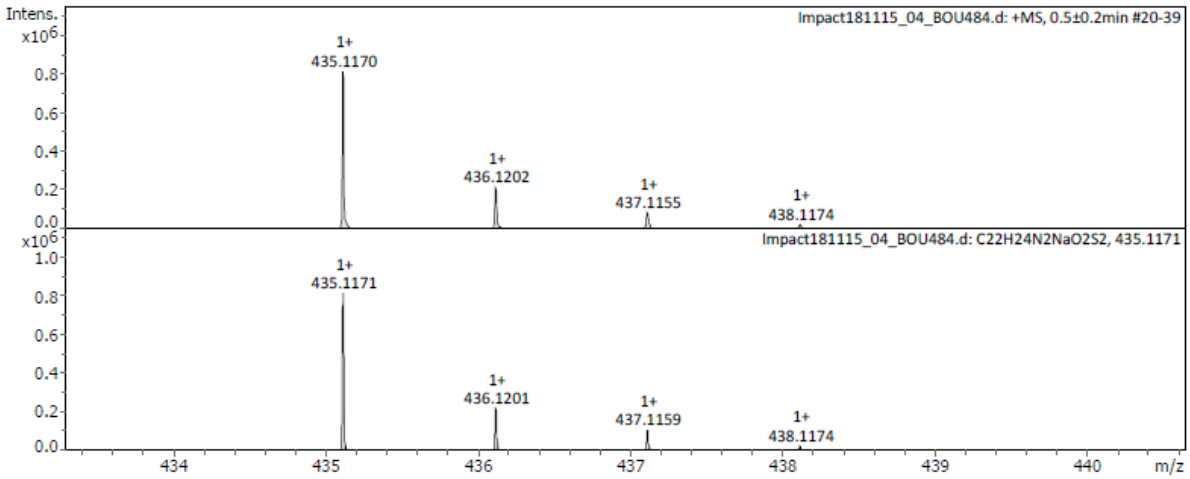

Meas. m/z	Ion Formula	m/z	Sum Formula	err [ppm]	mSigma	Adduct	z
413.1351	C22H25N2O2S2	413.1352	C22H24N2O2S2	0.1	15.9	M+H	1+
435.1170	C22H24N2NaO2S2	435.1171		0.4	13.2	M+Na	1+

Figure S40: HRMS spectrum of compound ***B-5***

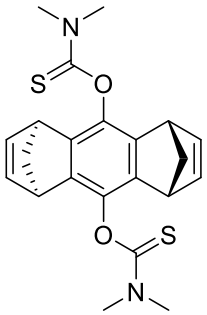

C-5 O,O'-((1R,4S,5S,8R)-1,4,5,8-tetrahydro-1,4:5,8-dimethanoanthracene-9,10-diyl) bis(dimethylcarbamothioate)

To a solution of **C-4** (1R,4S,5S,8R)-1,4,4a,5,8,9a-hexahydro-1,4:5,8-dimethanoanthracene-9,10-dione (4,50 g, 18.9 mmol, 1 eq) and NaH (1,822 g, 75.9 mmol, 4 eq) in dimethylformamide (39 mL) was added at 0°C dimethylthiocarbamoyl chloride (9.34 g, 75.9 mmol, 4 eq) in 16 mL of dry N, N-dimethylacetamide. The mixture was stirred at room temperature for 24 h. The precipitate was then filtrated and washed extensively with water. Drying of the resulting solid gave a brown powder (7.78 g, 98 %).

Brown powder, mp: degradation, 273.4 °C; HRMS (ESI) $[M + H]^+$ found 413.1351, calculated 413.1352 for $[C_{22}H_{25}N_2O_2S_2]^+$; ^{1}H NMR (400 MHz , $CDCl_3$) δ ppm = 6.94 - 6.76 (m, 4 H, $\mathbf{H_a}C{=}C\mathbf{H_a}$), 3.88 - 3.77 (m, 4 H, $C\mathbf{H_b}$), 3.52 (s, 6 H, $C\mathbf{H_{3c}}$), 3.38 (s, 6 H, $C\mathbf{H_{3d}}$), 2.29 (td, J = 1.6, 6.8 Hz, 2 H, $C\mathbf{H_{2e}}$), 2.19 (td, J = 1.7, 7.1 Hz, 2 H, $C\mathbf{H_{2e}}$); ^{13}C NMR (101MHz, $CDCl_3$) δ ppm = 187.7 ($\mathbf{C_f}S$), 142.8 ($\mathbf{C_{ArIVg}}$-O), 140.6 ($H\mathbf{C_a}{=}\mathbf{C_a}H$), 69.4 ($\mathbf{C_e}H_2$), 47.5 ($\mathbf{C_c}H$), 43.3 ($\mathbf{C_b}H_3$), 38.5 ($\mathbf{C_d}H_3$)

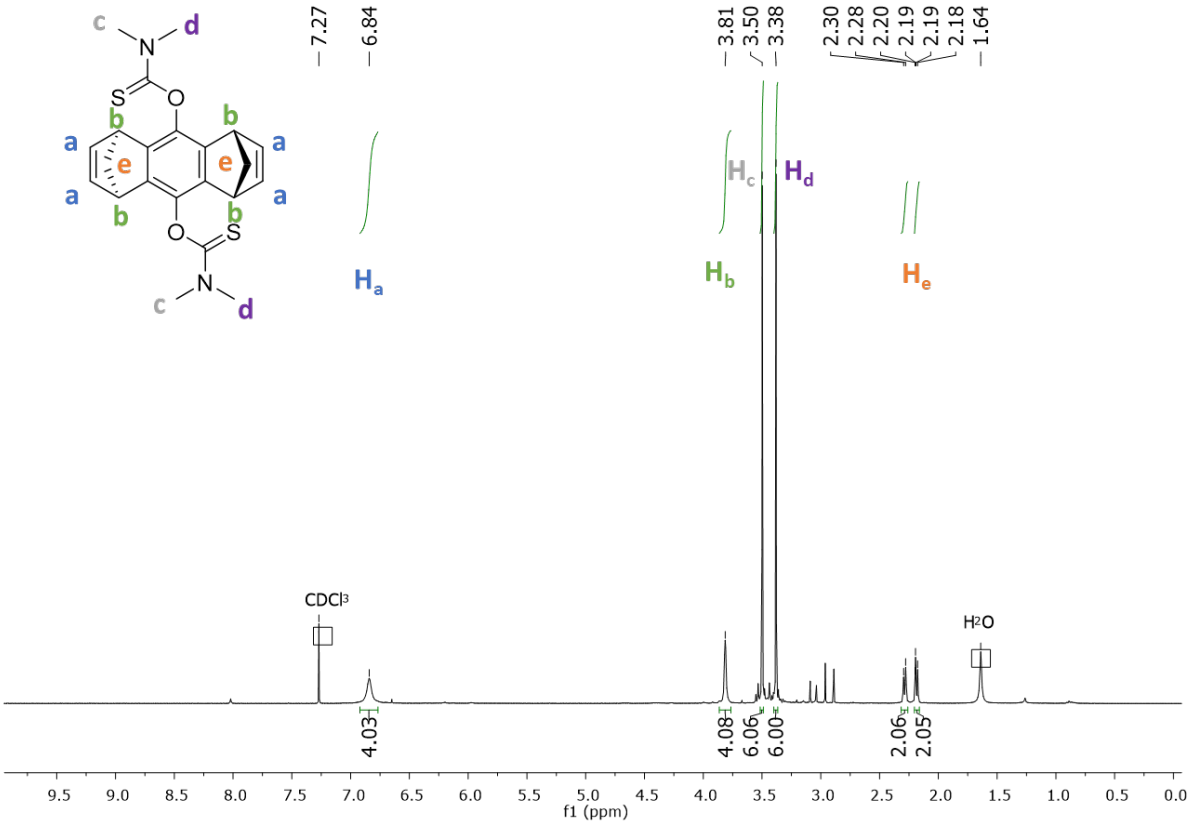

*Figure S41: ^{1}H NMR spectrum of compound **C-5***

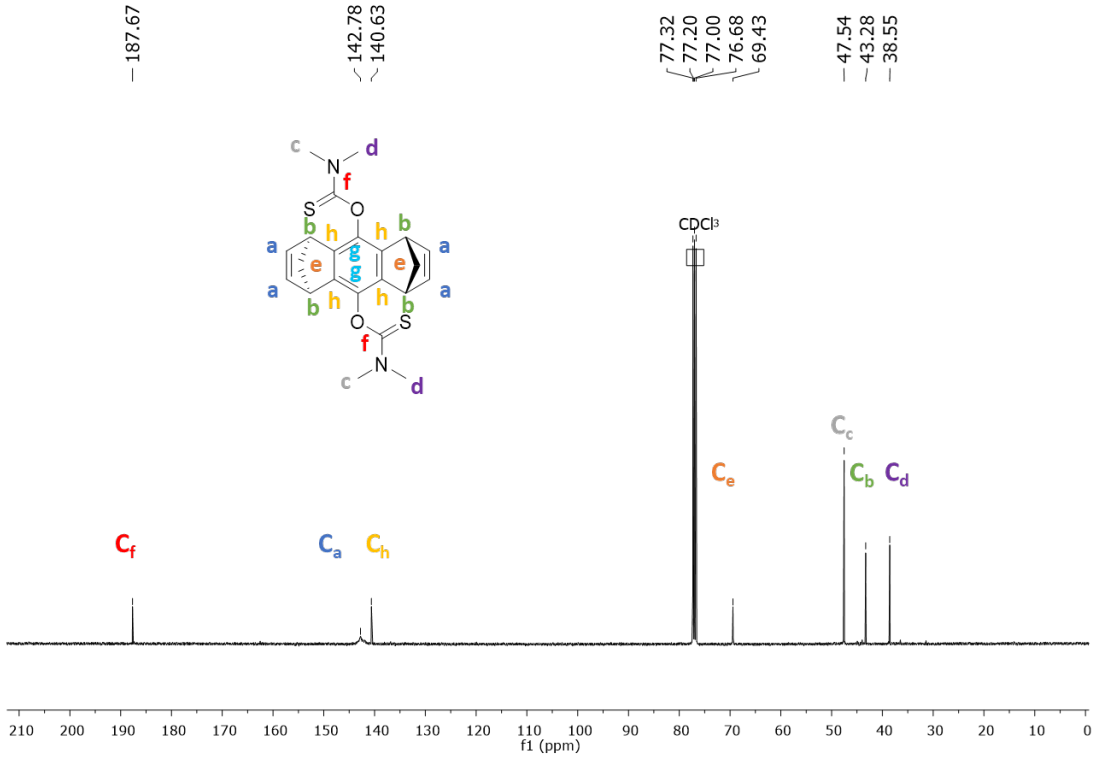

*Figure S42: ^{13}C NMR spectrum of compound **C-5***

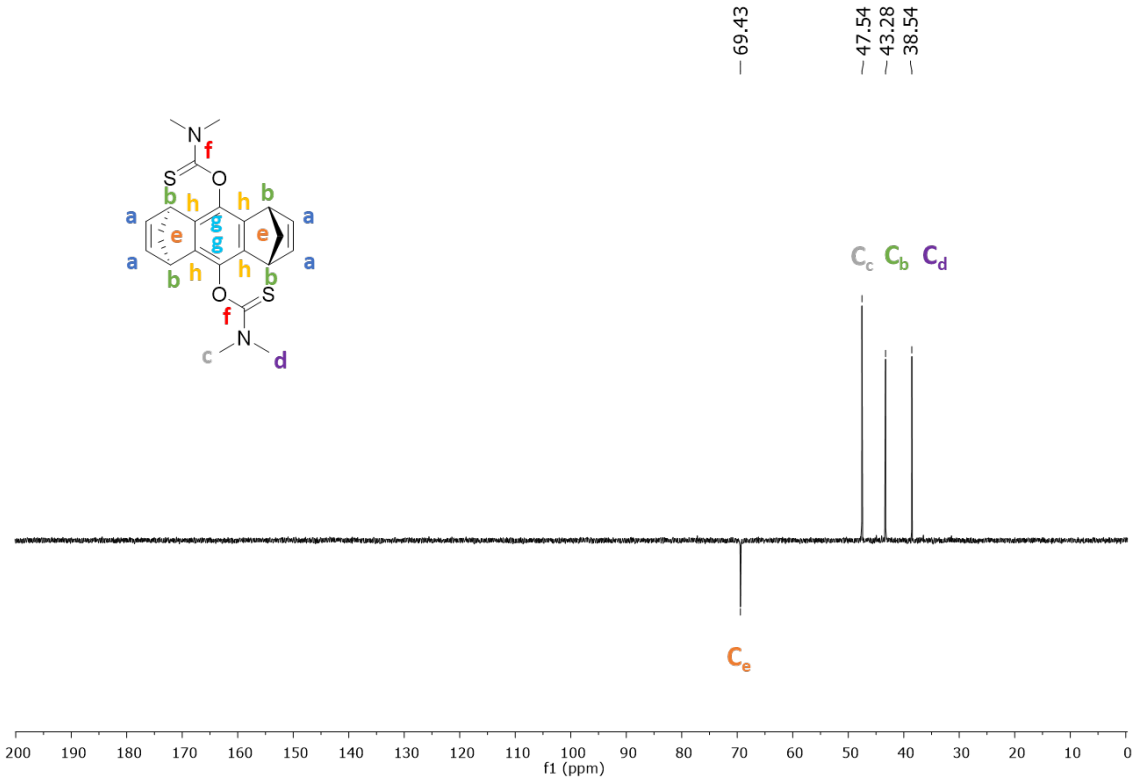

Figure S43: DEPT ^{13}C NMR spectrum of compound ***C-5***

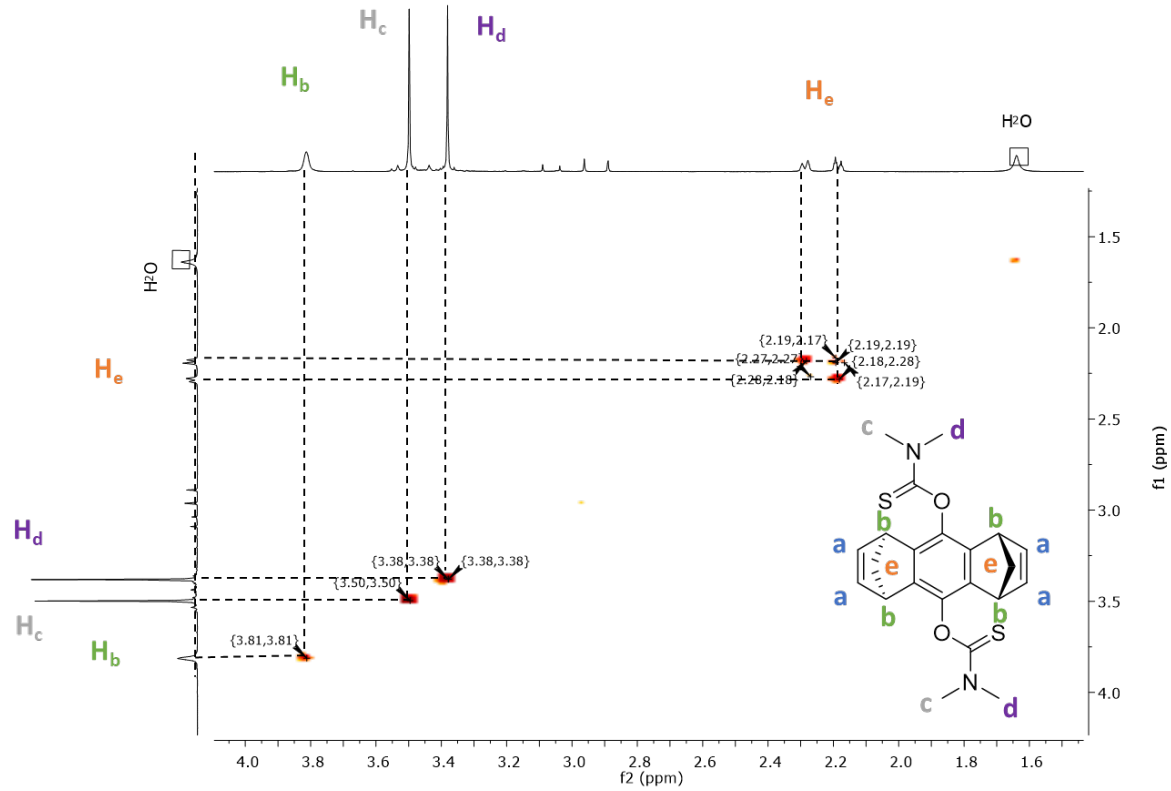

Figure S44: COSY NMR spectrum of compound ***C-5***

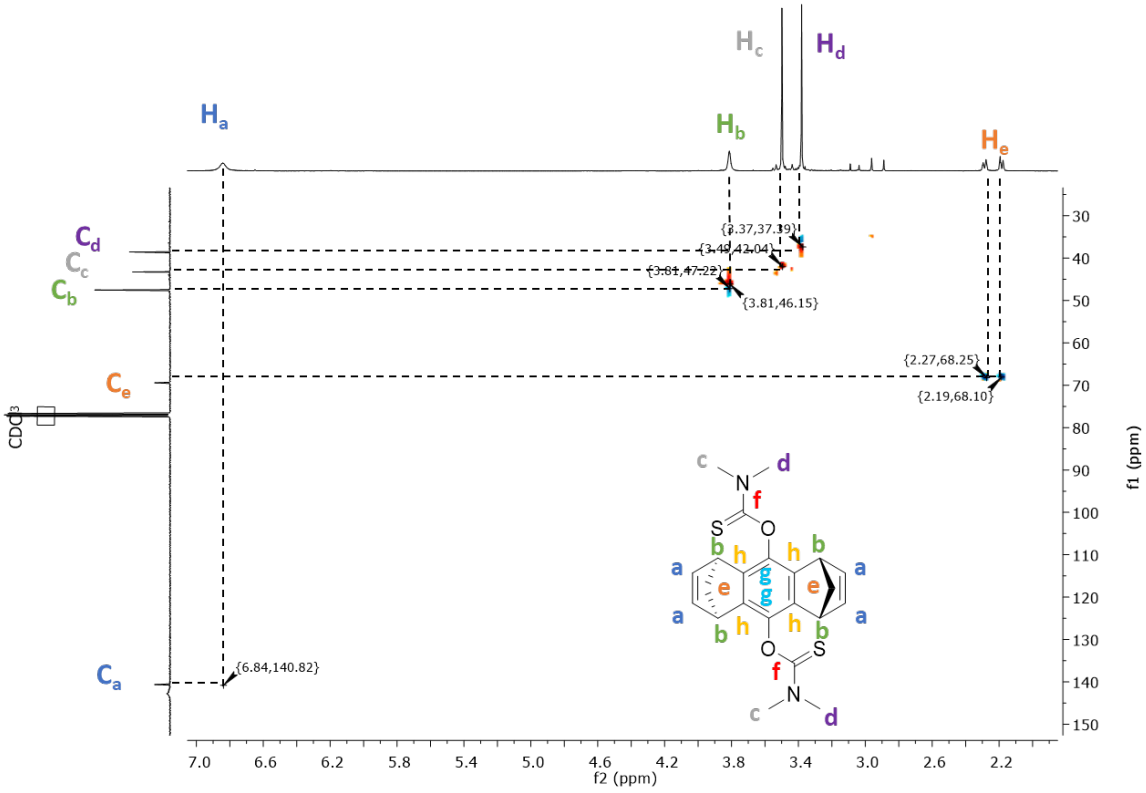

Figure S45: HSQC NMR spectrum of compound ***C-5***

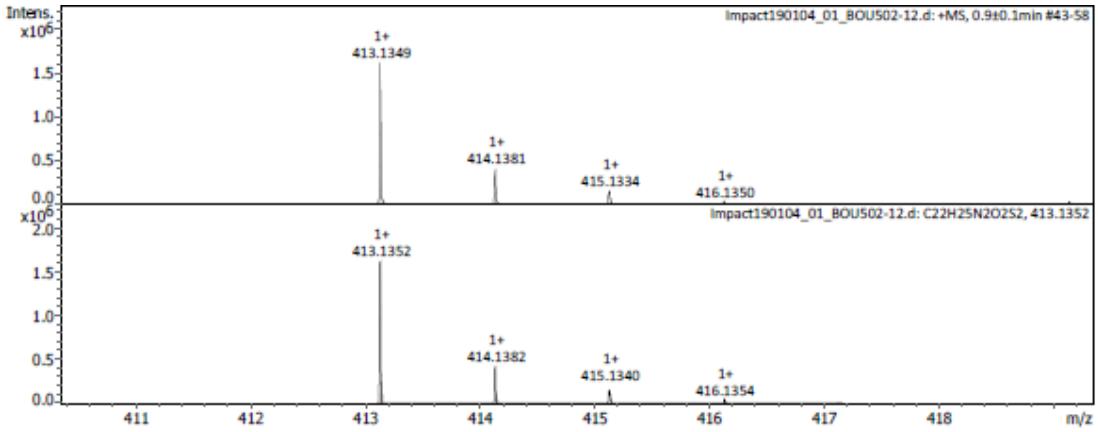

Meas. m/z	Ion Formula	m/z	Sum Formula	err [ppm]	mSigma	Adduct	z
413.1349	C22H25N2O2S2	413.1352	C22H24N2O2S2	0.7	17.0	M+H	1+
435.1170	C22H24N2NaO2S2	435.1171		0.3	14.8	M+Na	1+

Figure S46 : HRMS spectrum of compound ***C-5***

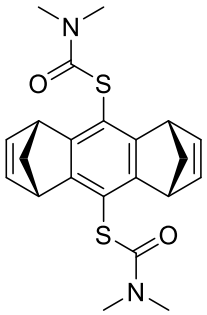

B-6 S,S'-((1R,4S,5R,8S)-1,4,5,8-tetrahydro-1,4:5,8-dimethanoanthracene-9,10-diyl) bis(dimethylcarbamothioate)

A solution of **B-5** O,O'-((1R,4S,5R,8S)-1,4,5,8-tetrahydro-1,4:5,8-dimethanoanthracene-9,10-diyl) bis(dimethylcarbamothioate) (357 mg, 0.87 mmol, 1 eq) in diphenyl ether (3 mL) was heated at 230 °C for 4 h. The mixture was then cooled to room temperature. The resulting mixture was purified by column chromatography (SiO_2, pentane : ethyl acetate = 1:0 -> 1:1 -> 0:1) to give a yellow powder (175 mg, 49 %).

Yellow powder, mp: 226.3 - 228.1 °C; HRMS (ESI) $[M + H]^+$ found 413.1351, calculated 413.1352 for $[C_{22}H_{25}N_2O_2S_2]^+$; ^{1}H NMR (400 MHz, $CDCl_3$) δ ppm = 6.78 (t, J = 1.7 Hz, 4 H, $\mathbf{H_a}C{=}C\mathbf{H_a}$), 4.02 (t, J = 1.5 Hz, 4 H, $C\mathbf{H_b}$), 3.19 - 2.99 (m, 12 H, $C\mathbf{H_{3cd}}$), 2.35 (m, 2 H, $C\mathbf{H_{2e}}$), 2.24 (m, 2 H, $C\mathbf{H_{2e}}$); ^{13}C NMR (101 MHz, $CDCl_3$) δ ppm = 165.7 ($\mathbf{C_f}O$), 154.1 ($\mathbf{C}_{Ar,IV\mathbf{h}}$), 143.2 ($H\mathbf{C}{=}\mathbf{C_a}H$), 118.0 ($\mathbf{C}_{Ar\mathbf{fg}}$-S), 69.6 ($\mathbf{C_e}H_2$), 50.5 ($\mathbf{C_b}H$), 36.9 ($\mathbf{C_{cd}}H_3$)

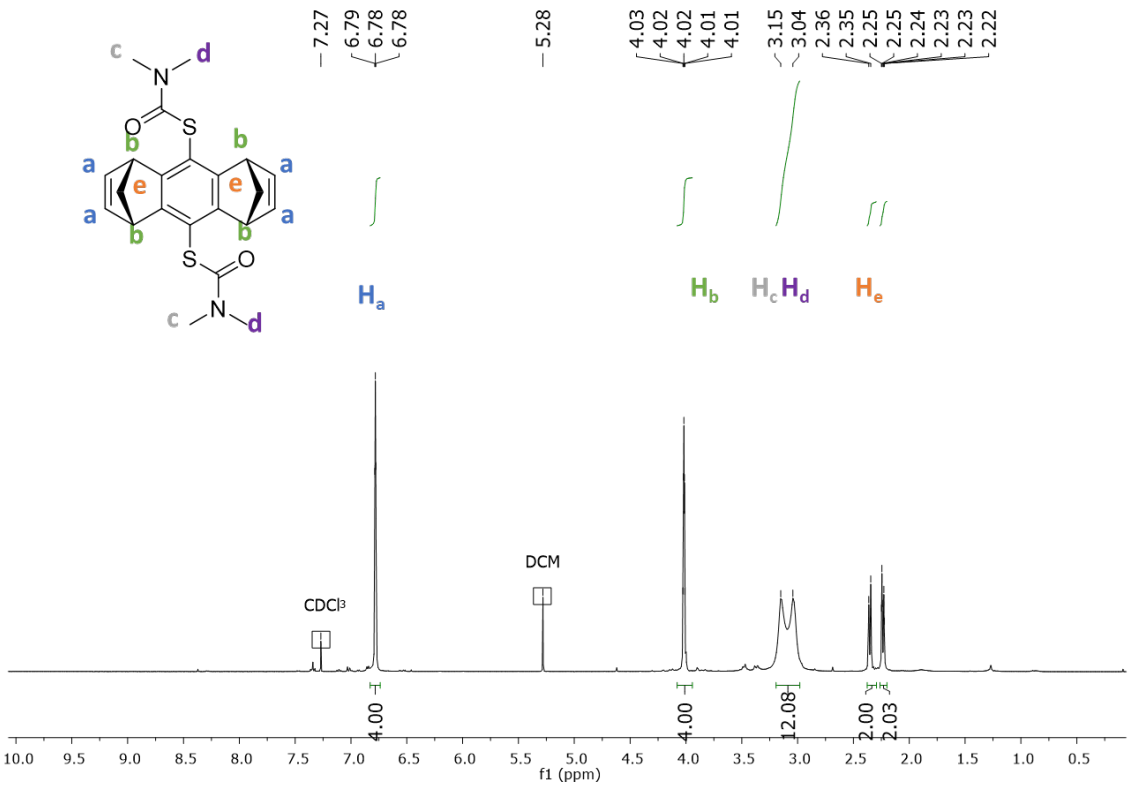

*Figure S47: ^{1}H NMR spectrum of compound **B-6***

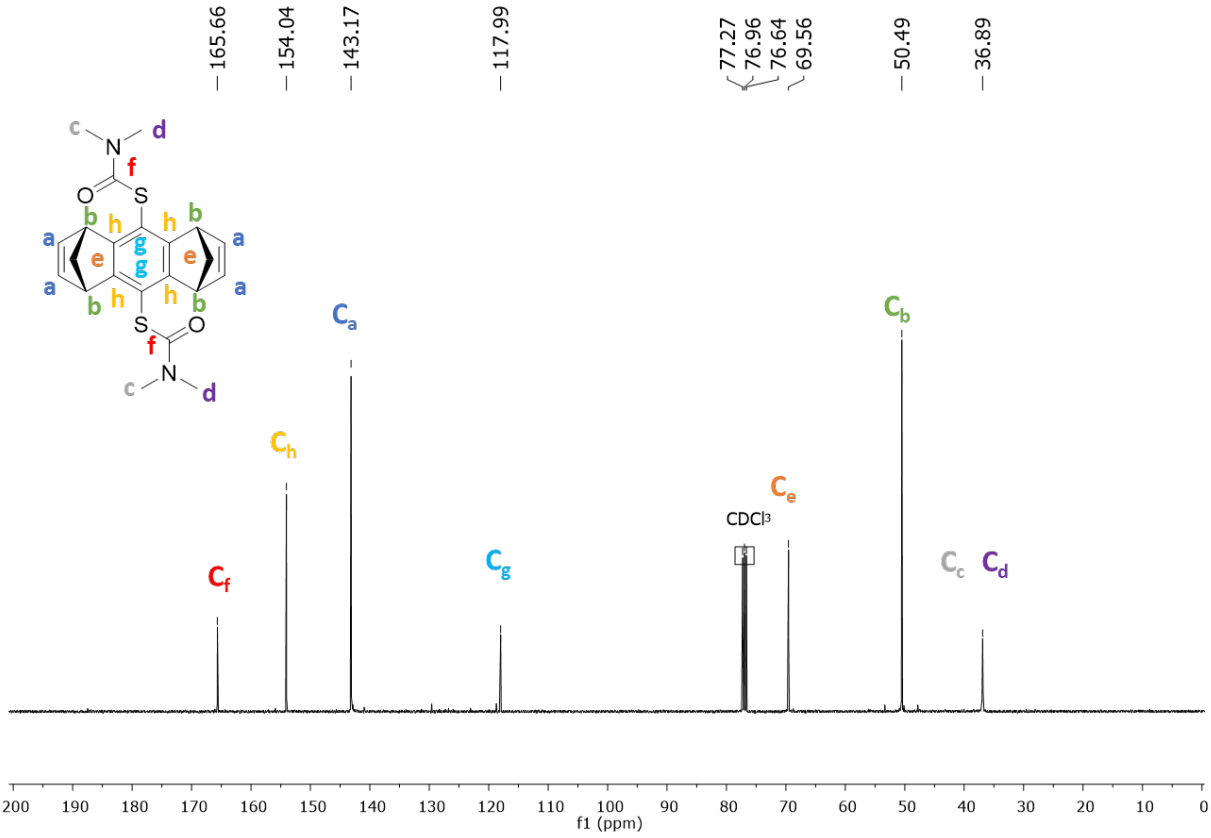

*Figure S48: ^{13}C NMR spectrum of compound **B-6***

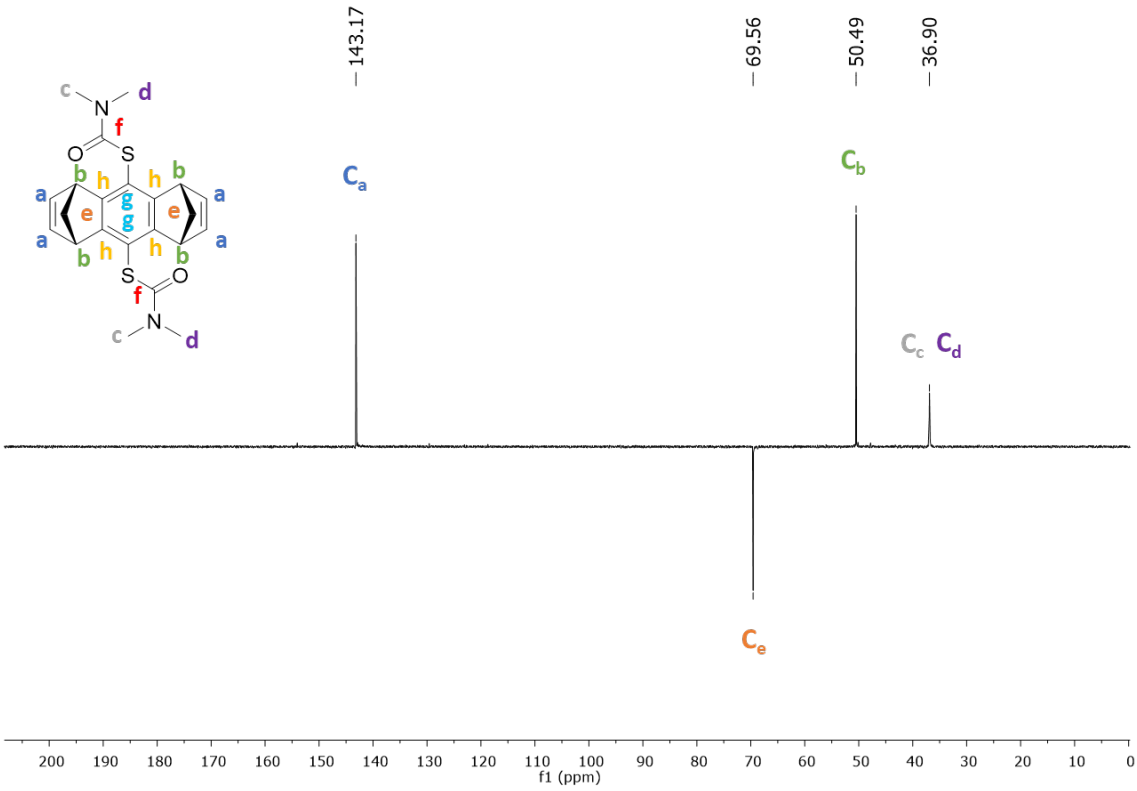

*Figure S49: DEPT ^{13}C NMR spectrum of compound **B-6***

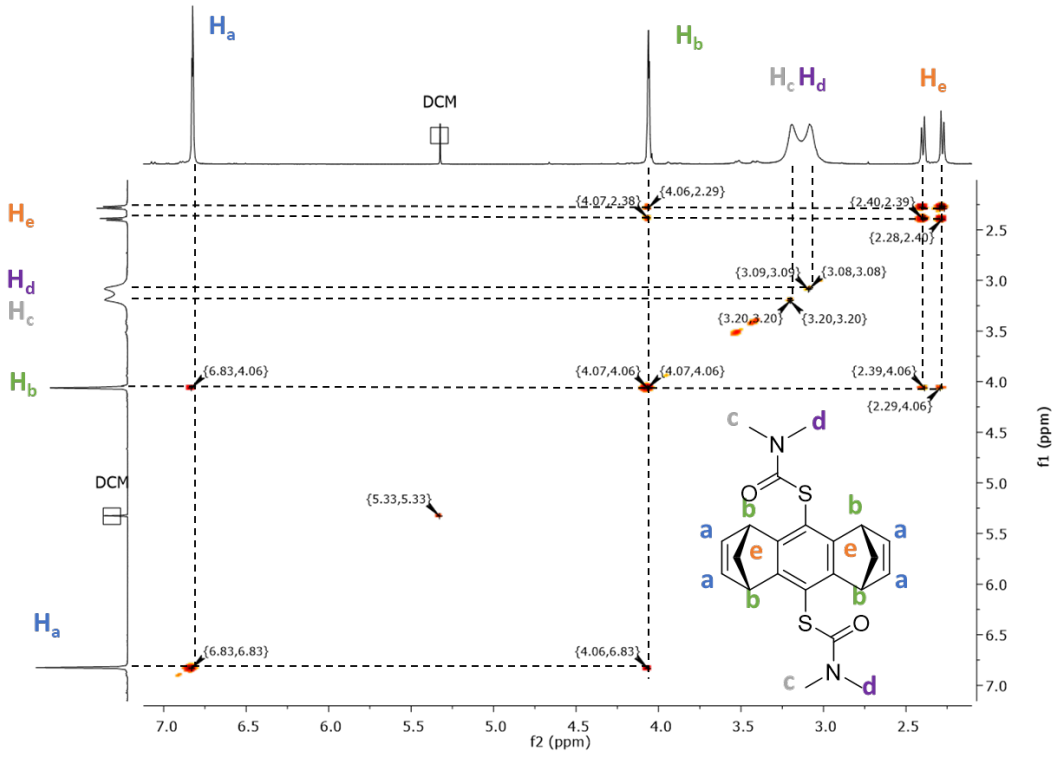

*Figure S50: COSY NMR spectrum of compound **B-6***

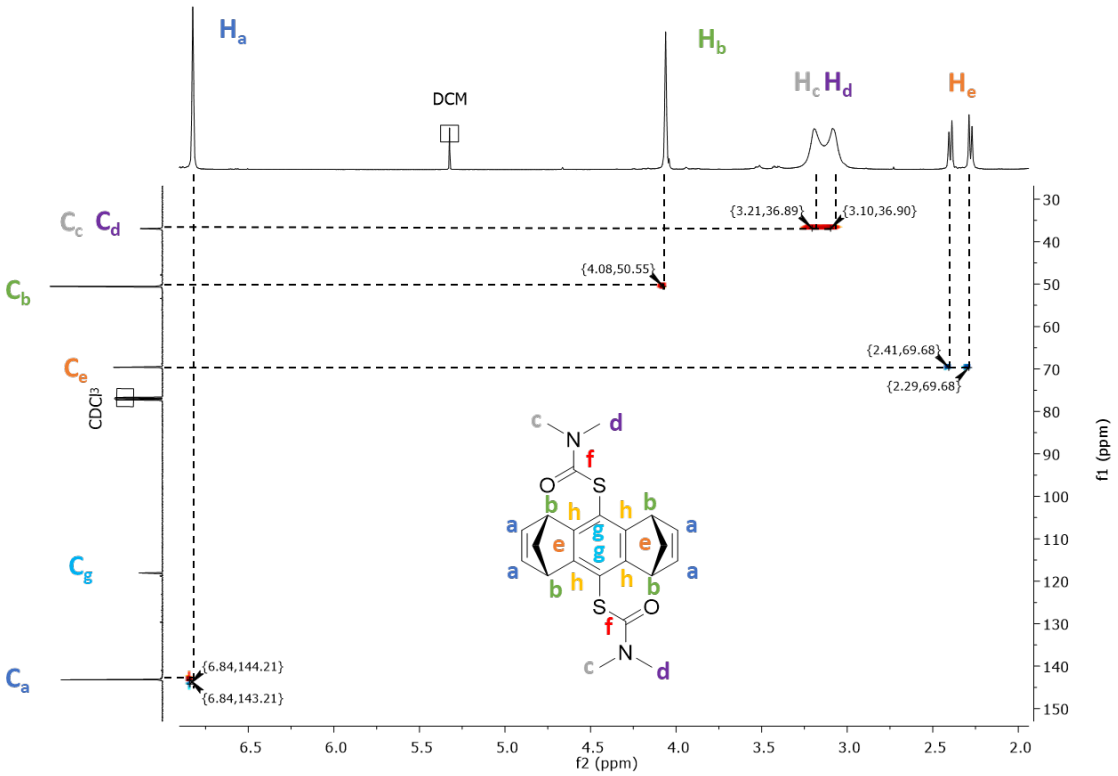

Figure S51: HSQC NMR spectrum of compound ***B-6***

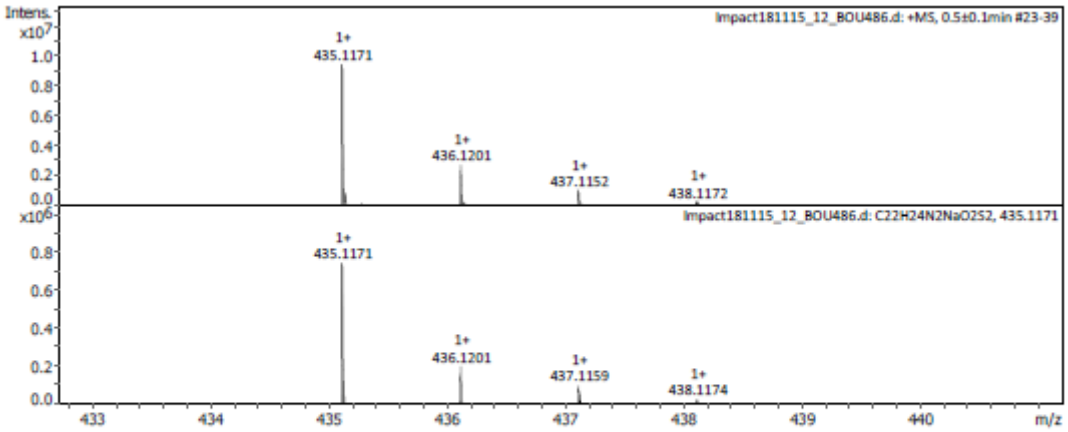

Meas. m/z	Ion Formula	m/z	Sum Formula	err [ppm]	mSigma	Adduct	z
413.1352	C22H25N2O2S2	413.1352	C22H24N2O2S2	0.1	22.6	M+H	1+
435.1171	C22H24N2NaO2S2	435.1171		0.0	16.4	M+Na	1+
451.0911	C22H24KN2O2S2	451.0911		-0.2	16.2	M+K	1+

Figure S52: HRMS spectrum of compound ***B-6***

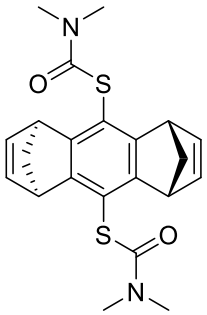

C-6 S,S'-((1R,4S,5S,8R)-1,4,5,8-tetrahydro-1,4:5,8-dimethanoanthracene-9,10-diyl) bis(dimethylcarbamothioate)

A solution of **C-5** O,O'-((1R,4S,5S,8R)-1,4,5,8-tetrahydro-1,4:5,8-dimethanoanthracene-9,10-diyl) bis(dimethylcarbamothioate) (357 mg, 0.87 mmol, 1 eq) in diphenylether (3 mL) was heated at 230 °C for 4 h. The mixture was then cooled to room temperature. The resulting mixture was purified by column chromatography (SiO_2, pentane : ethyl acetate = 1:0 -> 1:1 -> 0:1) to give a yellow powder (41 mg, 11 %).

Yellow powder, mp: degradation, 245.6 – 247.9 °C; HRMS (ESI) $[M + Na]^+$ found 435.1173, calculated 435.1171 for $[C_{22}H_{25}NaN_2O_2S_2]^+$; ^{1}H NMR (400 MHz, $CDCl_3$) δ ppm = 6.84 (t, J = 1.2 Hz, 2 H, $\mathbf{H_a}C=C\mathbf{H_a}$), 4.01 (t, J = 1.7 Hz, 2 H, $C\mathbf{H_b}$), 3.21 - 2.99 (m, 6 H, $C\mathbf{H_{3cd}}$), 2.24 (dd, J = 6.9, 28.0 Hz, 2 H, $C\mathbf{H_{2e}}$); ^{13}C NMR (101 MHz, $CDCl_3$) δ ppm = 165.7 ($\mathbf{C_f}O$), 154.0 ($\mathbf{C}_{Ar,IV\mathbf{h}}$), 143.2 ($H\mathbf{C_a}=\mathbf{C_a}H$), 118.0 ($\mathbf{C}_{Ar\mathbf{g}}$-S), 69.5 ($\mathbf{C_e}H_2$), 50.6 ($\mathbf{C_b}H$), 37.0 ($\mathbf{C_{cd}}H_3$)

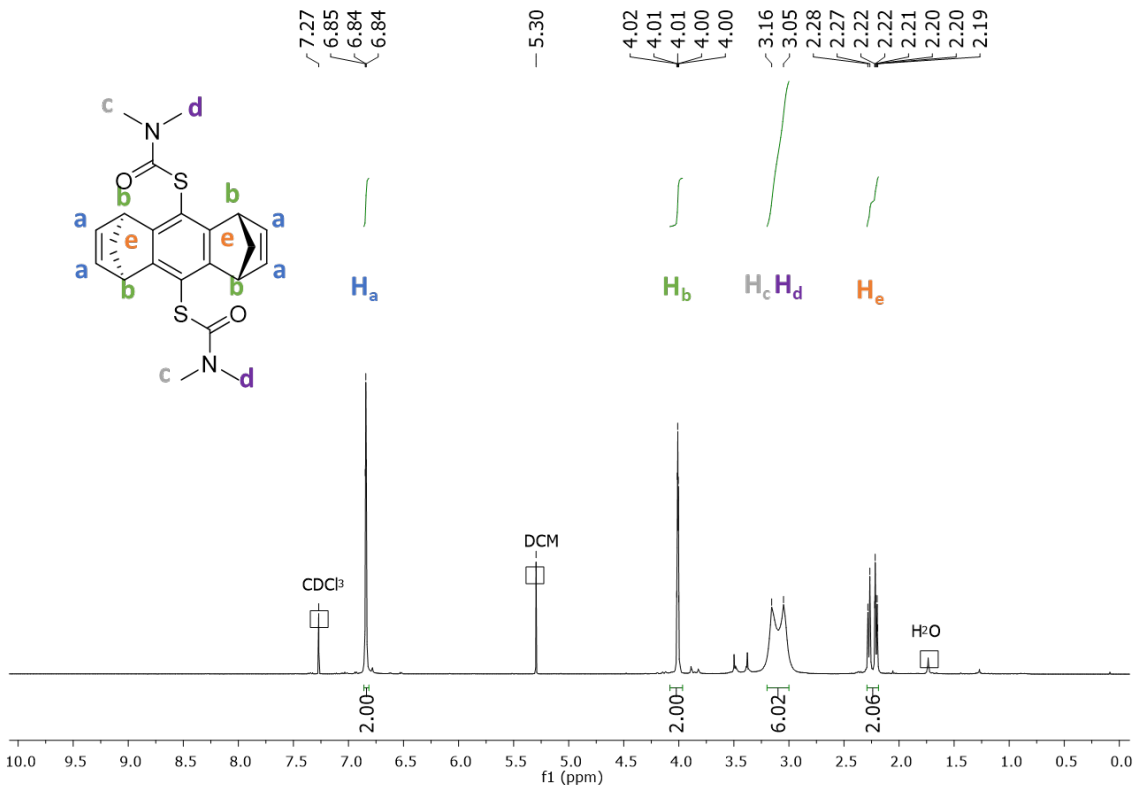

*Figure S53: ^{1}H NMR spectrum of compound **C-6***

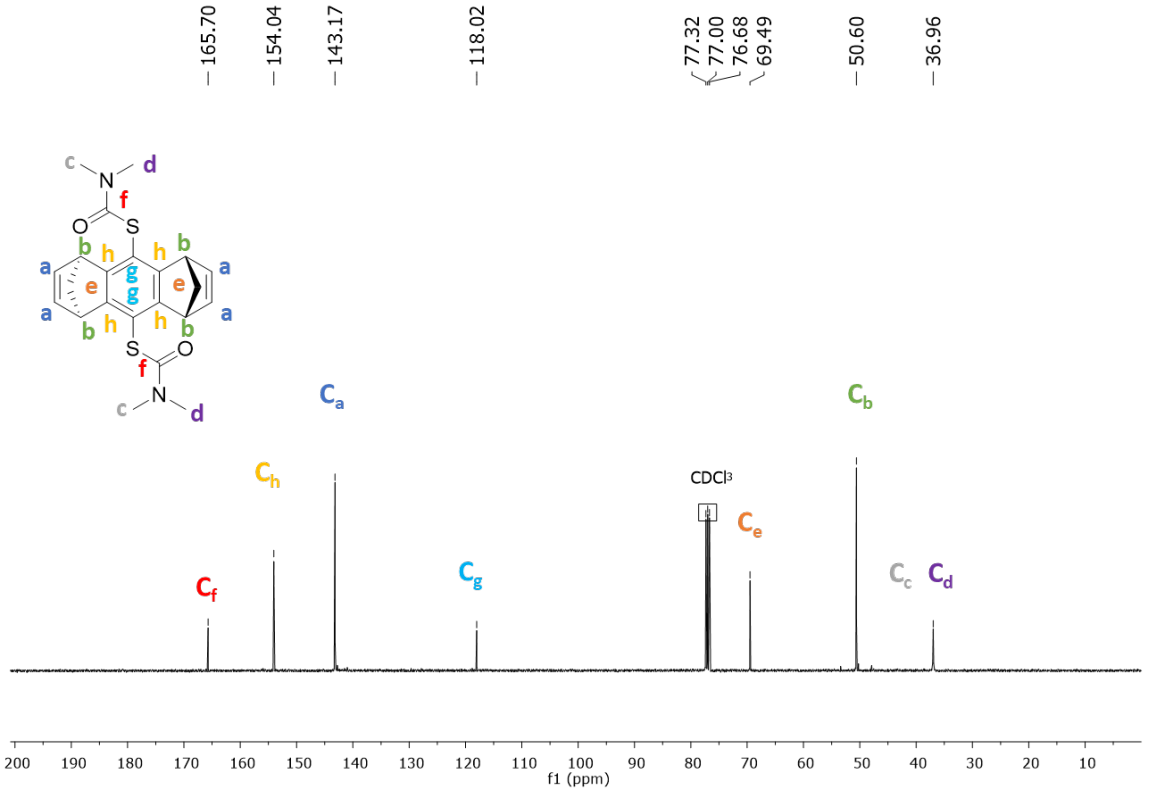

*Figure S54: ^{13}C NMR spectrum of compound **C-6***

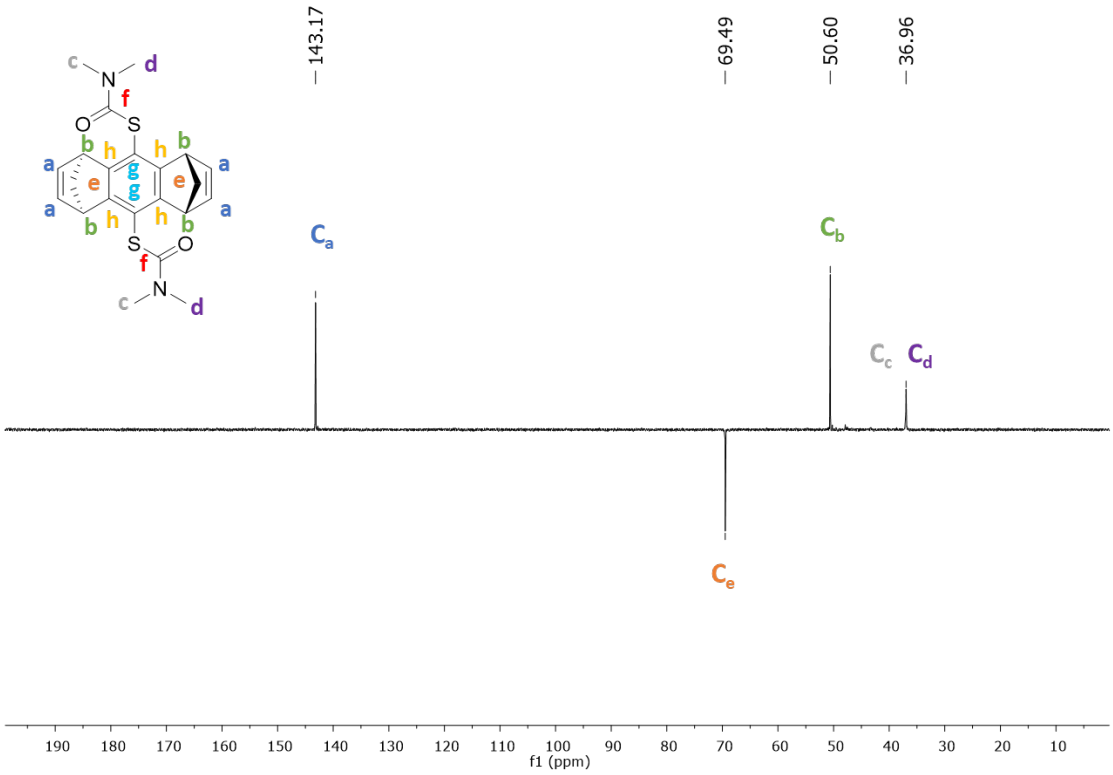

Figure S55: DEPT ^{13}C NMR spectrum of compound ***C-6***

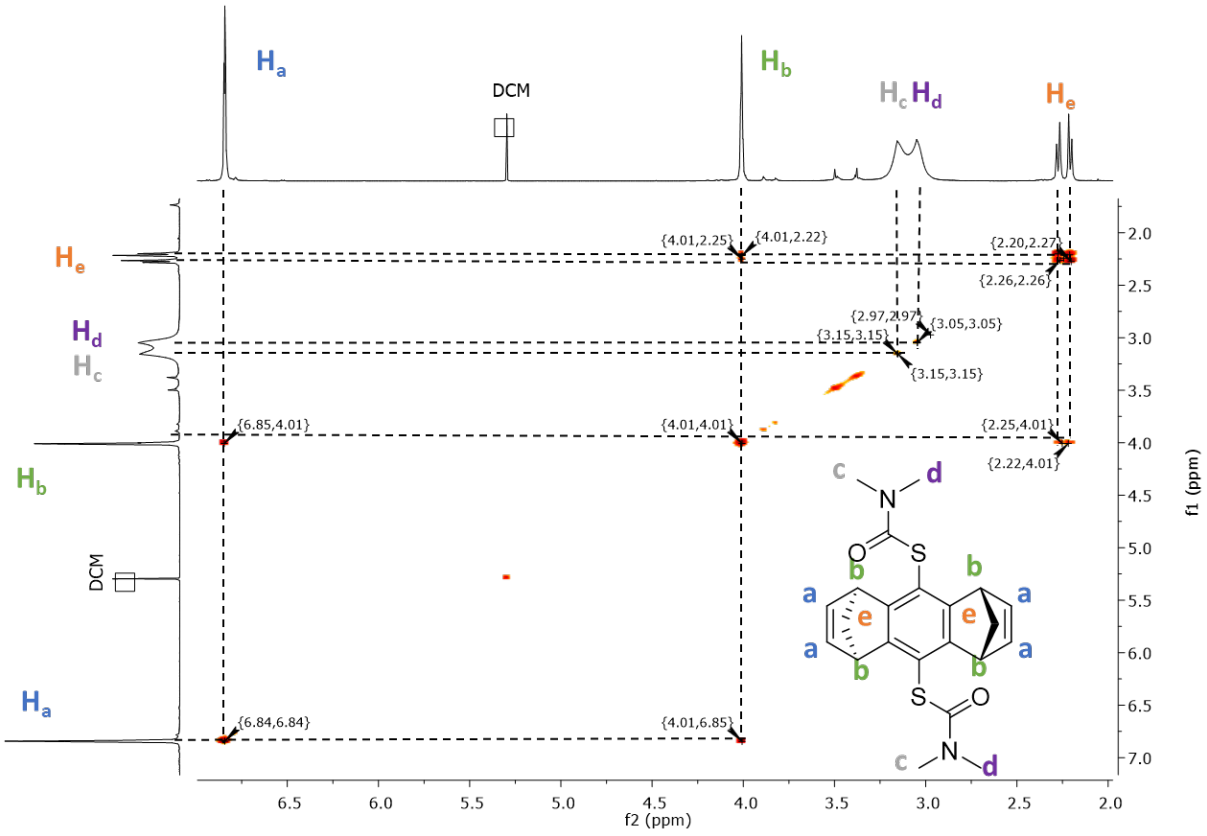

Figure S56: COSY NMR spectrum of compound ***C-6***

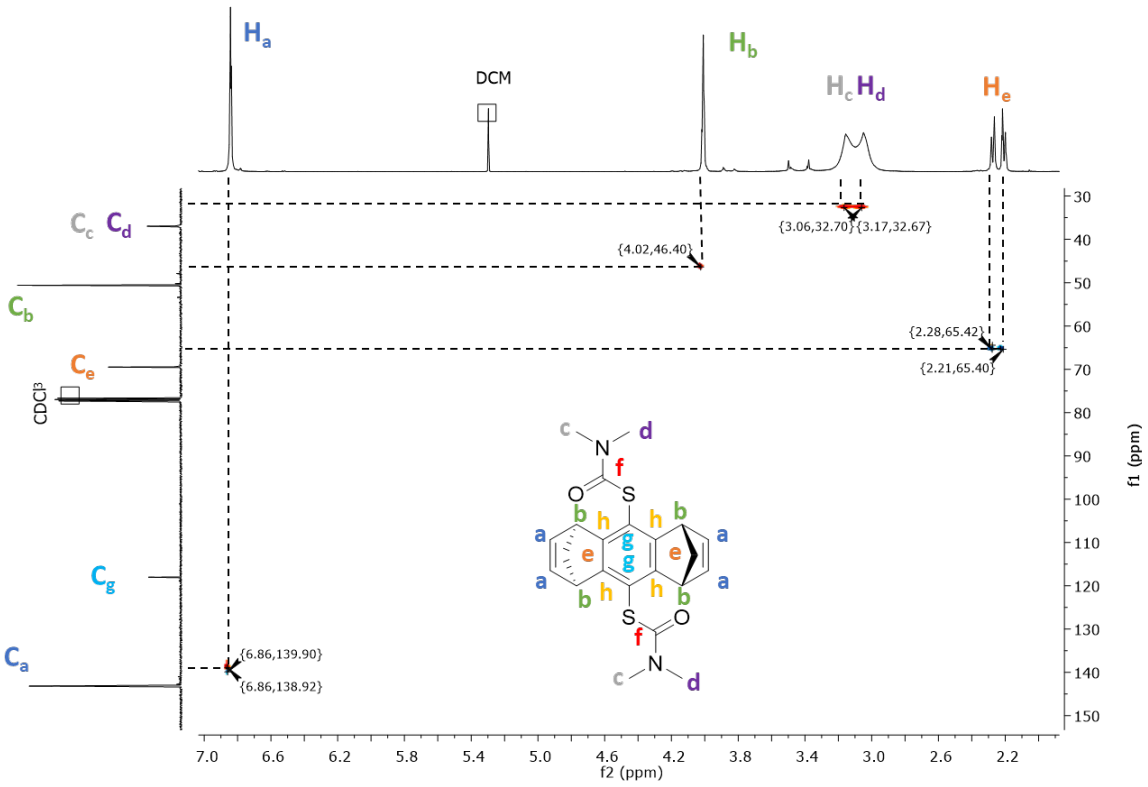

Figure S57: HSQC NMR spectrum of compound ***C-6***

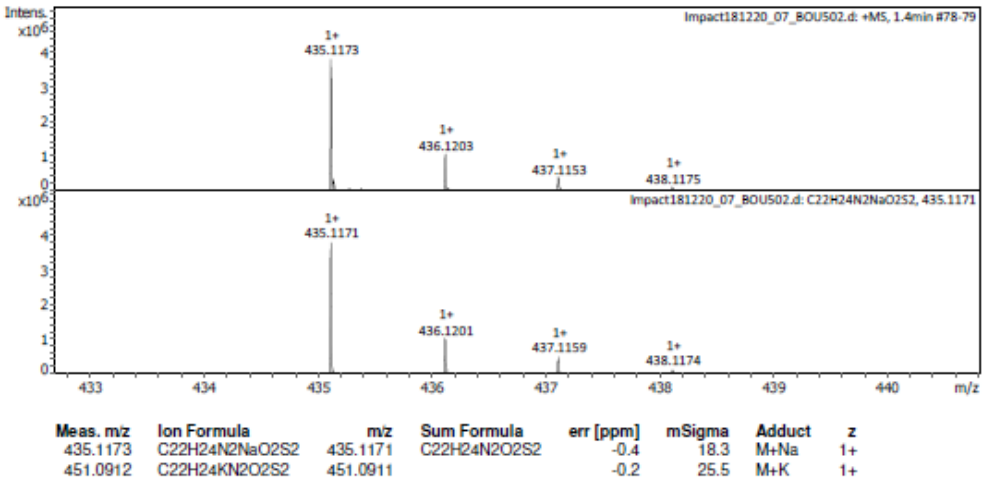

Meas. m/z	Ion Formula	m/z	Sum Formula	err [ppm]	mSigma	Adduct	z
435.1173	C22H24N2NaO2S2	435.1171	C22H24N2O2S2	-0.4	18.3	M+Na	1+
451.0912	C22H24KN2O2S2	451.0911		-0.2	25.5	M+K	1+

Figure S58: HRMS spectrum of compound ***C-6***

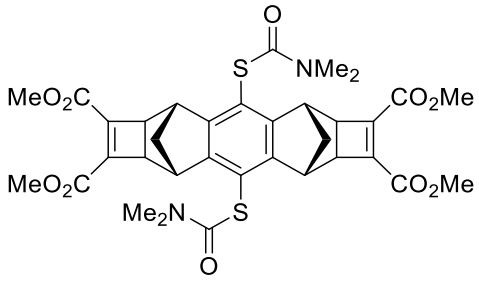

B-7 tetramethyl (3R,5S,8R,10S)-4,9-bis((dimethylcarbamoyl)thio)-2a,3,5,5a,7a,8,10,10a-octahydro-3,10:5,8-dimethanodicyclobuta[*b,i*]anthracene-1,2,6,7-tetracarboxylate

Dimethyl acetylenedicarboxylate (2.84 mL, 23.1 mmol, 2.6 eq) was added dropwise to a solution of **B-6** S,S'-((1R,4S,5R,8S)-1,4,5,8-tetrahydro-1,4:5,8-dimethanoanthracene-9,10-diyl) bis(dimethylcarbamothioate) (3.76 g, 8.89 mmol, 1 eq) with $RuH_2CO(PPh_3)_3$ (816 mg, 0.89 mmol, 0.1 eq) in anhydrous and degassed tetrahydrofurane (40 mL). The mixture was refluxed for 10 days under inert atmosphere. The solvent was removed under vacuum and the resulting residue was purified by SiO_2 column chromatography (dichloromethane: ethyl acetate 1 : 1) to give a yellow solid (2.9 g, 47 %).

Grey powder, mp: degradation, 301.3 °C; HRMS (ESI) $[M + Na]^+$ found 719.1704, calculated 719.1703 for $[C_{34}H_{36}NaN_2O_{10}S_2]^+$; ^{1}H NMR (400 MHz, $CDCl_3$) δ ppm = 3.81 (m, 12 H, C**H**$_{\mathbf{3a}\text{ester}}$), 3.44 (m, 4 H, C**H**$_{\mathbf{b}\ \text{6-membered ring}}$), 3.27 - 2.99 (m, 12 H, C**H**$_{\mathbf{3cd}\ \text{carbamate}}$), 2.87 (m, 4 H, C**H**$_{\mathbf{f}\ \text{4-membered ring}}$), 1.92 - 1.79 (m, 2 H, C**H**$_{\mathbf{2e}}$), 1.75 - 1.69 (m, 2 H, C**H**$_{\mathbf{2e}}$); ^{13}C NMR (101 MHz, $CDCl_3$) δ ppm = 165.6 (**C**$_{\mathbf{g}}O_{\text{ester}}$), 161.8 (**C**$_{\mathbf{i}}O_{\text{carbamate}}$), 150.0 ($C_{\mathbf{k}}$=$C_{\mathbf{k}}$), 143.2 (**C**$_{\text{Ar,IV}\mathbf{h}}$), 118.7 (**C**$_{\mathbf{j}\text{Ar}}$-S), 51.9 (**C**$_{\mathbf{a}}H_3$), 45.3 (**C**$_{\mathbf{f}}$H), 40.8 (**C**$_{\mathbf{b}}$H), 40.3 (**C**$_{\mathbf{k}}H_2$), 37.1 ($CH_{2\mathbf{cd}}$)

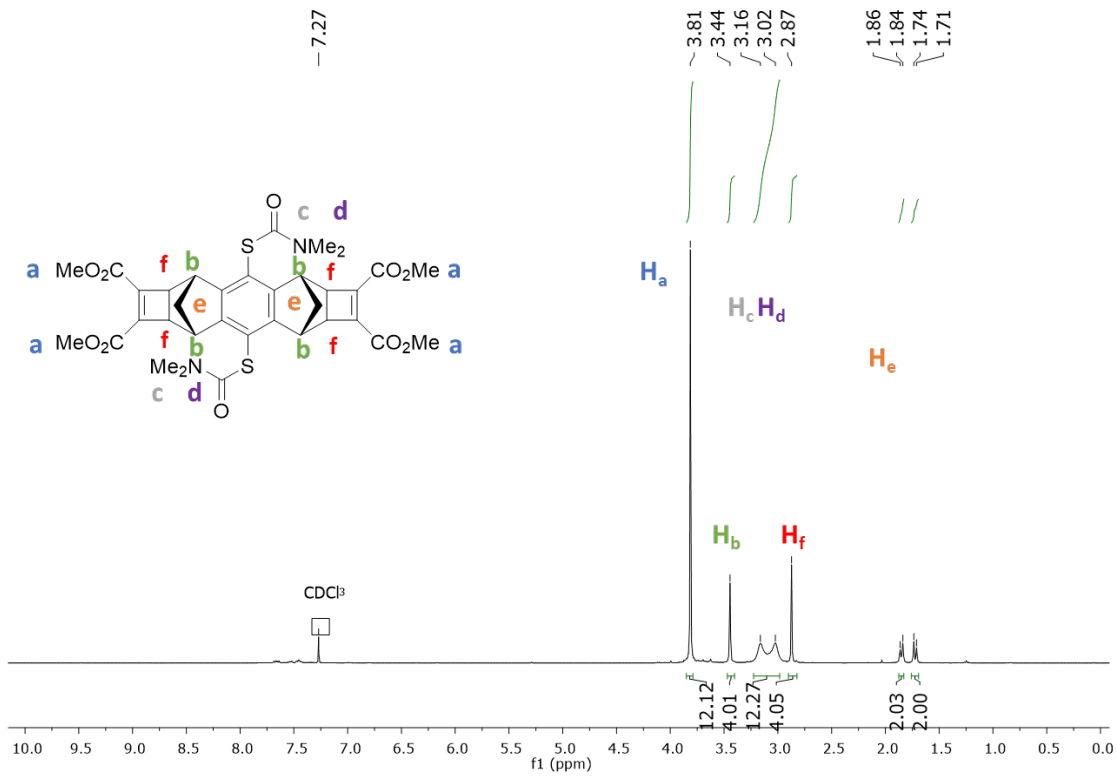

*Figure S59: [1]H NMR spectrum of compound **B-7***

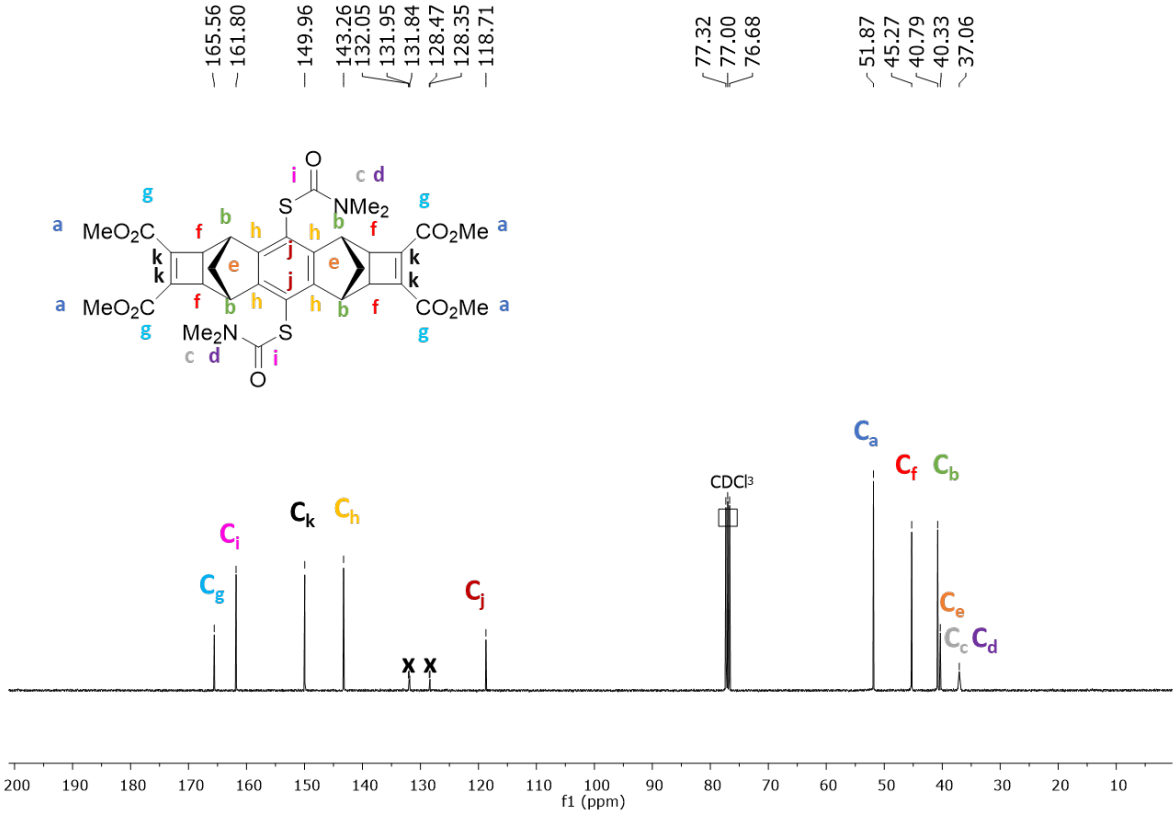

*Figure S60: [13]C NMR spectrum of compound **B-7***

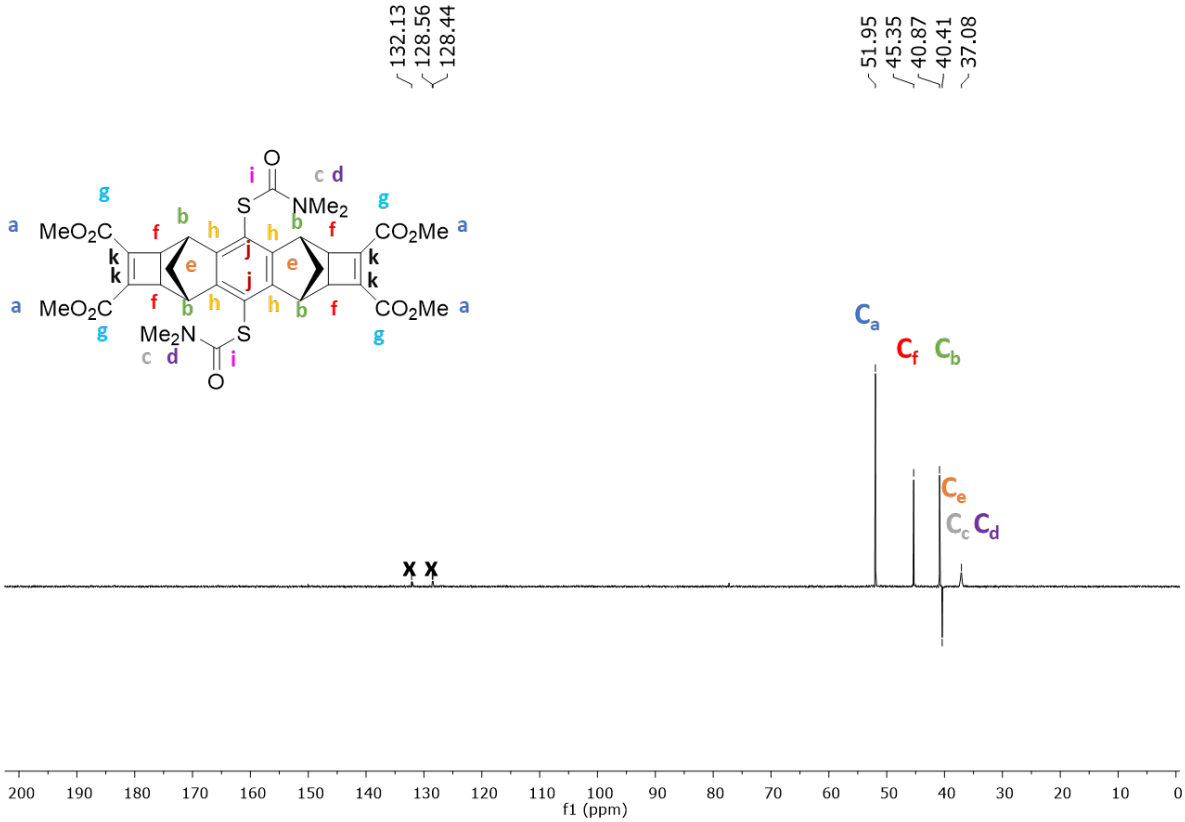

*Figure S61: DEPT ^{13}C NMR spectrum of compound **B-7***

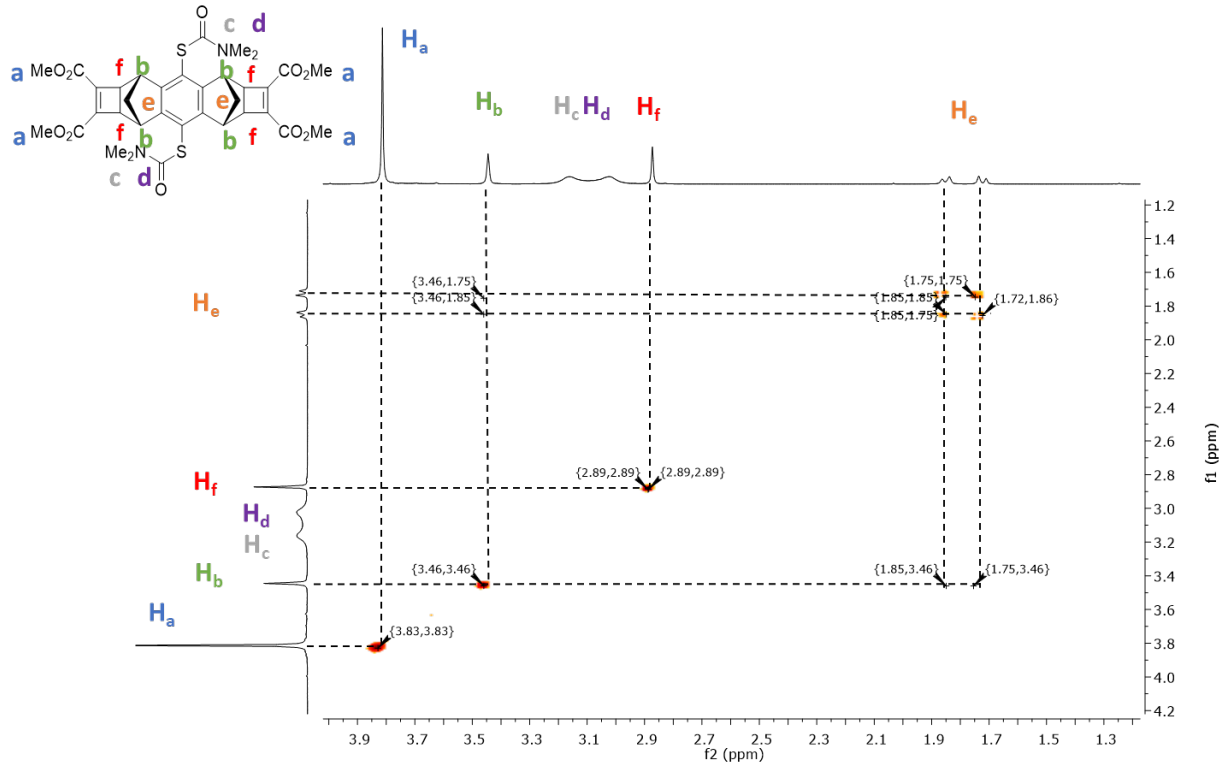

*Figure S62: COSY NMR spectrum of compound **B-7***

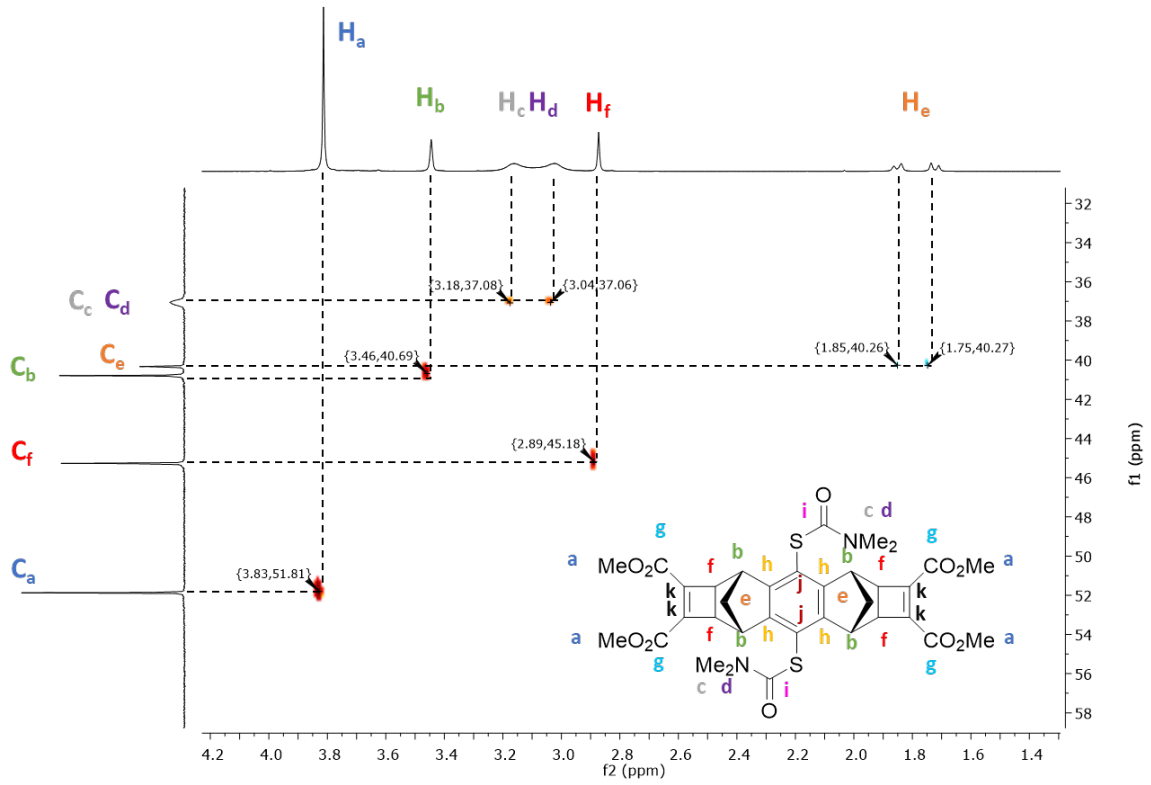

Figure S63: HSQC NMR spectrum of compound ***B-7***

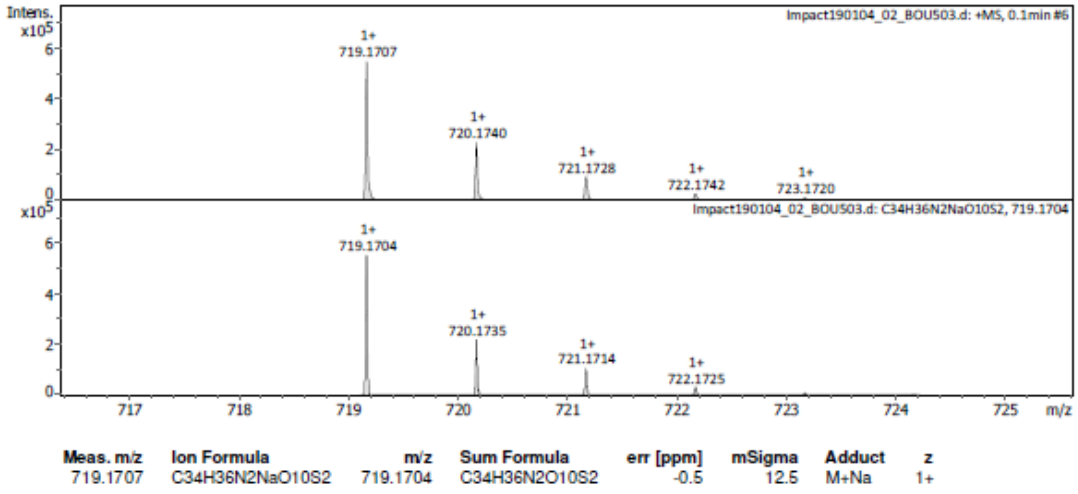

Meas. m/z	Ion Formula	m/z	Sum Formula	err [ppm]	mSigma	Adduct	z
719.1707	C34H36N2NaO10S2	719.1704	C34H36N2O10S2	-0.5	12.5	M+Na	1+

Figure S64: HRMS spectrum of compound ***B-7***

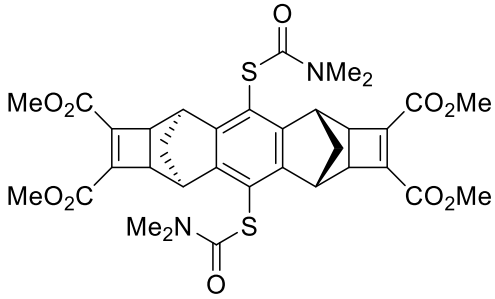

C-7 tetramethyl (3R,5R,8S,10S)-4,9-bis((dimethylcarbamoyl)thio)-2a,3,5,5a,7a,8,10,10a-octahydro-3,10:5,8-dimethanodicyclobuta[*b,i*]anthracene-1,2,6,7-tetracarboxylate

Dimethyl acetylenedicarboxylate (0,66 mL, 5.28 mmol, 2.6 eq) was added dropwise to a solution of **C-6** S,S'-((1R,4S,5R,8S)-1,4,5,8-tetrahydro-1,4:5,8-dimethanoanthracene-9,10-diyl) bis(dimethylcarbamothioate) (855 mg, 2.07 mmol, 1 eq) with $RuH_2CO(PPh_3)_3$ (190 mg, 0,207 mmol, 0.1 eq) in anhydrous and degassed tetrahydrofuran (9.3 mL). The mixture was refluxed for 10 days under inert atmosphere. The solvent was removed under vacuum and the resulting residue was purified by SiO_2 column chromatography (dichloromethane : ethylacetate 1 : 1) to give a grey solid (587 mg, 41 %).

Grey powder, mp: 261.2 – 263.3 °C; HRMS (ESI) $[M + Na]^+$ found 719.1707, calculated 719.1703 for $[C_{34}H_{36}NaN_2O_{10}S_2]^+$; ^{1}H NMR (400 MHz, $CDCl_3$) δ ppm = 3.80 (m, 12 H, C**H**$_{\mathbf{3a}\ \text{ester}}$), 3.44 (m, 4 H, C**H**$_{\mathbf{b}\ \text{6-membered ring}}$), 3.25 - 2.96 (m, 12 H, C**H**$_{\mathbf{3cd}\ \text{carbamate}}$), 2.81 (m, 4 H, C**H**$_{\mathbf{f}\ \text{4-membered ring}}$), 1.85 (m, 2 H, C**H**$_{\mathbf{2e}}$), 1.74 - 1.65 (m, 2 H, C**H**$_{\mathbf{2e}}$); ^{13}C NMR (101 MHz, $CDCl_3$) δ ppm = 165.4 (**C**$_{\mathbf{g}}$O$_{\text{ester}}$), 161.7 (**C**$_{\mathbf{i}}$O$_{\text{carbamate}}$), 149.8 (**C**$_{\mathbf{k}}$=**C**$_{\mathbf{k}}$), 143.2 (**C**$_{\text{Ar,IV}\mathbf{h}}$), 118.7 (**C**$_{\text{Ar}\mathbf{j}}$-S), 51.8 (**C**$_{\mathbf{a}}H_3$), 45.3 (C$_{\mathbf{j}}$H), 40.8 (**C**$_{\mathbf{b}}$H), 40.0 (**C**$_{\mathbf{e}}H_2$), 37.0 (**C**H$_{3\mathbf{cd}}$)

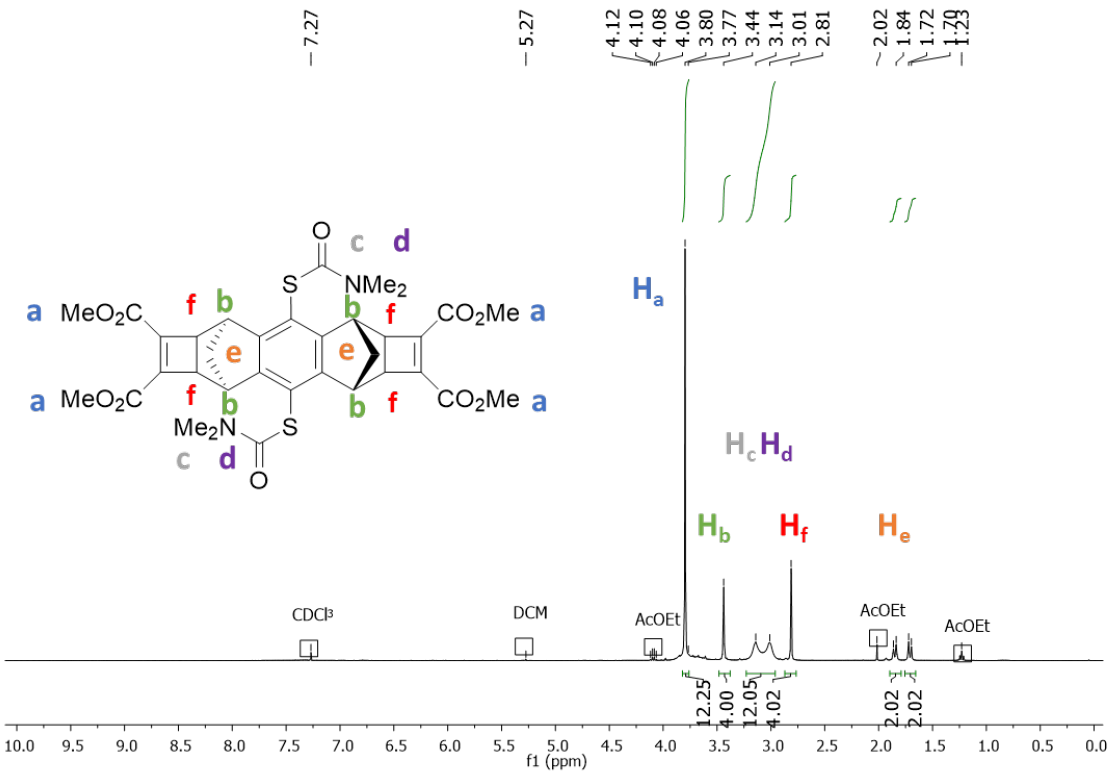

*Figure S65: [1]H NMR spectrum of compound **C-7***

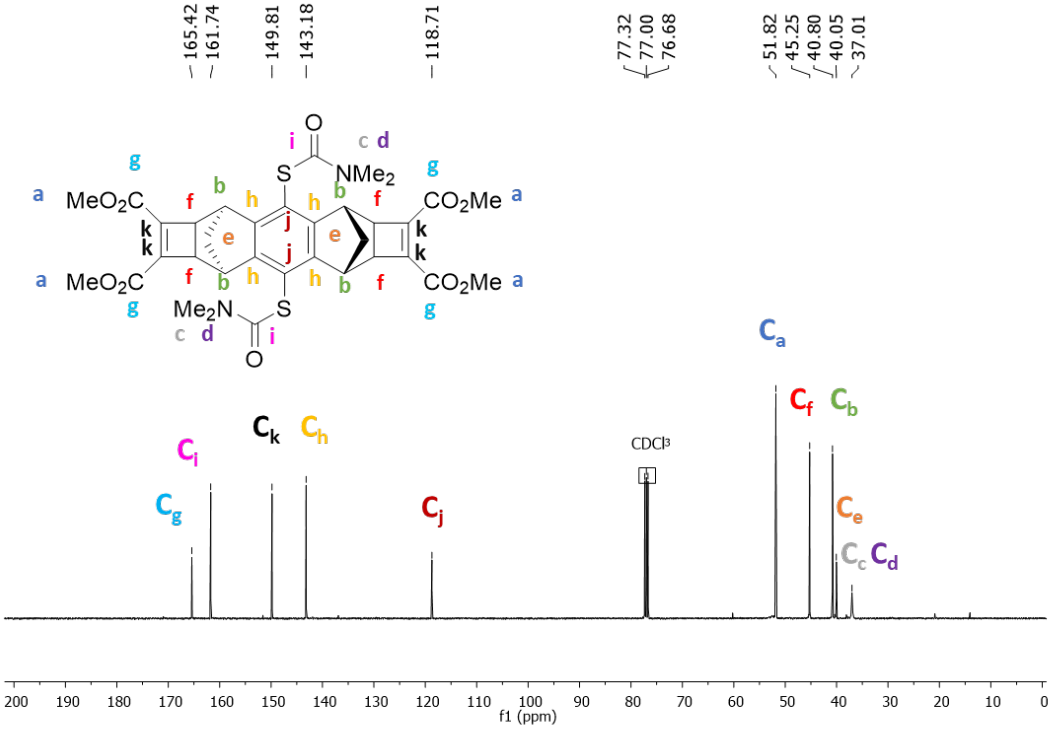

*Figure S66: [13]C NMR spectrum of compound **C-7***

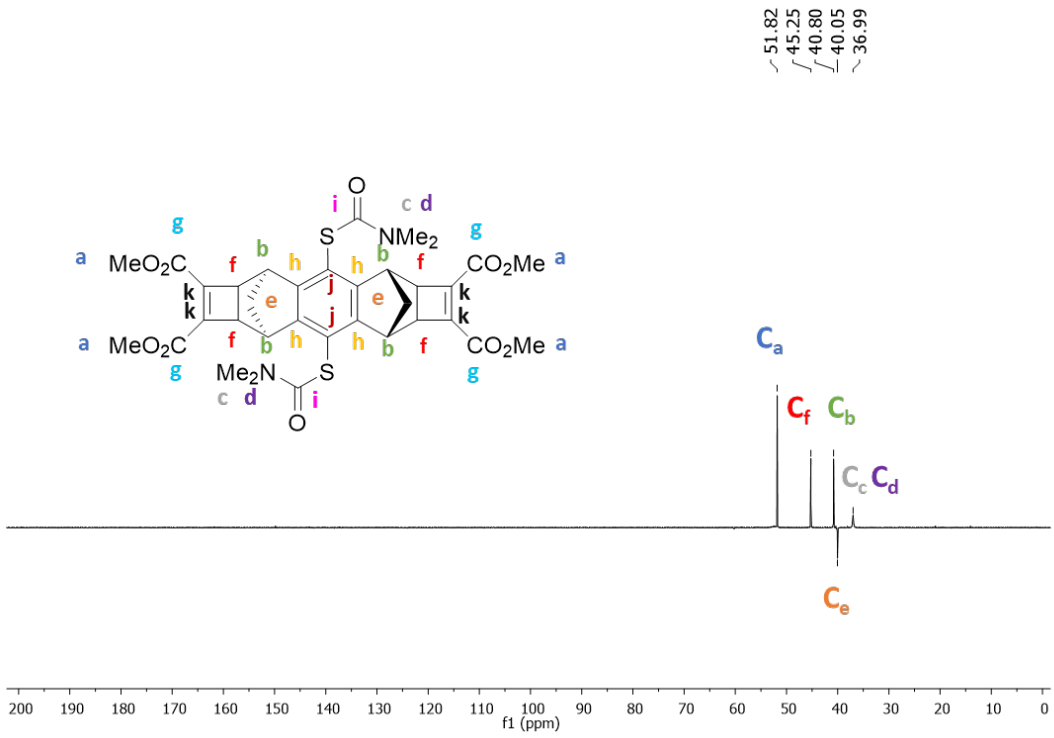

Figure S67: DEPT ^{13}C NMR spectrum of compound ***C-7***

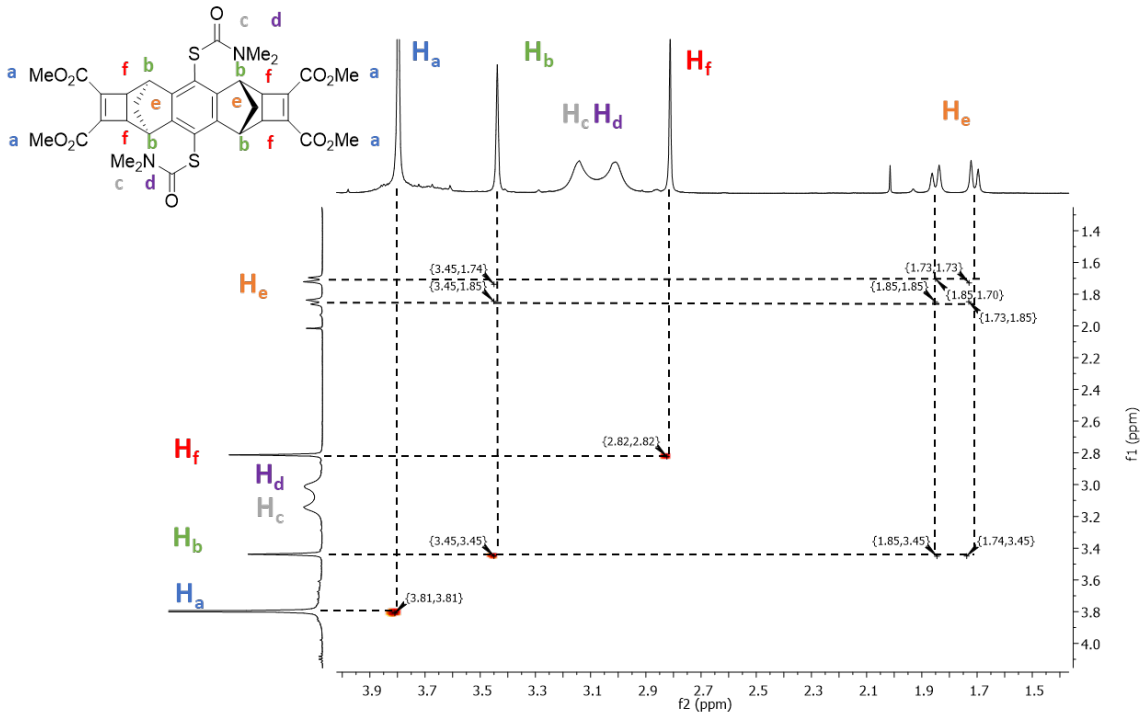

Figure S68: COSY NMR spectrum of compound ***C-7***

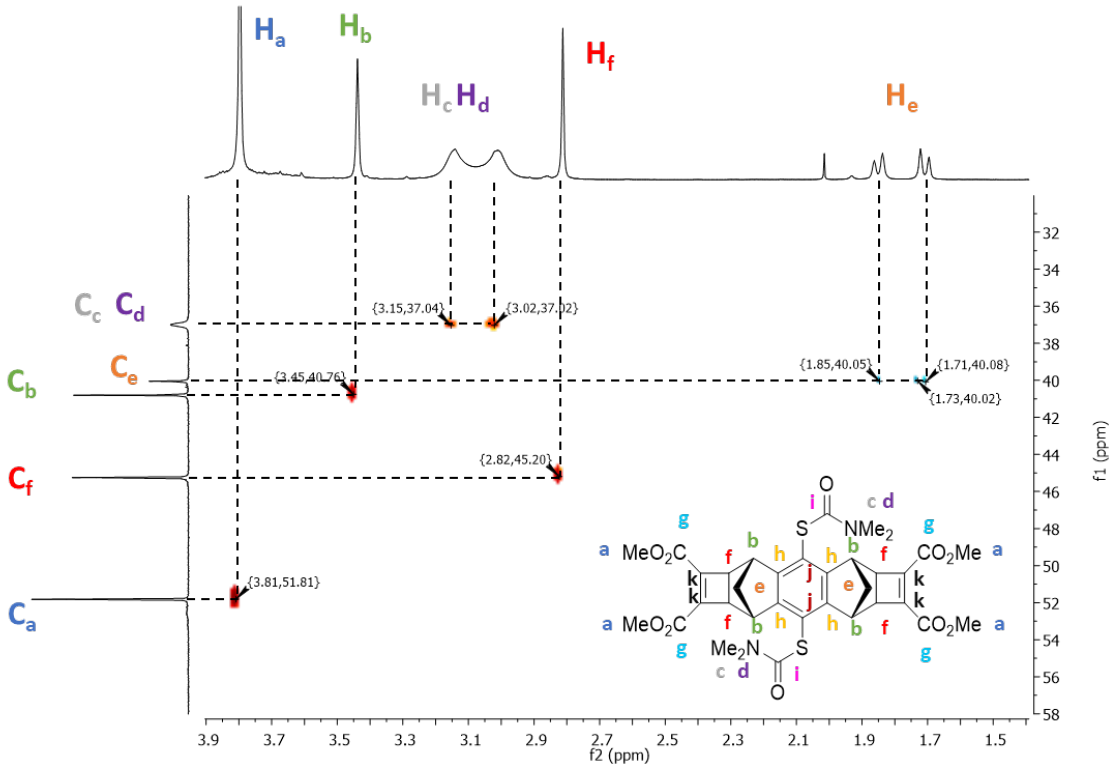

Figure S69: HSQC NMR spectrum of compound ***C-7***

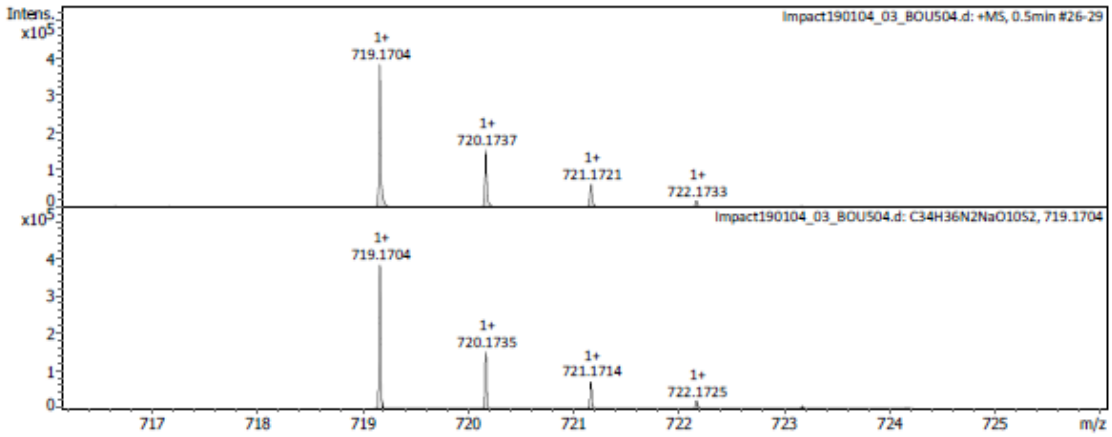

Meas. m/z	Ion Formula	m/z	Sum Formula	err [ppm]	mSigma	Adduct	z
697.1886	C34H37N2O10S2	697.1884	C34H36N2O10S2	-0.2	13.6	M+H	1+
719.1704	C34H36N2NaO10S2	719.1704		-0.1	12.4	M+Na	1+

Figure S70: HRMS spectrum of compound ***C-7***

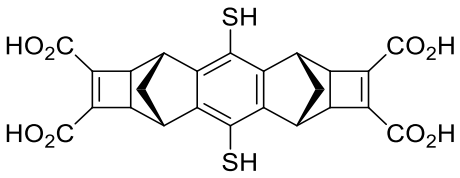

B (3R,5S,8R,10S)-4,9-dimercapto-2a,3,5,5a,7a,8,10,10a-octahydro-3,10:5,8-dimethanodicyclobuta[*b,i*]anthracene-1,2,6,7-tetracarboxylic acid

A solution of **B-7** (3R,5S,8R,10S)-tetramethyl 4,9-bis((dimethylcarbamoyl)thio)-3,5,8,10-tetrahydro-3,10:5,8-dimethanodicyclobuta[b,i]anthracene-1,2,6,7-tetracarboxylate (1.729 g, 2.52 mmol, 1 eq) in degassed 1.1 M NaOH (5.0 g, 125.7 mmol, 50 eq) in a degassed mixture of EtOH 1 / 1 H_2O (117 mL) was refluxed under an inert atmosphere for 16 h (monitored by ^1H NMR). The reaction mixture was cooled in ice, and concentrated HCl was added until pH 1. A precipitate was formed, filtered, and washed with water, yielding compound **B** as a brown solid (438 mg, 35 %).

brown solid; mp: decomposition 306.1 °C; HRMS (ESI) $[M - H]^+$ found 497.0369, calculated 497.0370 for $[C_{24}H_{17}O_{18}S_2]^-$; ^1H NMR (400 MHz, D_2O, NaOD) δ ppm = 3.34 - 3.31 (m, 4 H, C**H**$_{\mathbf{a}}$ $_{\text{6-membered ring}}$), 2.58 - 2.55 (m, 4 H, CH$_{\mathbf{b}}$ $_{\text{6-membered ring}}$), 1.61 - 1.55 (m, 2 H, C**H**$_{\mathbf{2c}}$), 1.48 - 1.43 (m, 2 H, C**H**$_{\mathbf{2c}}$); ^{13}C NMR (101 MHz, D_2O, NaOD) δ ppm = 168.1 (**C**$_{\mathbf{d}}$O), 147.2 (C$_{\mathbf{e}}$=C$_{\mathbf{e}}$), 144.6 (**C**$_{\text{iV Arf}}$), 119.9 (**C**$_{\text{Arg}}$-S), 44.0 (**C**$_{\mathbf{a}}$H $_{\text{4-membered ring}}$), 39.8 (**C**$_{\mathbf{a}}$H $_{\text{6-membered ring}}$), 38.7 (**C**$_{\mathbf{c}}H_2$)

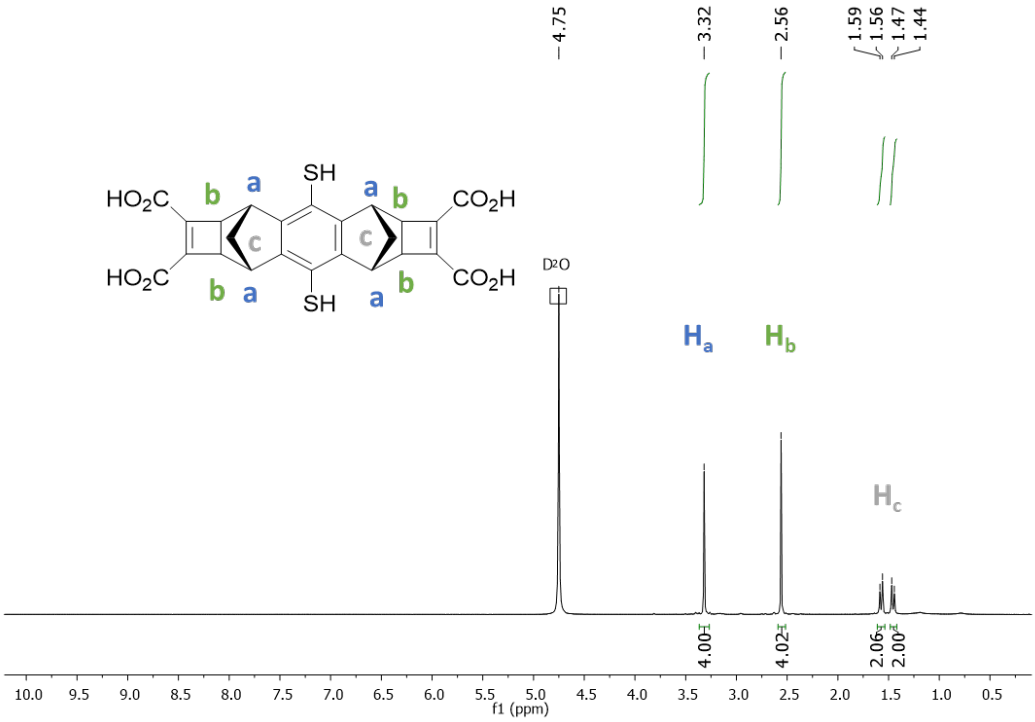

*Figure S71: ^1H NMR spectrum of compound **B***

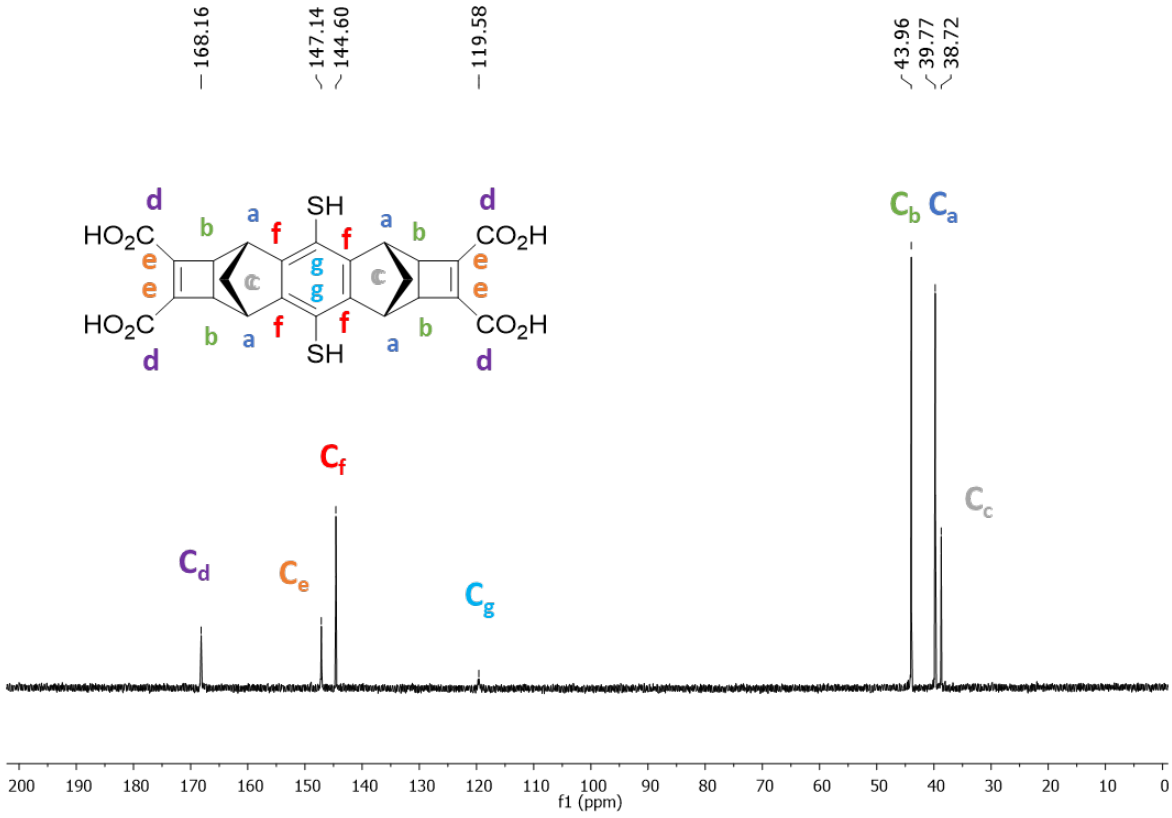

*Figure S72: ^{13}C NMR spectrum of compound **B***

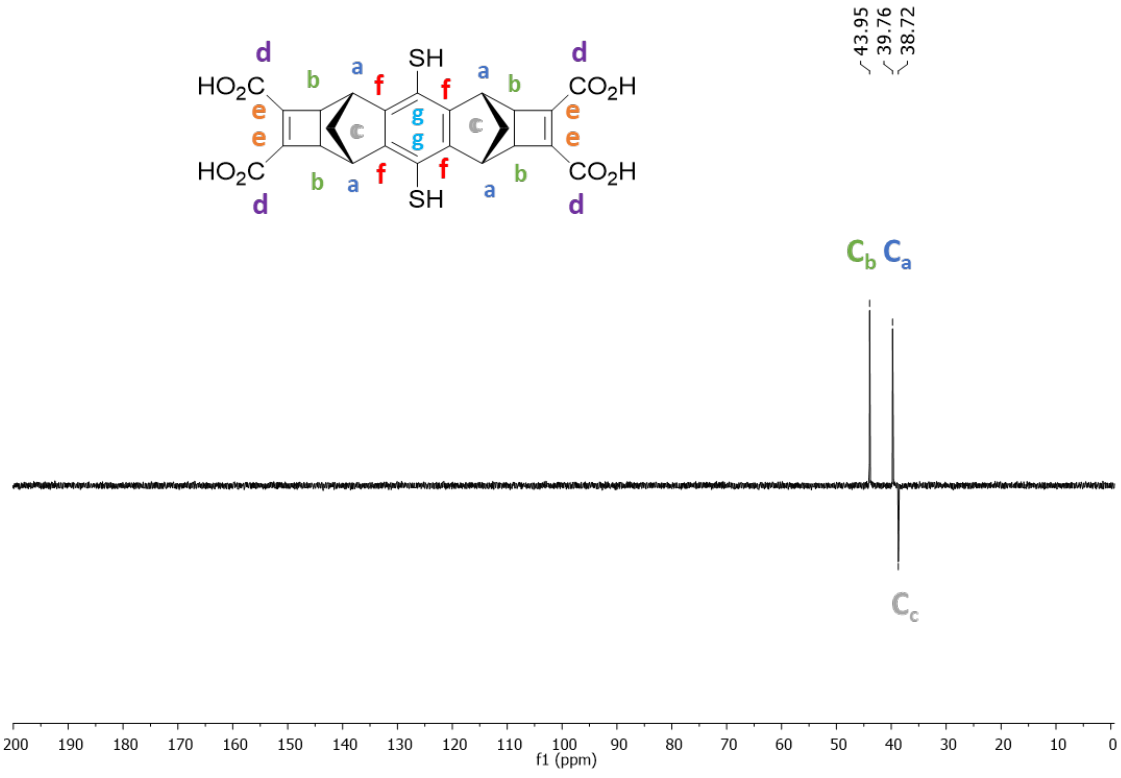

*Figure S73: DEPT ^{13}C NMR spectrum of compound **B***

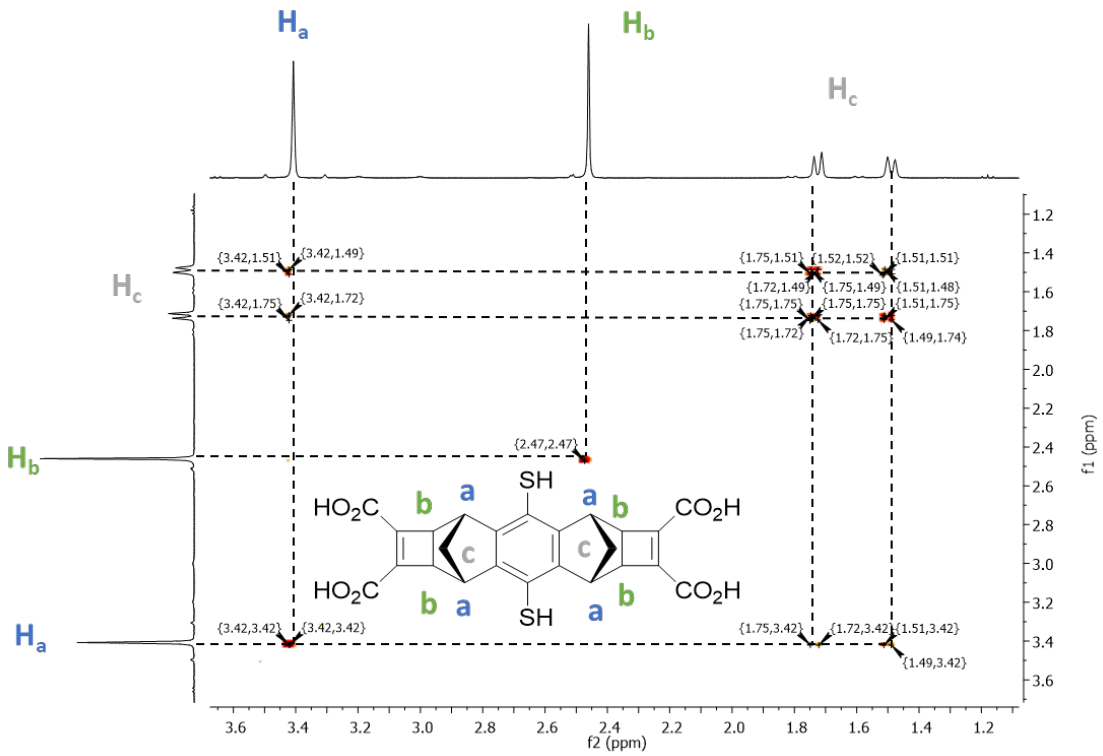

*Figure S74: COSY NMR spectrum of compound **B***

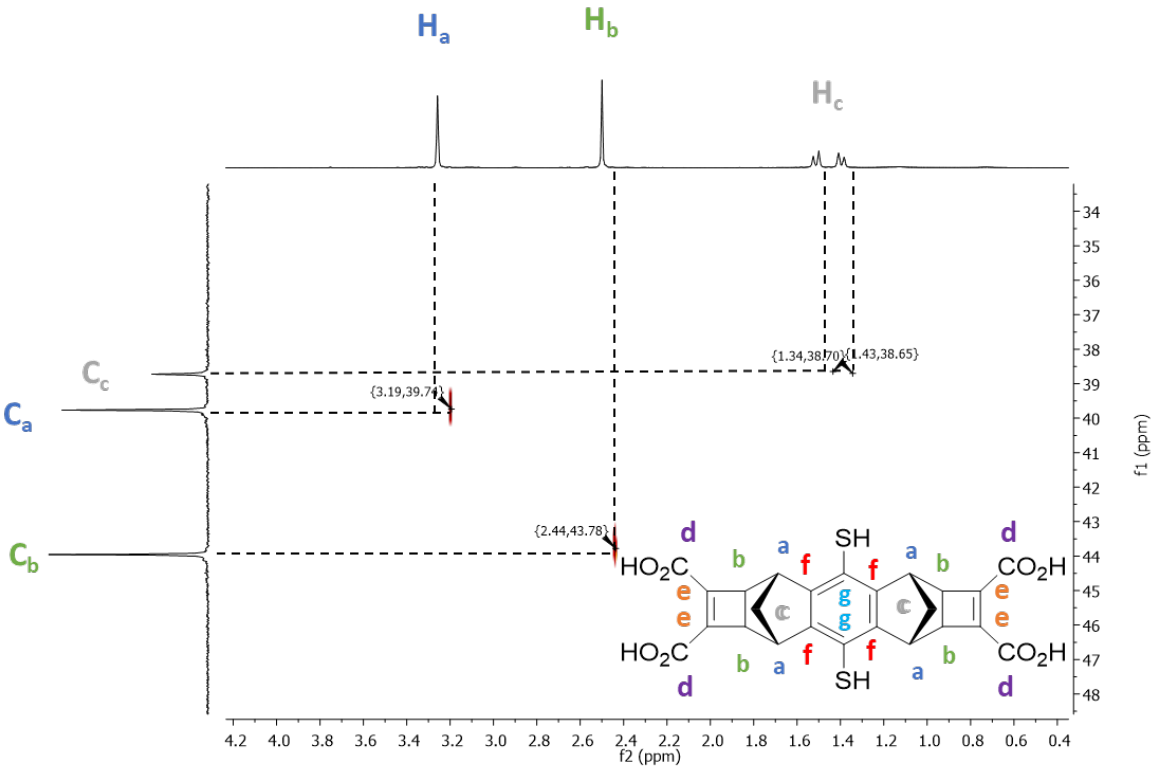

*Figure S75: HSQC NMR spectrum of compound **B***

Peak name	F2 [ppm]	D [m2/s]	error	name	R_H object	ΔR_H	status
1	1.626175717	3.32498E-10	1.87303E-12	**B-b**	5.76	0.032433	analyte
2	1.492433882	3.32524E-10	1.94695E-12	**B-b**	5.76	0.033707	analyte
3	2.560686884	3.35896E-10	1.33816E-12	**B-c**	5.70	0.022705	analyte
4	3.321077404	3.40801E-10	1.32157E-12	**B-a**	5.62	0.021782	analyte
5	3.675163735	9.02982E-10	4.14026E-12	dioxane	2.12	0.00972	ref
6	4.701965391	1.96271E-09	1.16805E-11	water	0.98	0.005805	solv

*Table S10 : ^{1}H DOSY data of builing block **B***

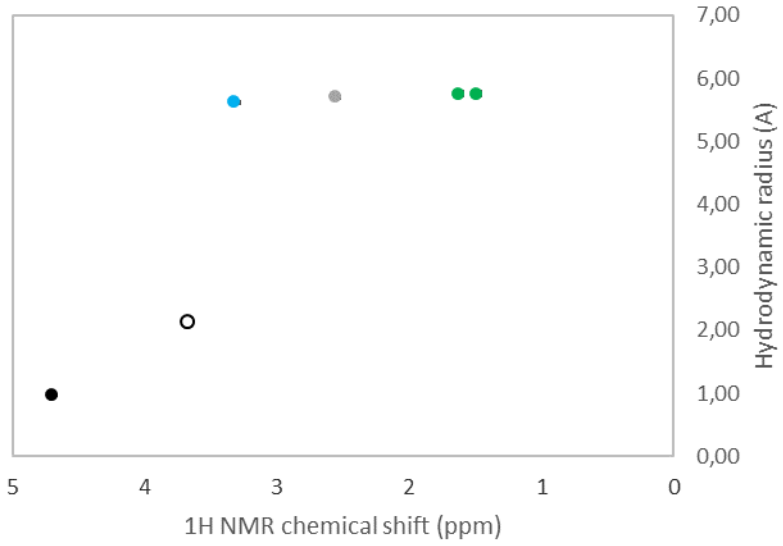

*Figure S76 : ^{1}H DOSY data plot of builing block **B***

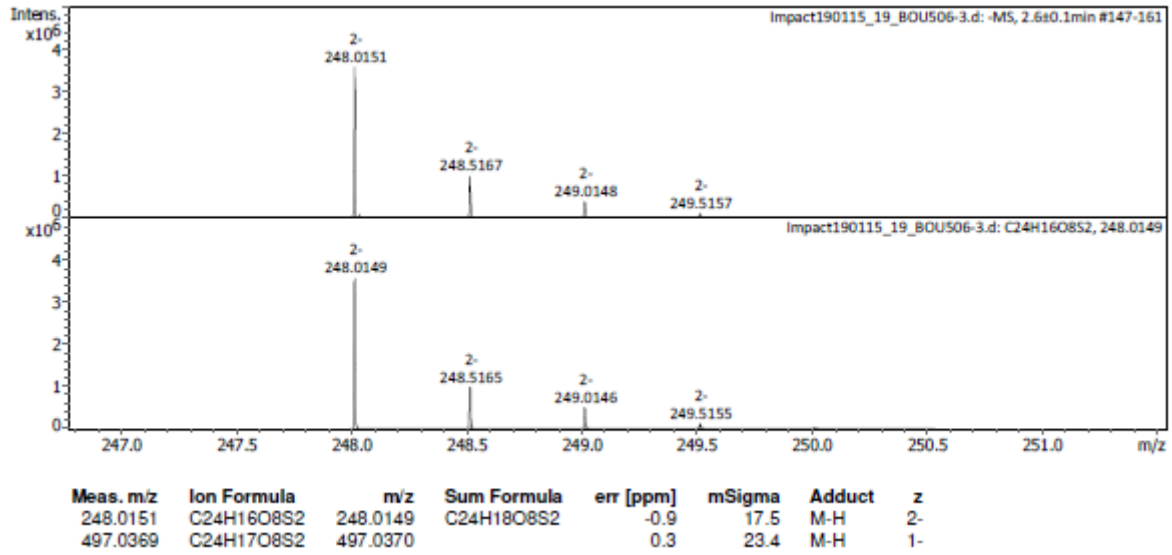

Meas. m/z	Ion Formula	m/z	Sum Formula	err [ppm]	mSigma	Adduct	z
248.0151	C24H16O8S2	248.0149	C24H18O8S2	-0.9	17.5	M-H	2-
497.0369	C24H17O8S2	497.0370		0.3	23.4	M-H	1-

*Figure S77: HRMS spectrum of compound **B***

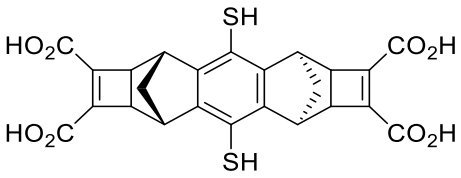

C (3R,5R,8S,10S)-4,9-dimercapto-2a,3,5,5a,7a,8,10,10a-octahydro-3,10:5,8-dimethanodicyclobuta[b,i]anthracene-1,2,6,7-tetracarboxylic acid

A solution of **C**-7 (3R,5R,8S,10S)-tetramethyl 4,9-bis((dimethylcarbamoyl)thio)-3,5,8,10-tetrahydro-3,10:5,8-dimethanodicyclobuta[b,i]anthracene-1,2,6,7-tetracarboxylate (587 mg, 0.86 mmol, 1 eq) in degassed 1.1 M NaOH (1.720 mg, 42.9 mmol, 50 eq) in a degassed mixture of EtOH 1 / 1 H_2O (40 mL) was refluxed under an inert atmosphere for 16 h (monitored by NMR). The reaction mixture was cooled in ice, and concentrated HCl was added until pH 1. A precipitate was formed, filtered, and washed with water, yielding compound **C** as a beige solid (161 mg, 38 %).

Beige solid; mp: decomposition 372.6 °C; HRMS (ESI) $[M - H]^+$ found 497.0368, calculated 497.0370 for $[C_{24}H_{17}O_{18}S_2]^-$; ^{1}H NMR (400 MHz, D_2O, NaOD) δ ppm = 3.47 - 3.41 (m, 4 H, CH $_{\text{6-membered ring}}$), 2.51 - 2.46 (m, 4 H, C**H**$_{\mathbf{a}}$ $_{\text{6-membered ring}}$), 1.80 - 1.72 (m, 2 H, C**H**$_{\mathbf{b}}$ $_{\text{4-membered ring}}$), 1.55 - 1.48 (m, 2 H, C**H**$_{\mathbf{2b}}$); ^{13}C NMR (101 MHz, D_2O, NaOD) δ ppm = 172.1 (**C**$_{\mathbf{d}}$O), 145.5 (**C**$_{\mathbf{e}}$=**C**$_{\mathbf{e}}$), 143.6 (**C**$_{\text{iV Arf}}$), 124.8 (**C**$_{\text{Arg}}$-S), 44.0 (**C**$_{\mathbf{a}}$H $_{\text{6-membered ring}}$), 40.9 (**C**$_{\mathbf{b}}$H $_{\text{4-membered ring}}$), 38.2 (**C**$_{\mathbf{c}}H_2$)

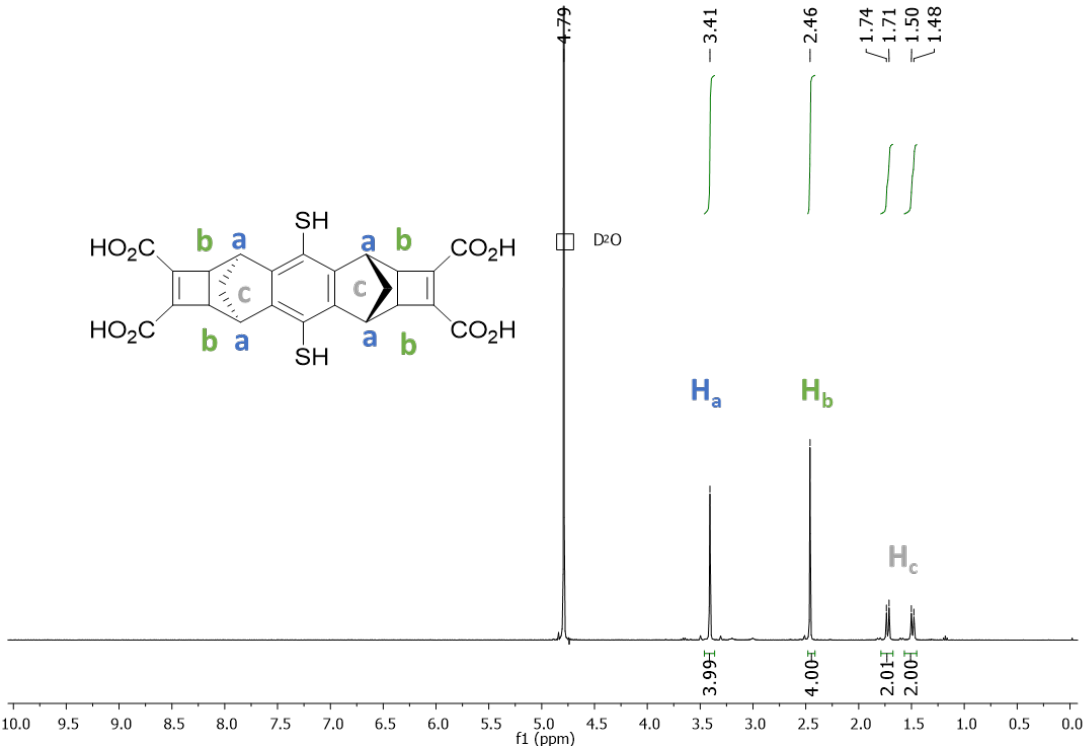

*Figure S78: ^{1}H NMR spectrum of compound **C***

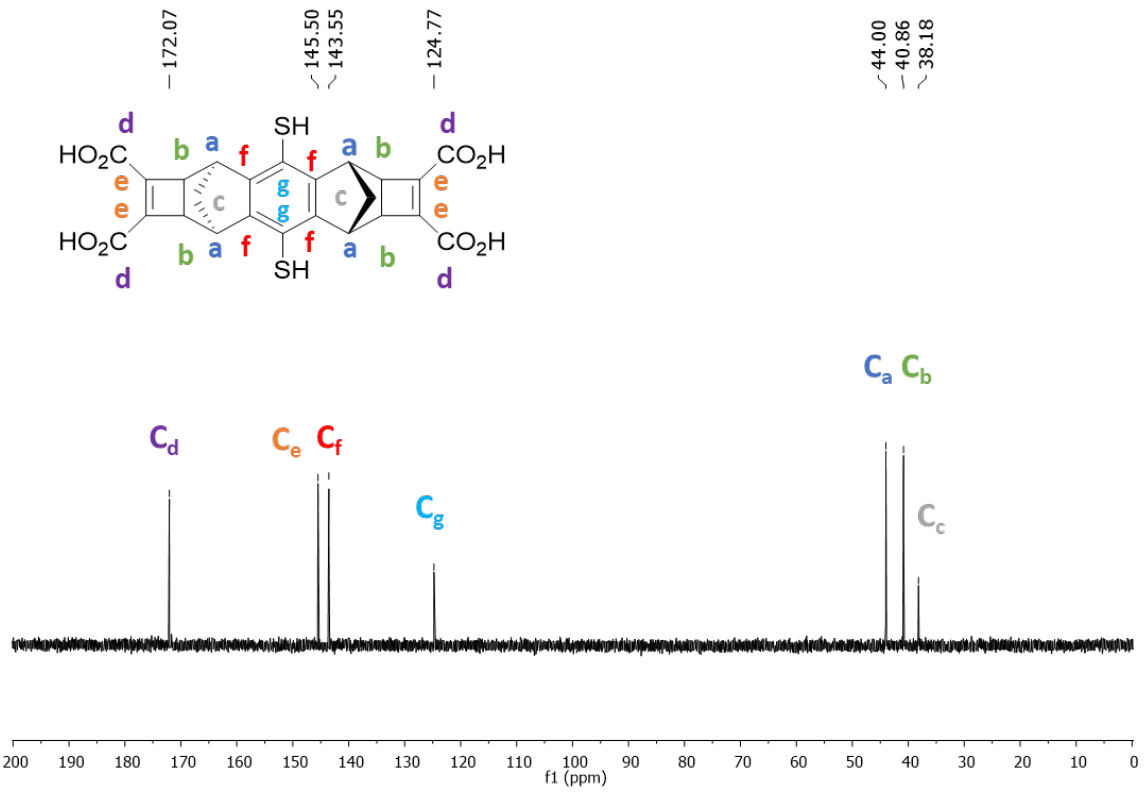

*Figure S79: ^{13}C NMR spectrum of compound **C***

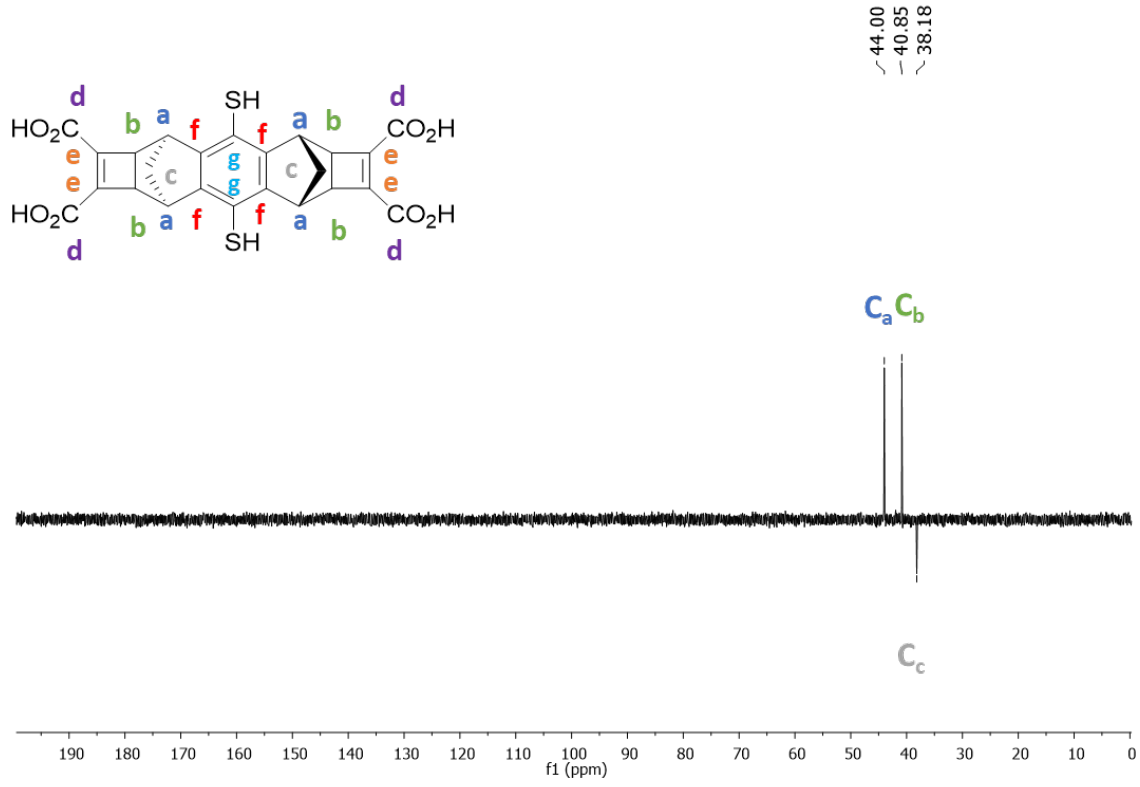

*Figure S80: DEPT ^{13}C NMR spectrum of compound **C***

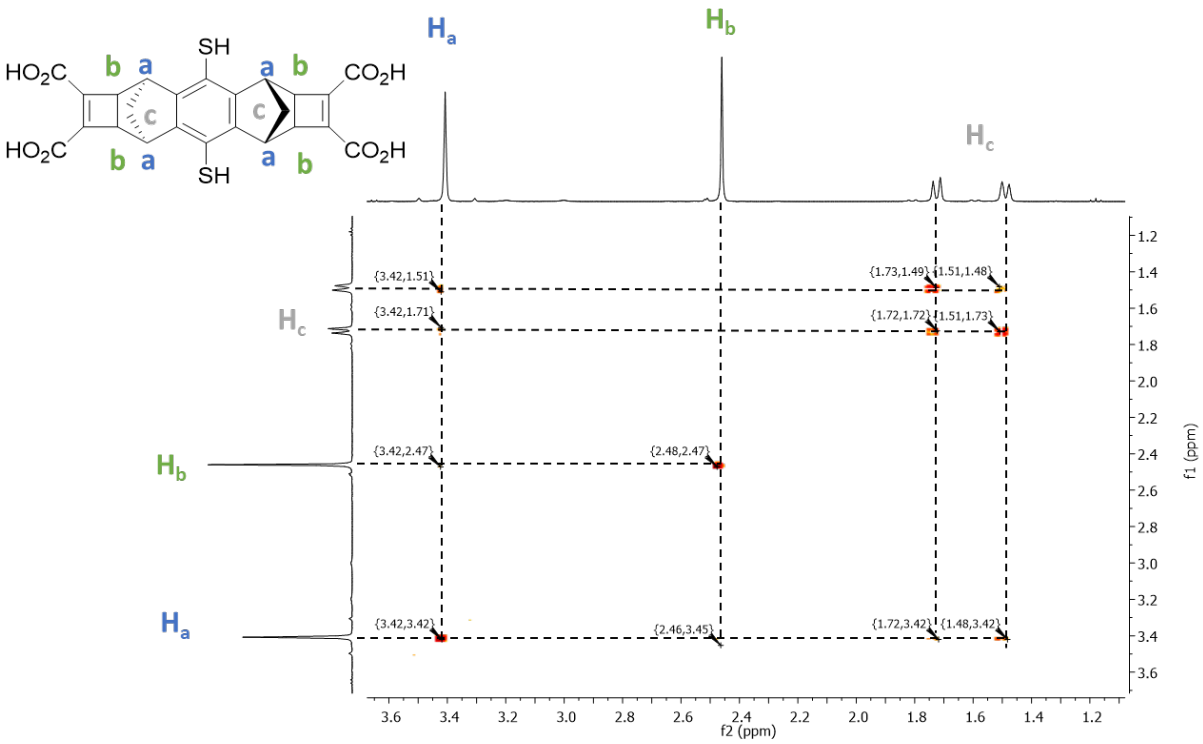

*Figure S81: COSY NMR spectrum of compound **C***

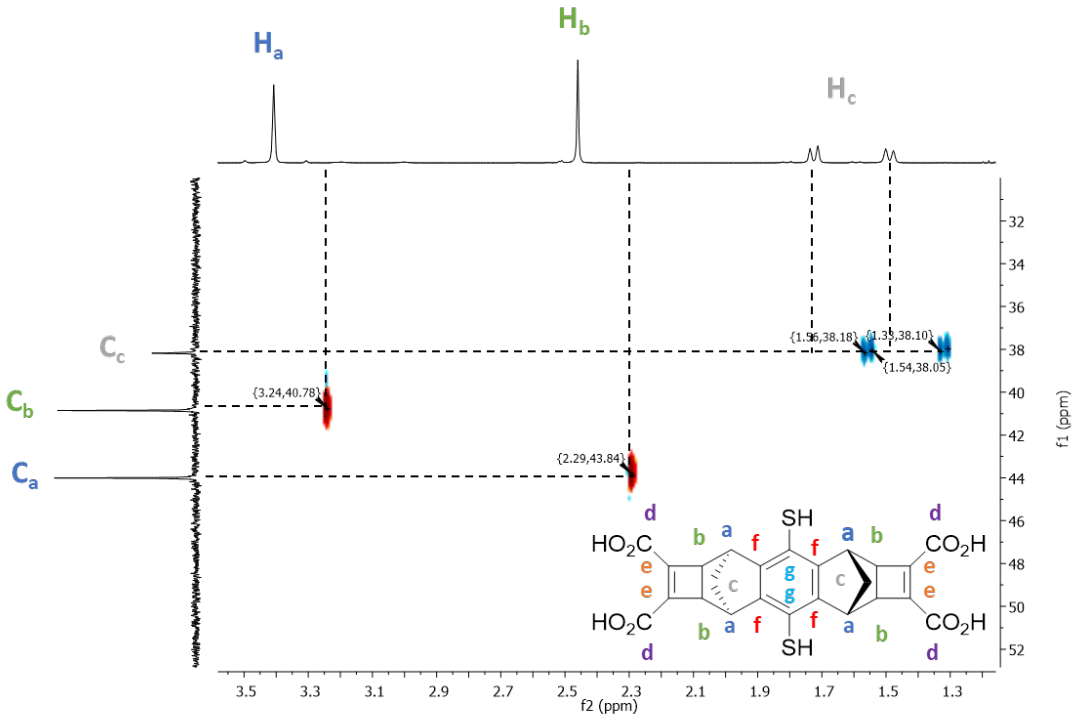

*Figure S82: HSQC NMR spectrum of compound **C***

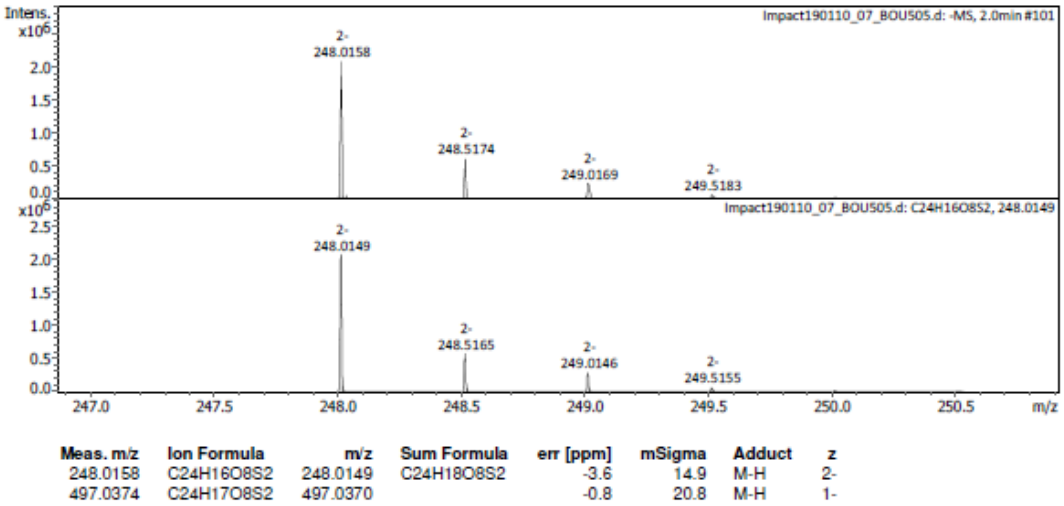

Meas. m/z	Ion Formula	m/z	Sum Formula	err [ppm]	mSigma	Adduct	z
248.0158	C24H16O8S2	248.0149	C24H18O8S2	-3.6	14.9	M-H	2-
497.0374	C24H17O8S2	497.0370		-0.8	20.8	M-H	1-

Figure S83: HR (-) ESI-MS spectrum of compound **C**

b. Aerobic oxidation of B and C

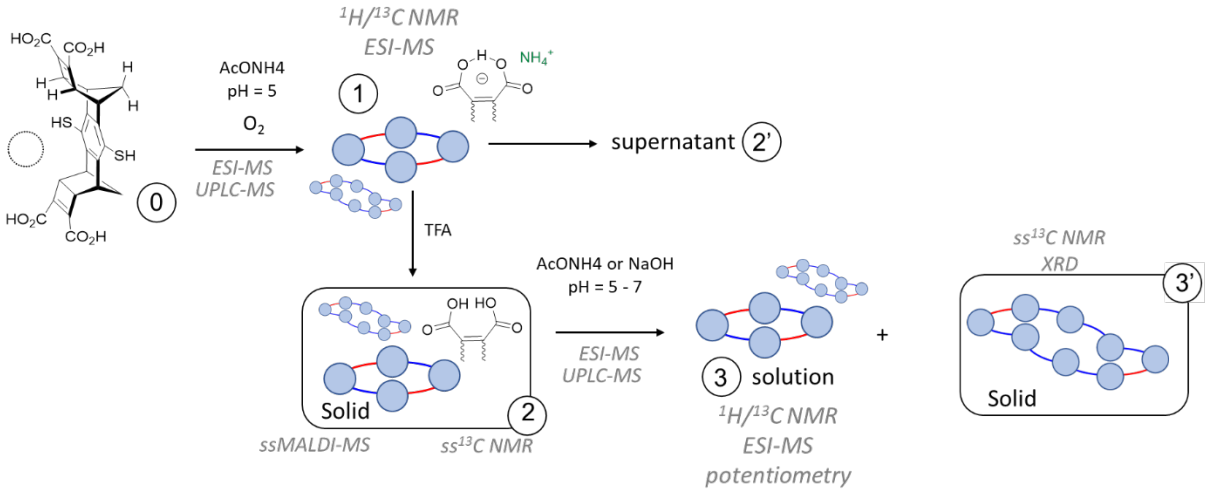

*Figure S84: Overview of the assembling procedure involving building block **B** and analyses conducted at each stage 1-3'.*

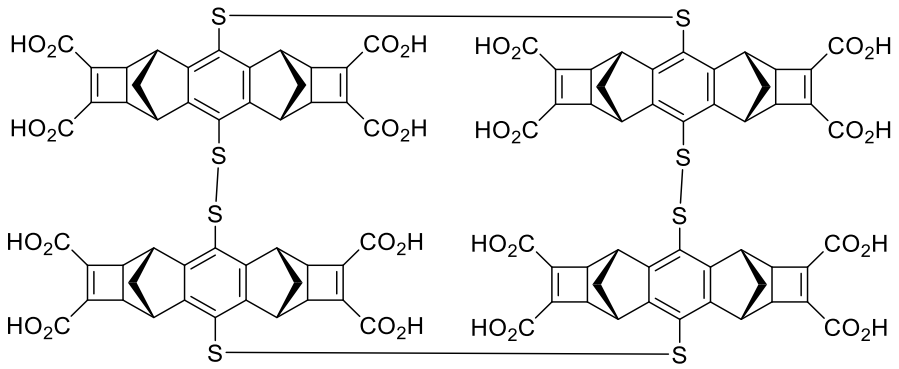

B_4

Self-assembling of B into B_4/B_8 (from stage 0 to 2).

A solution of **B** (3R,5S,8R,10S)-4,9-dimercapto-2a,3,5,5a,7a,8,10,10a-octahydro-3,10:5,8-dimethanodicyclobuta[b,i]anthracene-1,2,6,7-tetracarboxylic acid (stage, 0, Figure S84. 123 mg, 0.25 mmol, 1 eq) in aqueous ammonium acetate or $CD_3CO_2ND_4$ in D_2O (50 mL, 50 mM) was stirred for 36 h under air (reaching stage 1, Figure S84). The assembling process was monitored by ESI-MS, UPLC-MS (injection of 5 µL aliquots) or NMR. The same procedure was applied to isomer C. Then, TFA was added until pH 1 was reached. The resulting precipitate was filtrated and washed with water. Evaporation of the solvent gave a brown powder (stage 2, solid, 62 mg, 62 %).

Brown solid; mp: degradation, 321.7°C; MS (ESI) $[M - 2\ H]^{2-}$ found 991.047499, calculated 991.050042 for $[C_{96}H_{62}O_{32}S_8]^{2-}$; ^1H NMR (500 MHz, D_2O + 50 mM ND_4 CD_3COOD) δ ppm = 4.04 - 3.99 (m, 8 H), 3.11 - 3.06 (m, 8 H), 2.78 - 2.74 (m, 8 H), 2.50 - 2.46 (m, 8 H), 1.90 (d, J = 10.5 Hz, 4 H), 1.76 (d, J = 10.1 Hz, 4 H), 1.04 (d, J = 9.6 Hz, 4 H), 0.39 (d, J = 9.2 Hz, 4 H) (full attribution is described below); ^{13}C NMR (101 MHz, D_2O + 50 mM ND_4 CD_3COOD) δ ppm = 177.9, 167.1, 166.5, 149.5, 148.2, 147.8, 124.0, 123.9, 44.4, 43.8, 40.0, 39.4, 39.1, 39.0 (full attribution is described below).

c. Qualitative ESI-MS monitoring

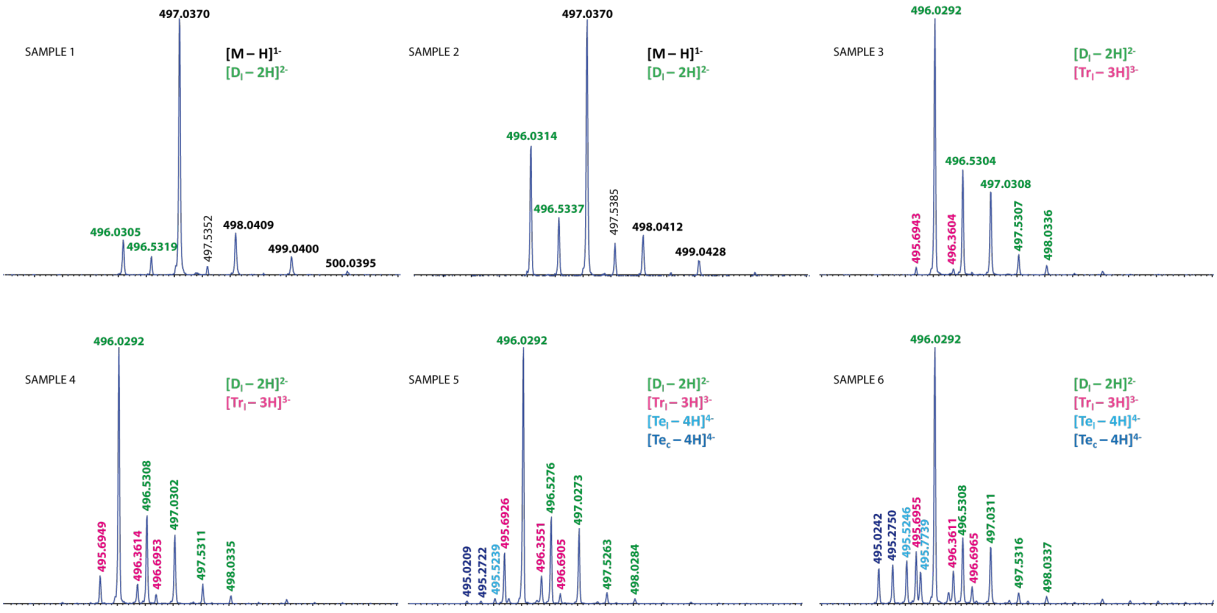

*Figure S85 : Qualitative overview of the chain elongation and ring closure process from **B** (5 mM) in 50 Ammonium acetate over time (M: monomer **B** D_l : linear dimer **B-B**; Tr_l :linear trimer **B-B-B;** Te_l : linear tetramer **B-B-B-B;** . Te_c:cyclic tetramer **B_4***

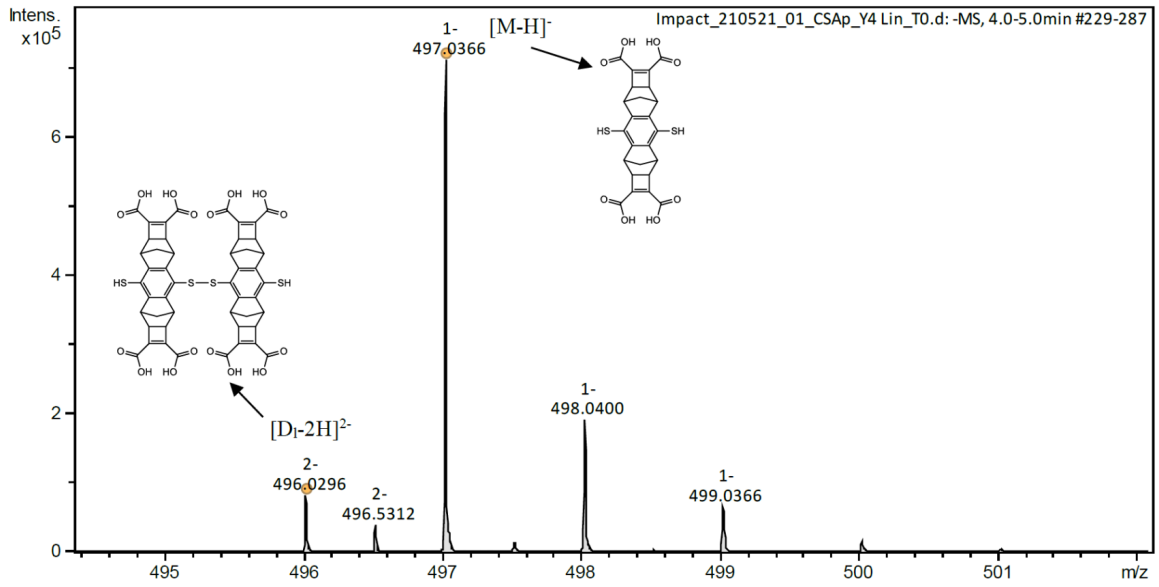

Meas. m/z	Ion Formula	Sum Formula	m/z	err [ppm]	mSigma	Adduct	z
496.0296	C48H32O16S4	C48H34O16S4	496.0292	-0.7	500.1	M-H	2-
497.0366	C24H17O8S2	C24H18O8S2	497.0370	0.9	24.5	M-H	1-

*Figure S86 : Detailed (-)ESI-MS spectrum (495-502 m/z range) of the library obtained immediately upon dissolution of **B** in 50 mM ammonium acetate*

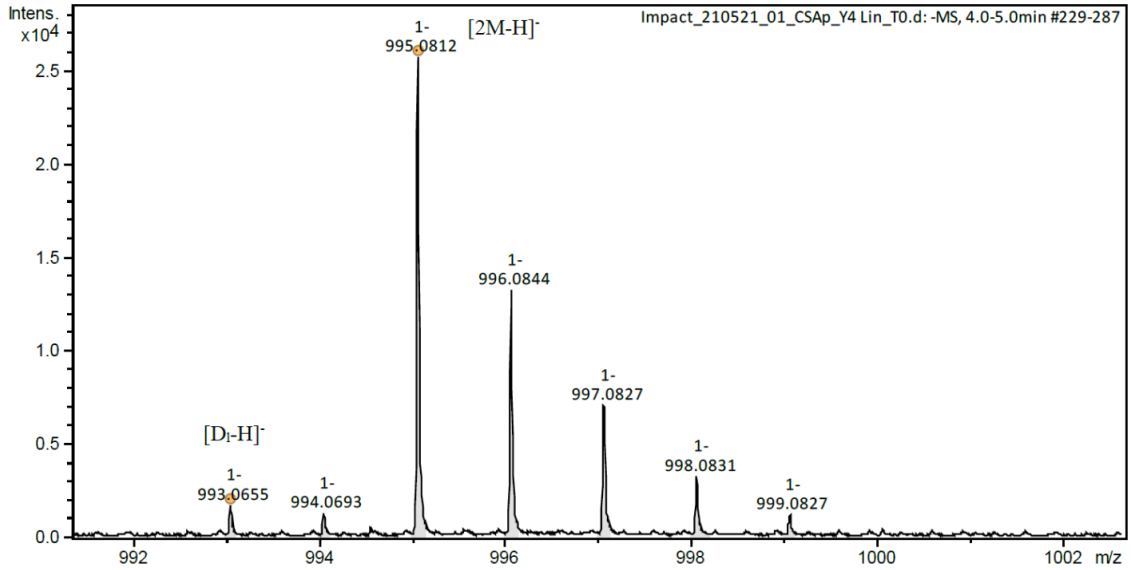

Meas. m/z	Ion Formula	Sum Formula	m/z	err [ppm]	mSigma	Adduct	z
993.0655	C48H33O16S4	C48H34O16S4	993.0657	0.2	175.7	M-H	1-
995.0812	C48H35O16S4	C24H18O8S2	995.0813	0.2	42.8	2M-H	1-

*Figure S87 : Detailed (-)ESI-MS spectrum (991-1003 m/z range) of the library obtained immediately upon dissolution of **B** in 50 mM ammonium acetate*

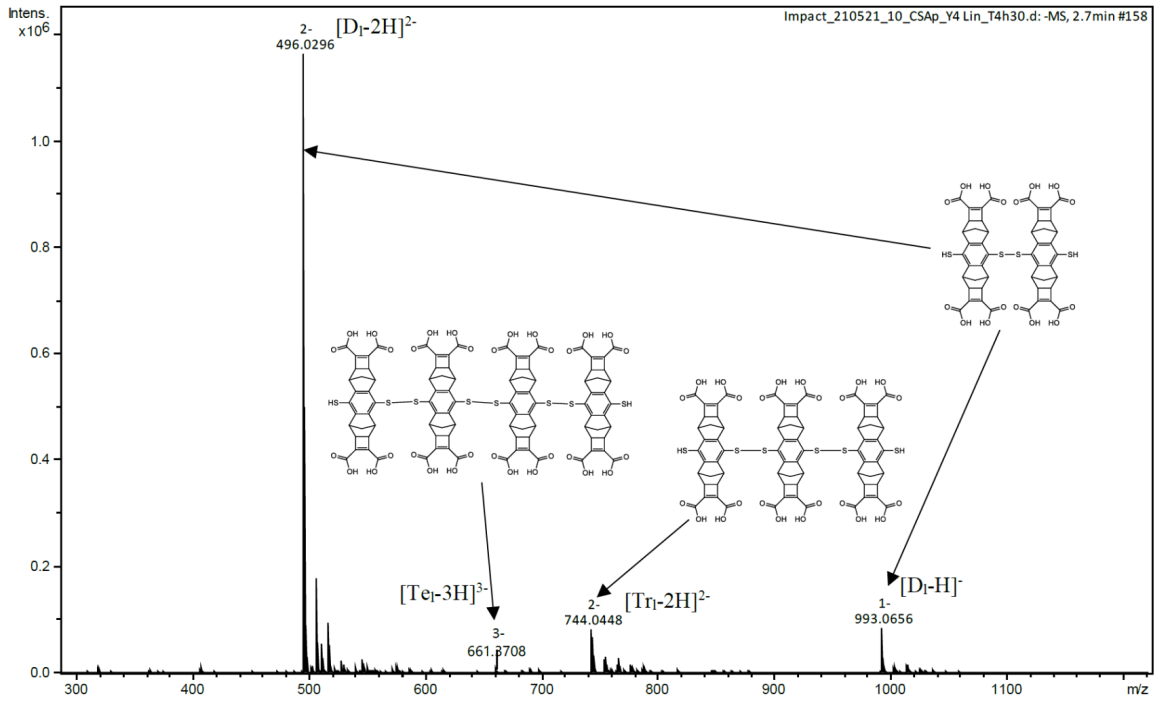

Meas. m/z	Ion Formula	Sum Formula	m/z	err [ppm]	mSigma	Adduct	z
496.0296	C48H32O16S4	C48H34O16S4	496.0292	-0.8	37.3	M-H	2-
993.0656	C48H33O16S4		993.0657	0.1	26.9	M-H	1-
661.0361	C96H63O32S8	C96H66O32S8	661.0362	0.1	40.1	M-H	3-
744.0448	C72H48O24S6	C72H50O24S6	744.0435	-1.7	38.7	M-H	2-

*Figure S88: Detailed (-)ESI-MS spectrum (300-1200 m/z range) of the library obtained 4h after dissolution of **B** in 50 mM ammonium acetate at stirring at 500 rpm*

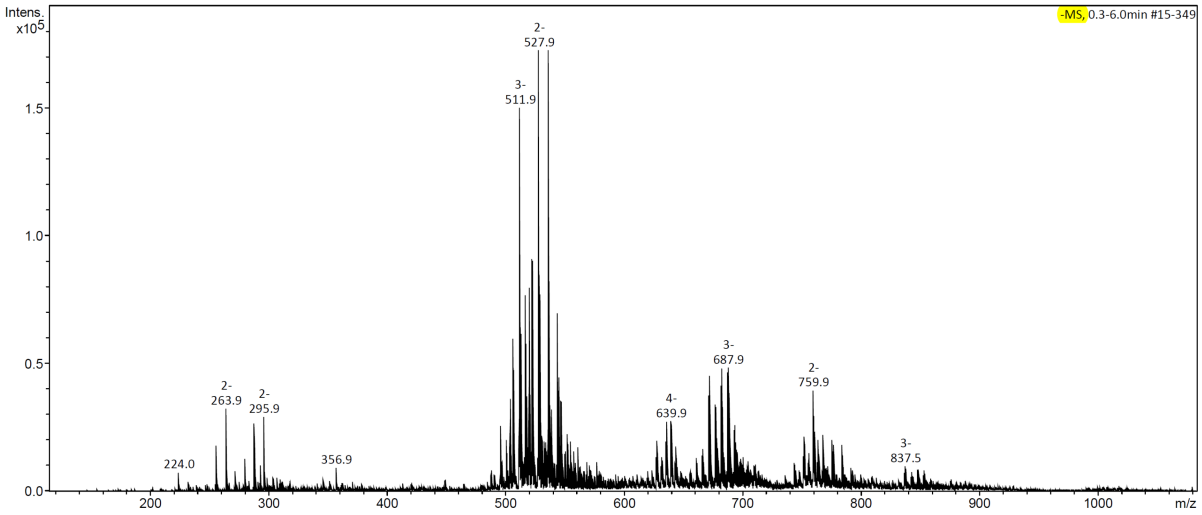

*Figure S89: broad range (-)ESI-MS spectrum (100-900 m/z range) of the library obtained 4h after dissolution of **C** in 50 mM ammonium acetate at stirring at 500 rpm*

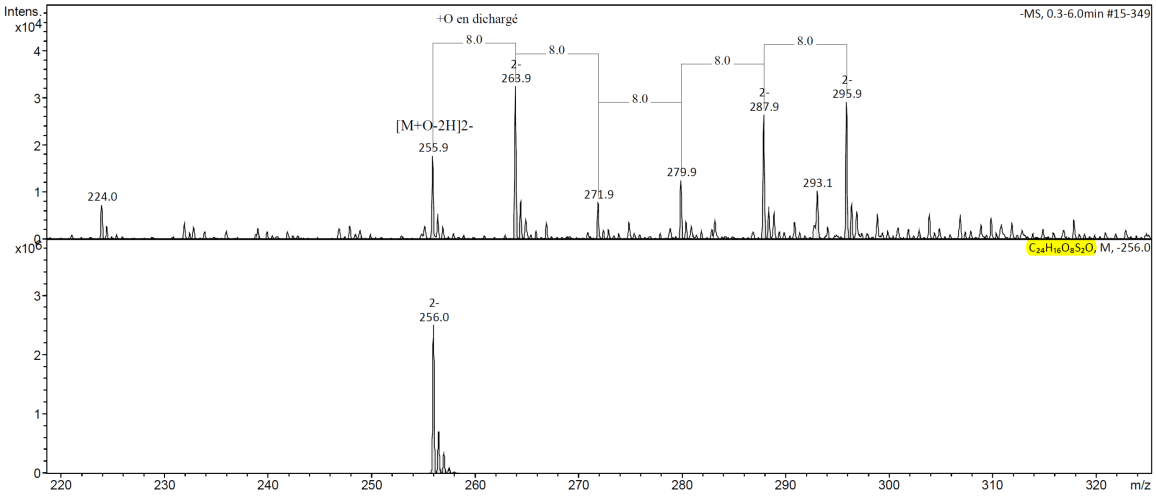

*Figure S90: zoomed (-)ESI-MS spectrum (220-320 m/z range) of the library obtained 4 h after dissolution of **C** in 50 mM ammonium acetate at stirring at 500 rpm highlighting the formation of **C**$(O)_{1\text{-}6}$ overoxidized species*

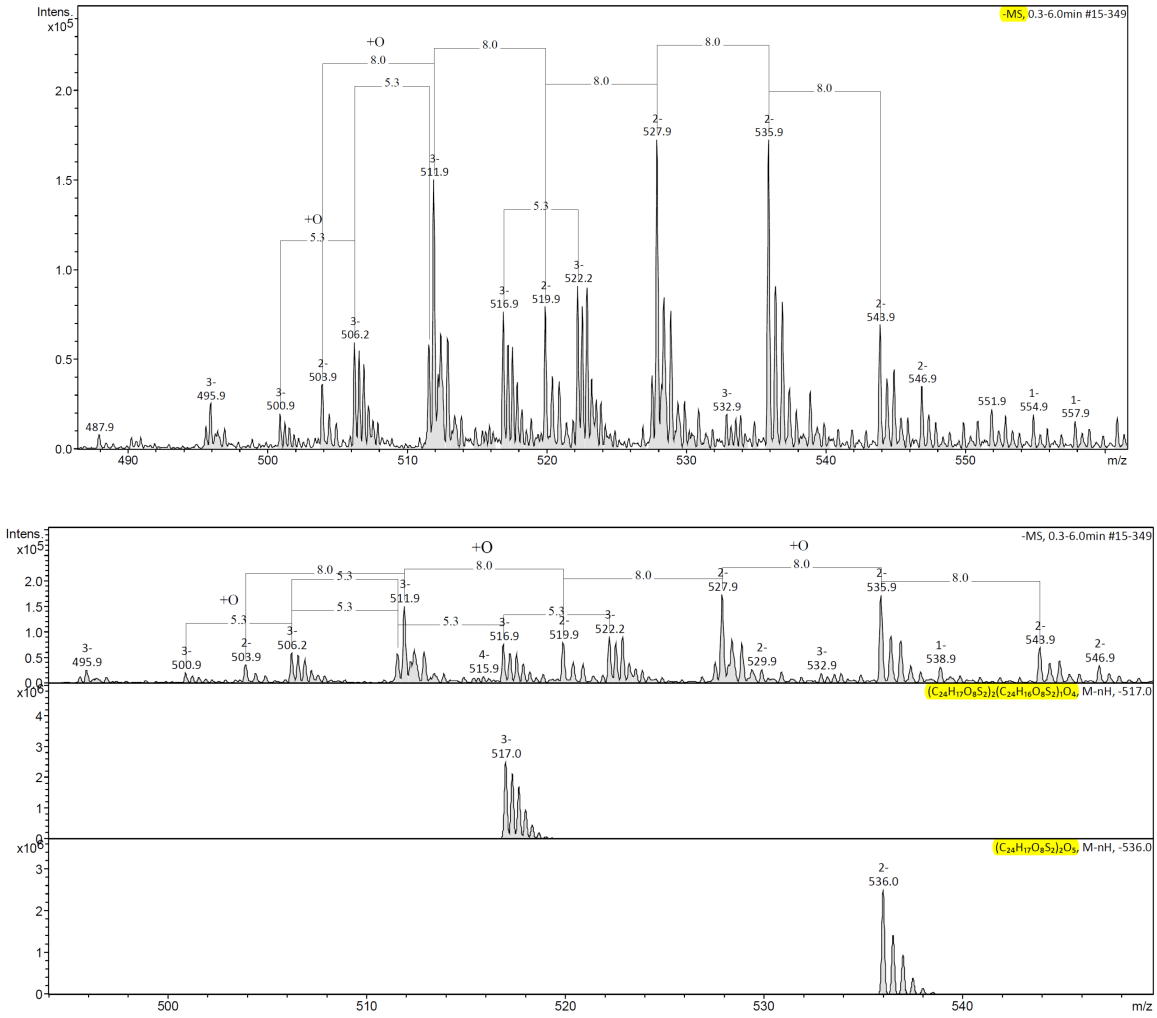

*Figure S91: zoomed (-)ESI-MS spectrum (480-560 m/z range) of the library obtained 4h after dissolution of **C** in 50 mM ammonium acetate at stirring at 500 rpm highlighting the formation of **CC**$(O)_{1\text{-}6}$ and **CCC**$(O)_{1\text{-}7}$ overoxidized species*

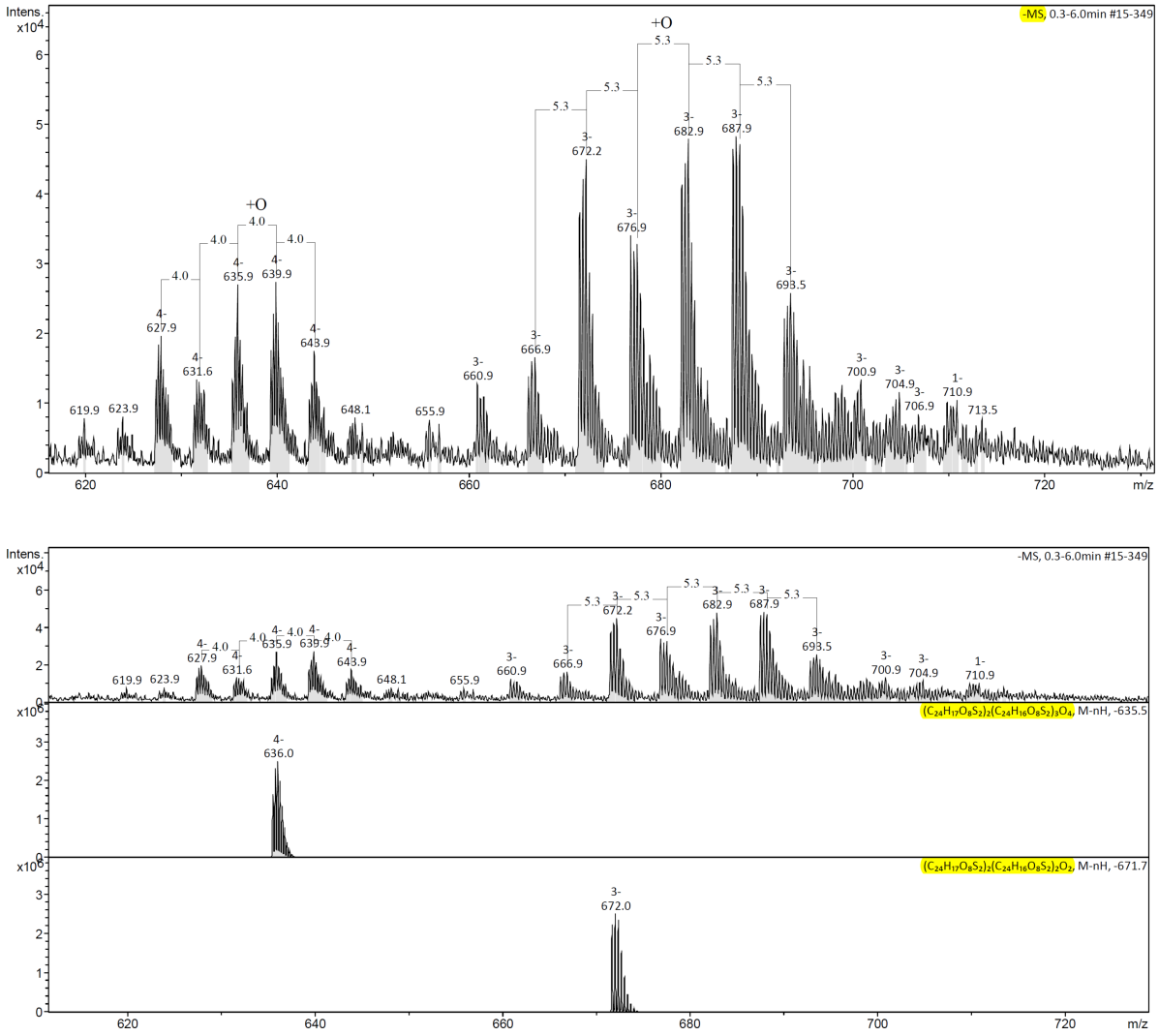

Figure S92: zoomed (-)ESI-MS spectrum (610-730 m/z range) of the library obtained 4h after dissolution of ***C*** *in 50 mM ammonium acetate at stirring at 500 rpm highlighting the formation of* ***CCCC****(O)*$_{1\text{-}9}$ *and* ***CCCCC****(O)*$_{1\text{-}7}$ *overoxidized species*

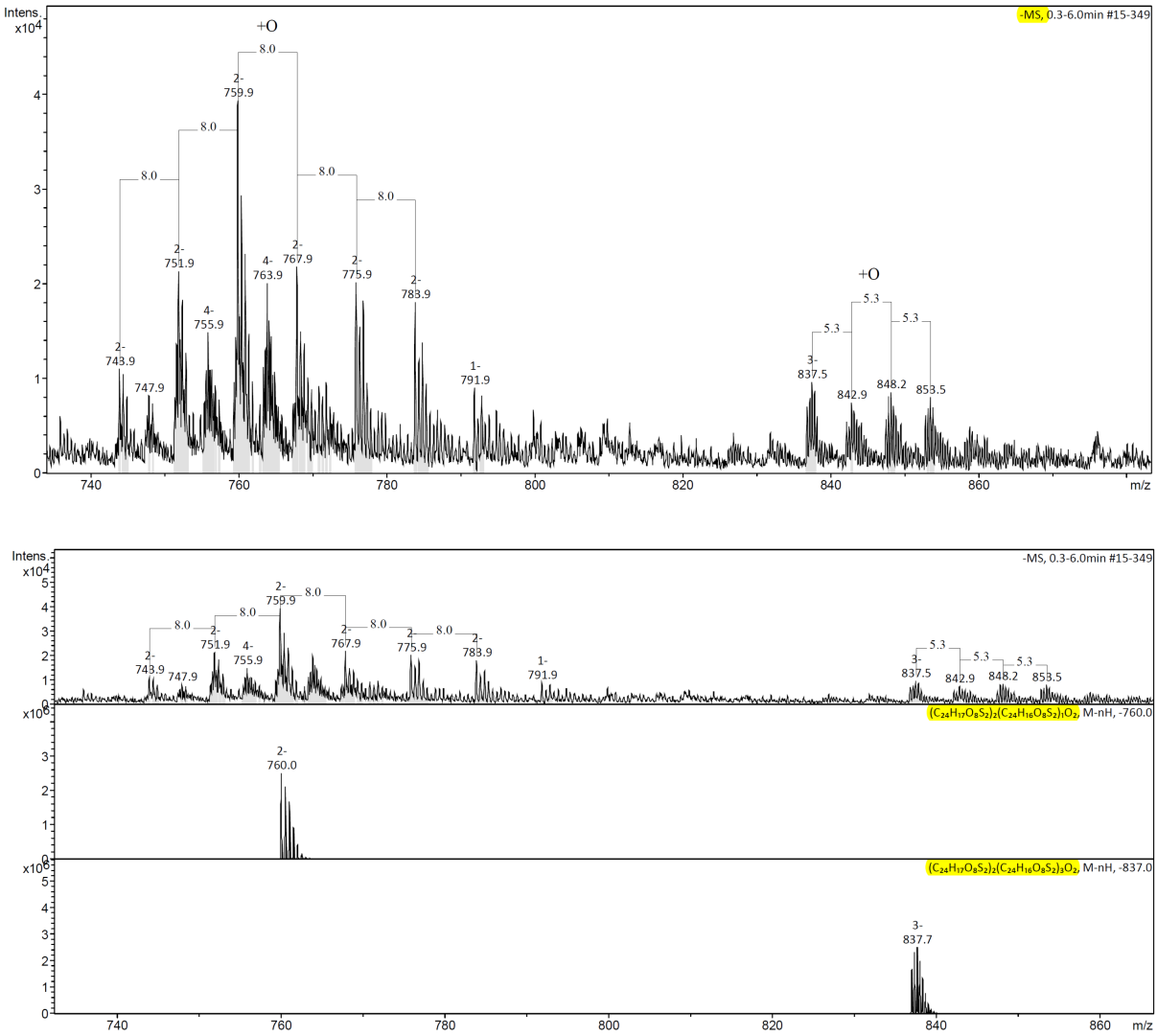

Figure S93: zoomed (-)ESI-MS spectrum (730-870 m/z range) of the library obtained 4h after dissolution of ***C*** *in 50 mM ammonium acetate at stirring at 500 rpm highlighting the formation of* ***CCC****(O)*$_{1\text{-}6}$ *and* ***CCCCC****(O)*$_{1\text{-}5}$ *overoxidized species*

d. Quantitative UPLC MS monitoring

UPLC-UV traces

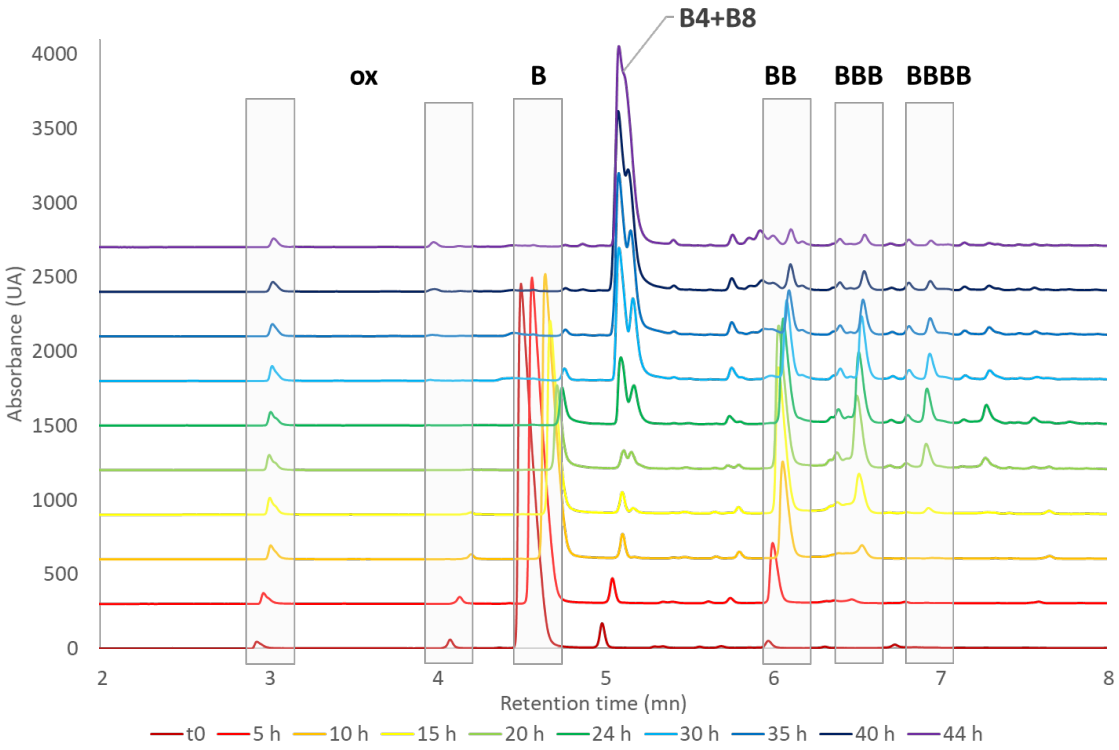

*Figure S94 :UV-UPLC monitoring at 250 nm of the library generated from **B** (5 mM) in $AcONH_4$ 50 mM stirred at 500 rpm*

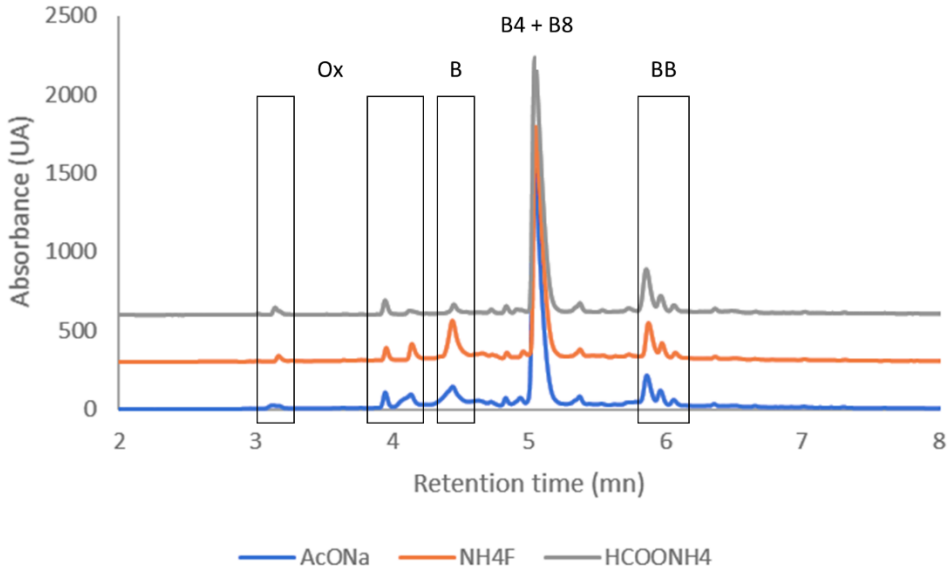

*Figure S95 :UV-UPLC monitoring at 250 nm of the library generated from **B** (5 mM) in the presence of 50 mM concentration of various salt, at pH 5.5 and stirred at 500 rpm for 48 hours*

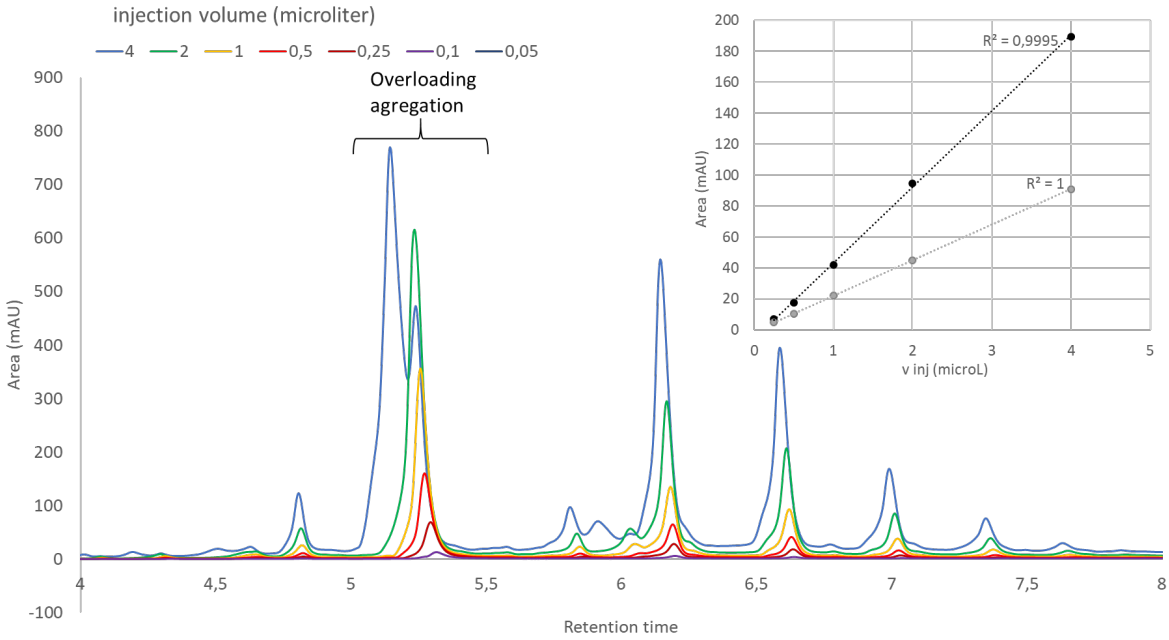

*Figure S96: Decreasing volume injection of the unstirred library prepared from **B** (5 mM) in ammonium acetate 50 mM after 50h. Shouldering of the **B**$_4$/**B**$_8$ peak at 5.2 min can be attributed to overloading and aggregation. Linearity of the integration (black dots: total area, grey dots: peak and shoulder from 5 – 5.5 min) confirms the absence that no fraction of the library remains retained by the column.*

UPLC-UV integration

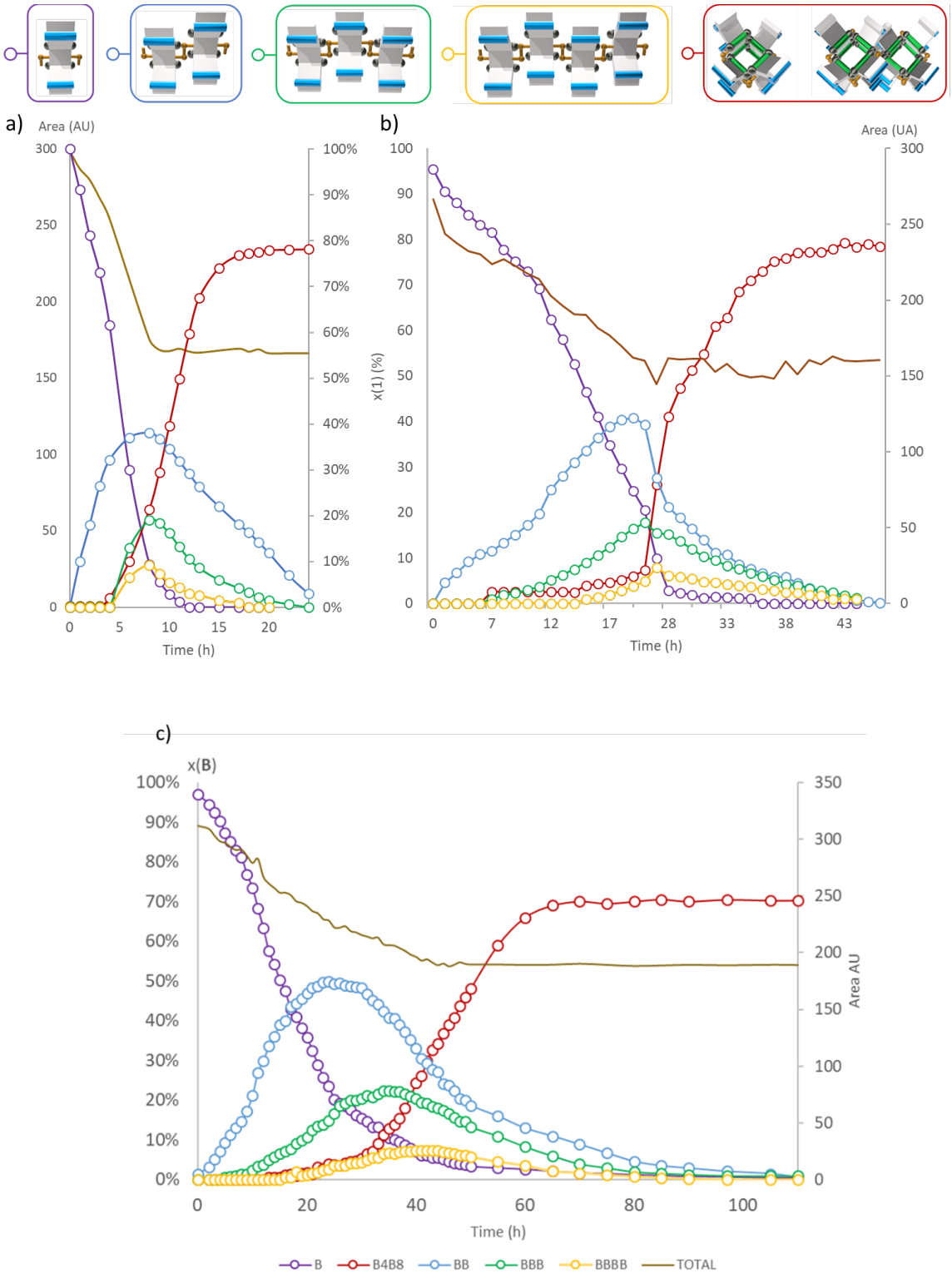

*Figure S97 :Relative quantification of cyclic oligomers generated from **B** (5mM) in 50 mM $CH_3CO_3NH_4$ pH 5.5 by UPLC-UV (250 nm) and total area (brown curve) with stirring rates of: a) 1000, b): 500 and c): 0 rpm*

MS data

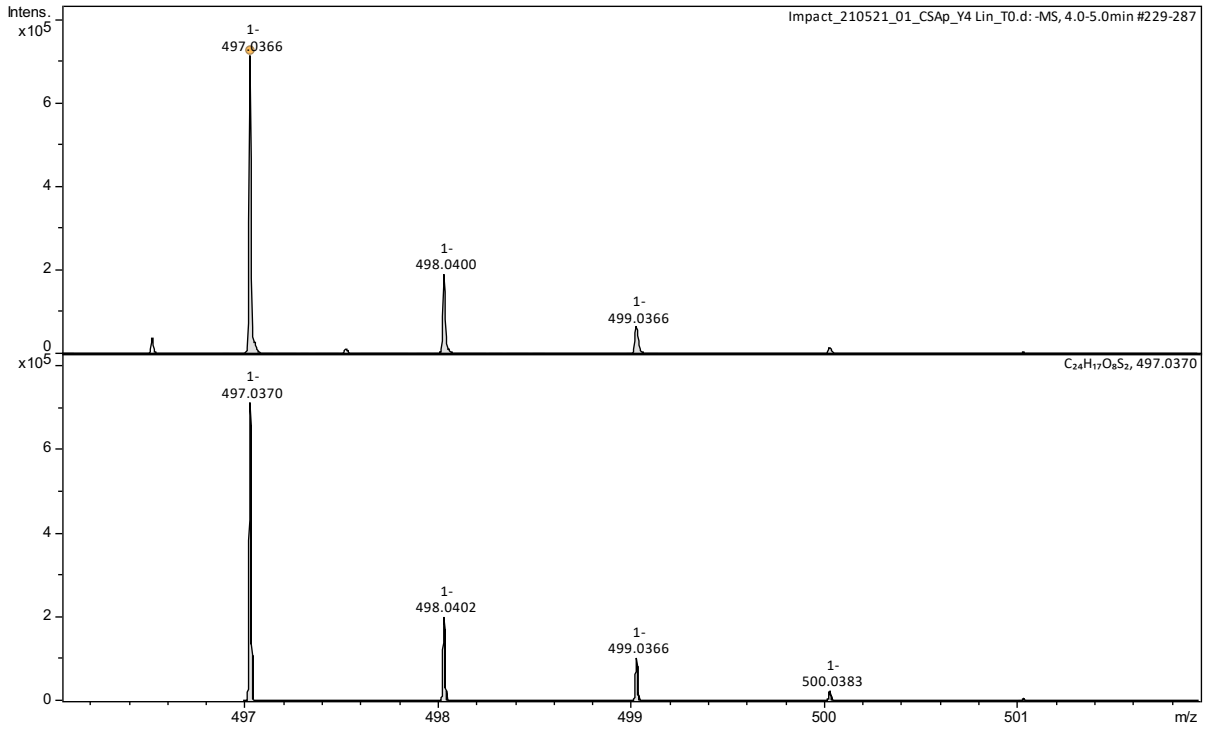

Meas. m/z	Ion Formula	Sum Formula	m/z	err [ppm]	mSigma	Adduct	z
497.0366	C24H17O8S2	C24H18O8S2	497.0370	0.9	24.5	M-H	1-

*Figure S98 :(-)ESI-MS snapshot of the **B** peak at 4.7 min ([**B**-H]$^-$ species) and comparison with the theoretical spectrum*

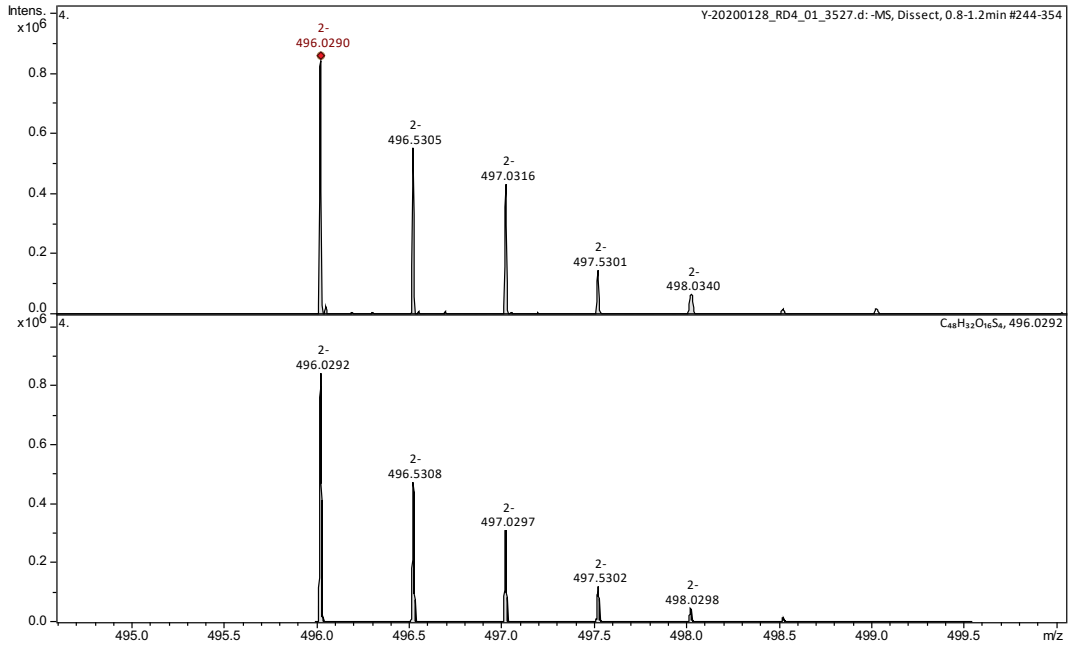

Meas. m/z	Ion Formula	Sum Formula	m/z	err [ppm]	mSigma	Adduct	z
496.0290	C48H32O16S4	C48H34O16S4	496.0292	0.5	45.6	M-H	2-

*Figure S99 :(-)ESI-MS snapshot of the **BB** peak at 4.7 min ([**BB**-2H]$^{2-}$ species) and comparison with the theoretical spectrum*

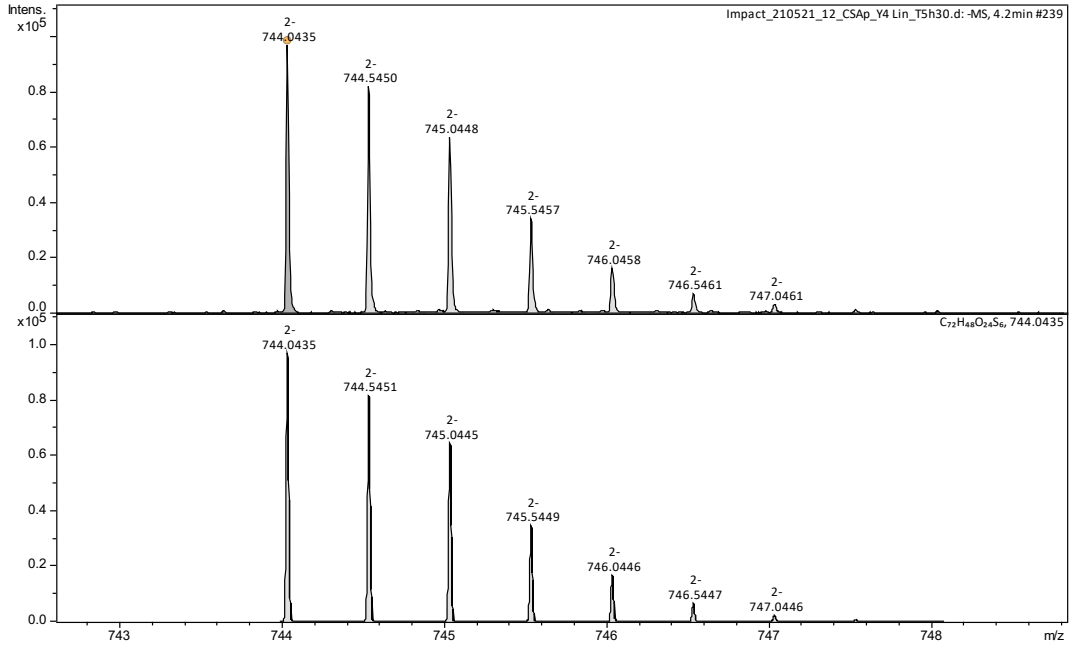

Meas. m/z	Ion Formula	Sum Formula	m/z	err [ppm]	mSigma	Adduct	z
744.0435	C72H48O24S6	C72H50O24S6	744.0435	0.1	6.4	M-H	2-

*Figure S100 :(-)ESI-MS snapshot of the **BBB** peak at 6.7 min ([**BBB**-2H]$^{2-}$ species) and comparison with the theoretical spectrum*

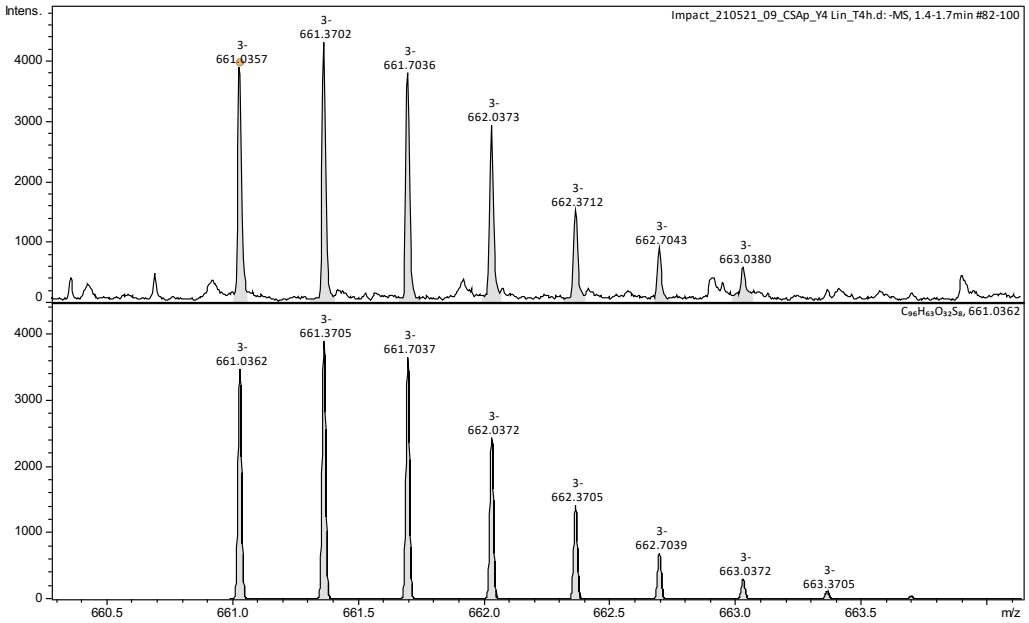

Meas. m/z	Ion Formula	Sum Formula	m/z	err [ppm]	mSigma	Adduct	z
661.0357	C96H63O32S8	C96H63O32S8	661.0362	0.7	37.5	M	3-

*Figure S101 :(-)ESI-MS snapshot of the **BBBB** peak at 7.0 min ([**BBBB**-3H]$^{3-}$ species) and comparison with the theoretical spectrum*

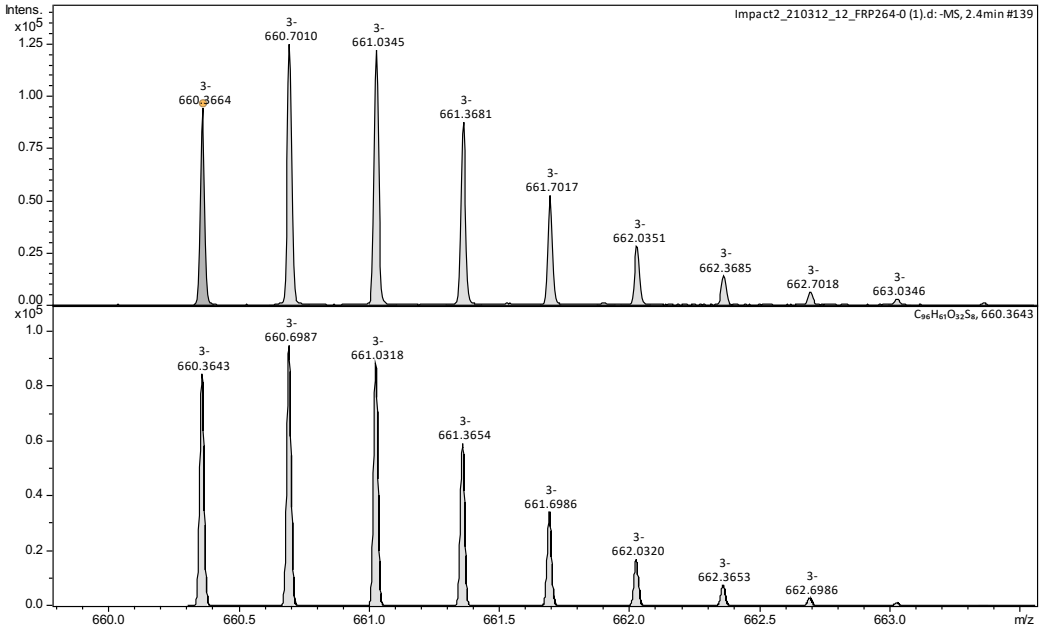

Meas. m/z	Ion Formula	Sum Formula	m/z	err [ppm]	mSigma	Adduct	z
660.3664	C96H61O32S8	C96H64O32S8	660.3643	-3.2	65.2	M-H	3-

*Figure S102 :(-)ESI-MS snapshot of the **B$_4$-B$_8$** peak at 5.3 min ([**B$_4$**-3H]$^{3-}$ species) and comparison with the theoretical spectrum*

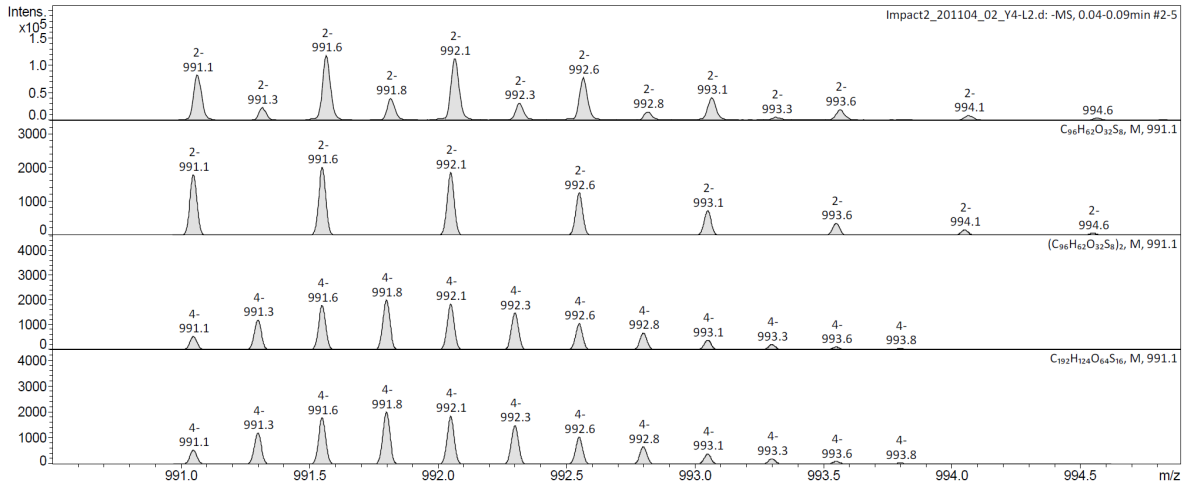

*Figure S103 :(-)ESI-MS snapshot of the **B_4-B_8** peak at 5.3 min ($[B_4\text{-}2H]^{2-}$ $[B_8\text{-}4H]^{4-}$ and species) and comparison with the theoretical spectrum*

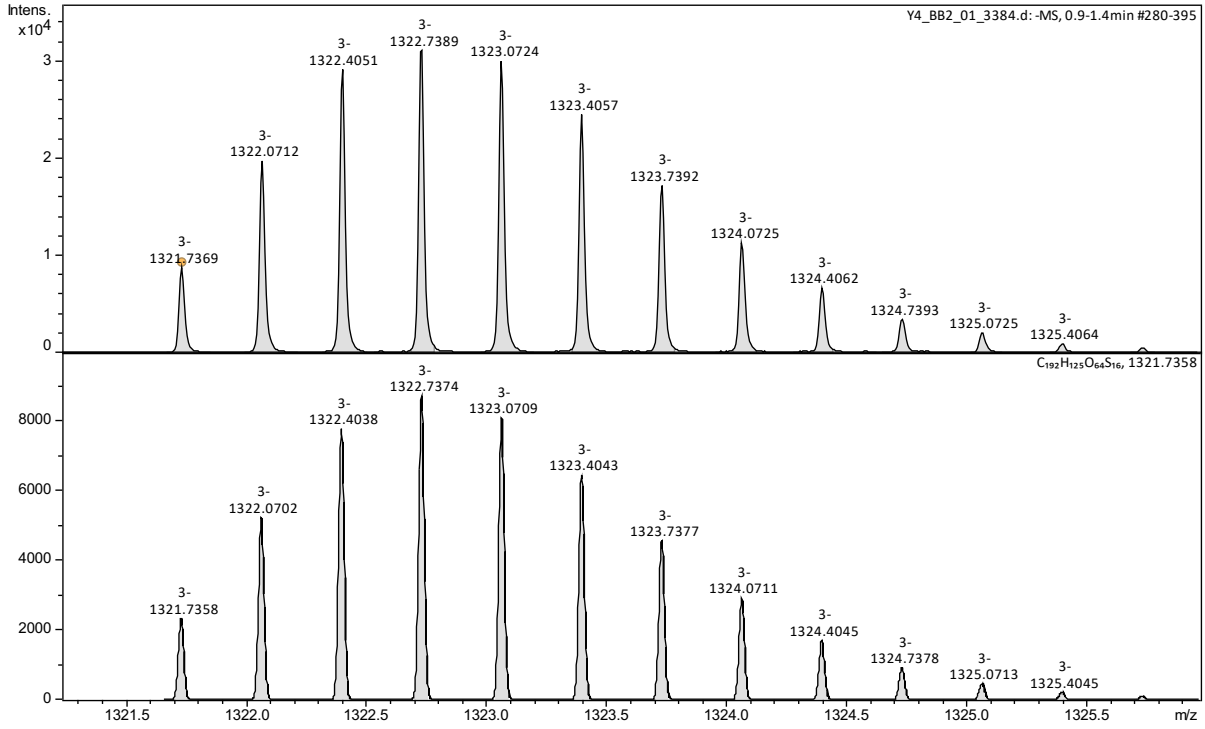

Meas. m/z	Ion Formula	Sum Formula	m/z	err [ppm]	mSigma	Adduct	z
1321.7369	C192H125O64S16	C192H128O64S16	1321.7358	-0.8	26.8	M-H	3-

*Figure S104 :(-)ESI-MS snapshot of the **B_4-B_8** peak at 5.3 min ($[B_8\text{-}3H]^{3-}$ species) and comparison with the theoretical spectrum*

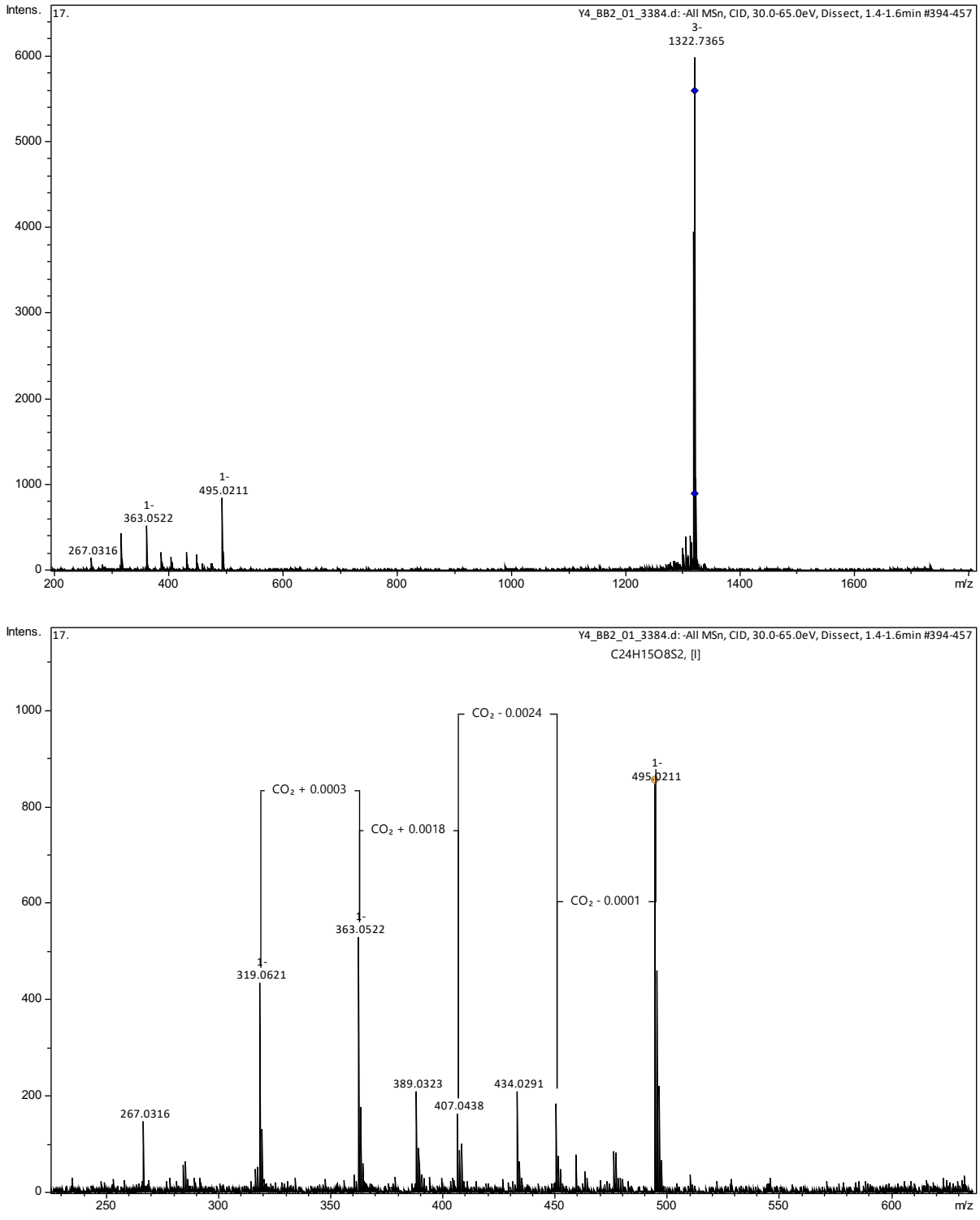

Figure S105 :(-)ESI-MS/MS fragmentation of the $[\boldsymbol{B_8}\text{-}3H]^{3-}$ species yielding the $[\boldsymbol{B}\text{-}H]^-$ ion

e. Solid state analysis of **B_4/B_8** solid (stage 2)

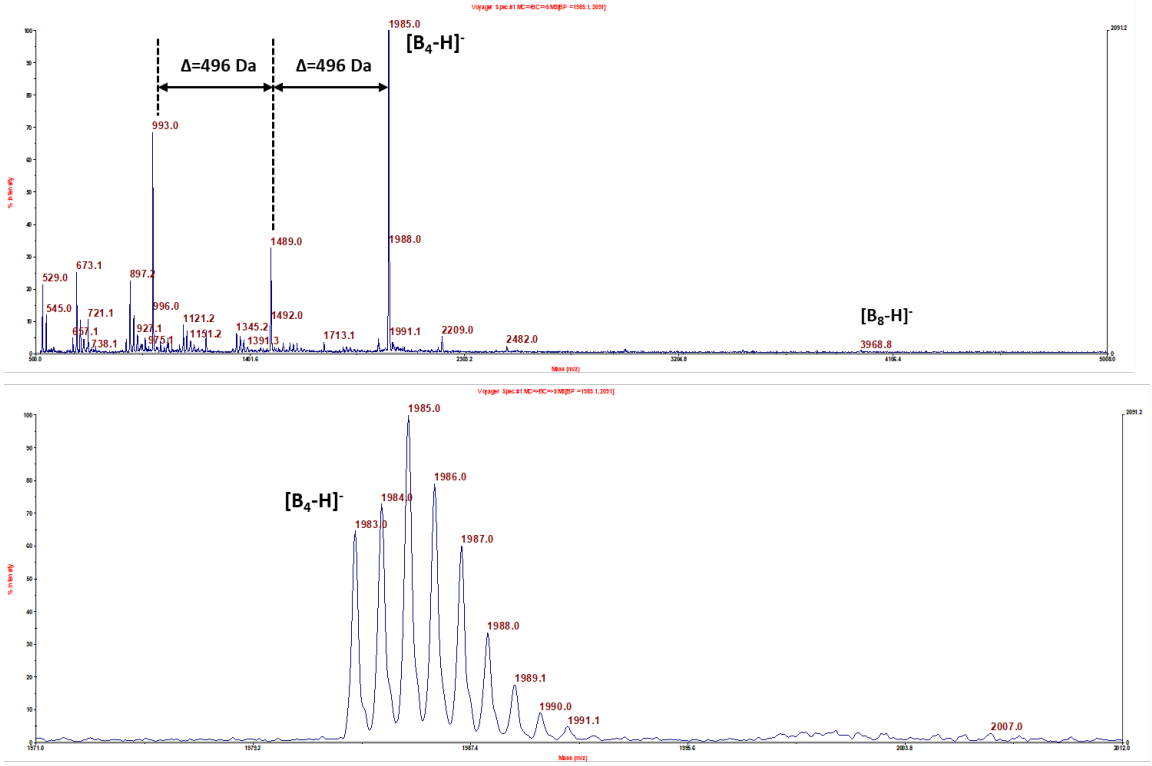

*Figure S106: Solid state MALDI spectrum of solid **B_4/B_8** after acidic precipitation (stage 2)*

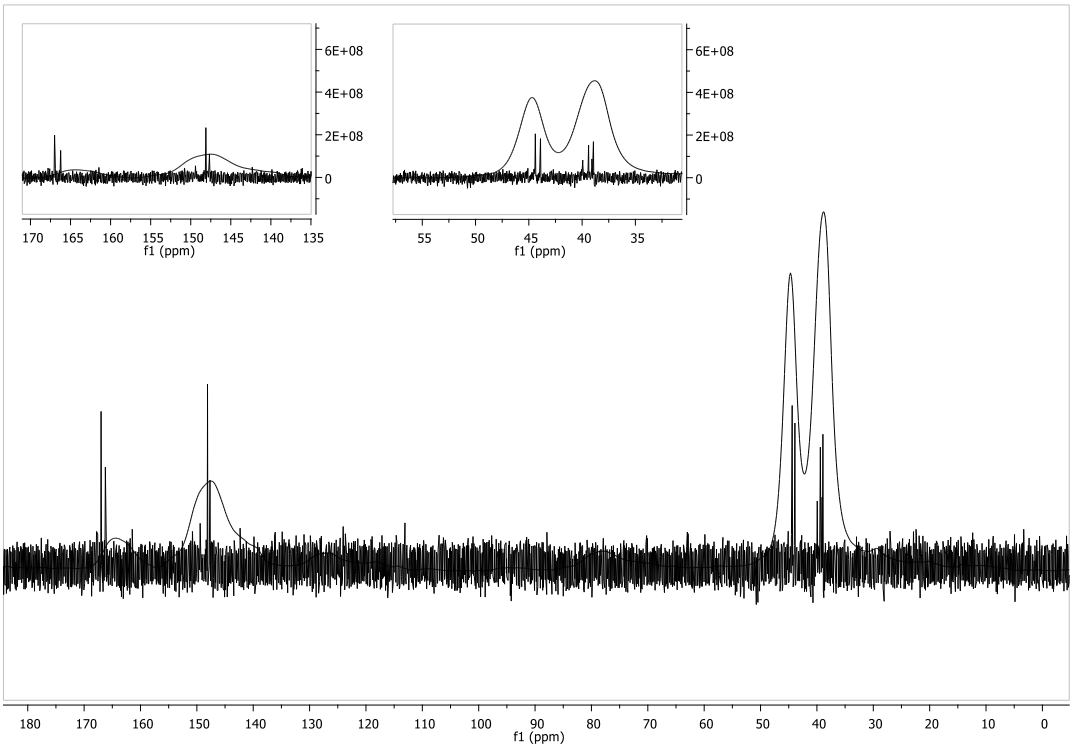

*Figure S107: Comparison between solid CP-MAS and liquid state ^{13}C spectra of **B_4-B_8** mixture obtained upon precipitation with TFA (stage 2) and upon redissolution at 1 mM (stage 3)*

f. Analysis of the redissolved **B_4/B_8**

Potentiometric titration on B_4/B_8

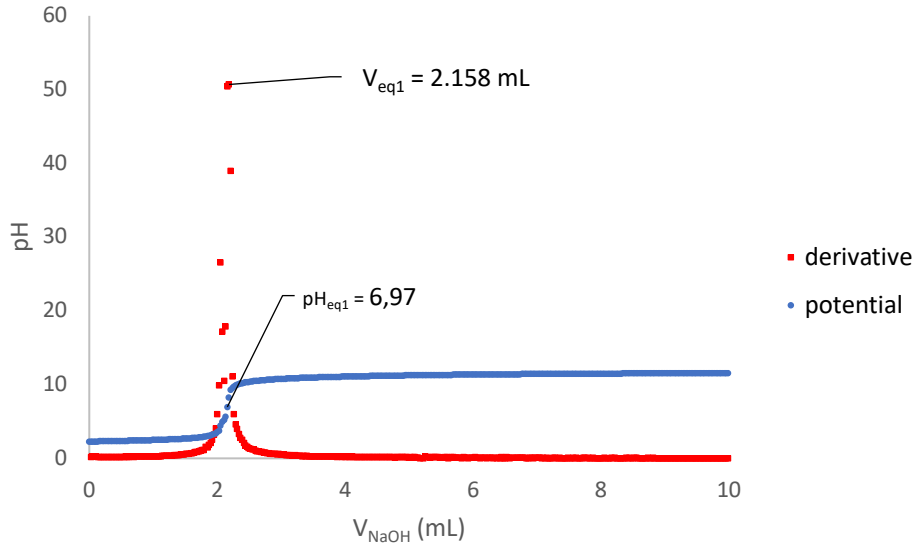

Figure S108 : Potentiometric reference titration (1 mL HCl (0,0958 mM) + 9 mL milliQ water)

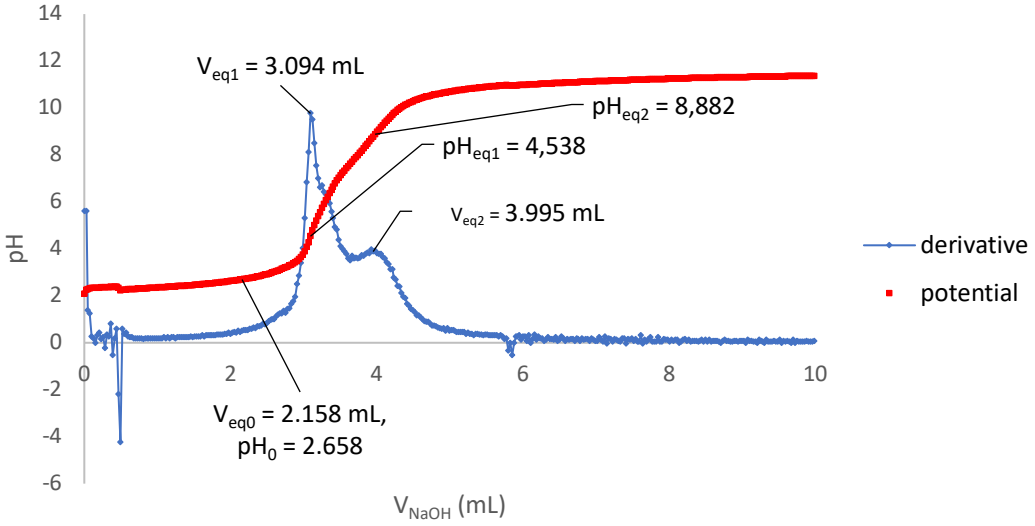

*Figure S109 : Potentiometric titration of **B_4-B_8** (11.0 mg of B_4 + 1 mL HCl (0,0958 mM) + 9 mL milliQ water)*

NMR data on 5 mM unsaturated samples

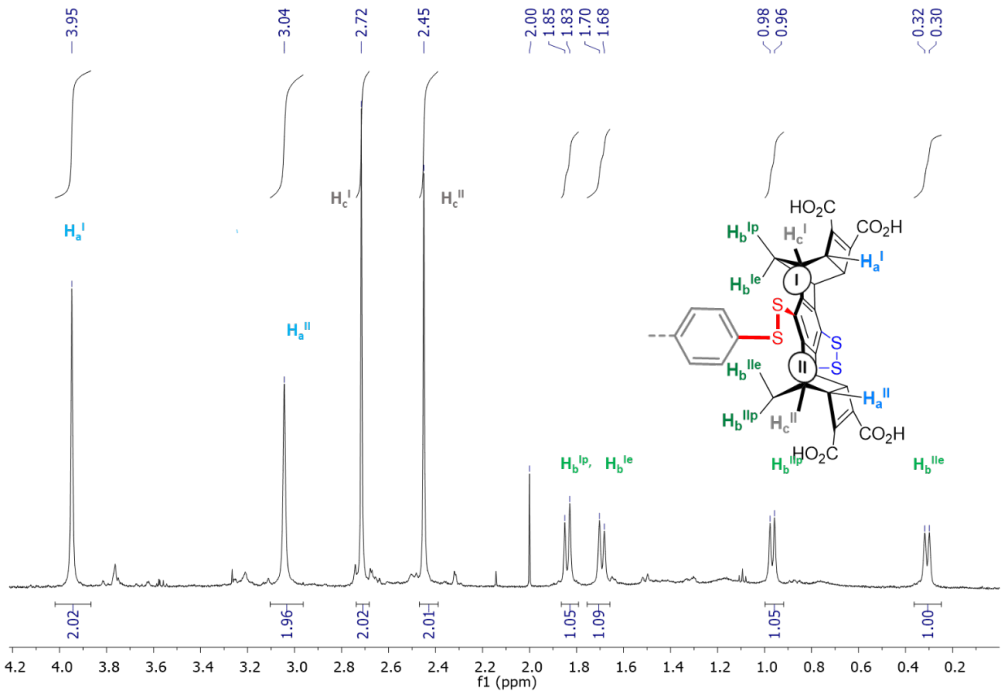

*Figure S110: ^{1}H NMR spectrum of the **B_4-B_8** system obtained after precipitation and redissolution in 50 mM $CD_3CO_2ND_4$ in D_2O*

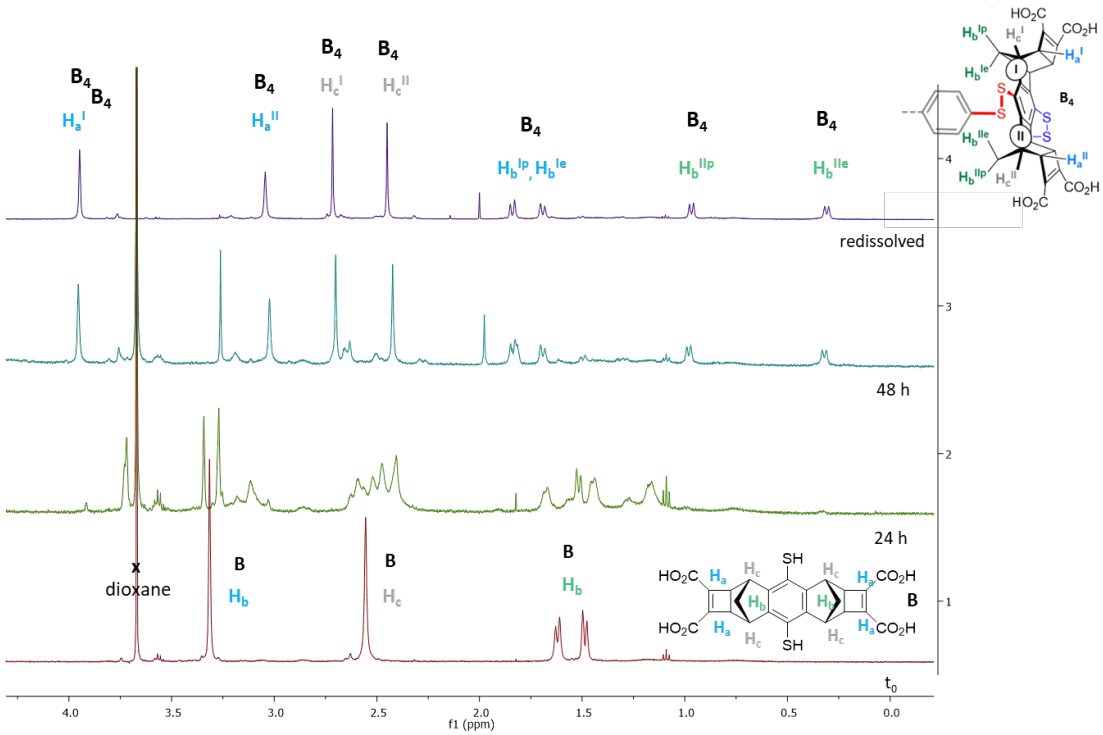

*Figure S111: Comparison between the ^{1}H spectrum of library generated from **B** (bottom) in $CD_3CO_2ND_4$ 50 mM, at 24h (green) and 48h (cyan) and of the system obtained after precipitation and redissolution in 50 mM $CD_3CO_2ND_4$ in D_2O (purple)*

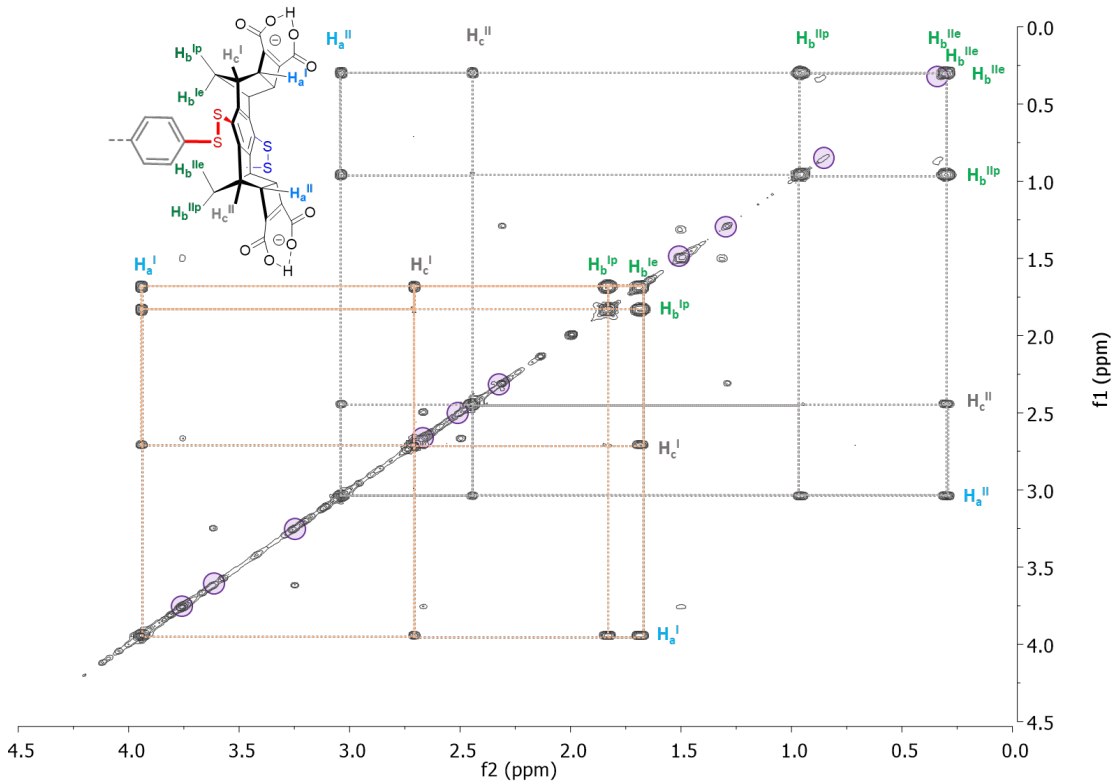

*Figure S112: ^{1}H COSY spectrum of the **B_4-B_8** system obtained after precipitation and redissolution in 50 mM $CD_3CO_2ND_4$ in D_2O*

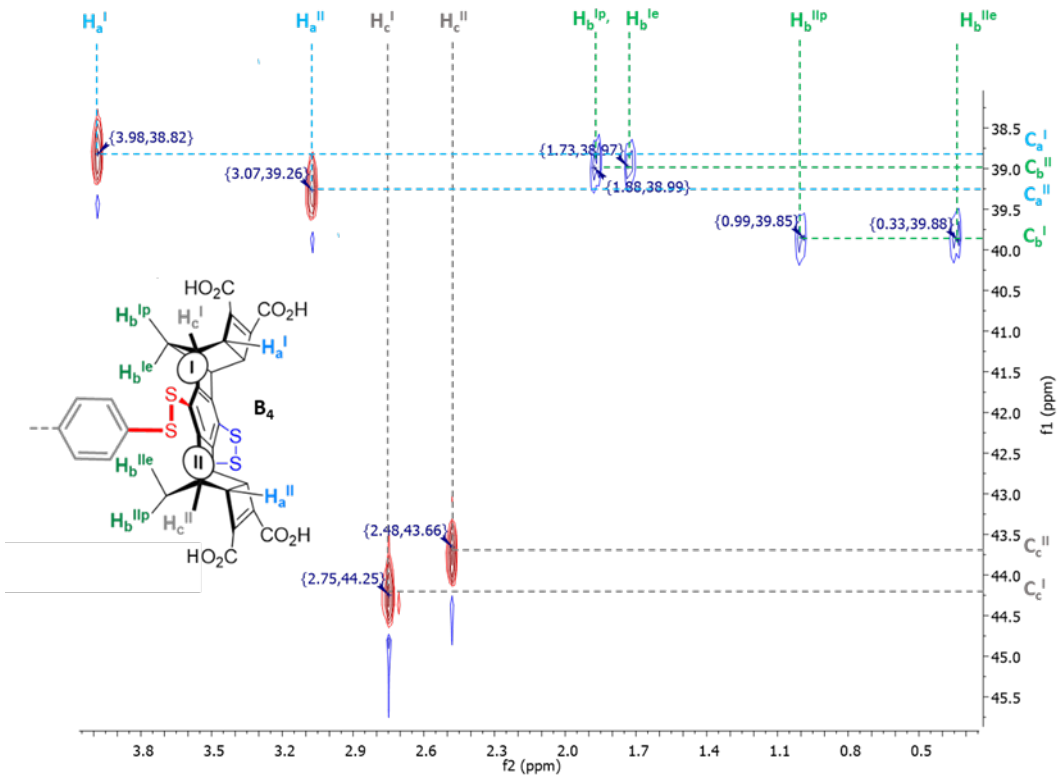

*Figure S113: ^{1}H-^{13}C HSQC spectrum of the **B_4-B_8** system obtained after precipitation and redissolution in 50 mM $CD_3CO_2ND_4$ in D_2O*

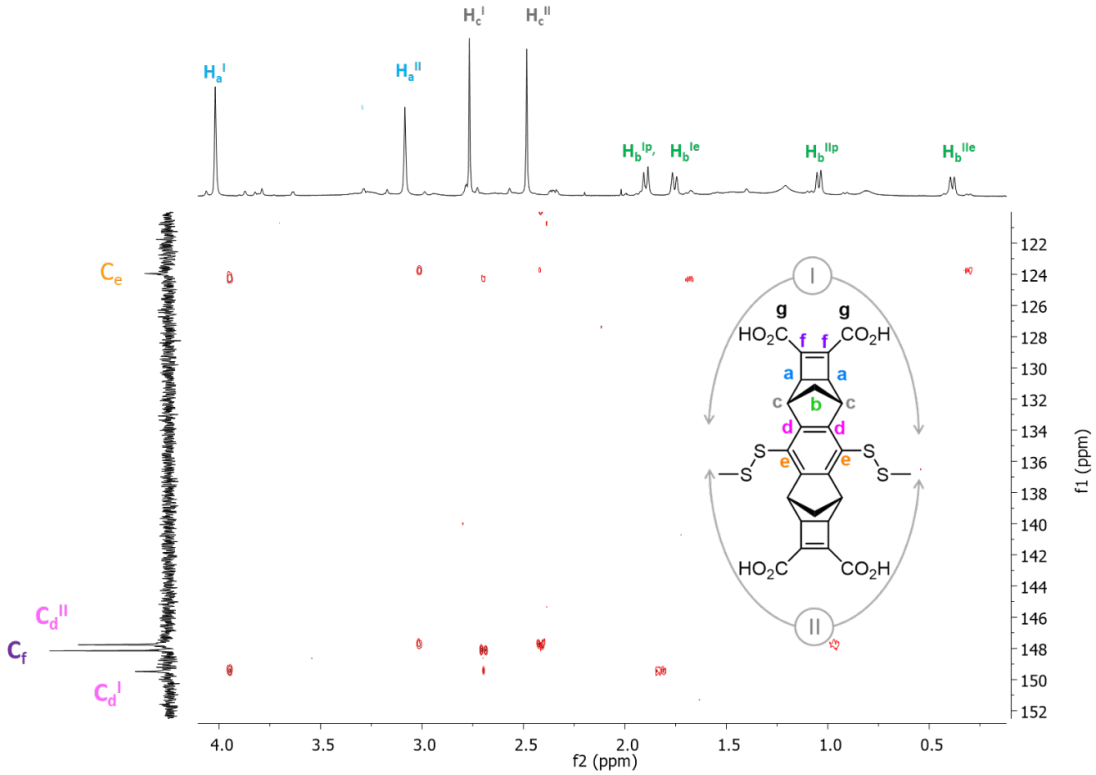

*Figure S114: ^{1}H-^{13}C HMBC spectrum of the **B_4-B_8** system obtained after precipitation and redissolution in 50 mM $CD_3CO_2ND_4$ in D_2O in the ^{13}C 120 – 150 ppm area*

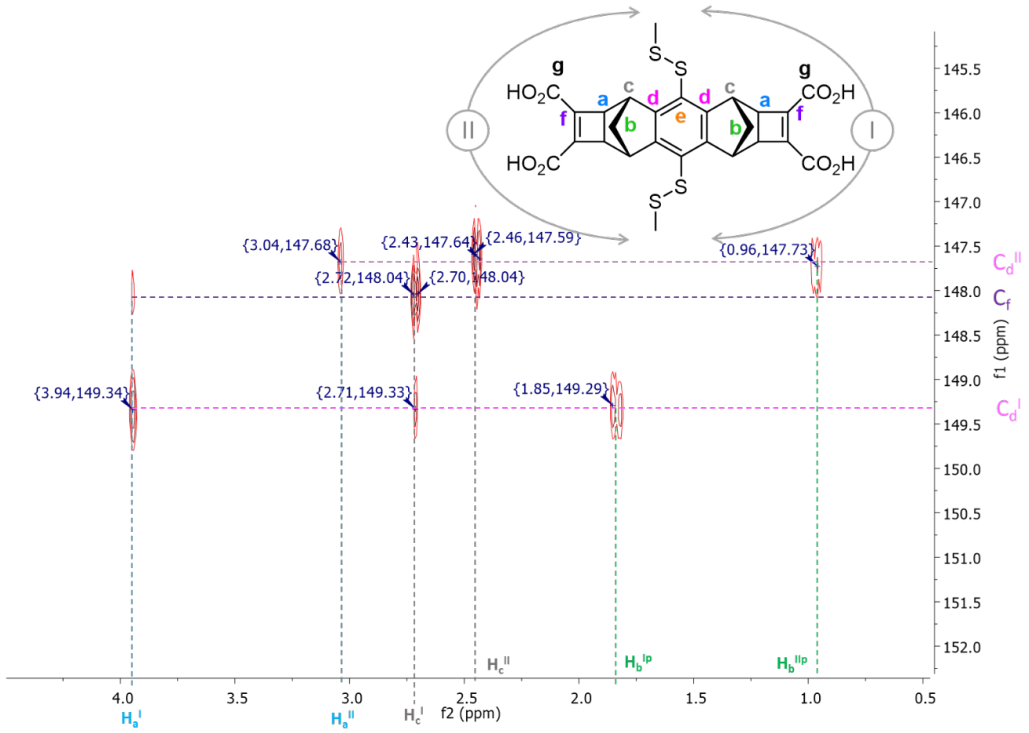

*Figure S115: ^{1}H-^{13}C HMBC spectrum of the **B_4-B_8** system obtained after precipitation and redissolution in 50 mM $CD_3CO_2ND_4$ in D_2O in the ^{13}C 145 – 155 ppm area*

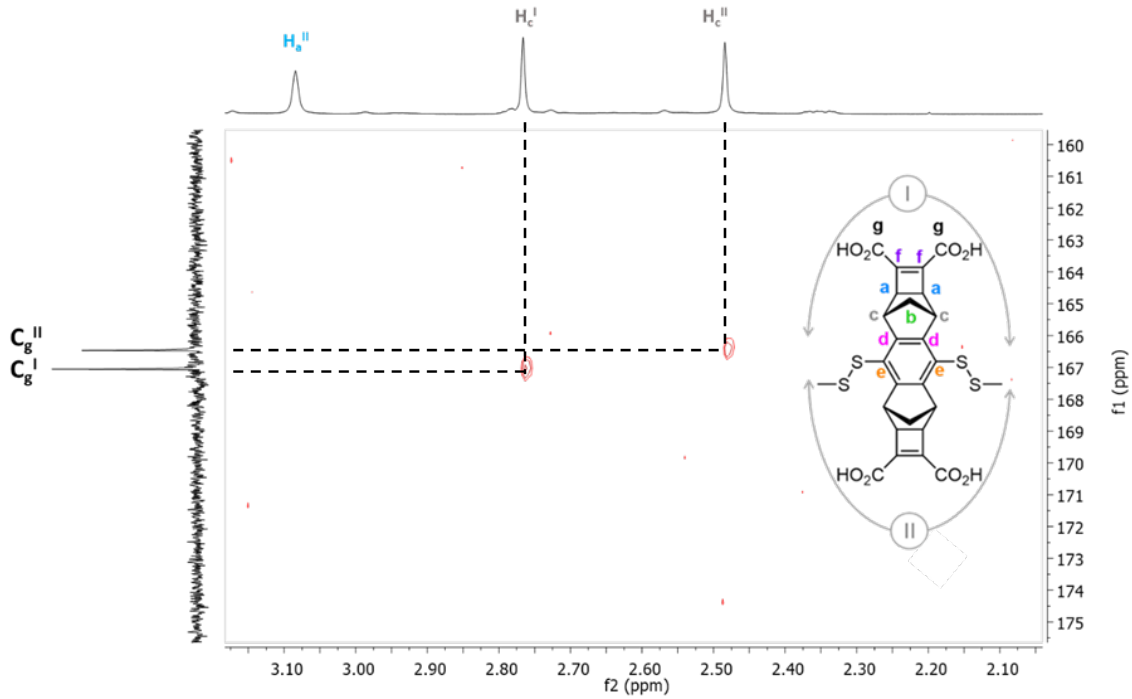

*Figure S116: ^{1}H-^{13}C HMBC spectrum of the **B_4-B_8** system obtained after precipitation and redissolution in 50 mM $CD_3CO_2ND_4$ in D_2O in the ^{13}C 160 – 175 ppm area*

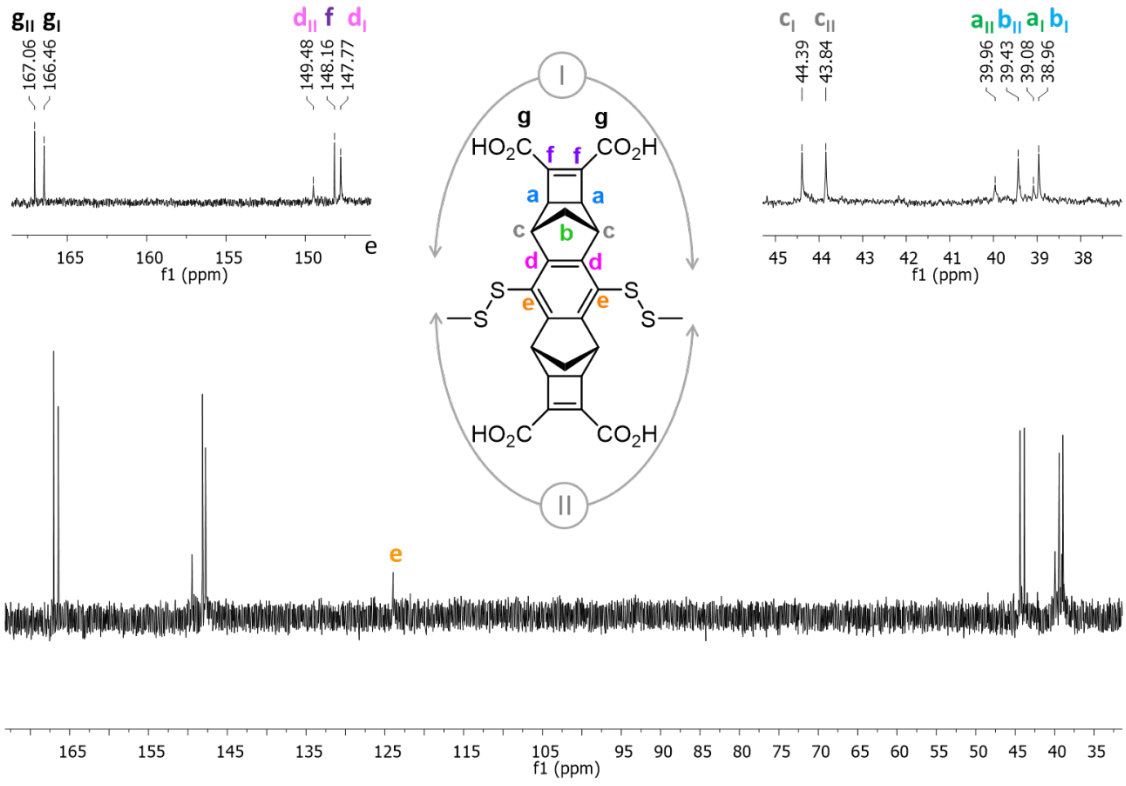

*Figure S117: ^{13}C spectrum of the **B_4-B_8** system obtained after precipitation and redissolution in 50 mM $CD_3CO_2ND_4$ in D_2O with full assignment of the **B_4** fraction*

Peak name	F2 [ppm]	D [m2/s]	error	name	status	RH object	DR_H
1	4.705320862	1.89752E-09	4.18055E-12	water	solvent	1.10	0.002421
2	3.956912989	2.13944E-10	2.27412E-12	H_a^I	analyte	**9.74**	0.103578
3	3.678025017	9.8337E-10	2.00417E-10	dioxane	reference	2.12	0.43207
4	3.021402701	2.2635E-10	3.08575E-12	H_a^{II}	analyte	**9.21**	0.12556
5	2.710742681	2.1307E-10	1.62801E-12	H_c^I	analyte	**9.78**	0.074759
6	2.428795751	2.14409E-10	1.83447E-12	H_c^{II}	analyte	**9.72**	0.083191
7	1.838400475	1.9701E-10	1.19778E-11	H_b^{Ip}	analyte	**10.58**	0.643363
8	1.693824444	2.09452E-10	2.91095E-12	H_b^{Ie}	analyte	**9.95**	0.13833
9	0.979477287	1.96606E-10	4.73905E-12	H_b^{IIp}	analyte	**10.60**	0.255595
10	0.321654594	2.10576E-10	4.73923E-12	H_b^{IIe}	analyte	**9.90**	0.222813

*Table S11 : DOSY NMR data of the **B_4-B_8** system obtained after precipitation and redissolution at 5 mM in 50 mM $CD_3CO_2ND_4$ in D_2O*

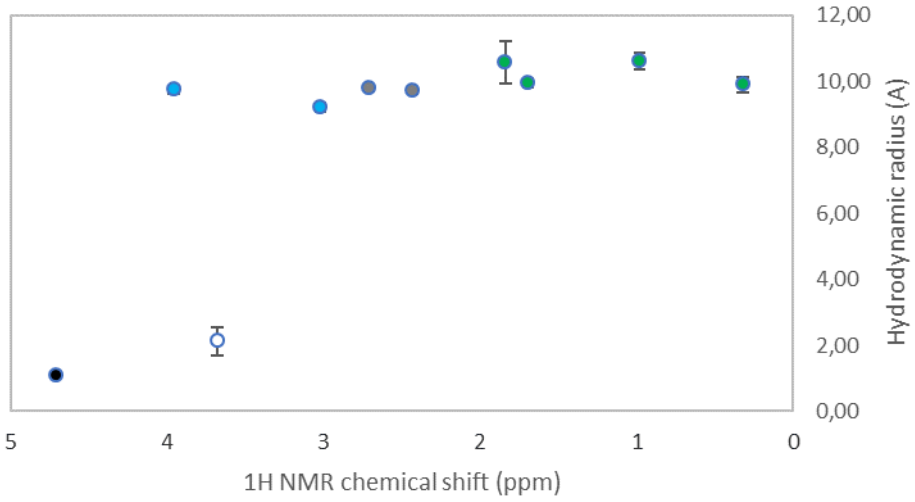

*Figure S118 : DOSY NMR data of **B_4** from a **B_4-B_8** system obtained after precipitation and redissolution at 5 mM in 50 mM $CD_3CO_2ND_4$ in D_2O*

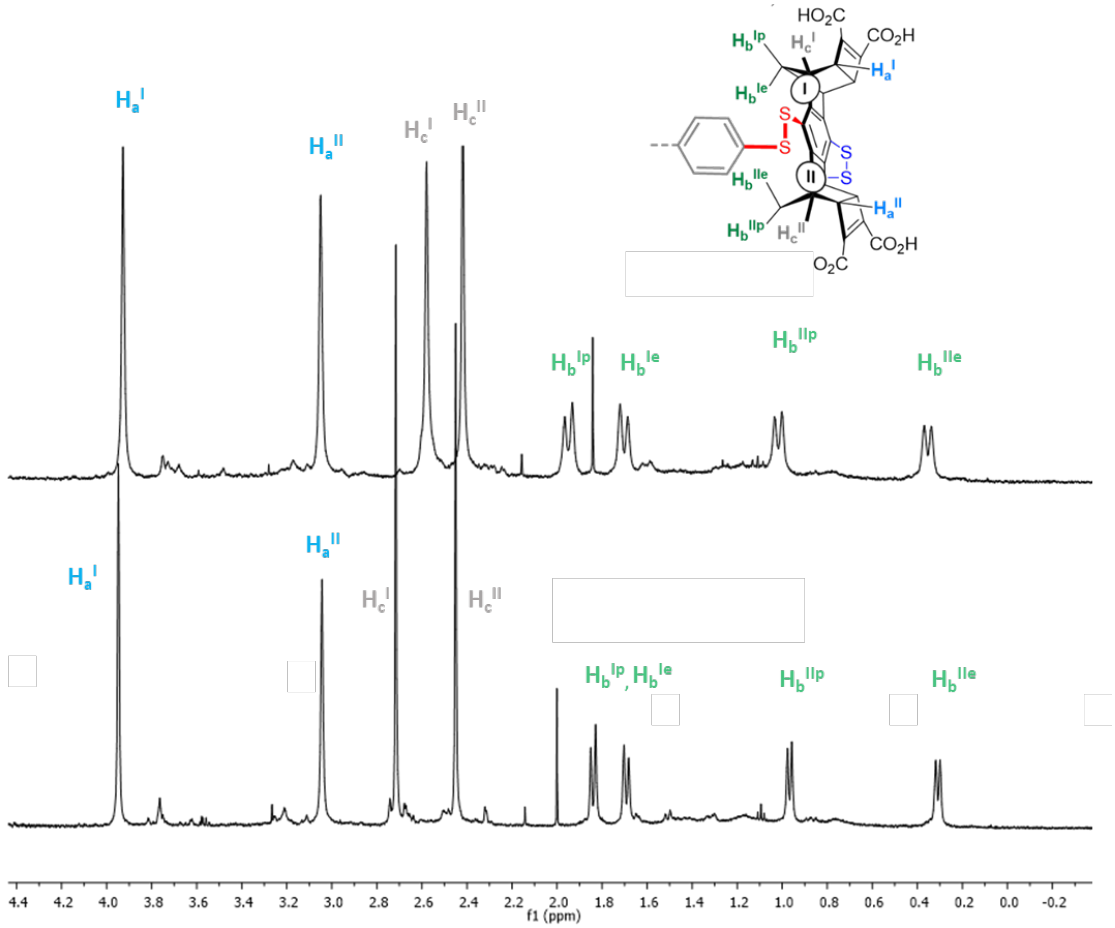

*Figure S119: comparison between ^{1}H NMR spectra of **B_4-B_8** systems before (stage 1, bottom) and after (stage 3, top) precipitation of **B_8** insoluble material*

B_8 precipitation from supersaturated solutions (from stage 2 to 3)

Sample preparation

In an UPLC vial of 2 mL equipped with a small stirrer, 7.936 mg (4 mM), 15.872 mg (8 mM), 31.744 mg (16 mM) of **B_4-B_8** mixture (solid stage 2) were suspended in 1 mL of water. Sonication dispersed the powder in water. Then, aliquots of a solution of sodium hydroxide 2 M were added (*m* µL) until full dissolution of the powder upon stirring. The pH was determined thanks was read with a Mettler Toledo 877 plus. The sample were analysed immediately and were left open or closed for some days without stirring before additional analyses. When a solid appeared (stage 3'), the vial was centrifuged for 5 min at 1200 rpm at 4°C and the supernatant removed with a filtering syringe equipped with a pore filter.

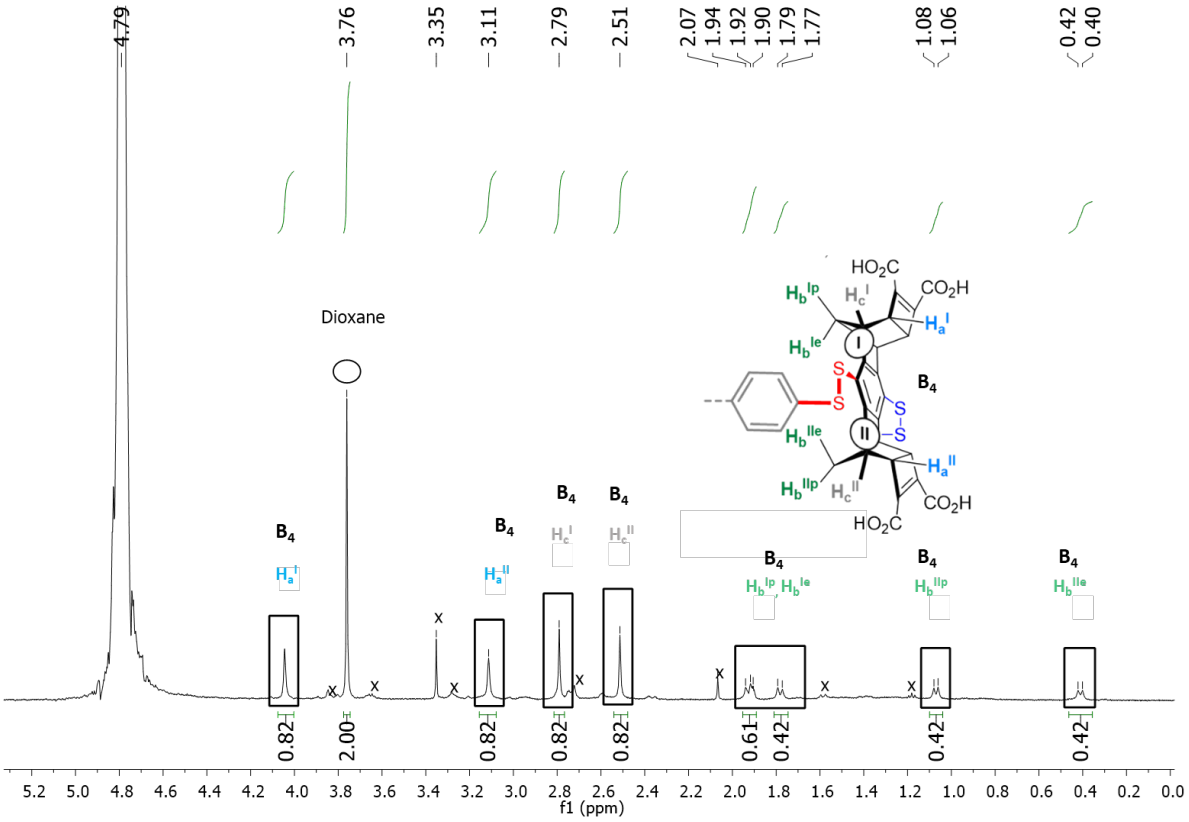

*Figure S120: q^{1}H NMR analysis of the **B$_4$-B$_8$** sample (stage 3) used for (-)ESI-MS calibration studies of the **B$_8$/B$_4$** ratio*

MS data on unsaturated and supersaturated samples (stage 3)

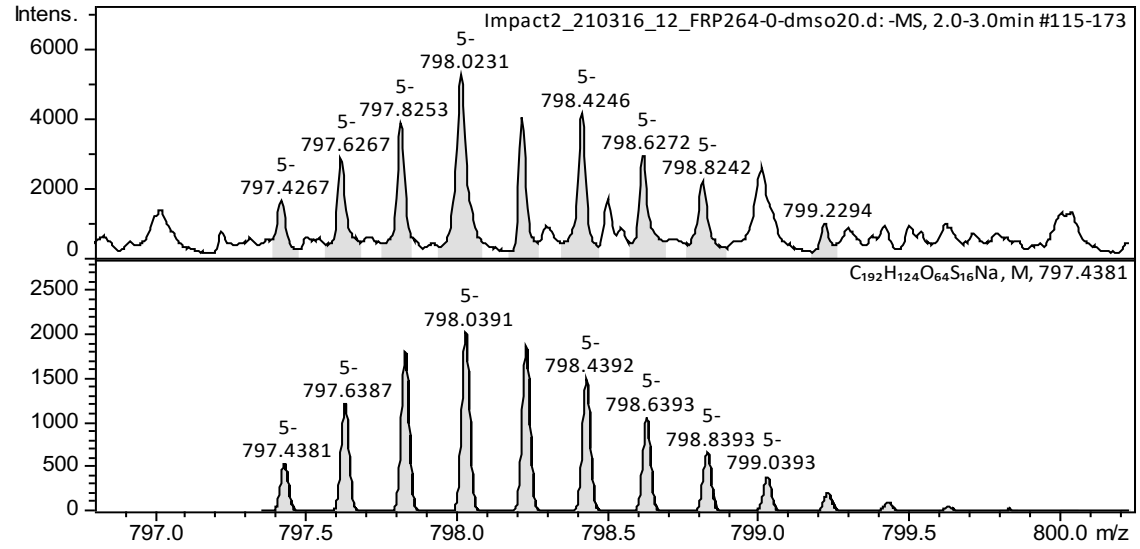

*Figure S121 : Detailed (-)ESI-MS spectrum (797-800 m/z range) of the **B$_4$-B$_8$** mixture analysed by q^{1}H NMR with area/intensity quantification of [**B$_8$**-6H+Na]$^{5-}$ species*

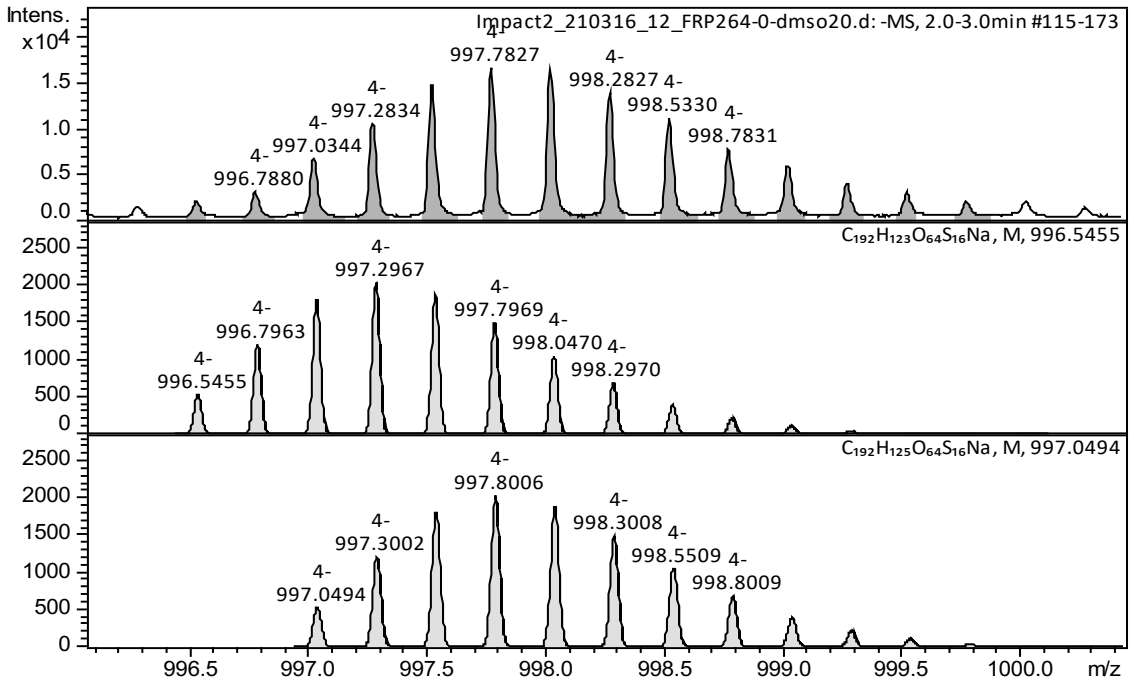

Figure S122 : Detailed (-)ESI-MS spectrum (996-1000 m/z range) of the ***B₄-B₈*** *mixture analysed by q¹H NMR with area/intensity quantification of [B₈-5H+Na]⁴⁻ and [****B₄****-7H+2D+Na]²⁻ species*

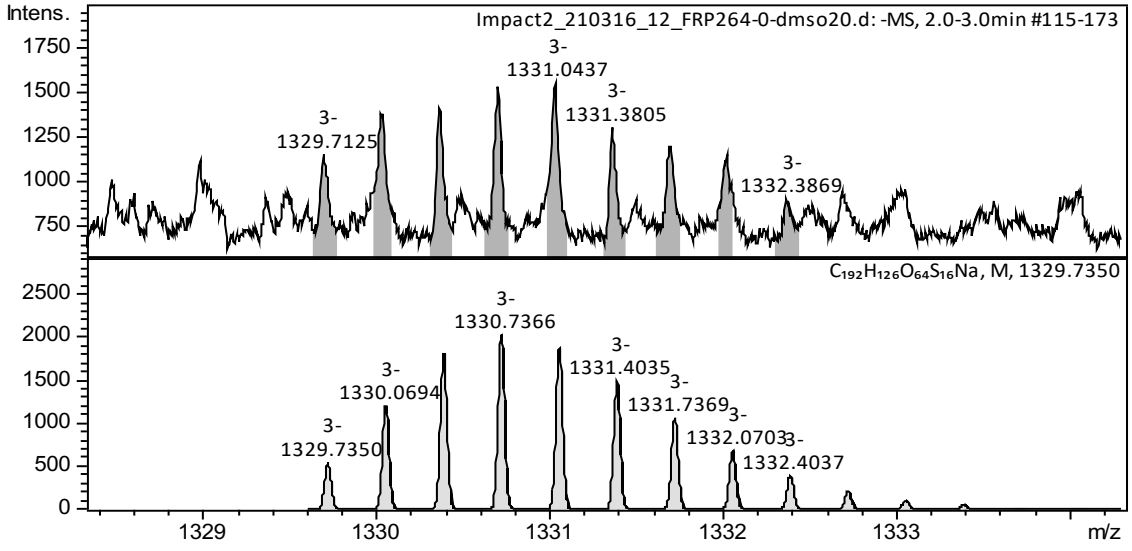

Figure S123 : Detailed (-)ESI-MS spectrum (1329-1333 m/z range) of the ***B₄-B₈*** *mixture analysed by q¹H NMR with area/intensity quantification of [****B₈****-6H+Na]⁵⁻*

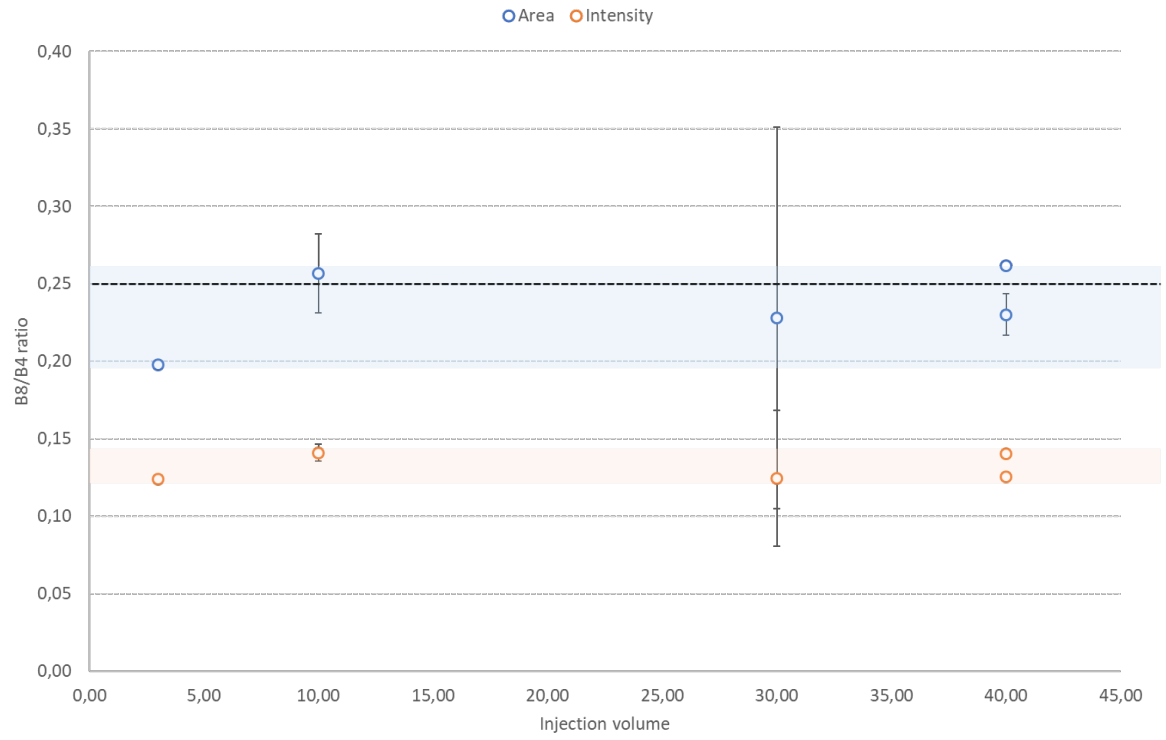

Figure S124 Summary of ESI-MS calibration of the $\boldsymbol{B_8/B_4}$ *ratio measured from peak area (blue mark) or intensity (red mark) with increasing injection volume of a 5 mM stage 3 solution. Dotted line indicates the ratio measured by* ^{1}*H NMR on the same sample*

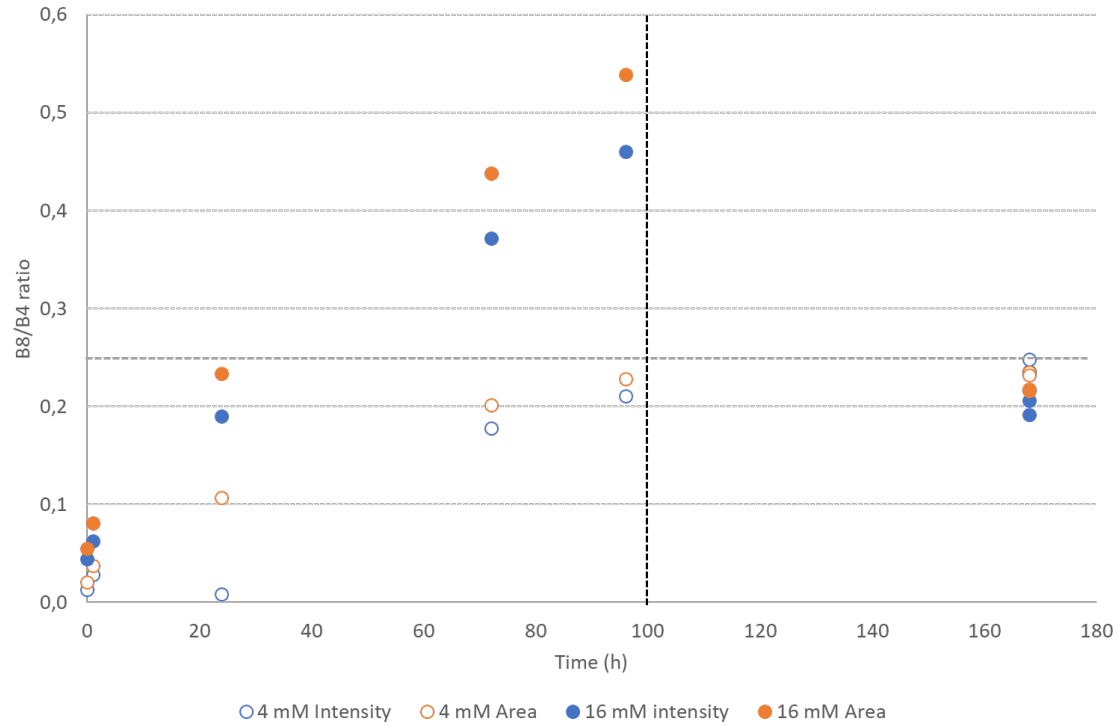

Figure S125 : Assessment of $\boldsymbol{B_8/B_4}$ *ratio by (-)ESI-MS (peak intensity blue, area : orange) from 16 mM (full dots) and 4 mM (empty dots) solutions obtained from stage 3. Precipitation occurs after 100 h (black dotted line). Grey dotted line corresponds to the ratio measured by q* ^{1}*H NMR*

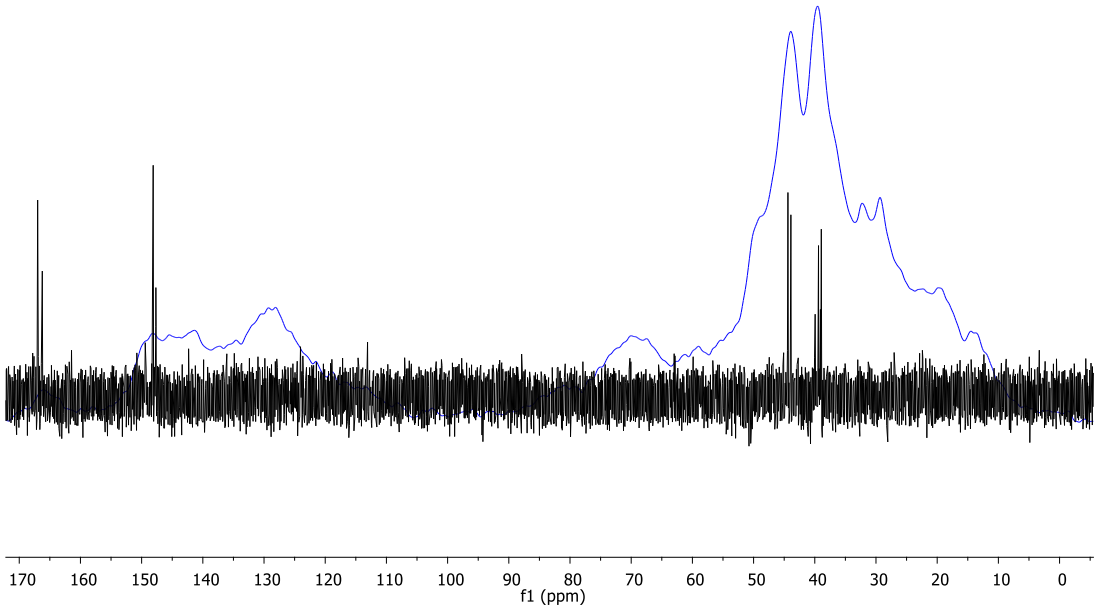

Figure S126: Comparison between solid CP-MAS and liquid state ^{13}C spectra of ***B_4-B_8*** *mixture obtained after precipitation with TFA and upon redissolution at 16 mM (stage 3, supernatant, black; stage 3', solid, blue)*

g. Modelling DFT data for **B_4**

Geometry	E hartree	E hartree	E hartree	dispersion hartree	Delta E kcal/mol	Delta E kcal/mol	Delta E kcal/mol	Delta disp kcal/mol
	B3LYP	B3LYP-D3BJ	m062X	B3LYPD3BJ	B3LYP	B3LYP-D3BJ	M062X	B3LYP-D3BJ
In_In_In_In_PPPP	-9285,966998	-9286,587673	-9283,49424	-0,620675166	14,36740731	14,36740731	12,9367986	3,979039434
In_In_In_Out_PPPP	-9285,958322	-9286,590536	-9283,494039	-0,632214707	15,8328177	12,57067819	13,06265191	-3,262132169
In_In_Out_Out_PPPP	-9285,947947	-9286,587474	-9283,494223	-0,639526735	22,34305933	14,49259546	12,94762942	-7,850498953
In_Out_In_Out_PPPP	-9285,950216	-9286,586343	-9283,488912	-0,636127292	20,91924028	15,20185062	16,27982409	-5,717316364
In_Out_Out_Out_PPPP	-9285,918636	-9286,562066	-9283,468346	-0,643430116	40,73622246	30,43631291	29,1857304	-10,29990799
Out_Out_Out_Out_PPPP	-9285,893989	-9286,544944	-9283,447355	-0,650955773	56,20247421	41,18014151	42,35720501	-15,02232906
In_In_In_In_MMMP	-9285,976408	-9286,602063	-9283,506804	-0,625654418	4,483323199	5,337620907	5,052932398	0,854511689
In_In_In_Out_MMMP	-9285,965457	-9286,599519	-9283,501659	-0,634061676	11,35524876	6,934124302	8,281311898	-4,421123077
In_In_Out_Out_MMMP	-9285,941837	-9286,578875	-9283,478489	-0,637037952	26,17730553	19,88853082	22,82033678	-6,288764353
In_Out_In_Out_MMMP	-9285,949087	-9286,588648	-9283,491021	-0,639561384	21,62791813	13,7556734	14,95658853	-7,872241529
In_Out_Out_Out_MMMP	-9285,933553	-9286,584147	-9283,485554	-0,650594028	31,3755252	16,58019406	18,38732102	-14,79533057
Out_Out_Out_Out_MMMP	-9285,905018	-9286,560853	-9283,462324	-0,65583438	49,28141466	31,19745055	32,96402785	-18,08370143
In_In_In_In_MPMP	-9285,983553	-9286,610569	-9283,514856	-0,627016169	0	0	0	0
In_In_In_Out_MPMP	-9285,971332	-9286,59949	-9283,50114	-0,628157224	7,668749674	6,952485231	8,606964227	-0,716022853
In_In_Out_Out_MPMP	-9285,958917	-9286,59949	-9283,498739	-0,640057302	15,45921736	6,952158926	10,11332588	-8,507052981
In_Out_In_Out_MPMP	-9285,948968	-9286,585768	-9283,486862	-0,636800109	21,70237213	15,56261838	17,56662644	-6,139515548
In_Out_Out_Out_MPMP	-9285,933809	-9286,58088	-9283,482068	-0,647022999	31,21502082	18,62987854	20,57472501	-12,55447639
Out_Out_Out_Out_MPMP	-9285,913091	-9286,570579	-9283,468946	-0,657487829	44,21559321	25,09433081	28,8092247	-19,12125663
In_In_In_In_MMPP	-9285,966575	-9286,591403	-9283,49751	-0,624827673	10,65374334	12,02703533	10,88464801	1,373301591
In_In_In_Out_MMPP	-9285,953531	-9286,584565	-9283,490425	-0,631034226	18,83908393	16,31770684	15,33043987	-2,521369253
In_In_Out_Out_MMPP	-9285,920276	-9286,550007	-9283,456387	-0,629860562	39,70708178	38,00308601	36,68975255	-1,784883566
In_Out_In_Out_MMPP	-9285,943755	-9286,585375	-9283,489661	-0,641619512	24,9735415	15,80980065	15,80985085	-9,163736904
In_Out_Out_Out_MMPP	-9285,905745	-9286,547307	-9283,446403	-0,641562413	48,82521525	39,69746206	42,95483878	-9,127906801
Out_Out_Out_Out_MMPP	-9285,890411	-9286,543084	-9283,443814	-0,652673738	58,44720119	42,34729036	44,57969305	-16,10036842

Table S12: Set of energetical data for the 24 possible diastereoisomers of $\boldsymbol{B_4}$

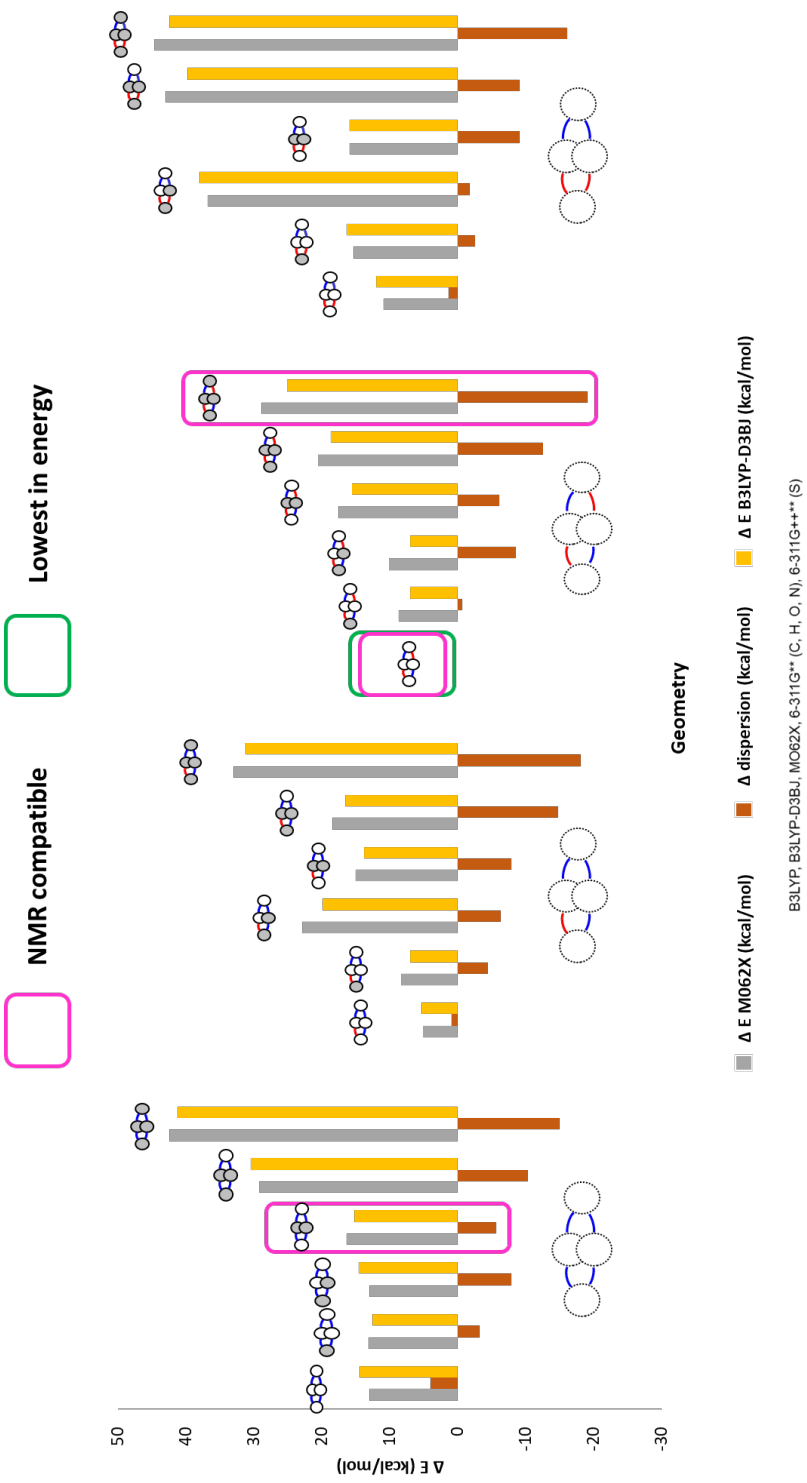

Figure S127 : Energies and dispersion contribution of the 24 diastereoisomers of ***B*****4***, relatively to the lowest in energy: In_In_In_In_MPMP. The structures were optimised with B3LYP and then single point energy were calculated with B3LYP-D3BJ (Yellow), B3LYP and M062X (Grey). Each series of 6 represents a set of diastereisomers with the same P (blue) / M (red) distribution. In each series, the diastereoisomers are represented from the left all In (white cercle) to the right all Out orientation (grey cercle). The dispersion contribution is obtained by the difference between the energy of B3LYP and B3LYP-D3BJ.*

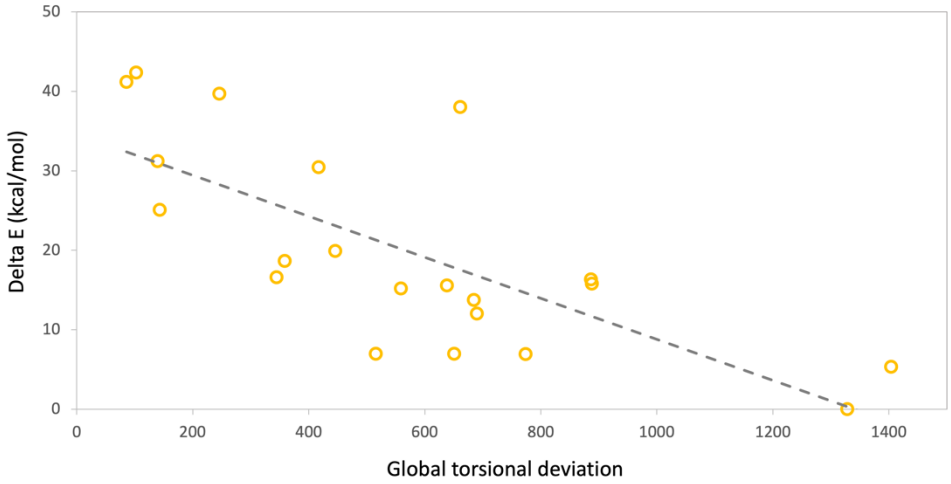

Figure S128 : Relationship between the single point energy (calculated with B3LYP-D3BJ, and relatively to the lowest in energy: In_In_In_In_MPMP) and global torsional deviation of the disulfide bridges (i.e. the sum of the squares of the difference between the measured torsion angles and the theoretical torsion angle of ± 90°) for the 24 diastereoisomers of ***B*****$_4$**.

h. X-ray crystallography data

CheckCIF validation

Refinement of **B$_8$** faced problems due to the disordered carboxylic side chains, weak diffraction intensity and low resolution. A number of A-level and B-level alerts were detected using IUCR's checkcif algorithm. These alerts are inherent to the data and refinement procedures and do not reflect errors. They are listed below and have been divided into two groups.

Group 1 alerts illustrate the weak quality of diffraction data and refinement statistics:

THETM01_ALERT_3_A The value of sine(theta_max)/wavelength is less than 0.550
Calculated sin(theta_max) = 0.4545

PLAT026_ALERT_3_B _Ratio observed / unique reflections (too) low	31%
PLAT084_ALERT_3_B High wR2 Value (i.e. > 0.25) …….	0.36 Report
PLAT241 ALERT_2_B High 'MainMol' Ueq as Compared to Neighbors	12 Check
PLAT242 ALERT_2_B Low 'MainMol' Ueq as Compared to Neighbors	17 Check
PLAT260_ALERT_2_B Large average Ueq of Residue S1, S5	Check
PLAT340_ALERT_3_B Low bond precision on C-C Bonds	0.02511 Ang.

Group 2 alerts are concerned with decision made during refinement and explained below:

PLAT201_ALERT_2_B _Isotropic non-H Atoms in main residue (s) Report

As described above, all non-H atoms of **B_8** were refined with anisotropic or isotropic displacement parameters.

Atomic coordinates and structure factors for **B_8** was deposited in the Cambridge Crystallographic Data Centre (CCDC) with accession code 2003509. The data is available free of charge upon request (www.ccdc.cam.ac.uk/).

CCDC #	2003509
Empirical Formula	$C_{192}H_{96}O_{64}S_{16}$
Formula weight	3939.64
Temperature	100 K
Diffraction source	PetraIII, DESY, Hamburg
Wavelength	0.97625 Å
Crystal system	Hexagonal
Space group	*P*622
Unit cell parameters	$a = b = 49.495$ (7) Å $c = 35.697$ (5) Å
Unit cell volume	75733 (2) $Å^3$
Z	6
Density	0.518 g cm^{-3}
Absorption coefficient	0.262 mm^{-1}
F(000)	12096.0
Theta range	1.567 to 26.343°
Index range	$h = -43 \rightarrow 43$ $k = -44 \rightarrow 44$ $l = -32 \rightarrow 32$
Total reflections	251908
Unique reflections	19896
R_{int}	0.1503
Completeness	0.9992
Data/Restraints/Parameters	19896/1035/855
R1, wR2 (Fo > 4σ (Fo))	0.1083, 0.2740
R1, wR2 (all data)	0.1871, 0.3616
Goodness-of-fit	0.966
Largest diff. Peak/hole/e $Å^{-3}$	0.26/-0.25

*Table S13 : Crystallographic data for **B_8**.*

Set of crystallographic data

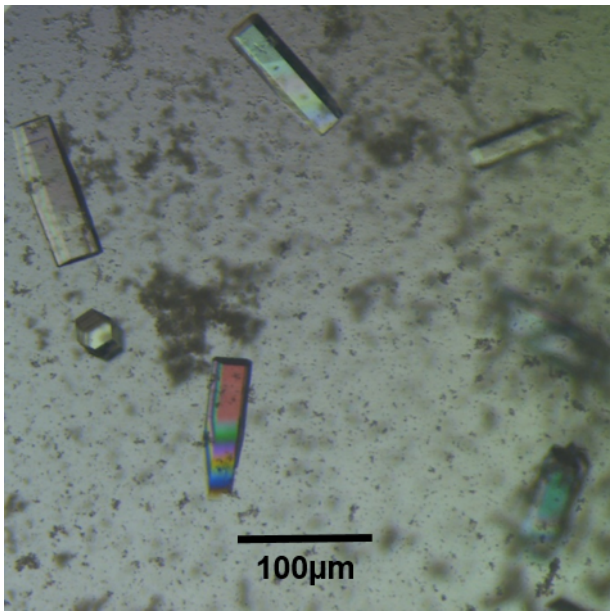

*Figure S129 : **B**$_8$ crystals seen under cross-polarizing microscope*

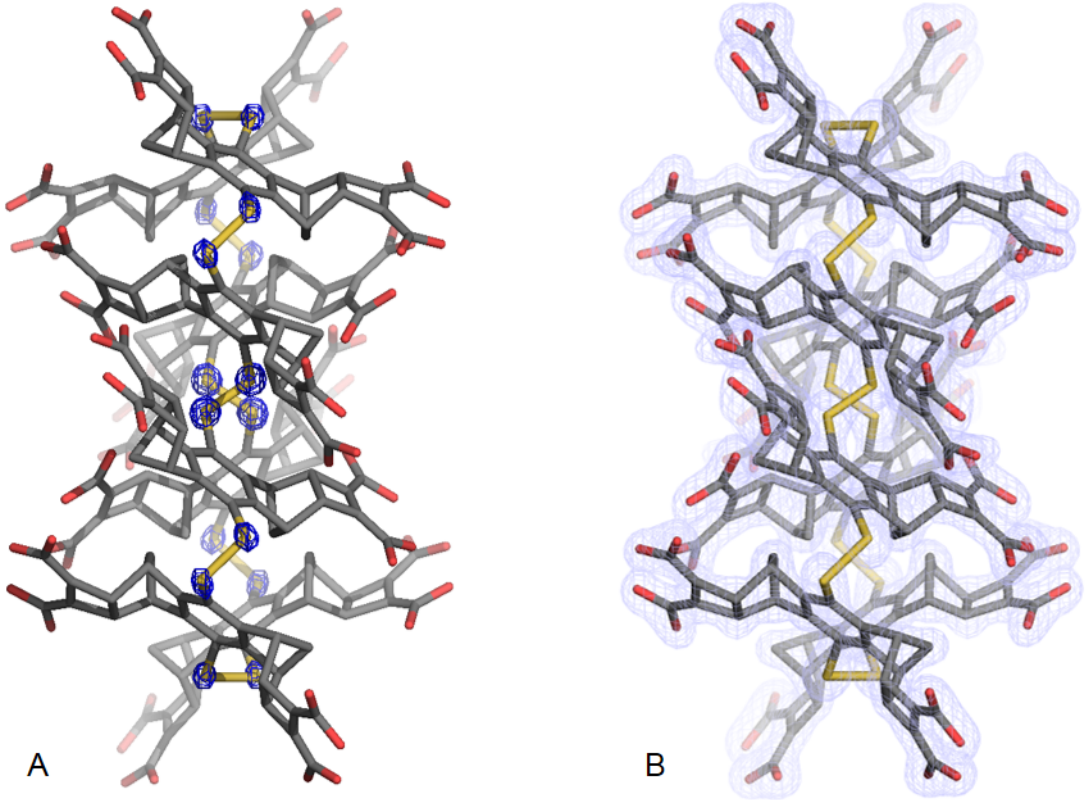

Figure S130 : *Sigma weighted $2F_o$-F_c electron density map superimposed on a **B**$_8$ macrocycle. A) Blue mesh, contoured at 8σ level showing sulphur atoms; B) Light blue mesh, contoured at 2σ level showing*

the shape of macrocycle. Values of the torsion angles of the disulfide bridges (in degrees): -58.88, 93.54, -58.88, 104.2, -58.88, 93.54, -58.88, 104.2.

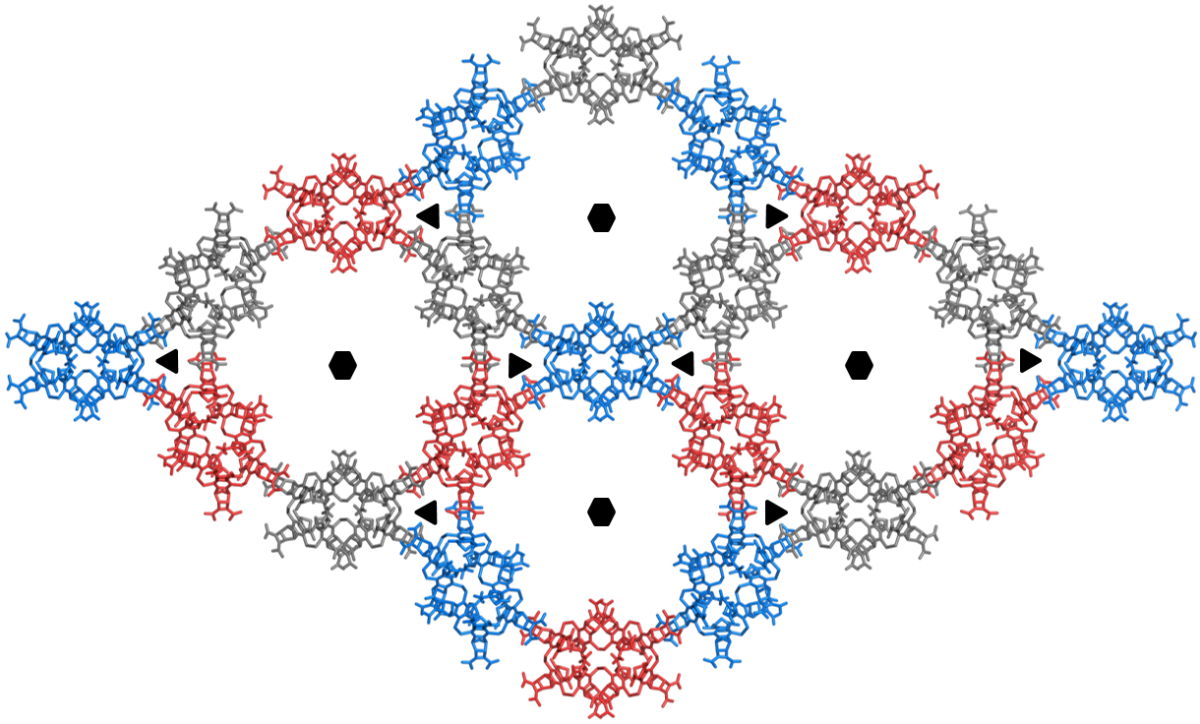

Figure S131 : Crystal lattice of ***B*****$_8$** *showing ring-like arrangements where each ring consists of six* ***B*****$_8$** *molecules.*

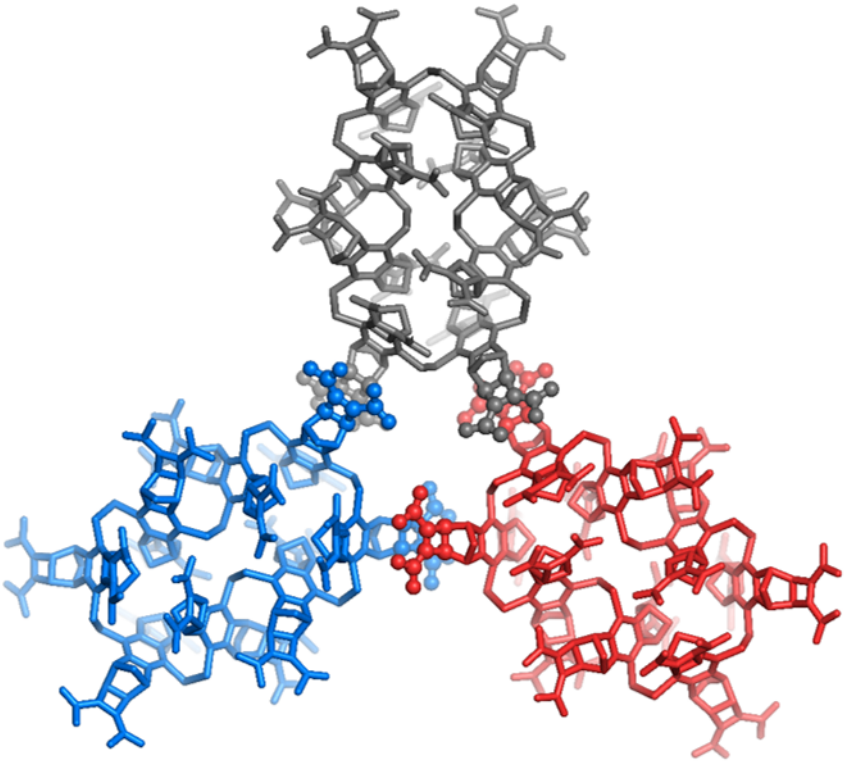

Figure S132 : Arrangement of stacking of one ***B*****$_8$** *molecule bifurcating to two neighbouring* ***B*****$_8$** *molecules at end of its long dimension.*

III. REFERENCES

(1) W. L. F. Armarego, in *Purification of Laboratory Chemicals (Eighth Edition)*, ed. W. L. F., Butterworth-Heinemann, 2017; pp 95–634. https://doi.org/10.1016/B978-0-12-805457-4.50003-3.

(2) A. Chevalier, A. Osypenko, J.-M. Lehn and D. Meyer, Phase Transfer of Metal Cations by Induced Dynamic Carrier Agents: Biphasic Extraction Based on Dynamic Covalent Chemistry, *Chem. Sci.*, 2020, **11**, 11468–11477. https://doi.org/10.1039/D0SC04098C.

(3) M. Cianci, G. Bourenkov, G. Pompidor, I. Karpics, J. Kallio, I. Bento, M. Roessle, F. Cipriani, S. Fiedler and T. R. Schneider, P13, the EMBL Macromolecular Crystallography Beamline at the Low-Emittance PETRA III Ring for High- and Low-Energy Phasing with Variable Beam Focusing, *J. Synchrotron Radiat.*, 2017, **24**, 323–332. https://doi.org/10.1107/S1600577516016465.

(4) A. A. McCarthy, R. Barrett, A. Beteva, H. Caserotto, F. Dobias, F. Felisaz, T. Giraud, M. Guijarro, R. Janocha, A. Khadrouche, M. Lentini, G. A. Leonard, M. Lopez Marrero,S. Malbet-Monaco, S. McSweeney, D. Nurizzo, G. Papp, C. Rossi, J. Sinoir, C. Sorez, J. Surr, O. Svensson, U. Zander, F. Cipriani, P. Theveneau and C. Mueller-Dieckmann, ID30B – a Versatile Beamline for Macromolecular Crystallography Experiments at the ESRF, *J. Synchrotron Radiat.*, 2018, **25**, 1249–1260. https://doi.org/10.1107/S1600577518007166.

(5) CrysAlisPRO, Oxford Diffraction /Agilent Technologies UK Ltd, Yarnton, England.

(6) W. Kabsch, Integration, Scaling, Space-Group Assignment and Post-Refinement, *Acta Cryst. D*, 2010, **66**, 133–144. https://doi.org/10.1107/S0907444909047374.

(7) W. Kabsch, XDS, *Acta Cryst. D*, 2010, **66**, 125–132. https://doi.org/10.1107/S0907444909047337.

(8) G. M. Sheldrick, Crystal Structure Refinement with SHELXL., *Acta Cryst. C*, 2015, **71**, 3–8. https://doi.org/10.1107/S2053229614024218.

(9) O. V. Dolomanov, L. J. Bourhis, R. J. Gildea, J. A. K. Howard and H. Puschmann, OLEX2: A Complete Structure Solution, Refinement and Analysis Program, *J. Appl. Cryst.*, 2009, **42**, 339–341. https://doi.org/10.1107/S0021889808042726.

(10) P. Emsley and K. Cowtan, Coot: Model-Building Tools for Molecular Graphics, *Acta Cryst. D*, 2004, **60**, 2126–2132. https://doi.org/10.1107/S0907444904019158.

(11) A. L. Spek, PLATON SQUEEZE: A Tool for the Calculation of the Disordered Solvent Contribution to the Calculated Structure Factors, *Acta Cryst. C*, 2015, **71**, 9–18. https://doi.org/10.1107/S2053229614024929.

(12) C. Lee, W. Yang and R. G. Parr, Development of the Colle-Salvetti Correlation-Energy Formula into a Functional of the Electron Density, *Phys. Rev. B*, 1988, **37**, 785–789. https://doi.org/10.1103/PhysRevB.37.785.

(13) M. Frisch, G. Trucks, H. Schlegel, G. Scuseria, M. Robb, J. Cheeseman, J. Montgomery, T. Vreven, K. Kudin, J. Burant, J. Millam, S. Iyengar, J. Tomasi, V. Barone, B. Mennucci, M. Cossi, G. Scalmani, N. Rega, G. Petersson, H. Nakatsuji, M. Hada, M. Ehara, K. Toyota, R. Fukuda, J. Hasegawa, M. Ishida, T. Nakajima, Y. Honda, O. Kitao, H. Nakai, M. Klene, X. Li, J. Knox, H. Hratchian, J. Cross, V. Bakken, C. Adamo, J. Jaramillo, R. Gomperts, R. Stratmann, O. Yazyev, A. Austin, R. Cammi, C. Pomelli, J. Ochterski, P. Ayala, K. Morokuma, G. Voth, P. Salvador, J. Dannenberg, V. Zakrzewski, S. Dapprich, A. Daniels, M. Strain, O. Farkas, D. Malick, A. Rabuck, K. Raghavachari, J. Foresman, J. Ortiz, Q. Cui, A. Baboul, S. Clifford, J. Cioslowski, B. Stefanov, G. Liu, A. Liashenko, P. Piskorz, I. Komaromi, R. Martin, D. Fox, T. Keith, A. Laham, C. Peng, A. Nanayakkara, M. Challacombe, P. Gill, B. Johnson, W. Chen, M. Wong, C. Gonzalez and J. Pople, Gaussian 03, Revision C.02. 2003.

(14) D. A. Case, H. M. Aktulga, K. Belfon, I. Y. Ben-Shalom, S. R. Brozell, D. S. Cerutti, T. E. Cheatham, III, G. A. Cisneros, V. W. D. Cruzeiro, T. A. Darden, R. E. Duke, G. Giambasu, M. K. Gilson, H. Gohlke, A. W. Goetz, R. Harris, S. Izadi, S. A. Izmailov, C. Jin, K. Kasavajhala, M. C. Kaymak, E. King, A. Kovalenko, T. Kurtzman, T. S. Lee, S. LeGrand, P. Li, C. Lin, J. Liu, T. Luchko, R. Luo, M. Machado, V. Man, M. Manathunga, K. M. Merz, Y. Miao, O. Mikhailovskii, G. Monard, H. Nguyen, K. A. O'Hearn, A. Onufriev, F. Pan, S. Pantano, R. Qi, A. Rahnamoun, D. R. Roe, A. Roitberg, C. Sagui, S. Schott-Verdugo, J. Shen, C. L. Simmerling, N. R. Skrynnikov, J. Smith, J. Swails, R. C. Walker, J. Wang, H. Wei, R. M. Wolf, X. Wu, Y. Xue, D. M. York, S. Zhao and P. A. Kollman (2021), Amber 2021, University of California, San Francisco.

(15) W. D. Cornell, P. Cieplak, C. I. Bayly, I. R. Gould, K. M. Merz, D. M. Ferguson, D. C. Spellmeyer, T Fox, J. W. Caldwell and P. A. Kollman, A Second Generation Force Field for the

Simulation of Proteins, Nucleic Acids, and Organic Molecules, *J. Am. Chem. Soc.*, 1995, **117**, 5179–5197. https://doi.org/10.1021/ja00124a002.

(16) J. Wang, R. M. Wolf, J. W. Caldwell, P. A. Kollman and D. A. Case, Development and Testing of a General Amber Force Field, *J. Comput. Chem.*, 2004, **25**, 1157–1174. https://doi.org/10.1002/jcc.20035.

(17) P. Mark and L. Nilsson, Structure and Dynamics of the TIP3P, SPC, and SPC/E Water Models at 298 K, *J. Phys. Chem. A*, 2001, **105**, 9954–9960. https://doi.org/10.1021/jp003020w.

(18) D. R. Roe and T. E. Cheatham, PTRAJ and CPPTRAJ: Software for Processing and Analysis of Molecular Dynamics Trajectory Data, *J. Chem. Theory Comput.*, 2013, **9**, 3084–3095. https://doi.org/10.1021/ct400341p.

(19) B. R. Miller, T. D. McGee, J. M. Swails, N. Homeyer, H. Gohlke and A. E. Roitberg, MMPBSA.Py: An Efficient Program for End-State Free Energy Calculations, *J. Chem. Theory Comput.*, 2012, **8**, 3314–3321. https://doi.org/10.1021/ct300418h.

(20) E. F. Pettersen, T. D. Goddard, C. C. Huang, G. S. Couch, D. M. Greenblatt, E. C. Meng and T. E. Ferrin, UCSF Chimera—A Visualization System for Exploratory Research and Analysis, *J. Comput. Chem.*, 2004, **25**, 1605–1612. https://doi.org/10.1002/jcc.20084.

(21) P.-T. Skowron, M. Dumartin, J. Jeamet, F. Perret, C. Gourlaouen, A. Baudouin, B. Fenet, J.-V. Naubron, F. Fotiadu, L. Vial and J. Leclaire, J. On-Demand Cyclophanes: Substituent-Directed Self-Assembling, Folding, and Binding, *J. Org. Chem.* 2016, **81**, 654–661. https://doi.org/10.1021/acs.joc.5b02605.